Johannes Mathes

Protein Adsorption to Vial Surfaces

Quantification, Structural and Mechanistic Studies

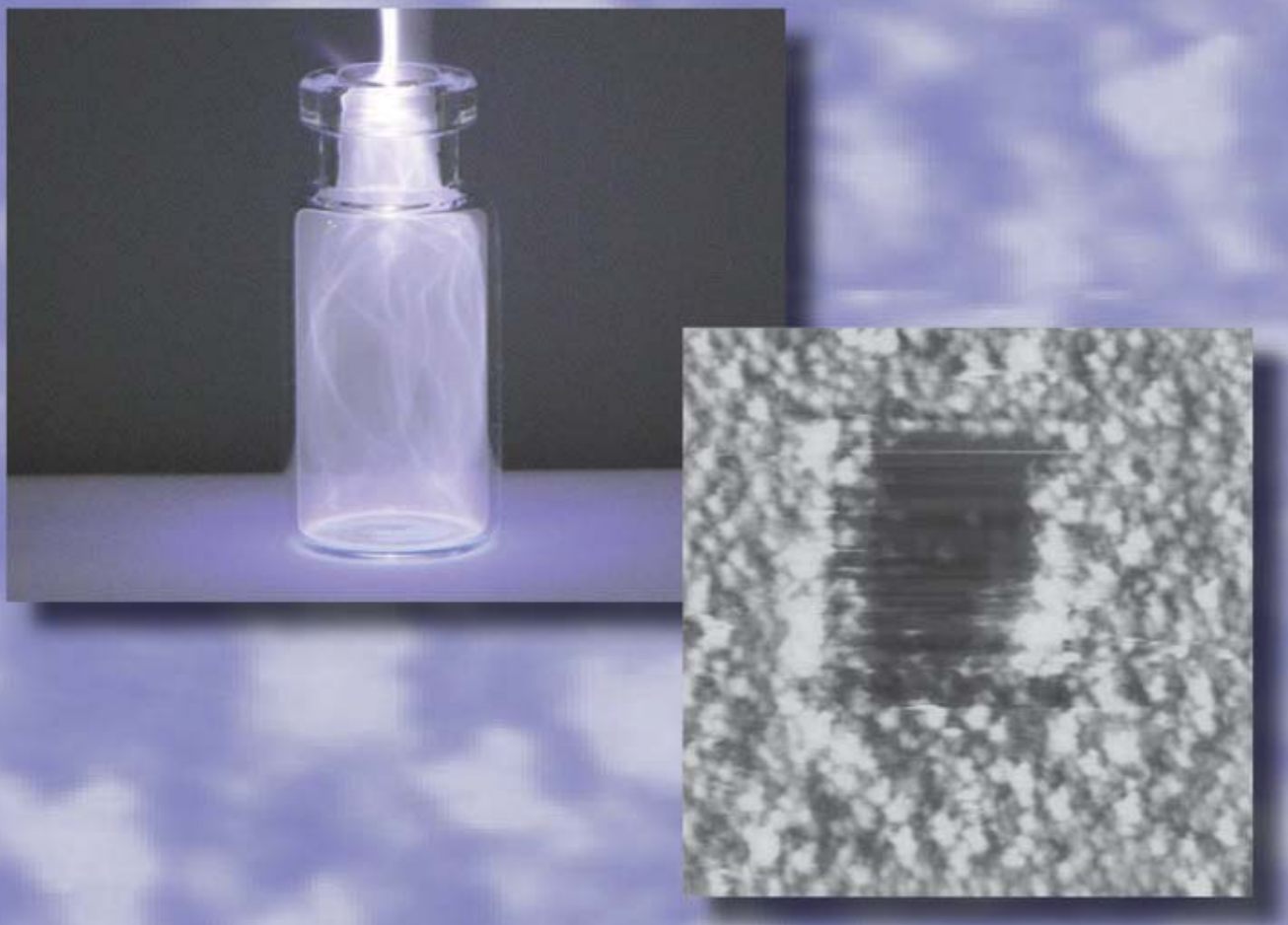

Cuvillier Verlag Göttingen
Internationaler wissenschaftlicher Fachverlag

Dissertation zur Erlangung des Doktorgrades
der Fakultät für Chemie und Pharmazie
der Ludwig-Maximilians-Universität München

Protein Adsorption to Vial Surfaces – Quantification, Structural and Mechanistic Studies

Johannes Maximilian Mathes

aus

Oberviechtach

2010

Bibliografische Information der Deutschen Nationalbibliothek
Die Deutsche Nationalbibliothek verzeichnet diese Publikation in der Deutschen Nationalbibliografie; detaillierte bibliografische Daten sind im Internet über http://dnb.d-nb.de abrufbar.
1. Aufl. - Göttingen : Cuvillier, 2010
Zugl.: München, Univ., Diss., 2010

978-3-86955-481-5

Erklärung

Diese Dissertation wurde im Sinne von § 13 Abs. 3 bzw. 4 der Promotionsordnung vom 29. Januar 1998 von Herrn Prof. Dr. Wolfgang Frieß betreut.

Ehrenwörtliche Versicherung

Diese Dissertation wurde selbständig, ohne unerlaubte Hilfe erarbeitet.

München, am 29. Juni 2010

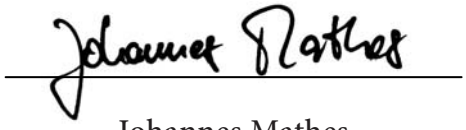

Johannes Mathes

Dissertation eingereicht am 29. Juni 2010

1. Gutachter: Prof. Dr. Wolfgang Frieß

2. Gutachter: Prof. Dr. Gerhard Winter

Mündliche Prüfung am 27. Juli 2010

Nonnenstieg 8, 37075 Göttingen
Telefon: 0551-54724-0
Telefax: 0551-54724-21
www.cuvillier.de

1. Auflage, 2010
Gedruckt auf säurefreiem Papier

978-3-86955-481-5

Acknowledgements

Foremost, I would like to express my deepest gratitude to my supervisor Prof. Dr. Wolfgang Frieß, who gave me the opportunity to work in the fascinating field of protein pharmaceuticals. I hold his valuable advice, his scientific guidance, and the inspiring discussions in high regard. Also, many thanks for the pleasant working atmosphere in the group.

I want to thank the leader of the chair, Prof. Dr. Gerhard Winter, for providing such excellent working conditions and his continuous efforts for the excellent technical equipment in the laboratories.

I am much obliged to the cooperating companies:

I am thankful for the generous material and scientific support which SCHOTT AG provided. I wish to thank the whole department FTV-1 in Mainz, with its head Dr. Uwe Rothhaar, for kindly welcoming and supporting me during this project. I am indebted to Volker Scheumann, who kindly performed the AFM and ToF-SIMS measurements. Also, I would like to thank Heike Koglin for ToF-SIMS measurements. Dr. Klaus Bange is acknowledged for his scientific contribution.

I am deeply indebted to Dr. Holger Roehl, also from SCHOTT AG. Thank you for all your support in the course of this thesis. Special thanks for your introduction to ToF-SIMS analytics and PCA. I have many fond memories of my days in Mainz; thank you for your friendship.

Merck Serono is gratefully acknowledged for the generous material support. I would like to thank Dr. Daniel Schwartz for his support within the project. Also, I am grateful to Dr. Mirelle Krier and Dr. Friedrich Rippmann for their introduction to molecular modeling.

From the IFOS institute in Kaiserslautern, I want to thank Dr. Michael Wahl for his high interest in the subject and for conducting the measurements in the ToF-SIMS project. Furthermore, I want to express my sincere thanks to Dr. Birgit Merz and Dr. Dr. Rolf Merz for conducting the XPS measurements.

From the Departments of Chemistry and Pharmacy of the LMU Munich, I would like to thank Dr. Sebastian Guenther for his introduction to XPS analysis, Tina Reuter for the gas sorption measurements, and Dr. Steffen Schmidt for taking the high quality SEM pictures.

I am very grateful to my lab partner Imke Leitner for the nice time in our lab and for the outstanding assistance whenever I needed help.

Thanks are also extended to the assisting students Julia Miller, Katrin Schaffenroth, Laura Liekmeier, Christiane Krettek, and Wolfgang Gulbins for the excellent job they did in their internships.

I want to thank all my former Munich colleagues for the outstanding working climate. Particularly, I want to mention Virginie, Miriam, Katja, Melanie, Frank, Lars, and Cornelius. Thanks for your support, for your friendship, and for the good times we spent together.

Outside the university, special thanks go to Carolin, Brian, and Susan.

My parents, my grandmother, my sister Carolin with André and Cecilia, and my parents-in-law, I want to thank for their encouragement and great support in all the years.

Finally, I want to sincerely thank my wife Sylvia and my daughter Elena. Heartfelt thanks for your encouragement over the past years, for your endless patience, and for your love!

For my parents,
for my wife Sylvia,
and for my daughter Elena

Table of Contents

Chapter 1

Introduction and Objectives of the Thesis

Chapter 2

Development of Sensitive Methods for the Quantification of Protein Adsorption to Pharmaceutical Containers

Chapter 3

Influence of Vial Surface Properties on IgG1 Adsorption

Chapter 4

Influence of the Protein Formulation on IgG Adsorption to Vials

Chapter 5

Modeling of IgG1 Adsorption to Vials – Isotherm Considerations and Affinity Aspects

Chapter 6

Advanced Investigations on Adsorbed IgG1 Molecules with XPS and ToF-SIMS

Chapter 7

Structural Stability Investigations and Atomic Force Microscopy Imaging of IgG1 Adsorbed on Borosilicate Glass

Chapter 8

APPENDIX

Chapter 1

Introduction and Objectives of the Thesis

Abstract

The adsorption of therapeutic proteins on a variety of surface types, e.g. from the production line and the storage containers through to administration equipment, has shown to cause severe problems which should not be underestimated. Among them is the loss of content but also the potential of severe protein structural changes, accompanied by the risk of therapy failure or immunological reactions. Protein pharmaceuticals play an important role in today's pharmacotherapy. Aside from common coatings or the use of plastic equipment, which is increasing in use, borosilicate glass is still the material of choice for the primary packaging of parenteral drugs. Against this background, a general summary on the phenomenon of protein adsorption on solid surface is given in the introductory chapter. Aside from external factors as, e.g. temperature, the adsorption of proteins generally depends on three main components which are the protein itself, the sorbent surface, and the surrounding liquid. The driving forces, whose interplay determines the overall adsorption process, are pointed out. Moreover, a short overview on adsorption quantification procedures and on approaches to identify the structural changes upon adsorption is provided.

1 INTRODUCTION

1.1 Adsorption of Therapeutic Proteins on Solid Surfaces

The understanding of adsorption of recombinant therapeutic proteins on various kinds of surfaces, e.g. in the course of up-stream and down-stream processing, fill and finish, storage, or administration is crucial in the pharmaceutical industry. In addition, it has been well known for a long time that proteins adsorb to glass and plastic, which can result in a reduced dose reaching the patient [1,2]. Table 1 gives some striking examples of protein loss to a selection of different surfaces. This summary underlines fatal consequences which potentially arise from adsorption, especially from solutions of low concentration. One of the most intensively investigated proteins of clinical relevance in this regard is insulin [2-5].

The main problem arises from the protein loss in solution. Without other optimizations, one approach to handle this problem is an appropriate increase of the starting concentration. Closely related to this is the inevitable financial effort for the surplus of the active ingredient. Moreover, the formulation can be adequately adapted with respect to the parameters pH and ionic strength or by the addition of suitable excipients. However, changes in the formulation are limited by the necessary conservation of protein stability on the one hand and an adequate biocompatibility on the other hand. Only in very rare cases will the protein itself be subject to changes with the intention to reduce its adsorption tendency. Another option is the selection of appropriate container material that has

Table 1: Selected examples for the adsorptive loss of therapeutic protein to different surfaces utilized during the production process, storage, or administration.

Protein	Surface	Concentration	Protein loss	Reference
Insulin	Glass bottle	30 U/l	52% after 5 min	[2]
Secretin	Siliconized glass container	40 CHR Units/ml	20%	[6]
Cetrorelix	Glass and plastic vials	0.2 - 0.4 µg/ml	30% after 2 h	[7]
Factor VIII	PVC mini bag	146 IU/ml	Approx. 60% after 48 h	[8]
Interleukin 2	Silicone rubber catheter tubing	50 - 100 µg/ml	Approx. 90% activity loss after 24 h	[9]
Salmon calcitonin and bovine serum albumin	Glass and polypropylene	25 - 150 µg/ml	30 - 75% after 12 h	[10]

low binding properties for the respective protein. However, a universal and at the same time stable coating countervailing protein adsorption has not been found to this day. Additional problems can arise from the adsorption of proteins on solid surface. One of the major difficulties is the structural instability of the proteins, and adsorption may result in unfolding and aggregation phenomena. Both are critical with regard to an increasing potential of causing immunogenicity problems (see below). It is particularly worrisome that these entities, once formed through contact with the interface, may get back into the bulk solution, a process which may possibly be facilitated by collision with dissolved molecules [11]. Thus, an extensive study of the different factors involved in the adsorption process is essential for selecting the right actions to avoid or at least to reduce the above-mentioned serious consequences.

1.2 Recombinant Proteins and their Formulation

Recombinant proteins play an important role in modern pharmacotherapy, and special requirements are needed for the formulation of these protein-based active ingredients. In the majority of cases, proteins are administered parenterally as an aqueous solution. Either the aqueous solution is the stored dosage form or a freeze-dried product is reconstituted prior to administration. In order to preserve the biological activity of the proteins, the formulation must ensure the integrity of the protein conformation while also retaining a wide range of functional groups from degradation. A multiplicity of excipients can be considered, of which buffers, sugars, polyols, amino acids, salts, and surfactants play the most important role. In terms of protein stability, the most critical factors are the pH value and the ionic strength [12]. The mechanism of stabilizing the protein structure by means of general protein stabilizers, such as sugars, is explained by the theory of preferential exclusion/interaction, discussed by Timasheff and coworkers [13-15], in which the protein molecule preferentially interacts with either water or the excipient molecules. Surfactants protect the protein from surface-mediated unfolding or aggregation. They also prevent the protein molecules from reaching the solution/air or the solution/packaging container interface [16]. Through this, concentration-dependent phenomena and the range of the critical micelle concentration (CMC) as a typical lower limit for the formulation concentration can be explained. Direct interactions between surfactant and protein molecules, especially with hydrophobic side chains, are an issue as well [17,18]. In the absence of unfolding, interactions between protein molecules are reduced. However, if the surfactant preferentially binds to the more hydrophobic unfolded state, the free energy of the denatured state would be lowered, and this state would be thermodynamically stabilized by the surfactant. Thus, the addition of surfactant can result in both stabilization and destabilization of a protein. Moreover, a chaperon-like effect of the surfactants, which promotes refolding of protein molecules, is discussed [19,20].

1.3 Immunogenicity of Proteins

The risk of immunogenicity reactions associated with therapeutic proteins should not be underestimated. By breaking the immune tolerance, therapy may fail, or an autogenic protein with an essential biological activity may be inactivated. A dramatic example in this regard is the sudden appearance of erythroblastopenia in erythropoietin-medicated patients, which occurred in temporal relation to a formulation change [21]. This crisis has encouraged scientific researchers, companies, and administration agencies (FDA, EMEA) to elucidate such relationships.

Sources affecting the immune response can be roughly categorized by either treatment or processing-related factors [22]. Treatment-related factors involve the immune tolerance of the patient as well as the dosing schedule, the route of administration, and treatment duration. Processing-related factors include intrinsic protein properties, such as sequence, three-dimensional structure, and glycosylation pattern but also the whole manufacturing process, container closure, as well as storage and handling [23,24]. The presence of aggregates, which are typically formed during processing and storage, has received particular attention [25]. Especially protein aggregates have shown to increase immunogenicity due to their size together with newly formed recognition patterns, analogous to virus-like arrays, which may be specifically recognized by the immune system [25].

1.4 Glass – a Primary Packaging Material for Parenteral Dosage Forms

From the beginning of the 20th century, primary packaging (vials, ampoules, carpules, and syringes) for liquid parenteral dosage forms or lyophilisates mainly consists of borosilicate glass because of its high chemical resistance, formability, and tightness. This circumstance has hardly changed with regard to contemporary protein pharmaceuticals. Hence, today's packaging materials were virtually developed several decades ago for low molecular weight active pharmaceutical ingredients. For some time, polymeric materials have been gaining ground in the primary packaging sector because of their high break resistance, their excellent drainability, and solvent resistance [26]. However, these advantages are accompanied by a considerable permeability for oxygen and humidity [27].

Overall, vials, ampoules, and syringes are, for the most part, made out of glass tubes. Due to the manufacturing process of both the glass tube and the primary packaging container, the surface of the glass exhibits a different composition than the bulk material [28]. The surface of the glass resembles a fire-polished material, featuring roughness in the sub-nanometer scale. An influence of surface roughness on protein adsorption, which should be taken into consideration when in the nanometer scale, is therefore assumed to be negligible [29]. However, defects from the manufacturing process as well as corrosion reac-

tions may lead to a significant roughening of the surface [30,31]. Furthermore, it has to be considered, that in the pharmaceutical field, glass containers are commonly cleaned, rinsed, and then subjected to a heat sterilizing or depyrogenizing step at 180 - 350°C directly before filling. This treatment can have a significant impact on the nature of the outermost glass surface due to the removal of contaminants or the alteration of the chemical glass composition. Although glass basically features high resistance, its surface chemically reacts with the liquid formulation. Thereby, the pH value is of particular importance. In an acidic medium, an exchange of H^+ or H_3O^+ with the mobile cations Na^+ or other network modifiers, such as K^+, Mg^{2+}, or Ca^{2+}, occurs. As a consequence of the alkali or earth alkali release, the pH value in the solution increases. This can appreciably affect the stability of the respective biomolecule. On the other hand, hydroxyl ions of a basic solution are able to break up siloxane bonds, leading to a degradation of the glass matrix. Thereupon, $Si(OH)_4$ or larger moieties all the way up to glass particles, as well as all other glass components such as boron or aluminum, can get into the drug solution. Through the autoprotolysis of water, the contact of glass with a solution at pH 7 equals a combined mechanism comprising a simultaneous acidic and alkaline attack. For kinetic reasons, the acidic attack predominates in the beginning and leads to an increase in the OH^- concentration, whereupon an alkaline degradation can be triggered.

1.5 Surface Modifications of Glass Containers for Parenteral Pharmaceuticals

There are numerous ways to modify a glass surface, such as coatings or chemical modifications pursuing protective or different functional goals [32]. However, only a few are applied in the pharmaceutical industry. Among them, primarily the coating with silicon oil (siliconization) is of higher relevance [33]. This kind of hydrophobization is often applied to prefilled syringes as a lubricant for the rubber plunger in order to facilitate ease of movement within the barrel. Moreover, by adjusting the surface hydrophobicity, the drainability of the containers is improved and the glass surface stability with regard to the aforementioned corrosion effects is increased. However, siliconization, which is inevitably associated with increased hydrophobic interactions, may be associated with an increased protein adsorption on the container surface [34]. Furthermore, despite the application of a thermal baking process, silicon oil may partially detach from the surface and get into the solution [35]. It is discussed that the formed droplets induce protein aggregation [36]. A recently developed plasma polymerization step could improve the deposition of hydrophobic layers on glass [37]. Another surface modification is a quartz-like inner coating, which drastically reduces the amount of ions dissolved from the glass [38]. Several other surface coatings, among them coatings on the basis of polyethylene

glycol (PEG), are described in literature to reduce protein adsorption on a wide range of materials, e.g. glass, plastic, and metal [39,40]. PEG chains form an extremely polar and well-hydrated surface that is free of charges in aqueous media. Hence, van-der-Waals interactions and (possibly) electrostatic and hydrophobic interactions are minimized. Polysaccharides and phospholipids are discussed as alternatives [41].

1.6 Protein Adsorption at the Solid Liquid Interface

Proteins are intrinsically surface-active and tend to accumulate at interfaces. The individual steps involved in the adsorption process of a protein molecule at solid liquid interface, as well as its detachment, are schematically depicted in Figure 1. One can differentiate between:

① The transport of the protein molecule from the solution towards the surface by diffusion and convection, influenced by the electrostatic potential of the solid surface.

② The interaction of the protein with the surface. Protein attachment is driven by a decrease of the Gibbs energy in the system. Theoretically, the adsorption of a protein per se is a reversible step, whereas in practice, mostly irreversibility is observed. The reason behind this phenomenon is that proteins usually interact with the solid surface through a plethora of contact regions at the same time, depending on, for example,

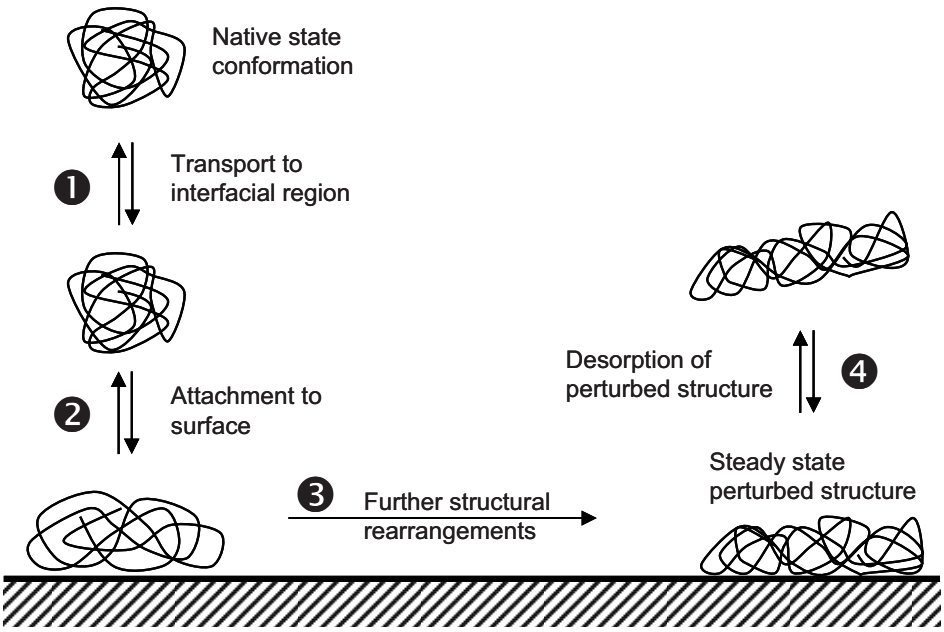

Figure 1: Schematic representation of the mechanism of protein adsorption on a solid surface (adapted from Norde and Haynes [42]).

their amino acid composition, their size, and their overall physical and chemical properties. Thereby, already changes in the proteins' secondary or tertiary structure can emerge.

③ The optimization of the protein - surface binding. Over time, the number of interaction points is further increased with the possibility of simultaneous molecular restructuring. Especially on hydrophobic surfaces, alterations of the proteins' secondary and tertiary structure often arise, caused by hydrophobic interactions.

④ Desorption and the diffusion back into the solution. This is less probable for unfolded proteins than for native ones due to a high number of interaction points with the surface and a more stable binding after protein unfolding.

The driving forces which facilitate protein adsorption were discussed by many authors [43-45]. They are basically equivalent to the forces that also account for the formation and the persistence of the proteins' three-dimensional structure. Regardless of the mechanism and the kinetics of the adsorption step, protein adsorption can only take place if the Gibbs energy G of the system decreases, provided that the temperature and pressure are constant [43]. The relation is depicted in Equation 1.

$$\Delta_{ads} G = \Delta_{ads} H - T \cdot \Delta_{ads} S < 0 \quad (1)$$

Therein, H, S, T, and Δ_{ads} equal the enthalpy, the entropy, the absolute temperature, and the change in each thermodynamic function through the adsorption process, respectively. For a basic understanding of the adsorption process, it is important to know how different kinds of interactions affect $\Delta_{ads}G$ [45]. In the following, the most important interaction types are outlined briefly.

(a) Interaction between electrical double layers (electrostatic interactions)

Both the protein molecules and the sorbent surface are electrostatically charged. In an aqueous medium, they are surrounded by counter ions which neutralize surface charges and by which means an electrical double layer is formed. Electrostatic interactions basically follow the Coulomb law. For systems that consist of multiply charged biomolecules and solid substrates, the resulting total electrostatic energy is equivalent to the sum of every single Coulomb pair [44].

(b) Changes in the hydration state (hydrophobic interactions)

Nonpolar groups are generally forced back from the aqueous system since favorable interactions such as hydrogen bonding towards water molecules are largely or completely missing. The overall hydrophobic surface area of proteins with water contact

decreases through the adsorption of such groups to solid surfaces. Furthermore, the entropy in the system increases because the ordered orientation of water molecules in the proximity of the hydrophobic areas is also forced back. Thus, dehydration resembles a driving force for adsorption. The principle of hydrophobic interactions is also reflected in the three-dimensional structure of proteins. While hydrophilic patches are directed outwards, i.e. towards the aqueous phase, hydrophobic residues largely shield themselves in the interior of the protein from hydrophilic interactions. As a final result, the adsorption tendency dramatically increases with increasing hydrophobicity of the protein surface [46] or with an increasing share of the hydrophobic protein interior in interaction with the solid surface after a possible protein unfolding step.

(c) *Dispersion interactions*

Dispersive interactions, also known as London forces, are attractive forces. They are based on the permanent electron density fluctuation of an atom species which, in turn, polarizes the electron system of another species. Dispersive forces cannot be saturated but are rather additive in nature. These forces are the dominating ones among the three van-der-Waals force components: London forces, Keesom forces (interactions between permanent electric moments), and Debye forces (interactions between permanent and induced dipoles) [44].

The actual binding energies of the above interaction components vary significantly. According to Auterhoff, ion-ion interactions amount to 5 - 80 kJ/mol, depending on the permittivity of the surrounding medium, whereas dipole - dipole interactions and H-bonds add up to 1 - 30 kJ/mol. In comparison, dispersive interactions and hydrophobic interactions amount to approx. 2 kJ per mol methylene group [47]. According to Norde, the contribution from the hydrophobic amino acid dehydration inside the proteins is approx. 9.2 kJ/mol/nm^2 with regard to hydrophobic interactions [43].

It was described above that hydrophobic protein structures are largely located inside the proteins, although hydrophobic amino acids on the surface area of proteins are not exceptional. Nevertheless, hydrophilic areas are mainly located at the protein's interface to the aqueous medium. This stabilizes the ordered α-helical and β-sheet structures. When the protein comes in contact with a hydrophobic surface, the hydrophobic interactions inside the proteins lose their influence on the three-dimensional structure, and hydrophobic patches turn out from the interior of the protein towards the sorbent surface [43]. The promotion of protein unfolding and aggregation through hydrophobic surfaces was shown for insulin [48] and β-lactoglobulin [49]. Also the wetting behavior of the surface, which is strongly associated with its contact angle and its hydrophobicity, directly affects the adsorbed amount of protein and the extent of structural alterations [50]. But ordered protein structures may also get notably lost when new hydrogen bonds are built

towards a polar interface. As a result, the conformational entropy of the protein increases and, as a consequence, adsorption increases as well [51]. In this regard, Arai and Norde observed appreciable adsorption of the structurally less stable α-lactalbumin on a hydrophilic surface of the same electrical charge [52]. If both electrostatic attraction and hydrophobic interactions were missing, adsorption was mainly mediated through the entropy gain of adsorption-induced unfolding.

1.7 Factors Influencing the Adsorption of Therapeutic Proteins on Solid Surfaces

Protein adsorption is a highly complex process. With regard to therapeutic protein pharmaceuticals, the extent of adsorption, as well as the structural stability and the irreversibility, predominantly depend on three key components, which are the protein, the solid surface, and the formulation composition. Norde classified proteins into "hard proteins" and "soft proteins" according to their adsorption behavior [53]. The former adsorb on hydrophilic surfaces only under electrostatic attraction. On the contrary, soft proteins are structurally more labile and adsorb on hydrophilic surfaces, even in the case of electrostatic repulsive conditions under structural reorientation. Besides stability factors, basic chemical properties of the proteins are of particular importance (see Table 2). The factors on the part of the sorbent surface chemistry, which influence the adsorption process, were for the most part already mentioned above in connection with the adsorption driving

Table 2: A selection of important factors influencing the adsorption behavior of proteins on solid surfaces.

Protein	Sorbent surface	Formulation
• Surface distribution of amino acids • Molecule size • 3D-structure in solution • (Net) charge and sign / location of protein IEP • Charge distribution on the protein surface • Protein stability	• Chemical composition • Hydrophilicity / hydrophobicity • Interfacial energy • Charge (sign) • Charge density • Electron donator and acceptor potentials • Sterical influences (surface roughness)	• pH value • Buffer type • Ionic strength • Polarity / dielectric constant • Excipients (like sugars, polyols and surfactants)

forces. Among others, these are charge, interfacial energy, and chemical composition. But also sterical properties in terms of surface roughness have shown to exert influence on the amount of protein bound [54].

Various studies demonstrate that the composition of the protein formulation, especially the pH value of the aqueous solution, is of supreme importance for the adsorption behavior. Provided a constant ionic strength, several protein adsorption studies denoted in literature exhibit pH-dependent adsorption maxima in the area of the isoelectric point of the respective protein [55-57]. This is typically explained by the increased protein stability, hence, by less space required per molecule at this pH, and by decreased electrostatic repulsion among the protein molecules, resulting in a denser packing on the surface. According to the common adsorption theory, the incorporation of charges in the defined contact area of a protein and the surface is energetically very unfavorable [43], and consequently, maximum adsorption would be most likely reached if free charges of the protein and the surface exactly compensated each other. Therefore, an adsorption maximum at a pH different from the protein isoelectric point (IEP) is suggested. Another approach which could explain such an observation is provided by Xu *et al.*, who argued that adsorption at conditions with an oppositely charged protein and surface increases due to an increased adsorption irreversibility [58]. The ionic strength of the protein formulation affects the aforementioned electrostatic interactions. For example, a high salt content can screen pronounced intermolecular repulsion forces and hence lead to an increased adsorbed amount of protein [59]. Besides, adsorption can be diminished by 15 - 90% through the addition of a surfactant, such as polysorbate 20, depending on the type of surfactant, its concentration, as well as the surface properties [60,61]. Sugars and polyols, which are often added to protein solutions, were described to show less or no adsorption-reducing effect [62]. However, it is feasible to reduce the adsorption of the API-protein by the addition of another indifferent protein such as human serum albumin (HSA) due to a competitive adsorption effect, as concluded by Lassen and Malmsten for an IgG and fibrinogen [63].

Proteins represent a very heterogeneous group of biomolecules, and generalizations concerning their adsorption behavior are difficult. For example, proteins were described to adsorb in larger quantities on hydrophobic surfaces than on hydrophilic ones [46,64]. However, the opposite result was observed as well [46,65]. Furthermore, the protein net charge is not always determining, and proteins can bind strongly on surfaces wearing the same net charge as the protein [66,67]. Finally, the adsorption behavior of an unknown protein on the surface of interest cannot be reliably predicted.

1.8 Characterization of Protein Adsorption on Solid Surfaces

A large number of investigations dealt with protein adsorption phenomena on solid surfaces. Special focus was on the total amount adsorbed, the adsorption kinetics, the reversibility of adsorption, morphology, and thickness of the protein layer, but also on the organization and orientation of molecules on the surface, as well as the extent of structural alterations. Typically, model proteins are utilized for adsorption studies. Their selection depends on different aspects, which, besides price and availability, involve intrinsic protein properties, such as IEP, shape, and stability. The selection of substrates conforms to the same principles. Model surfaces have a limited practical relevance but provide more fundamental and comparable results and allow the application of special methods. Oxidized silica (SiO_2) wafers are frequently utilized as hydrophilic model surface because they exhibit a very low surface roughness and because they are optically reflecting and very well characterized [58]. The following examples served as hydrophobic model surfaces: C_x-derivatized SiO_2 [68], polystyrene [69,70], or polytetrafluoroethylene (PTFE) [71]. In adsorption studies, the use of dispersive materials was also described, such as silicon dioxide micro and nanoparticles [72,73], polystyrene latices, or sols of silver iodide, hematite, silica, or polyoxymethylene [74]. To the contrary, adsorption studies on non-ideal solid surface were described by Duncan *et al.*, who studied protein adsorption on borosilicate glass vials and glass beads [10]. The adsorption of protein on glass surface has already been subject to investigations some decades ago [1]. Mizutani studied protein adsorption on porous glass as a model for glass containers [75,76]. Among the few further studies that dealt with protein binding on pharmaceutical surfaces, Qadry *et al.* investigated the adsorption behavior of proteins on plastic Resin CZ® vials [27]. Beyond that, several reviews give an overview of materials, methods, and proteins possible for adsorption investigations [77,78].

Measuring the protein concentration decrease in the "supernatant" liquid with the aid of coloring assays, high performance liquid chromatography (HPLC), or other quantification techniques is the simplest way to quantify adsorbed protein (solution depletion method). If a sufficiently large surface area is not available, protein is often radiolabeled with e.g. ^{125}I to increase sensitivity, which in addition represents a relatively precise reference quantification method. However, such a labeling step may have adverse effects on the structure and hence also on the adsorption behavior of proteins [79]. In quantitative adsorption measurements of salmon calcitonin on borosilicate glass, Duncan *et al.* found comparable results with a colorimetric protein assay, an HPLC procedure, and a radiolabeling method [80]. However, it turned out that these techniques differ in their applicable concentration range, their performance, and their versatility. Because of their high surface sensitivity, also spectroscopic ultrahigh vacuum techniques such as X-ray photoelectron spectroscopy (XPS) can be used to quantify adsorbed protein in a direct way [70].

Additional information on the structure and the organization [81], as well as on the surface coverage rate and the layer thickness of the protein adsorbate, can be gained [82]. However, it has to be mentioned that the protein layer and its structure is extensively altered by drying [83].

In order to receive meaningful quantification results of adsorbed protein, equilibrium conditions in the adsorption process are crucial. Many of the above-mentioned methods are suited for the investigation of protein adsorption kinetics. In the field of spectroscopic methods, ellipsometry has become important for the investigation of protein adsorption kinetics [84,85]. The new generation techniques are based on the perturbation of an evanescent electromagnetic field decaying from the adsorbent surface into the bulk solution [86]. Examples of modern methods applied are optical waveguide lightmode spectroscopy (OWLS) [87] or surface plasmon resonance (SPR) [88]. Taking HSA as an example, protein adsorption kinetics and hydration phenomena have recently been studied by using quartz crystal microbalance (QCM) systems, which, in addition, provide information on adsorption reversibility, distribution, and structural alterations [89]. Authors found adsorption equilibria on hydrophilic surface after approx. 1 h. On hydrophobic surfaces, time frames for reaching adsorption equilibria were between 1 h (ellipsometry) [90] and 6 h (QCM) [89]. However, a fundamental knowledge of protein adsorption kinetics offers by far more profound information on the whole adsorption process than only the point of adsorption equilibrium. This has been reviewed elsewhere [91,92].

Another important issue is the investigation of the structure of adsorbed proteins. It has been mentioned before that protein structures are often altered in the course of adsorption and are subject to the type and number of protein - surface interactions, particularly when the protein is in contact with hydrophobic surfaces. By means of ellipsometric measurements, for instance, one can infer structural alterations of the adsorbed protein from the changes of the refractive index or from the film density variations [93]. In this regard, primarily the surface properties are of particular importance. By using fluorescence spectroscopy, Maste *et al.* demonstrated the absence of structural changes for a bacterial serine protease adsorbed on hydrophilic silica, but not on hydrophobic Teflon® particles [94]. Moreover, alterations of the secondary structure of fibrinogen could be demonstrated with the aid of Fourier transform infrared (FT-IR) spectroscopy after adsorption on hydrophobic, but again not on hydrophilic surface [95]. However, a decrease in the β-sheet content of adsorbed IgG and the corresponding $F(ab')_2$ fragments was found on both hydrophobic and hydrophilic SiO_2 surfaces, using attenuated total reflection (ATR) FT-IR spectroscopy [96]. Partial unfolding of lysozyme adsorbed on SiO_2 could be proven by total internal reflection fluorescence spectroscopy (TIRF) [97]. The latest techniques utilize extrinsic fluorescence dyes which bind to hydrophobic protein structures. By using 8-anilino-1-naphtalene-sulfonate (ANS), Bilsten *et al.* revealed changes in the structure of human carbonic anhydrase II after adsorption to SiO_2 nano-

particles [98]. Another technique with regard to protein structure is the molecular imaging of adsorbed molecules under physiologic conditions by means of atomic force microscopy (AFM). Protein unfolding and denaturation was inferred from film thickness evaluations and a subsequent comparison with X-ray crystallographic data [99]. Moreover, the authors elucidated the adsorption process and observed a nucleation phenomenon of antibodies on the surface with a preferential binding of new molecules. Others visualized randomly distributed antibody aggregates with a diameter of 25 - 150 nm [100].

2 OBJECTIVES OF THE THESIS

The goal of this thesis was to investigate the adsorption of a monoclonal IgG1 antibody on primary packaging material, mostly on uncoated vials made of borosilicate glass, but also on siliconized glass vials and plastic vials. These represent the most common materials for packaging of parenteral drugs. The first main objective was to find suitable ways to quantify adsorbed protein and to investigate influencing parameters. An accurate and robust routine quantification method for adsorbed protein had to be developed and validated, which should be suitable as a routine examination technique (Chapter 2). In addition, it was our intention to reveal the main parameters which affect the final adsorbed quantity, regarding both the solid substrate (Chapter 3) and the protein formulation (Chapter 4). Firstly, parameters like surface hydrophilicity/hydrophobicity and the kind of surface pretreatment prior to the adsorption experiment needed to be analyzed. Secondly, the influence of solution pH, ionic strength, and the addition of selected excipients with an alleged effect, such as sugars, polyols, and surfactants had to be taken into consideration. Within the scope of adsorption isotherm investigations, the mathematical description of the adsorption processes by at least one theoretical adsorption model was pursued. The aim was to evaluate the adsorption affinity and the cooperative binding behavior, as well as to prove the previously established adsorption theories (Chapter 5). The confirmation of the achieved adsorption results, space-resolved information, as well as more profound information on the glass substrate chemistry were goals to be accomplished through additional sophisticated spectroscopic analytics (Chapter 6). A second main objective was the imaging of the protein adsorbates on the surface, as well as the elucidation of the structural integrity of adsorbed proteins, taking the pH value of the protein formulation into particular consideration (Chapter 7). Finally, this thesis should clarify the trilateral relation of protein, solid surface, and formulation composition, mostly concerning monoclonal IgG1, borosilicate glass, and typical formulation compositions, with respect to surface adsorption quantities and associated consequences regarding structure and stability.

3 REFERENCES

[1] Bull, H. B., Adsorption of bovine serum albumin on glass, *Biochim. Biophys. Acta* **19** (1956) 464-471.

[2] Petty, C., Cunningham, N. L., Insulin adsorption by glass infusion bottles, poly(vinyl chloride) infusion containers, and intravenous tubing, *Anesthesiology* **40** (1974) 406-410.

[3] McElnay, J. C., Elliott, D. S., D'Arcy, P. F., Binding of human insulin to burette administration sets, *Int. J. Pharm.* **36** (1987) 199-203.

[4] Zahid, N., Taylor, K. M. G., Gill, H., Maguire, F., Shulman, R., Adsorption of insulin onto infusion sets used in adult intensive care unit and neonatal care settings, *Diabetes Res. Clin. Pract.* **80** (2008) e11-e13.

[5] Mollmann, S. H., Jorgensen, L., Bukrinsky, J. T., Elofsson, U., Norde, W., Frokjaer, S., Interfacial adsorption of insulin conformational changes and reversibility of adsorption, *Eur. J. Pharm. Sci.* **27** (2006) 194-204.

[6] Ogino, J., Noguchi, K., Terato, K., Adsorption of secretin on glass surfaces, *Chem. Pharm. Bull.* **27** (1979) 3160-3163.

[7] Grohganz, H., Rischer, M., Brandl, M., Adsorption of the decapeptide Cetrorelix depends both on the composition of dissolution medium and the type of solid surface, *Eur. J. Pharm. Sci.* **21** (2004) 191-196.

[8] McLeod, A. G., Walker, I. R., Zheng, S., Hayward, C. P., Loss of factor VIII activity during storage in PVC containers due to adsorption, *Haemophilia* **6** (2000) 89-92.

[9] Tzannis, S. T., Hrushesky, W. J. M., Wood, P. A., Przybycien, T. M., Irreversible inactivation of interleukin 2 in a pump-based delivery environment, *Proc. Natl. Acad. Sci. U. S. A.* **93** (1996) 5460-5465.

[10] Duncan, M. R., Lee, J. M., Warchol, M. P., Influence of surfactants upon protein/peptide adsorption to glass and polypropylene, *International Journal of Pharmaceutics* **120** (1995) 179-188.

[11] Brash, J. L., Semak, Q. M., Dynamics of interactions between human albumin and polyethylene surface, *Journal of Colloid and Interface Science* **65** (1978) 495-504.

[12] McNally, E. J., Hastedt, J. E., Protein Formulation and Delivery, (Informa Healthcare USA, Inc., New York) Ed. 2, 2008.

[13] Timasheff, S. N., Solvent effects on protein stability, *Curr. Opin. Struct. Biol.* **2** (1991) 35-39.

[14] Arakawa, T., Timasheff, S. N., Stabilization of protein structure by sugars, *Biochemistry* **21** (1982) 6536-6544.

[15] Arakawa, T., Timasheff, S. N., Preferential interactions of proteins with salts in concentrated solutions, *Biochemistry* **21** (1982) 6545-6552.

[16] Chang, B. S., Kendrick, B. S., Carpenter, J. F., Surface-Induced Denaturation of Proteins during Freezing and Its Inhibition by Surfactants, *J. Pharm. Sci.* **85** (1996) 1325-1330.

[17] Chi, E. Y., Krishnan, S., Randolph, T. W., Carpenter, J. F., Physical Stability of Proteins in Aqueous Solution: Mechanism and Driving Forces in Nonnative Protein Aggregation, *Pharm. Res.* **20** (2003) 1325-1336.

[18] Vermeer, A. W. P., Norde, W., The influence of the binding of low molecular weight surfactants on the thermal stability and secondary structure of IgG, *Colloids and Surfaces, A: Physicochemical and Engineering Aspects* **161** (2000) 139-150.

[19] Tandon, S., Horowitz, P. M., Detergent-assisted refolding of guanidinium chloride-denatured rhodanese. The effects of the concentration and type of detergent, *J. Biol. Chem.* **262** (1987) 4486-4491.

[20] Randolph, T. W., Jones, L. S., Surfactant-Protein Interactions, *Rational Design of Stable Protein Formulations: Theory and Practice. [In: Pharm. Biotechnol., 2002; 13]*, Carpenter, J. F., Manning, M. C., Eds. (Kluwer Academic/Plenum Publishers, 2002), 203.

[21] Schellekens, H., Jiskoot, W., Erythropoietin-associated PRCA: still an unsolved mystery, *J. Immunotoxicol.* **3** (2006) 123-130.

[22] Sharma, B., Immunogenicity of therapeutic proteins. Part 1: Impact of product handling, *Biotechnol. Adv.* **25** (2007) 310-317.

[23] Schellekens, H., Immunogenicity of therapeutic proteins: clinical implications and future prospects, *Clin. Ther.* **24** (2002) 1720-1740.

[24] Sharma, B., Immunogenicity of therapeutic proteins. Part 2: Impact of container closures, *Biotechnol. Adv.* **25** (2007) 318-324.

[25] Hermeling, S., Crommelin, D. J. A., Schellekens, H., Jiskoot, W., Structure-Immunogenicity Relationships of Therapeutic Proteins, *Pharmaceutical Research* **21** (2004) 897-903.

[26] Daikyo Resin CZ Product information brochure, Daikyo Seiko, Ltd., 2009.

[27] Qadry, S. S., Roshdy, T. H., Char, H., Del Terzo, S., Tarantino, R., Moschera, J., Evaluation of CZ-resin vials for packaging protein-based parenteral formulations, *Int. J. Pharm.* **252** (2003) 207-212.

[28] Pickles, C., Manufacturing Problems, *Pharmaceutical Technology Europe* **11** (2008) 20-23.

[29] Song, W., Chen, H., Protein adsorption on materials surfaces with nano-topography, *Chin. Sci. Bull.* **52** (2007) 3169-3173.

[30] Bange, K., Anderson, O., Rauch, F., Lehuede, P., Radlein, E., Tadokoro, N., Mazzoldi, P., Rigato, V., Matsumoto, K., Farnworth, M., Multi-method characterization of soda-lime glass corrosion. Part 1. Analysis techniques and corrosion in liquid water, *Glass Sci. Technol. (Frankfurt/Main, Ger.)* **74** (2001) 127-141.

[31] Schwarzenbach, M. S., Reimann, P., Thommen, V., Hegner, M., Mumenthaler, M., Schwob, J., Guentherodt, H. J., Topological structure and chemical composition of inner surfaces of borosilicate vials, *PDA J. Pharm. Sci. Technol.* **58** (2004) 169-175.

[32] Min'ko, N. I., Mikhal'chuk, I. N., Lipko, M. Y., Modification of the surface of sheet glass (A review), *Glass Ceram.* **57** (2000) 109-113.

[33] Mundry, T., Einbrennsilikonisierung bei pharmazeutischen Glaspackmitteln - Analytische Studien eines Produktionsprozesses, Thesis, 1999.

[34] Norde, W., Lyklema, J., Why proteins prefer interfaces, *J. Biomater. Sci. Polym. Ed.* **2** (1991) 183-202.

[35] Sharma, D. K., Oma, P., Krishnan, S., Silicone microdroplets in protein formulations. Detection and enumeration, *Pharm. Technol.* **33** (2009) 74-76 / 77-78.

[36] Jones, L. S., Kaufmann, A., Middaugh, C. R., Silicone oil induced aggregation of proteins, *Journal of Pharmaceutical Sciences* **94** (2005) 918-927.

[37] Bicker, Matthias, Bauch, Hartmut, Hahn, Andreas, Bauer, Stefan, Lohmeyer, Manfred, and Hormes, Robert., Container having improved ease of discharge product residue, and method for the production thereof, PCT Int. Appl., WO 2007-EP11493 / 2008071458 (2008)

[38] Schwarzenbach, M. S., Reimann, P., Thommen, V., Hegner, M., Mumenthaler, M., Schwob, J., Guntherodt, H. J., Interferon alpha -2a interactions on glass vial surfaces measured by atomic force microscopy, *PDA J. Pharm. Sci. Technol.* **56** (2002) 78-89.

[39] Gombotz, W. R., Wang, G., Horbett, T. A., Hoffman, A. S., Protein adsorption to and elution from polyether surfaces, *Poly(Ethylene Glycol) Chemistry - Biotechnical and Biomedical Applications*, Harris, J. M., Ed. (Plenum Press, New York, USA, 1992), Chapter 16, 247-261.

[40] Ito, Y., Hasuda, H., Sakuragi, M., Tsuzuki, S., Surface modification of plastic, glass and titanium by photoimmobilization of polyethylene glycol for antibiofouling, *Acta Biomater.* **3** (2007) 1024-1032.

[41] Holmberg, K., Control of protein adsorption at surfaces, *Encyclopedia of Surface and Colloid Science*, Arthur T. Hubbard, Ed. (Marcel Dekker, Inc., USA, 2002), 1242-1253.

[42] Norde, W., Haynes, C. A., Reversibility and the mechanism of protein adsorption, *ACS Symposium Series* **602** (1995) 26-40.

[43] Norde, W., Proteins at Solid Surfaces, *Physical Chemistry of Biological Interfaces*, Baszkin, A., Norde, W., Eds. (Marcel Dekker, Inc., Basel, 2000), Chapter 4, 115-135.

[44] Basiuk, V. A., Adsorption of biomolecules at silica, *Encyclopedia of Surface and Colloid Science*, Arthur T. Hubbard, Ed. (Marcel Dekker, Inc., USA, 2002), 277-293.

[45] Vermeer, A. W. P., Conformation of adsorbed proteins, *Encyclopedia of Surface and Colloid Science*, Arthur T. Hubbard, Ed. (Marcel Dekker, Inc., USA, 2002), 1193-1212.

[46] Malmsten, M., Ellipsometry studies of the effects of surface hydrophobicity on protein adsorption, *Colloids and Surfaces, B: Biointerfaces* **3** (1995) 297-308.

[47] Auterhoff, H., Lehrbuch der Pharmazeutischen Chemie, Knabe, Joachim and Hoeltje, Hans-Dieter, Eds., (Wiss. Verl.-Ges., Stuttgart) Ed. 13, 1994.

[48] Sluzky, V., Klibanov, A. M., Langer, R., Mechanism of insulin aggregation and stabilization in agitated aqueous solutions, *Biotechnol Bioeng* **40** (1992) 895-903.

[49] Nylander, T., Protein adsorption in relation to solution association and aggregation, *Surfactant Science Series* **110** (2003) 259-294.

[50] Sethuraman, A., Vedantham, G., Imoto, T., Przybycien, T., Belfort, G., Protein unfolding at interfaces: Slow dynamics of a-helix to b-sheet transition, *Proteins: Structure, Function, and Bioinformatics* **56** (2004) 669-678.

[51] Czeslik, C., Factors ruling protein adsorption, *Zeitschrift fuer Physikalische Chemie (Muenchen, Germany)* **218** (2004) 771-801.

[52] Arai, T., Norde, W., The behavior of some model proteins at solid-liquid interfaces. 1. Adsorption from single protein solutions, *Colloids and Surfaces* **51** (1990) 1-15.

[53] Norde, W., The behavior of proteins at interfaces, with special attention to the role of the structure stability of the protein molecule, *Clinical Materials* **11** (1992) 85-91.

[54] Deligianni, D. D., Katsala, N., Ladas, S., Sotiropoulou, D., Amedee, J., Missirlis, Y. F., Effect of surface roughness of the titanium alloy Ti-6Al-4V on human bone marrow cell response and on protein adsorption, *Biomaterials* **22** (2001) 1241-1251.

[55] Su, T. J., Lu, J. R., Thomas, R. K., Cui, Z. F., Penfold, J., The Conformational Structure of Bovine Serum Albumin Layers Adsorbed at the Silica-Water Interface, *Journal of Physical Chemistry B* **102** (1998) 8100-8108.

[56] Ortega-Vinuesa, J. L., Hidalgo-Alvarez, R., Study of the adsorption of F(ab')2 onto polystyrene latex beads, *Colloids and Surfaces, B: Biointerfaces* **1** (1993) 365-372.

[57] Serra, J., Puig, J., Martin, A., Galisteo, F., Galvez, M., Hidalgo-Alvarez, R., On the adsorption of IgG onto polystyrene particles: electrophoretic mobility and critical coagulation concentration, *Colloid Polym. Sci.* **270** (1992) 574-583.

[58] Xu, H., Lu, J. R., Williams, D. E., Effect of surface packing density of interfacially adsorbed monoclonal antibody on the binding of hormonal antigen human chorionic gonadotrophin, *Journal of Physical Chemistry B* **110** (2006) 1907-1914.

[59] Luey, J. K., McGuire, J., Sproull, R. D., The effect of pH and sodium chloride concentration on adsorption of b-lactoglobulin at hydrophilic and hydrophobic silicon surfaces, *Journal of Colloid and Interface Science* **143** (1991) 489-500.

[60] Zhang, M., Ferrari, M., Reduction of albumin adsorption onto silicon surfaces by Tween 20, *Biotechnology and Bioengineering* **56** (1997) 618-625.

[61] Hawe, A., Studies on Stable Formulations for a Hydrophobic Cytokine, Thesis, 2006.

[62] Hawe, A., Friess, W., Formulation Development for Hydrophobic Therapeutic Proteins, *Pharmaceutical Development and Technology* **12** (2007) 223-237.

[63] Lassen, B., Malmsten, M., Structure of protein layers during competitive adsorption, *Journal of Colloid and Interface Science* **180** (1996) 339-349.

[64] Elwing, H., Welin, S., Askendal, A., Nilsson, U., Lundstroem, I., A wettability gradient method for studies of macromolecular interactions at the liquid/solid interface, *J. Colloid Interface Sci.* **119** (1987) 203-210.

[65] Malmsten, M., Lassen, B., Van Alstine, J. M., Nilsson, U. R., Adsorption of complement proteins C3 and C1q, *J. Colloid Interface Sci.* **178** (1996) 123-134.

[66] Burns, N. L., Holmberg, K., Brink, C., Influence of surface charge on protein adsorption at an amphoteric surface: effects of varying acid to base ratio, *J. Colloid Interface Sci.* **178** (1996) 116-122.

[67] Bos, M. A., Shervani, Z., Anusiem, A. C. I., Giesbers, M., Norde, W., Kleijn, J. M., Influence of the electric potential of the interface on the adsorption of proteins, *Colloids Surf. B* **3** (1994) 91-100.

[68] Marsh, R. J., Jones, R. A. L., Sferrazza, M., Adsorption and displacement of a globular protein on hydrophilic and hydrophobic surfaces, *Colloids and Surfaces, B: Biointerfaces* **23** (2002) 31-42.

[69] Browne, M. M., Lubarsky, G. V., Davidson, M. R., Bradley, R. H., Protein adsorption onto polystyrene surfaces studied by XPS and AFM, *Surface Science* **553** (2004) 155-167.

[70] Lhoest, J. B., Detrait, E., Van Den Bosch De Aguilar, Bertrand, P., Fibronectin adsorption, conformation, and orientation on polystyrene substrates studied by radiolabeling, XPS, and ToF SIMS, *Journal of Biomedical Materials Research* **41** (1998) 95-103.

[71] Wagner, M. S., McArthur, S. L., Shen, M., Horbett, T. A., Castner, D. G., Limits of detection for time of flight secondary ion mass spectrometry (ToF-SIMS) and X-ray photoelectron spectroscopy (XPS): detection of low amounts of adsorbed protein, *Journal of Biomaterials Science, Polymer Edition* **13** (2002) 407-428.

[72] Kondo, A., Mihara, J., Comparison of adsorption and conformation of hemoglobin and myoglobin on various inorganic ultrafine particles, *Journal of Colloid and Interface Science* **177** (1996) 214-221.

[73] Docoslis, A., Wu, W., Giese, R. F., van Oss, C. J., Measurements of the kinetic constants of protein adsorption onto silica particles, *Colloids and Surfaces, B: Biointerfaces* **13** (1999) 83-104.

[74] Norde, W., MacRitchie, F., Nowicka, G., Lyklema, J., Protein adsorption at solid-liquid interfaces: reversibility and conformation aspects, *Journal of Colloid and Interface Science* **112** (1986) 447-456.

[75] Mizutani, T., Decreased activity of proteins adsorbed onto glass surfaces with porous glass as a reference, *Journal of Pharmaceutical Sciences* **69** (1980) 279-282.

[76] Mizutani, T., Adsorption of proteins on silicone-coated glass surfaces, *Journal of Colloid and Interface Science* **82** (1981) 162-166.

[77] Kingshott, P., Hoecker, H., Methods of assessing protein adsorption, *Encyclopedia of Surface and Colloid Science*, Arthur T. Hubbard, Ed. (Marcel Dekker, Inc., USA, 2002), 3342-3369.

[78] Nakanishi, K., Sakiyama, T., Imamura, K., On the adsorption of proteins on solid surfaces, a common but very complicated phenomenon, *Journal of Bioscience and Bioengineering* **91** (2001) 233-244.

[79] Lensen, H. G. W., Breemhaar, W., Smolders, C. A., Feijen, J., Competitive adsorption of plasma proteins at solid-liquid interfaces, *Journal of Chromatography* **376** (1986) 191-198.

[80] Duncan, M., Gilbert, M., Lee, J., Warchol, M., Development and comparison of experimental assays to study protein/peptide adsorption onto surfaces, *Journal of Colloid and Interface Science* **165** (1994) 341-345.

[81] Paynter, R. W., Ratner, B. D., Horbett, T. A., Thomas, H. R., XPS studies on the organization of adsorbed protein films on fluoropolymers, *Journal of Colloid and Interface Science* **101** (1984) 233-245.

[82] Ratner, B. D., Horbett, T. A., Shuttleworth, D., Thomas, H. R., Analysis of the organization of protein films on solid surfaces by ESCA, *Journal of Colloid and Interface Science* **83** (1981) 630-642.

[83] Ortega-Vinuesa, J. L., Tengvall, P., Lundstrom, I., Aggregation of HSA, IgG, and fibrinogen on methylated silicon surfaces, *Journal of Colloid and Interface Science* **207** (1998) 228-239.

[84] Alaeddine, S., Nygren, H., Logarithmic growth of protein films, *ACS Symposium Series* **602** (1995) 41-51.

[85] Wahlgren, M., Arnebrant, T., Lundstroem, I., The adsorption of lysozyme to hydrophilic silicon oxide surfaces: comparison between experimental data and models for adsorption kinetics, *J. Colloid Interface Sci.* **175** (1995) 506-514.

[86] Ramsden, J. J., Protein adsorption kinetics, *Surfactant Sci. Ser.* **110** (2003) 199-220.

[87] Hook, F., Voros, J., Rodahl, M., Kurrat, R., Boni, P., Ramsden, J. J., Textor, M., Spencer, N. D., Tengvall, P., Gold, J., Kasemo, B., A comparative study of protein adsorption on titanium oxide surfaces using in situ ellipsometry, optical waveguide lightmode spectroscopy, and quartz crystal microbalance/dissipation, *Colloids Surf. B* **24** (2002) 155-170.

[88] Snopok, B. A., Kostyukevich, E. V., Kinetic studies of protein-surface interactions: A two-stage model of surface-induced protein transitions in adsorbed biofilms, *Analytical Biochemistry* **348** (2006) 222-231.

[89] Lubarsky, G. V., Davidson, M. R., Bradley, R. H., Hydration-dehydration of adsorbed protein films studied by AFM and QCM-D, *Biosensors & Bioelectronics* **22** (2007) 1275-1281.

[90] Malmsten, M., Lassen, B., Ellipsometry studies of protein adsorption at hydrophobic surfaces, *ACS Symposium Series* **602** (1995) 228-238.

[91] Al-Malah, K., Abdellatif Hasan Mousa, H., Protein adsorption kinetics, *Surfactant Science Series* **107** (2002) 847-870.

[92] Ramsden, J. J., Adsorption kinetics of proteins, *Encyclopedia of Surface and Colloid Science*, Arthur T. Hubbard, Ed. (Marcel Dekker, Inc., USA, 2002) 240-276.

[93] Voeroes, J., The density and refractive index of adsorbing protein layers, *Biophysical Journal* **87** (2004) 553-561.

[94] Maste, M. C. L., Norde, W., Visser, A. J. W. G., Adsorption-induced conformational changes in the serine proteinase savinase: a tryptophan fluorescence and circular dichroism study, *Journal of Colloid and Interface Science* **196** (1997) 224-230.

[95] Steiner, G., Tunc, S., Maitz, M., Salzer, R., Conformational Changes during Protein Adsorption. FT-IR Spectroscopic Imaging of Adsorbed Fibrinogen Layers, *Analytical Chemistry* **79** (2007) 1311-1316.

[96] Buijs, J., Norde, W., Lichtenbelt, J. W. T., Changes in the Secondary Structure of Adsorbed IgG and F(ab')2 Studied by FTIR Spectroscopy, *Langmuir* **12** (1996) 1605-1613.

[97] Czeslik, C., Jackler, G., Royer, C., Driving forces for the adsorption of enzymes at the water/silica interface studied by total internal reflection fluorescence spectroscopy and optical reflectometry, *Spectroscopy (Amsterdam, Netherlands)* **16** (2002) 139-145.

[98] Billsten, P., Freskgard, P. O., Carlsson, U., Jonsson, B. H., Elwing, H., Adsorption to silica nanoparticles of human carbonic anhydrase II and truncated forms induce a molten-globule-like structure, *FEBS Letters* **402** (1997) 67-72.

[99] Cullen, D. C., Lowe, C. R., AFM studies of protein adsorption. 1. Time-resolved protein adsorption to highly oriented pyrolytic graphite, *Journal of Colloid and Interface Science* **166** (1994) 102-108.

[100] Caruso, F., Rodda, E., Furlong, D. N., Orientational aspects of antibody immobilization and immunological activity on quartz crystal microbalance electrodes, *Journal of Colloid and Interface Science* **178** (1996) 104-115.

Chapter 2

Development of Sensitive Methods for the Quantification of Protein Adsorption to Pharmaceutical Containers

Abstract

The fundamental adsorption behavior of a monoclonal IgG1 antibody (IgG1) from a common formulation was studied on the internal surface of borosilicate glass packaging vials. For this purpose, a standardized adsorption procedure was created. In addition, sensitive analytical methods tailored to the particular needs of an accurate quantification of proteins adsorbed in containers were developed. The first one was based on thorough desorption through the use of sodium dodecyl sulfate (SDS), followed by quantification via size exclusion high performance liquid chromatography (SE-HPLC) combined with fluorescence detection. The second approach pursued the exhaustive hydrolyzation of adsorbed proteins and the measurement of total organic carbon (TOC) content. The suitability of both methods for their intended purpose was verified by validating according to the ICH guideline. Both procedures proved to be superior to commercial protein quantification assays concerning their applicability for the problem. This was exemplified by means of relevant characteristics like linearity, limit of quantification, and limit of detection. Finally, the extent of IgG1 adsorption could be accurately determined. The adsorbed IgG1 quantities in borosilicate glass vials measured with TOC after protein hydrolyzation correlated with those obtained by using surfactant-desorption combined with SE-HPLC quantification. The equivalence of both procedures and thus the plausibility of the findings could be verified. Moreover, the measured values were in line with those described in literature for IgG adsorption on hydrophilic silica.

1 INTRODUCTION

The phenomenon of protein adsorption is very complex. Besides time-dependent changes in the protein orientation and conformation upon adsorption, predominantly the quantitative description of the adsorbed amount and possibly the rate of adsorption are of particular interest. Since an individual method is not capable of giving an overall picture of the adsorption process, a multi-technique approach is required [1]. Of all the well-established methods, only very few are applicable for investigating the problem of protein adsorption on pharmaceutical container surface. The difficulty is to follow protein adsorption on a rather small and non-ideal surface in terms of geometry, surface properties, and chemical composition. In this chapter, the focus will be set on the challenging quantification problem of proteins on container surfaces.

In literature, many techniques are described that are suitable for a sensitive quantification of adsorbed protein. The most common are ellipsometry [2,3], X-ray photoelectron spectroscopy (XPS) [4], detection of radiolabeled proteins [5-7], and the solution depletion approach [8,9]. Ellipsometry as a non-destructive method is the most common technique for monitoring *in situ* protein adsorption [10]. Furthermore, common applications of this method are the determination of layer thickness [11] and the quantification of the adsorbed protein [12,13]. From our experience, the main problem with ellipsometry arises from the curved surface geometry of the vial wall and the non-exact planarity of the vial bottom, as mentioned above (data not shown). XPS is a well established and very surface-specific technique which allows sensitive measuring of adsorbed protein films [14]. However, the method is inevitably limited by the necessary ultrahigh vacuum. It has been pointed out that vacuum leads to alterations in the protein film shape and in layer thickness, in contrast to the situation in aqueous environment [15,16]. Because XPS requires a rather high level of effort in sample preparation and "technical devices", it was not selected as our routine method for protein quantification. For further applications concerning XPS measurements, see Chapter 6. A highly accurate method, especially for investigating a small surface area, is radioactive labeling of proteins, most commonly with ^{125}I, ^{131}I, or ^{14}C. It is an accepted and reliable way to determine the absolute amount of adsorbed protein [1] and is therefore often used as a reference method. However, the labeling step itself may have adverse effects on the protein structure and therefore may influence the overall adsorption behavior of proteins [8,17,18]. In addition, the handling of radioactive material requires special expenditure on the involved equipment. This especially applies to γ-emitting nuclides.

Without doubt, the most straightforward approach to determine the portion of adsorbed protein is measuring the depletion of proteins in solution. The concentration is measured

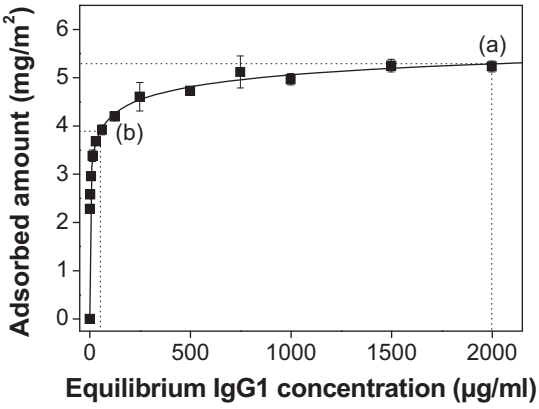

Figure 1: Adsorption isotherm of IgG1 on borosilicate glass vial surface determined at high affinity conditions leading to high IgG1 surface concentrations (n = 3).

before and after incubation, and the adsorbed quantity is obtained from the mass balance. Thus, one would most likely favor the latter method for the sole purpose of quantification. But in this regard, a mandatory requirement is a sufficiently large surface area. In our case, this implies the use of a rather small container size providing the highest surface-to-volume ratio. However, the solution depletion method would not lead to success if protein adsorption was analyzed at surface saturation conditions. The dilemma will be illustrated by an example. The magnitude of protein adsorption depends on the bulk concentration, as will be discussed later in further detail (Chapter 5). Figure 1 shows a high affinity isotherm of a monoclonal IgG1 antibody (IgG1) in 2R borosilicate glass vials. The adsorption conditions were chosen so that they led to very high adsorbed amounts. At IgG1 solution concentrations of 2 mg/ml, surface saturation was virtually reached. A thereby associated surface concentration of 5.2 mg/m^2 equals a protein quantity of 7.0 µg, by which the protein concentration in the vial is reduced. With a filling volume of 3.5 ml, the overall quantum of 7.0 mg is reduced by 0.1%, which is inside the range of typical analytical errors and would therefore not be resolved (a). If, for example, a concentration reduction by 10% should be measured, an equilibrium concentration of 52 µg/ml is required. But, as is indicated by Figure 1, at this point, saturation has not been reached and the isotherm is still in its initial phase (b). Concerning the commonly used solution depletion method, the error in adsorbed protein quantity strongly depends on the protein concentration and increases especially at high concentration levels, which are, however, common for antibody formulations. For this reason, proteins are preferably quantified in a direct manner, while protein modifications and labeling are avoided.

The practicability of quantification directly on surfaces is delicate, as already mentioned. By contrast, the method of choice is intended to be universally applicable on the diversity of packaging containers and proteins. One approach is based on a thorough removal of the molecules from the internal surface, followed by a sensitive quantification of the for-

merly adsorbed molecules. For desorption of proteins from solid surfaces, charged surfactants are well suited. The strongest eluting force for proteins on glass was ascribed to sodium dodecyl sulfate (SDS) [19]. Size exclusion high performance liquid chromatography (SE-HPLC) is a routine method in protein analytics and combines a number of advantages like low detection limits, high reproducibility, automatized processing, and high flexibility in terms of the post-chromatographic detection system. Therefore and for reasons of practicability, the combination of SDS protein desorption and SE-HPLC quantification was chosen as a possible procedure for adsorption quantification of IgG1 on container surfaces. However, the validity of this technique had to be verified by alternative methods. An acid-catalyzed total hydrolyzation step of adsorbed proteins was therefore applied, which simultaneously accomplished desorption of the protein from the solid surface. It was directly followed by highly sensitive total organic carbon (TOC) determination.

Newly implemented analytical approaches have to be validated and it needs to be shown that the procedure is suitable for its intended purpose [20]. According to the ICH guidance document "Validation of Analytical Procedures Q2(R1)" [20], various investigations need to be made pertaining to the particular directive. These are verification of linearity, determination of accuracy and precision/repeatability, determination of detection and quantification limits, verification of the robustness of the analytical method, as well as system suitability testing, all within the specified range, which in our case is defined from 0 to +20% above the maximum value expected. In the following, at first the validity of both the SE-HPLC and TOC quantification methods is verified by comparing these methods with other common protein quantification assays. Afterwards, the focus is on the development of an appropriate incubation, rinsing, and desorption method for the purpose of a standardized investigation of protein adsorption to packaging containers.

2 MATERIALS AND METHODS

2.1 Materials

2.1.1 Protein Formulation

For adsorption experiments, a monoclonal IgG1 antibody (MW ≈ 152 kDa) in 10 mM phosphate buffer and 145 mM NaCl (pH 7.2) was used, kindly provided by Merck Serono (Darmstadt, Germany). A second antibody was used within the scope of comparative studies. Human IgG from pooled serum (h-IgG) was purchased as a lyophilized powder from Sigma-Aldrich (Steinheim, Germany) and dissolved in the analogous buffer solution. The solutions were filtered through a hydrophilic 0.2 µm polyethersulfone membrane filter (Pall GmbH, Dreieich, Germany) before use.

2.1.2 Glass Vials and Closure Systems

Fiolax® 2R borosilicate glass vials with an overflow capacity of approx. 4 ml were used, kindly provided by SCHOTT AG (Mainz, Germany). The glass material is composed of approx. 75% SiO_2, 8 - 12% B_2O_3, and up to 5% alkaline earths and alumina (Al_2O_3) [21]. The glass quality is further described as glass type 1 Ph. Eur. Glasses were washed in a vial washing machine FAW 500 from Bausch & Stroebel GmbH & Co. KG (Ilshofen, Germany) with ultrapure water and heat sterilized at 250°C for 1 h before use. After filling, the glass vials were closed with FluroTec® stoppers and finally sealed with Flip-Off® seals, both kindly provided by West Pharmaceutical Services GmbH & Co. KG (Eschweiler, Germany)

2.1.3 Chemicals / Excipients

The eluent for SE-HPLC analysis was a PBS buffer consisting of 10 mM NaH_2PO_4/ Na_2HPO_4 and 145 mM NaCl (Merck Chemicals, Darmstadt, Germany). The pH value was adjusted to 7.2 by using 1 M NaOH or HCl (Sigma-Aldrich, Munich, Germany). Sodium dodecyl sulfate (Sigma-Aldrich, Munich, Germany) was added in different amounts to the buffer. The buffers were finally filtered through a hydrophilic 0.2 µm polypropylene membrane filter (Pall GmbH, Dreieich, Germany). Water for all buffers and applications was ultrapure water (0.055 µS/cm) from a Purelab Plus UV/UF system (ELGA LabWater, Celle, Germany) and was filtrated through a 0.22 µm membrane filter before use. The typical total organic carbon (TOC) level was 14.8 ± 1.4 ppb. Protein hydrolyzation was

performed with 6 M HCl, prepared by dilution of a concentrated (32%) HCl solution (Merck Chemicals, Darmstadt, Germany). All chemicals used were of analytical grade.

2.1.4 Test Tubes

Typical protein handling like dilution and sample preparation was done in 2 ml polypropylene Safe-Lock® microcentrifuge tubes (Eppendorf AG, Hamburg, Germany). Additional containers were 15 ml and 50 ml polypropylene tubes (GreinerBio-One GmbH, Frickenhausen, Germany). TOC measurements were conducted by using 40 ml device-specific, low TOC certified vials (< 10 ppb C) from GE Analytical Instruments (Boulder, CO, USA), equipped with a septum cap.

2.2 Methods

2.2.1 SE-HPLC

SE-HPLC was performed on an Agilent 1100 (Agilent Technologies GmbH, Boeblingen, Germany) equipped with a Tosoh TSKgel G3000SWXL and a TSKgel SWXL guardcolumn (Tosoh Bioscience GmbH, Stuttgart, Germany). The eluent was a PBS buffer (described above) containing SDS. Aside from the integrated variable wavelength UV detector, a Thermo Spectra 3000 fluorescence detector was included via an Agilent 35000E A/D-signal converter. All chromatograms were integrated manually by using the Agilent ChemStation software Rev. B 02.01 (Agilent Technologies GmbH, Boeblingen, Germany).

2.2.2 UV Spectroscopy

UV absorption measurements were conducted on a Thermo Spectronic UV 1 spectrophotometer from Thermo Electron Corporation (Dreieich, Germany). For protein content determination, UV absorption was determined at $\lambda = 280$ nm by applying an extinction coefficient of 1.40 cm^2/mg.

2.2.3 Fluorescence Spectroscopy

Fluorescence characteristics of the protein-containing samples were investigated by using a Varian Cary Eclipse fluorescence spectrophotometer (Varian Deutschland GmbH, Darmstadt, Germany). The IgG concentration was fixed at 0.05 mg/ml corresponding to an absorbance of 0.07 at 280 nm. For the determination of the maximum fluorescence

intensity, emission spectra were recorded from 310 - 410 nm and the excitation wavelength was increased iteratively in steps of 0.5 nm from 260 - 308 nm. Samples were measured in standard 10 x 10 mm quartz fluorescence cuvettes at 25°C. Excitation and emission bandwidth were both set to 5 nm. The typical scan rate was 30 nm/min (data interval 0.5 nm, averaging time 1.0 s). The PMT-voltage was set to 600 V.

2.2.4 Micro BCA™ Protein Assay Kit

The micro BCA (mBCA) assay used was purchased from Pierce Biotechnology Inc. (Rockford, IL, USA). It is based on the peptide bond mediated stoichiometric reduction of Cu^{2+} to Cu^{+}, followed by a coloring reaction with bicinchoninic acid. The absorbance was measured in 10 x 10 mm quartz cuvettes at 562 nm. According to the specification, the assay has a linear working range from 0.5 - 20 µg/ml protein.

2.2.5 Calbiochem Non Interfering Protein Assay

The copper-based Calbiochem Non Interfering Protein Assay (NI-assay) was purchased from Merck Chemicals (Darmstadt, Germany). In contrast to the mBCA assay, the excess of Cu^{2+} over the amount of peptide bonds is quantified via a color-producing reagent not further specified. Absorbance was measured in 10 x 10 mm quartz cuvettes at 480 nm. The assay is specified to a linear response from 0.5 - 50 µg protein and was done without a precipitation step, since the solutions did not contain any interfering agents.

2.2.6 Analysis of Total Organic Carbon

TOC analysis was applied on a Sievers 900 laboratory TOC analyzer (GE Analytical Instruments, Boulder, CO, USA). The measuring principle of this device is the oxidation of carbon species to CO_2 by a persulfate reagent combined with UV radiation. CO_2 is measured by "membrane conductometric detection". The device is split in two circuits, whereas inorganic carbon (IC), e.g. carbonate, is determined after acidification with phosphorous acid. The TOC content is calculated by Equation 1, where TC equals the total carbon content of the solution.

$$TOC = TC - IC \tag{1}$$

Before each analysis, the device was thoroughly rinsed with the sample liquid. Four independent measurements per sample were conducted. The first one was rejected and the remaining three were averaged.

2.2.7 Surface Tension Measurements

Surface tension measurements for the determination of critical micelle concentrations (CMC) were performed on a K100 MK2 tensiometer (Kruess GmbH, Hamburg, Germany). The device was equipped with a microprocessor-controlled dispenser, Metrohm® 765 Dosimat (Deutsche Metrohm GmbH & Co. KG, Filderstadt, Germany), and a temperature-controlled water bath Julabo F12 (Julabo Labortechnik GmbH, Seelbach, Germany). The Wilhelmy plate method was applied at 25°C. The Kruess LabDesk 3.1 software was used for control and curve analysis.

3 RESULTS AND DISCUSSION

3.1 Development and Optimization of a Standardized Quantification Method

Before any adsorption experiment could be accomplished, a highly sensitive, accurate, and robust quantification assay had to be developed. The need for a preferably low quantification limit arose from the quantum of adsorbed IgG attained on glass surface. Typical values for IgG adsorption on hydrophilic silica have been found in the area from 1.1 mg/m^2 [22], 2.3 mg/m^2 [23], 4.0 mg/m^2 [24] to 5.5 mg/m^2 [25], depending on time, concentration, pH, and ionic strength. From the dimensions of 2R vials and by implying a filling volume of 3.5 ml, the wetted surface area was calculated as 13.4 cm^2. Thus, effective IgG1 concentrations in the range of approx. 0.5 - 2.5 micrograms per milliliter after a thorough desorption were expected.

3.1.1 Determination of Fluorescence Properties of IgG1 and h-IgG

In general, intrinsic fluorescence of proteins can be used for their sensitive quantification [26]. For an automated and highly reproducible quantification, SE-HPLC with fluorescence detection was preferred. Concerning HPLC, fluorescence detectors are amongst the most sensitive LC detectors [27]. One limitation may be its restricted linear response over a concentration range of two orders of magnitude only [27]. However, in our case, fluorescence measurements for LC detection are limited by the lower concentration threshold. For obtaining the highest fluorescence response and the best sensitivity in protein quantification later on, the spectral properties including the quantum efficiency of both IgGs had to be evaluated thoroughly. Especially the effect of SDS on the fluorescence behavior

of the proteins had to be identified, as SDS was an essential part of the following methods. Both IgG1 and h-IgG were analyzed in two different buffer solutions, PBS pH 7.2 and PBS pH 7.2 containing 0.05% SDS. Therefore, emission spectra were recorded from 310 - 410 nm and the excitation wavelength was successively increased from 260 - 308 nm. Thus, the correlating wavelength pairs λ_{ex} / λ_{em} of maximum quantum yield could be determined. The 3D-fluorescence spectra are shown in Figure 2.

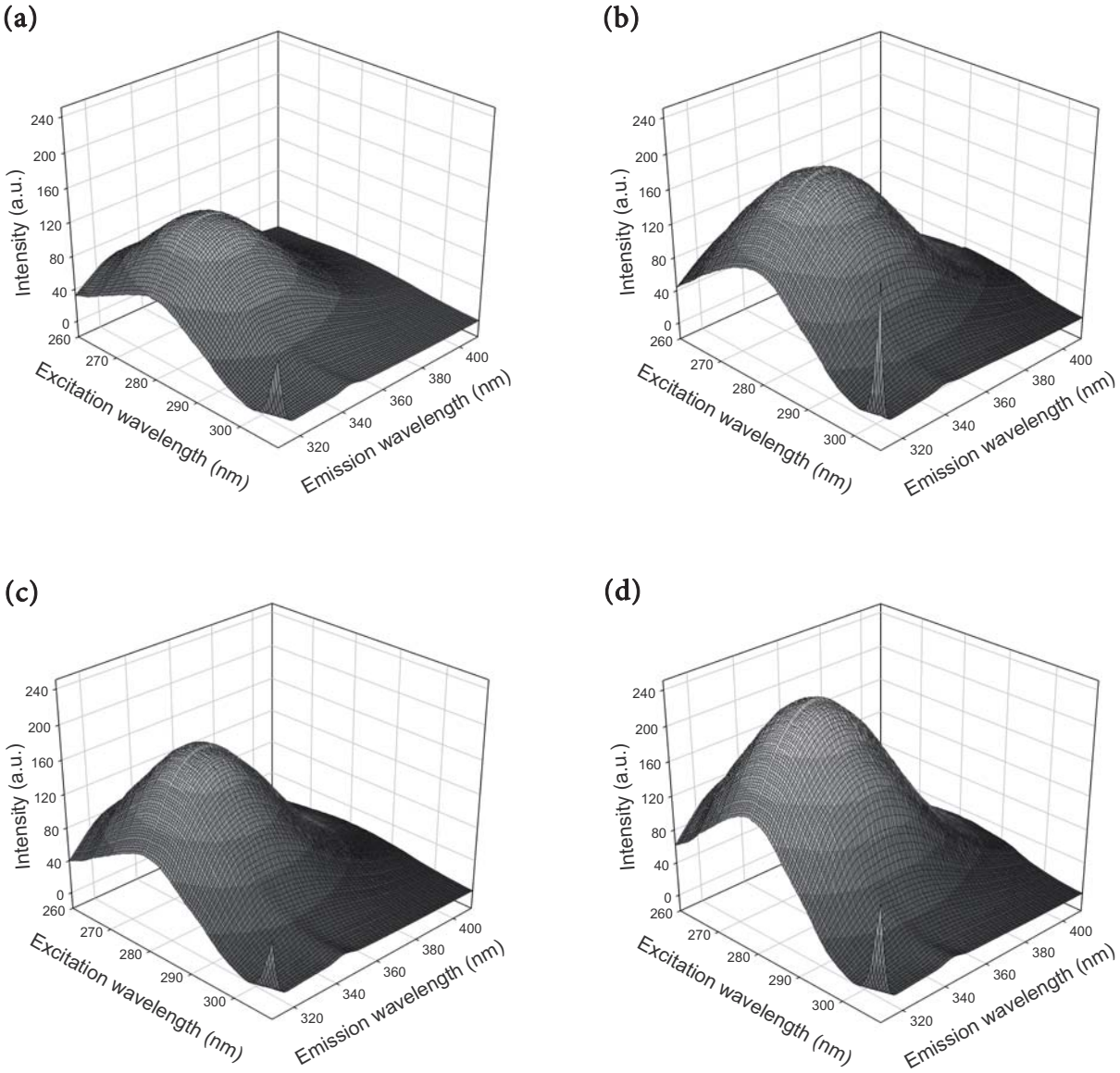

Figure 2: Fluorescence characterization of IgG1 and h-IgG; plots show fluorescence spectra of IgG1 in (a) PBS buffer and (b) PBS buffer containing 0.05% SDS as well as fluorescence spectra of h-IgG in (c) PBS buffer and (d) PBS buffer containing 0.05% SDS.

Table 1: Fluorescence characteristics of IgG1 and h-IgG dissolved in PBS buffer and PBS buffer containing 0.05% SDS.

Protein (dissolved in)	λ_{ex} maximum (nm)	λ_{em} maximum (nm)
IgG1 (PBS buffer)	279.5	333.0
IgG1 (PBS buffer + 0.05% SDS)	279.5	338.0
h-IgG (PBS buffer)	279.0	337.0
h-IgG (PBS buffer + 0.05% SDS)	279.5	337.0

With respect to the surfactant-free samples, it becomes obvious that human pooled IgG exhibits a higher quantum yield than the monoclonal IgG1. In either instance the fluorescence intensity was further increased by the addition of SDS. This is most likely caused by a decreased intramolecular quenching as a consequence of structural reorganizations arising from SDS binding. This increased fluorescence response improves the sensitivity when IgG is quantified. Moreover, the 3D-plots reveal a slight broadening effect in the fluorescence maximum area, induced by the surfactant. As for IgG1, the emission maximum was red-shifted, suggesting drastic structural alterations. For h-IgG, the emission wavelength maximum was generally found at longer wavelengths of 337 nm, but no shift could be observed upon the addition of SDS. The excitation wavelength causing the highest fluorescence intensity was consistently located at 280 nm, in accordance with the UV absorption maximum. A summary of the fluorescence characteristics is shown in Table 1.

As standard setting for IgG detection in SE-HPLC, a wavelength pair of 280 nm (excitation) and 334 nm (emission detection) was chosen. The latter value lies between the fluorescence maxima determined for IgG1 and h-IgG. Overall, differences in fluorescence intensities for both proteins were only marginal, and no adverse effect for a sensitive quantification was expected.

3.1.2 Validation of a New SE-HPLC Method for Sensitive IgG Quantification

SE-HPLC, which is a standard method for the investigation of protein stability, can be used for the quantification of proteins. In our case, a Tosoh TSKgel 3000 SWXL with a TSKguardcolumn SWXL (Tosoh Bioscience GmbH, Stuttgart, Germany) as an appropriate column set for IgG was utilized. The chromatographic parameters were adapted adequately in order to improve the overall sensitivity. First, the injected sample volume and therefore the protein quantum analyzed per chromatographic run had to be increased. Best results were found for an injection volume of 400 µl, accomplished by multiple drawing. In a second step, the most sensitive detection system had to be evaluated. Therefore,

UV detection, by applying absorption at 280 nm, where mainly tyrosine and tryptophan absorb, was compared with fluorescence detection at the wavelengths settings evaluated above (see 3.1.1). UV absorption measurements of amide bonds in the area of 210 - 220 nm were not attempted, since they are rather subject to interference with biological compounds and buffer solutions [28]. Although, according to the buffer composition, interference was not expected [28], the results, particularly the linearity derived at 210 nm, were not completely satisfying. Best results provided fluorescence detection, not necessarily due to a better signal-to-noise ratio but rather because of the specificity for protein. Especially at low protein concentrations, the UV signal was overlaid by significant peaks originating from the buffer matrix. The remaining chromatographic parameters were suitably adjusted. The flow was set to 0.75 ml/min, and the duration of a chromatographic run was set to 50 min. The eluent composition equaled the formulation buffer of IgG1 (PBS buffer pH 7.2). Accessorily, SDS in a final concentration of 0.05% (1.73 mM) was added. The application of SDS in SEC was investigated before [29-31]. According to the authors, SDS in denaturing SEC leads to a better resolution, an extended linear range, and an increased accuracy [32]. Reducing the adsorption tendency on column packaging material is crucial. While high salt contents are commonly used in native SEC, also detergents notably stop protein hydrophobic interactions with silica matrices. In addition, denaturing mobile phases are described as helpful in disrupting non-covalent protein - protein interactions [32]. In our case, SDS was, among others, added for the purpose of desorption of the adsorbed proteins, which will be commented on explicitly in 3.2.2. Since the desorption liquid equals the mobile phase of the SEC in terms of composition, the quality of the chromatographic spectra was further improved.

It was mentioned introductorily that the quantity of IgG adsorbed per 2R vial would at the most be about 7 µg. With a vial fill volume of 3.5 ml, the concentration of desorbed protein would be less than approx. 2 µg/ml. For the benefit of maximum flexibility concerning the adsorbed quantity, container material and geometry, the validated range was generously defined from 0.1 to 10 µg/ml. The linearity was studied for both IgG1 and h-IgG. Each value was prepared and measured in triplicate and the results are depicted in Figure 3. The correlation coefficient reflects an excellent linearity for both IgG fractions. The slope of h-IgG was less than the slope of IgG1. According to the fluorescence characterization, however, a higher quantum yield and therefore higher fluorescence intensities of h-IgG were expected. Most likely the lamp intensity of the fluorescence detector decreased distinctly in the period of several weeks between the two investigations. Nonetheless, the quality of linearity was thereby unaffected, as shown in Table 2, but the calculated limits of quantification and detection were indeed affected (see 3.1.4).

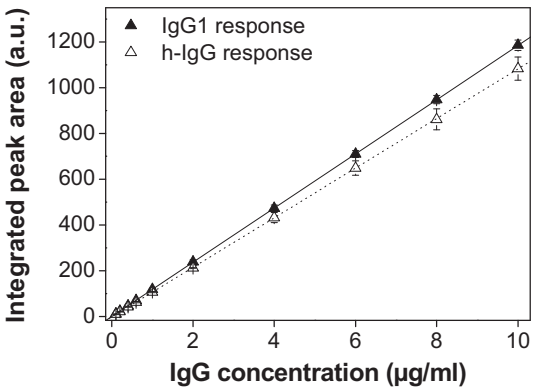

Table 2: Linear regression parameters by least square approach.

	Slope	y-intercept	R
IgG1	118.6	-0.5	0.9999
h-IgG	108.4	-2.2	0.9999

Figure 3: 10-Point linearity of IgG1 and h-IgG using the SE-HPLC quantification method with fluorescence detection at 280 nm / 334 nm for both proteins in the range from 0.1 - 10 µg/ml (n = 3).

Table 3: Day 1 percent recoveries obtained from HPLC assay (n = 3 per concentration).

Theoretical IgG1 content (µg/ml)[a]	Theoretical response (a.u.)	Observed response (a.u.)	Percent recovery (%)	RSD (precision) (%)
0.2034	23.7	24.5	103.3	2.2
1.0171	120.2	122.2	101.7	2.3
8.1368	964.4	965.6	100.1	1.6

[a] based on UV absorption measurement

Table 4: Day 2 percent recoveries obtained from HPLC assay (n = 3 per concentration).

Theoretical IgG1 content (µg/ml)[a]	Theoretical response (a.u.)	Observed response (a.u.)	Percent recovery (%)	RSD (precision) (%)
0.1958	22.8	22.5	98.7	8.3
0.9788	115.6	114.6	99.1	1.7
7.8301	928.1	919.2	99.0	1.6

[a] based on UV absorption measurement

Table 5: Time-course study of IgG1 dissolved in PBS buffer pH 7.2 containing 0.05% SDS, stored in HPLC glass vials at 25°C for the indicated time.

IgG1 content (µg/ml)[a]	Theoretical response (a.u.)	Observed response (a.u.)				Mean recovery (%)	RSD (%) (precision)
		0 h	6 h	32 h	72 h		
0.2198	25.6	26.5	26.2	26.2	26.1	102.5	0.7

[a] determined from UV absorption measurement (stock solution)

Accuracy and precision/repeatability were assessed according to the ICH document Q2(R1) [20], which recommends a minimum of nine determinations over a minimum of three concentration levels. To evaluate the repeatability, each measured value came from a freshly prepared dilution. Tables 3 and 4 provide the results of two independent tests on different days. Obviously, in the case of lower concentrations, the recovery differs more from the expected value, and the precision becomes poorer. The reason for this is an increased error in dilution and peak integration. However, the quantitative analysis of concentrations in the common range is precise and accurate.

The influence of storage time on the analyte in borosilicate HPLC-vials was investigated next. Low concentrations of IgG1, which were considered most critical, were prepared in SDS desorption buffer and filled into separate vials. Analysis covered a timeframe of 3 days, an internally set maximum for HPLC-analysis. As shown in Table 5, a high precision could be achieved. It can be concluded that IgG is prevented from adsorption due to the addition of SDS. The device-specific variations were in an acceptable range. Therefore, the lack of precision in low concentrations (shown above) was not due to adsorption effects but was most likely caused by dilution errors.

Altogether, the quantification method depicted above is robust in terms of sample stability and provides good recoveries and precision down to the upper nanogram range. It was considered sufficiently accurate for the quantification of adsorbed quantities after desorption and was implemented as the standard quantification method within the scope of this work. In order to avoid device-specific or environmental errors, as well as day-to-day variations, an independent calibration curve in the form of external standards was recorded in every HPLC batch run.

3.1.3 Validation of a New Total Organic Carbon Analysis Method for Sensitive IgG Quantification

At least one sensitive reference method with respect to the SE-HPLC quantification of desorbed protein within the vial had to be established. Moreover, there was the need for an alternative desorption method which proves the completeness of desorption by means of SDS. In the following, the implementation and validation of a new TOC-based method for the quantification of adsorbed protein is described.

TOC analysis is an approved and widely used method for monitoring water quality [33]. Furthermore, it is a suitable, FDA-accepted method for e.g. monitoring residual substances in cleaning validation [34,35]. Its applicability as a sensitive and reliable method to determine protein concentrations could be shown before as well [36,37]. Since, in our case, TOC analysis was intended to be applied for the quantification of IgG1 on surfaces, an appropriate desorption step had to be involved. SDS desorption was excluded since the

organic molecule would account for and influence the overall TOC value. For this reason, the exhaustive hydrolysis of adsorbed protein molecules was used instead and was derived from a standardized hydrolyzation procedure [38-40]. The vials containing adsorbed protein were filled with 200 µl of 6 M HCl and closed with FluroTec® stoppers, which were acid-resistant. Vials were crimped and finally heated to 110°C for 24 h without the addition of further reagents. After removal of the acid in a desiccator which contained drying agent and NaOH pellets, the vials were filled with 3.75 ml of TOC-grade water, and the hydrolysis products were dissolved during 15 min of sonication. To achieve a volume sufficient for the TOC measurement procedure, the content of five equivalent vials was merged. Initially, the system suitability was tested according to USP Chapter <643>, using a 500 ppb standard solution of 1,4-benzoquinone and sucrose, respectively. The test was passed with a response efficiency of 101.3%. In the following, the validated range was defined to IgG1 concentrations from 0.09 to 3 µg/ml and thus chosen narrower than the range of the HPLC method. The linearity of the intact IgG1 dissolved in TOC-water, as well as of the hydrolyzed IgG1 dissolved in TOC-water after drying, was investigated by a 7-point calibration curve (Figure 4). Each solution was measured in triplicate to confirm the validity of the response. Both exhibit a very good linearity in the range, which is apparent from the correlation coefficient (Table 6). The blank value was slightly increased to approx. 50 ppb by the hydrolyzation procedure. The ratio carbon/protein (w/w) was determined from the slope of each calibration curve to 0.518 g C / g protein for the intact IgG and 0.526 g C / g protein for the hydrolyzed protein species. This is directly in line with the theoretical values derived from the amino acid sequence, which were determined to 0.520 with, and 0.521 without the inclusion of a typical glycosylation pattern. The

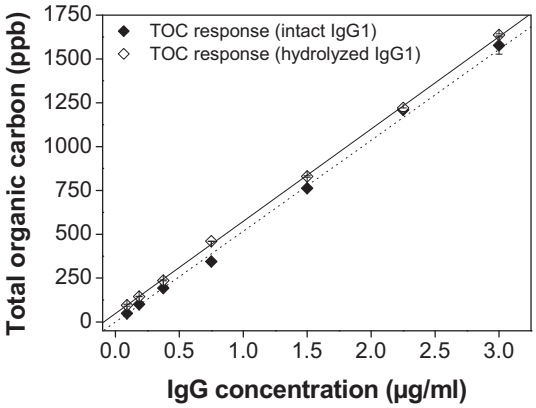

Table 6: Linear regression parameters by least square approach.

	Slope	y-intercept	R
Intact IgG1	518.0	-0.6	0.9992
Hydrolyzed IgG1 components	526.5	47.7	0.9998

Figure 4: 7-Point TOC linearity plot of intact IgG1 dissolved in ultrapure water as well as after an exhaustive hydrolyzation process, the removal of acid and re-dissolution in ultrapure water (n = 3).

Table 7: Day 1 percent recoveries obtained from protein hydrolyzation assay (n = 3).

Theoretical IgG1 content (µg/ml)[a]	Theoretical C (ppb)	Observed C (ppb)	Percent recovery (%)	RSD (precision) (%)
0.1788	141.8	137.2	96.8	2.9
0.7248	429.3	432.8	100.8	1.0
2.8991	1574.1	1531.1	97.3	1.4

[a] based on UV absorption measurement before hydrolyzation step

Table 8: Day 2 percent recoveries obtained from protein hydrolyzation assay (n = 3).

Theoretical IgG1 content (µg/ml)[a]	Theoretical C (ppb)	Observed C (ppb)	Percent recovery (%)	RSD (precision) (%)
0.1737	139.2	147.7	94.2	2.0
0.7043	418.5	407.9	102.6	3.1
2.8172	1531.0	1543.3	99.2	0.6

[a] based on UV absorption measurement before hydrolyzation step

numbers also correspond with the findings of Rouwenhorst *et al.* [36]. The increased value for pre-hydrolyzed molecules may have arisen from a more complete oxidation to CO_2 within the TOC device. It is known that certain substances may be under-quantitated by an insufficient oxidation to CO_2 [37].

Accuracy and precision/repeatability of the hydrolyzed protein method were assessed in the same manner as was utilized for the SE-HPLC method (Tables 7 and 8). For TOC measurements, the recovery is acceptable with values from 94.2 to 102.6% over the defined range. Decreased recovery values for the lower concentrations arose from the increased blind value. Precision was expressed by means of assay variability as relative standard deviation within one concentration and day-to-day variation. The former was less than ±5% and the latter was within the range of ±10%. Again, the relatively high variations were mainly provoked by the blank value, which affected measurement precision especially in the lower range.

A further substantial argument for the hydrolyzation step is the adsorption tendency of native protein molecules on the inside of the TOC test tubes, which was not expected for the individual amino acids. Accordingly, the time span between sample preparation and TOC measurement could become critical in case native proteins are measured. Therefore, a time-course experiment was performed on the recovery of intact IgG1 from solutions

Table 9: Time-course study of IgG1 in 10 mM phosphate buffer pH 7.2.

IgG1 content (µg/ml)[a]	Theoretical C (ppb)	Observed C (ppb)					Mean recovery (%)	RSD (%) (precision)
		0 h	3 h	6 h	9 h	24 h		
0.7233	335.2	306.0	297.3	231.7	205.7	202.0	74.1	20.1
2.8932	1337	1380	1136	1093	1113	1163	88.0	9.9

[a] determined from UV absorption measurement

stored in borosilicate glass containers over 24 h (Table 9). Native protein was dissolved in 10 mM phosphate buffer pH 7.2 so that adsorption/desorption was not influenced by slight pH shifts (in advance, linearity of the IgG1 response in phosphate buffer could also be demonstrated; data not shown). A decrease in concentration over the duration of the test appeared which becomes apparent by a poor recovery and an increased relative standard deviation. Especially at the lower IgG1 concentration, a steady decrease in the IgG1 concentration can be observed, whereas adsorption approaches an equilibrium value after approx. 9 h. The adsorption process was not as visible at an increased IgG1 concentration. However, the mean recovery was comparably poor over the 24 h experiment. As a conclusion, it can be stated that the TOC technique provides the possibility of online observation of protein adsorption in containers. But for the benefit of the robustness of the TOC quantification method, it could be shown that only the measurement of hydrolyzed protein samples makes sense, as adsorption of intact protein to the TOC sample vial leads to a distinct decrease in content over time.

3.1.4 Sensitivity of the New Methods in Comparison with Commercial Standard Assays

The quality of the newly developed methods was compared with two commercial standard assays. Both micro-BCA assay and NI-assay are designed for the analysis of very low protein concentrations and are compatible with the amounts of buffer salts, sodium chloride, and SDS applied. In analogy to the SE-HPLC method, the range was set to an IgG1 concentration from 0.1 to 10 µg/ml. In Figure 5 and Table 10, the linearity of both colorimetric standard assays is compared within the defined range. The NI-assay provides only a minor slope, which results in a poor limit of detection (LOD) and limit of quantification (LOQ) (see below). The slope of the mBCA assay is considerably higher, but, especially in the lower range, the variance of data clearly increases.

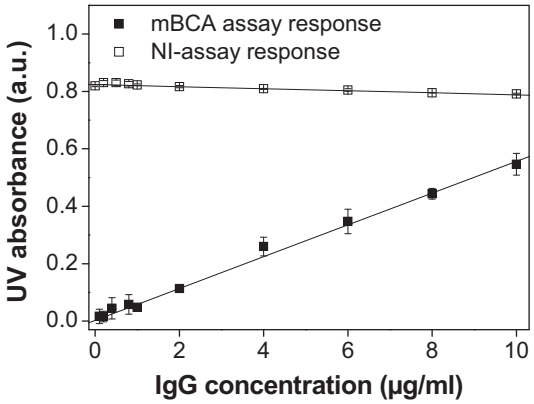

Table 10: Linear regression parameters by least square approach.

	Slope	y-intercept	R
mBCA assay	0.0554	0.003	0.9978
NI-assay	-0.0036	0.824	-0.9875

Figure 5: 10-Point calibration curves and linear fits of different copper-based protein quantification assays (mBCA and NI-assay) for IgG1 in the concentration range from 0.1 - 10 µg/ml (n = 3).

For a direct comparison of all methods, corresponding LOD as well as LOQ values were determined from the linearity plots, based on the standard deviation of the response and the slope [20]. Moreover, as for HPLC chromatograms, more precise LOD and LOQ values based on signal-to-noise ratios were determined graphically and additionally compared to the result for IgG1 and h-IgG. In Table 11, linear fit correlation coefficients for IgG1 and h-IgG in the range from 0.1 - 10 µg/ml (0.04 - 3 µg/ml for TOC) as well as LOD/LOQ values are summarized. According to correlation coefficients, the SE-HPLC method provides the best linearity by far, followed by TOC analysis. The same order applies to LOD and LOQ (Table 11), whereas graphically determined values differ slightly from the results determined from the linearization approach. The coloring assays are suited for a sensitive quantitative analysis of IgG1, but only to a limited extent. Due to the ease of handling and automation, HPLC quantification was preferred, and TOC was applied to verify the HPLC results.

Table 11: Correlation coefficients of different quantification assays for IgG1 and h-IgG in the concentration range from 0.1 - 10 µg/ml and calculated LOD and LOQ values based on the calibration curve.

	IgG1 mBCA assay	IgG1 NI-assay	IgG1 TOC analysis[a]	IgG1 SE-HPLC	h-IgG SE-HPLC
R	0.9978	-0.9875	0.9998	0.9999	0.9999
LOD (µg/ml)	33.16	848.3	0.073	0.027 (0.048)[b]	0.057 (0.036)[b]
LOQ (µg/ml)	100.5	2570	0.220	0.083 (0.130)[b]	0.171 (0.121)[b]

[a] TOC analysis of hydrolyzed protein fractions (6 M HCl, 110°C, 24 h), range: 0.04 - 3.0 µg/ml

[b] values determined from signal-to-noise approach

3.2 Development of a Standardized IgG Adsorption Quantification Assay for Glass Containers

3.2.1 Desorption Buffer and Timeframe of Desorption Process

As already described, SDS was added to the HPLC running buffer. In principle, the surfactant fulfils three functions. Firstly, it prevents proteins from adsorption to the surface of HPLC sample vials, as previously shown (3.1.2). In all probability, this applies to other surfaces like, for example, pipette tips or the column material as well. The addition of SDS therefore increases sample stability during analysis and minimizes sample variation. Secondly, SDS turned out to be ameliorative for the whole SE-HPLC quantification method in terms of peak quality and therefore the overall sensitivity (see above). However, the principal reason for the addition of surfactant was its ability to desorb protein adsorbates from the container surface. In this regard, the strongest eluting force for proteins from a glass surface has been ascribed to SDS [19]. The quantity of surfactant is a compromise between concentrations necessary for an exhaustive desorption step and the reduced column lifetime upon an excess of surfactant [41]. Froeberg *et al.* examined desorption of lysozyme layers on mica in detail [42]. According to them, at concentrations below the CMC, SDS binds to the protein layer and only leads to an increase in the interfacial charge. When surfactant concentration is further increased and reaches CMC, a complete desorption of protein occurs. A virtually complete desorption of proteins from hydrophilic silica was also proven by Svedsen *et al.*, using SDS in concentrations above its CMC dissolved in PBS buffer [43]. In the presence of SDS, proteins form flexible polyelectrolytic complexes by means of acquiring a high net negative charge [30], resulting in increased electrostatic repulsion. Upon changes in quaternary structure, the form will change from globular to elongated [32].

The CMC of SDS in water is in the area of 8.08 mM (0.23%) [44]. It is well known that the CMC of surfactants decreases upon increasing the ionic strength of the medium by the addition of salt [44]. In our case, the CMC of SDS in PBS buffer pH 7.2 at 25°C was determined to be 0.94 ± 0.02 mM (0.027%) by tensiometric measurements (Figure 6a). The result is very well in line with the value expected from an equation provided by Fuguet *et al.* [44]. A reduction of the antimicrobial effect of SDS in presence of sodium [45] was not considered critical. Hence, the concentration of the surfactant could be set to the above value without any problems. For an SDS/protein binding ratio of 1.4 g/g [46], the CMC will be exceeded at protein concentrations in the range investigated, in spite of unspecific surfactant adsorption on the laboratory glassware. The concentration of unbound SDS was consciously kept low to avoid unnecessary burden on the column [41] or possible interference of excess micelles [30].

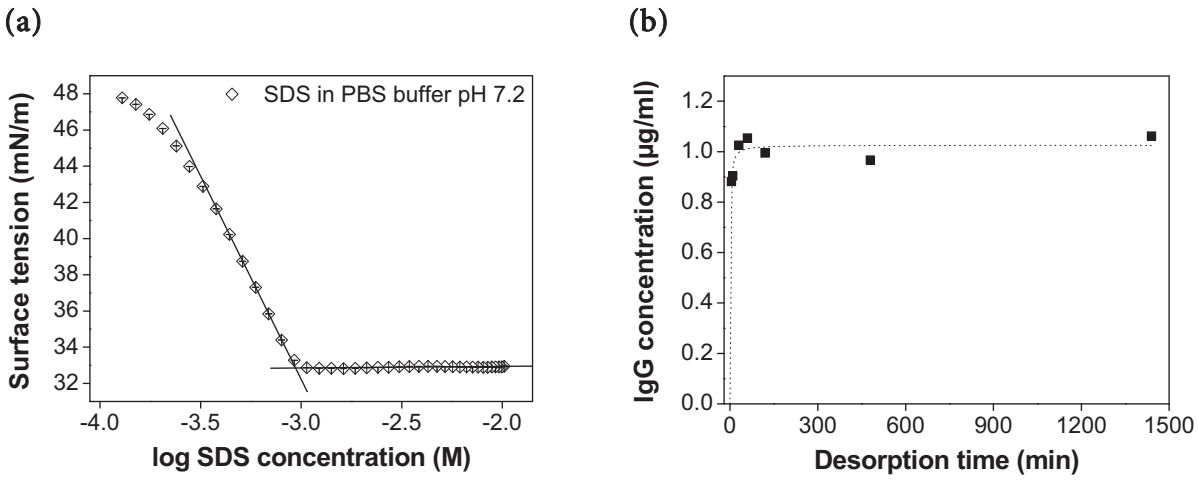

Figure 6: (a) CMC determination of SDS in PBS buffer pH 7.2 by surface tension measurement (n = 3). (b) Desorption kinetics of IgG1 from 2R glass vials in the timeframe up to 24 h using 0.05% SDS in PBS buffer pH 7.2 (dotted line equals a nonlinear curve fit).

The desorption kinetics of IgG1 from 2R borosilicate glass vials, using 0.05% SDS in PBS sample buffer pH 7.2, was determined by the SE-HPLC method (Figure 6b). The results indicate that desorption by the use of SDS is very fast, and a final protein concentration is reached within the first 30 min. A prolongation of the desorption period up to 62 h did not reveal any significant variations (data not shown). To ensure proper results and for practical reasons, the desorption interval was fixed to 14 h over night.

3.2.2 Rinsing Buffer and Number of Rinsing Steps

As a rule, protein adsorption on surfaces is considered irreversible upon concentration changes [47]. So, by dilution, no or hardly any of the bound protein is removed [48,49]. Hysteresis can therefore be observed between the adsorption and the desorption process. Furthermore, protein can alter its conformation over time and enhance contacts with the surface, resulting in a tighter binding [50]. However, it was also shown that a certain amount of protein could be removed from surfaces upon rinsing [26,51].

In the scope of this work, protein adsorption was consistently studied after defined rinsing steps. The purpose was to remove surface-adhering remainder of the protein bulk, as well as unbound or only loosely bound molecules. The especially tailored procedure of vial treatment can be summarized as follows. After the incubation step, the protein solution of 3.5 ml was carefully removed from the containers by using a syringe plus injection needle. Immediately after emptying, the vials were filled with 4.0 ml of rinsing solution, incubated for one minute, emptied again, and drained upside down on Kimtech Science Precision Wipes (Kimberly-Clark Corporation, WI, USA) for another minute. To evalu-

ate the number of rinsing steps required, the residual protein content of each rinsing fraction was determined, as illustrated in Figure 7a. The first rinse contains most of the adherent concentrated protein solution and therefore exhibits the highest protein content. The second fraction includes a small remainder of rinse #1 and the rest of the loosely attached molecules. The following fractions did not contain any IgG1. Four rinsing steps were performed for the default method, and they were limited to one minute each. Besides, the execution of four rinsing steps is an established procedure, which is for example applied for the removal of excess protein in ELISA assays [52]. In this regard, Buijs *et al.* studied the amount of IgG that was removed from hydrophilic silica after rinsing for 15 min using the correlating sample buffer [24]. Depending on the pH, they found desorption values in the range of 0.1 - 0.2 mg/m^2 in the majority of cases and less than 10% of the amount originally adsorbed. In our case, the removed quantity should be presumably less because the adsorption step we applied took 24 h instead of 30 min, and the irreversibility of adsorption usually increases with adsorption time (see below).

Care was taken that the inside of the vial along with the protein layer did not dry. Protein adsorption is highly affected by the ionic strength and pH of the protein formulation (see Chapter 4). Therefore, the effect of the ionic strength in the rinsing buffer was investigated as well. After incubation, separate vials were rinsed 4 times with a 10 mM sodium phosphate buffer (pH 7.2), containing varying amounts of sodium chloride. The protein

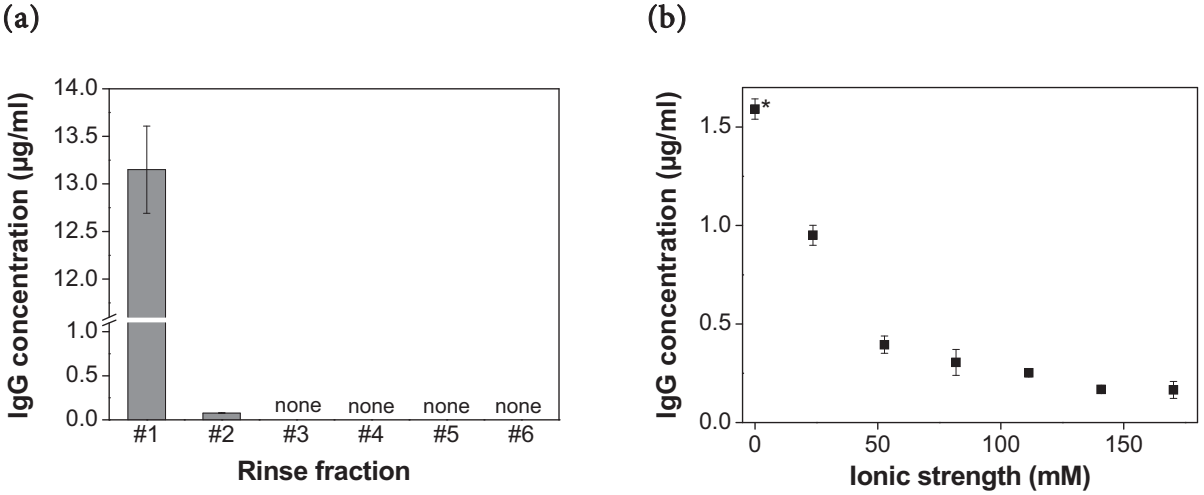

Figure 7: (a) SE-HPLC quantification of IgG1 in successive rinsing buffer fractions (1 min, n = 3); final rinse (#6) took 14 h; (b) IgG1 concentration in the SDS desorption buffer fraction as a function of the ionic strength in the rinsing buffer (10 mM phosphate buffer including variable amounts of sodium chloride adjusted to pH 7.2); non-pretreated glass vials were used for incubation (n = 3).

***deionized water was used for rinsing**

content remaining in the vials after rinsing was measured by desorption using standardized SDS desorption buffer. The results indicate that the ionic strength of the rinsing buffer drastically affected the determined amount of protein bound in the vial. According to Figure 7b, the lower the salt content in the rinsing solution, the less protein was washed out and hence, more protein was determined after the desorption step. Decreasing the salt content diminishes solvation and therefore the solubility of proteins. More importantly, it leads to increased electrostatic interaction between the proteins and the sorbent surface. The result would be a stronger binding at electrostatic attractive conditions. In addition, stronger binding of proteins to the surface may have been caused by increased hydrophobic interactions as a result of potentially reversible protein denaturation in hypotonic medium. In this regard, Docoslis *et al.* found increased adsorption or rather decreased desorption of HSA on silica particles by rinsing at zero ionic strength [26]. Beforehand, adsorption was accomplished using HSA dissolved in pure H_2O. Furthermore, Docoslis *et al.* reported an increased elution of protein in the presence of phosphate ions and ascribed that to competition with protein-attracting sites [26]. This does not coincide with our findings, as the reduction of NaCl concentration while retaining the phosphate concentration showed an effect as well. So, in our opinion, solely the differences in ionic strength were responsible for variations in the adsorbed amount. For lysozyme on hydrophilic silicon oxide surfaces, Wahlgren *et al.* also found increased adsorption and higher irreversibility at low ionic strength [51]. Adsorption was also found to be reversible upon pH shifts [48,53]. However, more detailed investigations on the adsorption reversibility and the dependency of adsorption on both pH and ionic strength are presented in Chapter 4 and 7 in more detail. In conclusion, it is absolutely essential that the rinsing medium equals the formulation used for incubation in every respect.

3.2.3 Timeframe of Adsorption Process

An unspecific adsorption of IgG1 to the inner surface of vials was accomplished by filling empty vials with protein solution, sealing, crimping, and incubating them in a perpendicular position in a temperature-controlled water bath. Temperature was set to 25°C for all incubation procedures described in this work. Furthermore, very slow horizontal movement at 25 rpm was applied to gently agitate the solution. Thus, the formation of concentration gradients was avoided, and concentration was kept consistent throughout the whole volume. The arising of weak shear forces was not meant to influence the adsorption process. The steps involved in the protein adsorption mechanism are manifold, and each can be time-determining for the overall process [54]. Like the adsorbed amount, also adsorption kinetics depends on many different factors. An incubation time of several hours is commonly considered to be sufficient for IgG to reach equilibrium adsorption

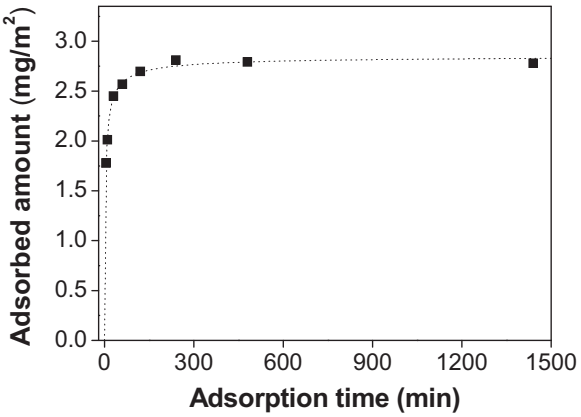

Figure 8: Adsorbed amount of IgG1 in 2R glass vials at pH 7.2 (PBS buffer) as a function of incubation time.

conditions on several surfaces [55]. The kinetics of IgG1 adsorption on borosilicate glass was investigated, taking the above requirements for rinsing and the desorption procedure into account. In Figure 8, adsorption kinetics of IgG1 for the pH 7.2 standard formulation is shown. The adsorption kinetics turned out to be considerably slower than the desorption step. In general, adsorption was found to increase fast within the first hour but slowed down steadily, approaching a final value within approx. 4 h. This again coincides roughly with the findings of Docoslis *et al.* [26]. In order to balance possible variations in adsorption kinetics due to varying formulation parameters and concentrations [12], the standard procedure was fixed to 24 h.

As already stated, adsorption irreversibility increases with adsorption time [51]. So after 24 h of incubation, a lower degree of displacement by rinsing was expected so that the measured adsorption values would most likely mirror the situation after long-term storage. Indeed, a longer adsorption interval of 3 days in borosilicate glass vials neither gave rise to a further adsorption increase nor a decrease (data not shown). Consequently, after 24 h, it is expected that the surface is saturated and adsorption is in equilibrium state. Extensive investigation of adsorption rates was not planned in the scope of this work. The phenomenon of IgG1 adsorption on container surfaces was studied exhaustively, mainly in equilibrium state. Nevertheless, importance should be attributed to this point in future investigations, as adsorption kinetics provides substantial insight into adsorption mechanisms [56].

3.3 IgG1 Adsorption on Glass Vials – Comparison of SE-HPLC and TOC Method

In previous sections, a standard method for incubation and surface rinsing, followed by the removal of surface-bound protein, was developed (24 h adsorption, four rinsing steps with buffer of the same pH and ionic strength as the formulation, followed by 14 h desorption with formulation buffer containing 0.05% SDS). The procedure was now applied by using the default protein formulation to determine the typical amount of IgG1 irreversibly bound on the glass vial surface. The results of this standard quantification practice were compared with those of the validated TOC reference technique after hydrolyzation, using 6 M HCl (see 3.1.3). The adsorption values determined by means of the SE-HPLC method are slightly higher compared to those determined by TOC (2.68 mg/m^2 vs. 2.29 mg/m^2), as depicted in Figure 9. However, the fact that both results are in a quite narrow range indicates that the desorption conditions described above were sufficient to determine the total adsorbed protein.

In literature, adsorption values for IgG on hydrophilic silica at moderate ionic strengths of 2.5 - 3.2 mg/m^2 before and 2.4 - 3.0 mg/m^2 after a rinsing step are described [24]. The values were determined by reflectometry after an incubation of 7.5 µg/ml IgG in phosphate-buffered solution pH 7 plus 100 mM NaCl for 30 min. The value of 2.3 ± 0.4 mg/ml at pH 7.5 in 150 mM NaCl for IgG on hydrophilic silica, described by Heinrich *et al.*, is

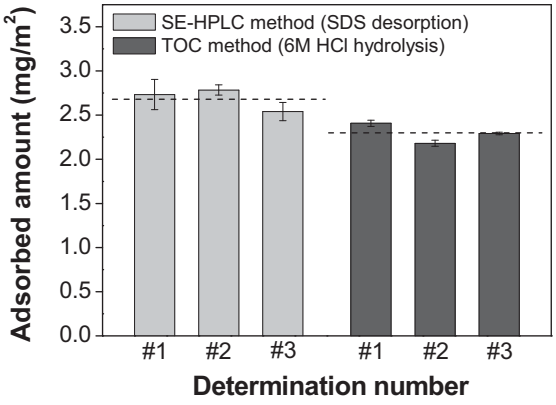

Table 12: Measured values for the application of two different quantification approaches on equal sample vials.

	SE-HPLC method		TOC method	
	Adsorbed amount (mg/m^2)	SD (mg/m^2)	Adsorbed amount (mg/m^2)	SD (mg/m^2)
#1	2.73[a]	0.17	2.41[b]	0.04
#2	2.78[a]	0.06	2.18[b]	0.03
#3	2.54[a]	0.10	2.29[b]	0.02

[a] mean value from 3 vials [b] mean value from 9 vials

Figure 9: Adsorbed IgG1 quantities in 2R borosilicate vials determined with the SE-HPLC method (SDS desorption) and TOC method (6 M HCl hydrolysis); dashed line indicates mean value of the three independent determinations.

also in accordance with our findings [23]. Although the ionic strength of 20 mM was considerably lower compared to the ionic strengths described in the above references, Xu *et al.* achieved similar results by applying ellipsometry on anti-β-hCG immunoglobulin adsorbed on hydrophilic silica, namely 3.4 mg/m^2 before and 2.5 mg/m^2 after thorough rinsing [12]. Compared to measurements on solid silica surface, a similar outcome was described for IgG on porous silica samples by using the solution depletion method. Surface concentrations of 2.5 ± 0.1 mg/m^2 were found in 100 mM phosphate buffer at pH 7.4 [55]. All these values are within a defined range, mostly depending on the particular adsorption conditions. Although these examples do not completely resemble our conditions regarding formulation, surface, timeframes, as well as the analytical method, the results confirm the validity and applicability of our techniques developed for the analysis of protein adsorption on the glass vial internal surface.

4 CONCLUSIONS

In this chapter, sensitive methods tailored to the quantification of protein adsorbed in pharmaceutical containers were developed. Desorption of adsorbed protein by means of SDS with subsequent quantification in SE-HPLC was shown to be a well-suited method for sensitive quantitative analysis of protein adsorption in glass vials. LOD and LOQ values of the SE-HPLC quantification method were within the range of 0.03 - 0.06 and 0.08 - 0.17 µg/ml of IgG, respectively. One reference technique was developed that was based on the determination of total organic carbon after an exhaustive hydrolyzation of the adsorbed protein. LOD and LOQ values (0.07 and 0.2 µg/ml) were in the same order of magnitude as those of the aforementioned HPLC method. Both quantification techniques were validated according to the ICH guideline. In contrast, commercial coloring quantification assays were found inappropriate for the intended purpose due to their poor sensitivity in the corresponding range.

For the investigation of equilibrium adsorption states, a standardized adsorption assay was developed. It included the 24 h incubation of the protein solution in vials at 25°C and slight horizontal agitation of 25 rpm. Incubation was followed by a standardized fourfold rinsing step of one minute each and a 14 h desorption step of protein via incubation with 0.05% SDS in PBS buffer pH 7.2. In the course of this, basic knowledge of the adsorption and desorption timeframe was gained. Through the example of varying ionic strengths, it was proven that the quality of the rinsing fluid directly affected the adsorbed protein quantity. As a consequence for further practice, this implies that the rinsing fluid essentially has to equal the formulation used for incubation in every respect, in spite of the

short timeframe it was in contact with the protein layer. Within the scope of method development, the equilibrium amount of monoclonal IgG1 antibody adsorbed in borosilicate glass vials was obtained, using a single formulation composition for incubation (pH 7.2, ionic strength 170 mM). The adsorbed amounts of IgG1 were in the area of approx. 2.7 mg/m^2. The results obtained by using TOC after protein hydrolyzation were consistent with those from surfactant desorption in combination with SE-HPLC quantification. Hence, the plausibility of the latter procedure was verified. The comparison of our results with those described in literature for similar surface and protein types also confirmed the outcomes of the new assays.

5 REFERENCES

[1] Kingshott, P., Hoecker, H., Methods of assessing protein adsorption, *Encyclopedia of Surface and Colloid Science*, Arthur T. Hubbard, Ed. (Marcel Dekker, Inc., USA, 2002), 3342-3369.

[2] De Feijter, J. A., Benjamins, J., Veer, F. A., Ellipsometry as a tool to study the adsorption behavior of synthetic and biopolymers at the air-water interface, *Biopolymers* **17** (1978) 1759-1772.

[3] Cuypers, P. A., Hermens, W. T., Hemker, H. C., Ellipsometry as a tool to study protein films at liquid-solid interfaces, *Analytical Biochemistry* **84** (1978) 56-67.

[4] Fitzpatrick, H., Luckham, P. F., Eriksen, S., Hammond, K., Bovine serum albumin adsorption to mica surfaces, *Colloids and Surfaces* **65** (1992) 43-49.

[5] Chan, B. M. C., Brash, J. L., Adsorption of fibrinogen on glass: reversibility aspects, *Journal of Colloid and Interface Science* **82** (1981) 217-225.

[6] Xu, S., Damodaran, S., Calibration of radiotracer method to study protein adsorption at interfaces, *J. Colloid Interface Sci.* **157** (1993) 485-490.

[7] Brash, J. L., Semak, Q. M., Dynamics of interactions between human albumin and polyethylene surface, *Journal of Colloid and Interface Science* **65** (1978) 495-504.

[8] Duncan, M., Gilbert, M., Lee, J., Warchol, M., Development and comparison of experimental assays to study protein/peptide adsorption onto surfaces, *Journal of Colloid and Interface Science* **165** (1994) 341-345.

[9] Arai, T., Norde, W., The behavior of some model proteins at solid-liquid interfaces. 1. Adsorption from single protein solutions, *Colloids and Surfaces* **51** (1990) 1-15.

[10] Arwin, H., Ellipsometry, *Physical Chemistry of Biological Interfaces*, Baszkin, A., Norde, W., Eds. (Marcel Dekker, Inc., Basel, 2000), Chapter 17, 577-607.

[11] Malmsten, M., Lassen, B., Ellipsometry studies of protein adsorption at hydrophobic surfaces, *ACS Symposium Series* **602** (1995) 228-238.

[12] Xu, H., Lu, J. R., Williams, D. E., Effect of surface packing density of interfacially adsorbed monoclonal antibody on the binding of hormonal antigen human chorionic gonadotrophin, *Journal of Physical Chemistry B* **110** (2006) 1907-1914.

[13] Malmsten, M., Ellipsometry studies of protein layers adsorbed at hydrophobic surfaces, *Journal of Colloid and Interface Science* **166** (1994) 333-342.

[14] Wagner, M. S., McArthur, S. L., Shen, M., Horbett, T. A., Castner, D. G., Limits of detection for time of flight secondary ion mass spectrometry (ToF-SIMS) and X-ray photoelectron spectroscopy (XPS): detection of low amounts of adsorbed protein, *Journal of Biomaterials Science, Polymer Edition* **13** (2002) 407-428.

[15] Paynter, R. W., Ratner, B. D., Horbett, T. A., Thomas, H. R., XPS studies on the organization of adsorbed protein films on fluoropolymers, *Journal of Colloid and Interface Science* **101** (1984) 233-245.

[16] Xia, N., May, C. J., McArthur, S. L., Castner, D. G., Time-of-flight secondary ion mass spectrometry analysis of conformational changes in adsorbed protein films, *Langmuir* **18** (2002) 4090-4097.

[17] Lensen, H. G. W., Breemhaar, W., Smolders, C. A., Feijen, J., Competitive adsorption of plasma proteins at solid-liquid interfaces, *Journal of Chromatography* **376** (1986) 191-198.

[18] Holmberg, M., Stibius, K. B., Ndoni, S., Larsen, N. B., Kingshott, P., Hou, X. L., Protein aggregation and degradation during iodine labeling and its consequences for protein adsorption to biomaterials, *Anal. Biochem.* **361** (2007) 120-125.

[19] Mizutani, T., Decreased activity of proteins adsorbed onto glass surfaces with porous glass as a reference, *J. Pharm. Sci.* **69** (1980) 279-282.

[20] ICH, Validation of Analytical Procedures: Text and Methodology Q2(R1), 2005

[21] SCHOTT AG, SCHOTT technical glasses: Physical and technical properties, 2007.

[22] Malmsten, M., Ellipsometry studies of the effects of surface hydrophobicity on protein adsorption, *Colloids and Surfaces, B: Biointerfaces* **3** (1995) 297-308.

[23] Heinrich, L., Mann, E. K., Voegel, J. C., Koper, G. J. M., Schaaf, P., Scanning Angle Reflectometry Study of the Structure of Antigen-Antibody Layers Adsorbed on Silica Surfaces, *Langmuir* **12** (1996) 4857-4865.

[24] Buijs, J., van den Berg, P. A. W., Lichtenbelt, J. W. T., Norde, W., Lyklema, J., Adsorption dynamics of IgG and its F(ab')2 and Fc fragments studied by reflectometry, *Journal of Colloid and Interface Science* **178** (1996) 594-605.

[25] Buijs, J., Norde, W., Lichtenbelt, J. W. T., Changes in the Secondary Structure of Adsorbed IgG and F(ab')2 Studied by FTIR Spectroscopy, *Langmuir* **12** (1996) 1605-1613.

[26] Docoslis, A., Rusinski, L. A., Giese, R. F., van Oss, C. J., Kinetics and interaction constants of protein adsorption onto mineral microparticles - measurement of the constants at the onset of hysteresis, *Colloids Surf. B* **22** (2001) 267-283.

[27] Scott, R. P. W., Journal of Chromatography Library, Vol. 11: Liquid Chromatography Detectors, (Elsevier Scientific Publishing Company, Amsterdam, Neth., 1977.

[28] Olson Bradley, J. S. C., Markwell, J., Assays for determination of protein concentration, *Current Protocols in Protein Science*, (John Wiley & Sons, Inc., 2007), Chapter 3.4, 1-29.

[29] Welling, G. W., Kazemier, B., Welling-Wester, S., Size-exclusion high-performance liquid chromatography of integral membrane proteins; effect of detergents on immunological activity, *Chromatographia* **24** (1987) 790-794.

[30] Takagi, T., Takeda, K., Okuno, T., Effect of salt concentration on the elution properties of complexes formed between sodium dodecylsulfate and protein polypeptides in high-performance silica gel chromatography, *J. Chromatogr.* **208** (1981) 201-208.

[31] Konishi, T., Sasaki, M., Separation of membrane proteins of H. halobium by gel permeation high-performance liquid chromatography, *Chem. Pharm. Bull.* **30** (1982) 4208-4212.

[32] Wu, C., Handbook of Size Exclusion Chromatography and Related Techniques, (Marcel Dekker Inc,) Ed. 2, 2002.

[33] Gesamter organischer Kohlenstoff in Wasser zum pharmazeutischen Gebrauch, *Ph. Eur. 6. Ausgabe, Grundwerk 2008*, (Deutscher Apotheker Verlag, Stuttgart, 2008), Chapter 2.2.44.

[34] Jenkins, K. M., Vanderwielen, A. J., Armstrong, J. A., Leonard, L. M., Murphy, G. P., Piros, N. A., Application of total organic carbon analysis to cleaning validation, *PDA Journal of Pharmaceutical Science and Technology* **50** (1996) 6-15.

[35] http://www.fda.gov/cder/guidance/cgmps/equipment.htm#TOC, U.S. Food and Drug Administration, 2008.

[36] Rouwenhorst, R. J., Jzn, J. F., Scheffers, W. A., Van Dijken, J. P., Determination of protein concentration by total organic carbon analysis, *Journal of Biochemical and Biophysical Methods* **22** (1991) 119-128.

[37] Baffi, R., Dolch, G., Garnick, R., Huang, Y. F., Mar, B., Matsuhiro, D., Niepelt, B., Parra, C., Stephan, M., A total organic carbon analysis method for validating cleaning between products in biopharmaceutical manufacturing, *Journal of Parenteral Science and Technology* **45** (1991) 13-19.

[38] Lottspeich, F., Engels, J. W., Simeon, A., Bioanalytik, (Spektrum Akademischer Verlag GmbH, Heidelberg) Ed. 2, 2006.

[39] Ng, L. T., Pascaud, A., Pascaud, M., Hydrochloric acid hydrolysis of proteins and determination of tryptophan by reversed-phase high-performance liquid chromatography, *Anal. Biochem.* **167** (1987) 47-52.

[40] Yan, G., Li, J. T., Huang, S. C., Caldwell, K. D., Calorimetric observations of protein conformation at solid-liquid interfaces, *ACS Symposium Series* **602** (1995) 256-268.

[41] Batey, I. L., Gupta, R. B., Mac Ritchie, F., Use of size-exclusion high-performance liquid chromatography in the study of wheat flour proteins: an improved chromatographic procedure, *Cereal Chem.* **68** (1991) 207-209.

[42] Froeberg, J. C., Blomberg, E., Claesson, P. M., Desorption of Lysozyme Layers by Sodium Dodecyl Sulfate Studied with the Surface Force Technique, *Langmuir* **15** (1999) 1410-1417.

[43] Svendsen, I. E., Lindh, L., Arnebrant, T., Adsorption behaviour and surfactant elution of cationic salivary proteins at solid/liquid interfaces, studied by in situ ellipsometry, *Colloids and Surfaces, B: Biointerfaces* **53** (2006) 157-166.

[44] Fuguet, E., Rafols, C., Roses, M., Bosch, E., Critical micelle concentration of surfactants in aqueous buffered and unbuffered systems, *Anal. Chim. Acta* **548** (2005) 95-100.

[45] Srinivasan, V. S., Narasimhan, C. L., Suryanarayanan, T. S., Raghavan, P. S., Effect of metal ions on the antimicrobial activity of sodium dodecylsulfate, *Curr. Sci.* **50** (1981) 22-23.

[46] Reynolds, J. A., Tanford, C., Gross conformation of protein-sodium dodecyl sulfate complexes, *J. Biol. Chem.* **245** (1970) 5161-5165.

[47] Norde, W., The behavior of proteins at interfaces, with special attention to the role of the structure stability of the protein molecule, *Clinical Materials* **11** (1992) 85-91.

[48] Bull, H. B., Adsorption of bovine serum albumin on glass, *Biochim. Biophys. Acta* **19** (1956) 464-471.

[49] Elgersma, A. V., Zsom, R. L. J., Norde, W., Lyklema, J., The adsorption of bovine serum albumin on positively and negatively charged polystyrene lattices, *J. Colloid Interface Sci.* **138** (1990) 145-156.

[50] Norde, W., Haynes, C. A., Reversibility and the mechanism of protein adsorption, *ACS Symposium Series* **602** (1995) 26-40.

[51] Wahlgren, M., Arnebrant, T., Lundstroem, I., The adsorption of lysozyme to hydrophilic silicon oxide surfaces: comparison between experimental data and models for adsorption kinetics, *J. Colloid Interface Sci.* **175** (1995) 506-514.

[52] ZeptoMetrix Corporation, Immuno-Tek: Quantitative Human IgG ELISA Manual, 2008.

[53] Su, T. J., Lu, J. R., Thomas, R. K., Cui, Z. F., Penfold, J., The Effect of Solution pH on the Structure of Lysozyme Layers Adsorbed at the Silica-Water Interface Studied by Neutron Reflection, *Langmuir* **14** (1998) 438-445.

[54] Norde, W., Adsorption of proteins from solution at the solid-liquid interface, *Advances in Colloid and Interface Science* **25** (1986) 267-340.

[55] Kamyshny, A., Lagerge, S., Partyka, S., Relkin, P., Magdassi, S., Adsorption of Native and Hydrophobized Human IgG onto Silica: Isotherms, Calorimetry, and Biological Activity, *Langmuir* **17** (2001) 8242-8248.

[56] Barnthip, N., Noh, H., Leibner, E., Vogler, E. A., Volumetric interpretation of protein adsorption: Kinetic consequences of a slowly-concentrating interphase, *Biomaterials* **29** (2008) 3062-3074.

Chapter 3

Influence of Vial Surface Properties on IgG1 Adsorption

Abstract

In this study, the influence of the surface state of packaging vials for pharmaceutical application on the extent of protein adsorption was investigated. It was found that the adsorption of an IgG1 antibody on borosilicate glass and hydrophobic vial surfaces (siliconized glass and cyclic olefin polymer plastic vials) largely depends on the surface polarity (γ_s^p / γ_s), which could be determined by dynamic advancing contact angle measurements. The adsorbed protein mass decreased linearly with increasing surface polarity. Furthermore, the elemental composition of the outermost surface layer of borosilicate glass was proven to vary when it was in contact with formulation buffers of different pH. The immediate effect of the elemental composition on adsorption was not further investigated. But the previous contact with formulation buffers of extreme pH led to a decrease of IgG1 adsorption on glass due to an increase in surface polarity. A decreased surface polarity was observed after a vial washing step, followed by sterilization in moist or dry heat. It is assumed that unspecific surface-deposited contamination gave rise to this decrease in surface polarity. Organic material could be found on the pretreated glass surface in time-of-flight secondary ion mass spectrometry measurements. Surface contamination could either be removed by heat treatment up to 600°C or by an Ar plasma treatment, both of which gave rise to a highly increased surface polarity. The total amount of IgG1 adsorbed to borosilicate glass containers within 24 h increased with precedent vial storage time at exposure to air. This effect applied to super-hydrophilic glass surfaces after plasma cleaning as well as to washed and heat sterilized reference vials.

1 INTRODUCTION

Before filling, primary packaging containers are normally pretreated, unless the packaging material is supplied in a clean and sterilized form. As a rule, chemical and particulate contamination from airborne and other environmental sources have to be considered [1]. Washing the containers with water or water with detergent along with an adequate rinsing procedure is used to remove potential contaminates like dirt, dust, salt depositions, fibers, or other particles. However, microbiological aspects of pharmaceuticals are of importance as well, not only for sterile products. Sterilization is the finite method for microbial control of packaging. Irradiation, gas treatment, and heat sterilization are most often applied. Common dry heat procedures include temperatures from 160 - 180°C for 1 h and more, whereas glass sterilization is often carried out in line with the filling operation and is performed in heat tunnels at 320°C or slightly higher for 3 - 4 min [1]. Autoclaving is an effective procedure as well, which is also applicable for a number of plastics materials.

The adsorption of proteins on solid surface largely depends on surface qualities like specific surface area, hydrophilicity, and electrical state [2]. It could be shown by many authors that proteins generally adsorb in higher quantities on hydrophobic surfaces than on hydrophilic ones [3-6]. The most important materials in the field of primary packaging of protein pharmaceuticals are blank hydrophilic borosilicate glass, hydrophobized (siliconized or silanized) borosilicate glass, as well as hydrophobic cyclic olefin polymers (COP), or cyclic olefin copolymers (COC). The hydrophobic materials should thus be prone to bind higher quantities of the therapeutic protein, which will be examined in detail in the scope of this work. Hydrophobic coating gives rise to an increased hydrophobicity. In addition, unspecific surface contamination, which was shown to build up on hydrophilic materials, can result in unintentional hydrophobization and potential complications [7,8]. This phenomenon is well known and crucial in semiconductor and silicon wafer technology. Contaminants were described to hamper effective cleaning of the surfaces. They impair good adhesion of deposited films and cause uncontrolled variations [9]. In the following, considerations are limited to molecular compounds, whereas adsorbed gases, ions, and larger particles are ignored. Atmospheric contaminants can originate from the laboratory or clean room air. The main sources are outgassing of construction materials or urban pollutants. In this regard, organic amines or volatile condensable organic chemicals like plasticizers, pump oils, or cleaning solvents come into consideration [9]. Because of their molecular dimensions, they are difficult to filter out with conventional HEPA filters. Contaminants can also deposit from liquids, e.g. deionized water, which come into contact with the surfaces. A number of cleaning procedures were established to restore the original surface properties. An extensive overview of cleaning procedures was provided by Reinhardt and Kern [9]. These comprise aqueous cleaning and dry cleaning processes, like etching, UV/O_3 treatment, plasma treatment, and others.

The problem of many common analytical methods is that they are usually too insensitive to detect or characterize such hydrocarbon contamination which usually does not form more than a monolayer on the surface [8]. In this respect, time-of-flight secondary ion mass spectrometry (ToF-SIMS) for instance, was shown to be suited and sufficiently sensitive for the detection and investigation of such surface contaminants [8]. Although only present in minor absolute quantity, hydrocarbon contamination from the environment is sufficient to dramatically alter surface properties like e.g. wettability [10]. The quality of the outermost surface layer is especially decisive for adsorption phenomena, not only with respect to proteins. Therefore, only marginal changes may directly affect adsorption characteristics. Moreover, the surface chemistry and morphology of the substrate, such as elemental composition, surface roughness, hydration state, and hydrophilicity, contribute to the adsorption tendency of proteins on the sorbent surface. Altogether, wettability is possibly the most important single surface parameter that affects the quantity and quality of adsorbed protein [11]. For the estimation of the surface free energy of a solid, usually contact angles of different liquids with well-known surface tension are evaluated [12]. According to Young, the contact angle θ depends on the surface tension of the solid γ_s, the surface tension of the liquid γ_l, and the interfacial tension of solid and liquid γ_{sl}, as described by Equation 1:

$$\gamma_s = \gamma_{sl} + \gamma_l \cos\theta \tag{1}$$

Fowkes suggested that the total free energy at a surface consists of contributions from different intermolecular forces [13]. He differentiated between dispersion forces among all molecules from temporary asymmetric charge distribution, and induced or permanent polar forces, which are inherent only in certain molecules [12]. According to Owens and Wendt, the dispersive component γ^d and the polar component γ^p together make up to the entire surface free energy γ (Equation 2) [14]:

$$\gamma = \gamma^d + \gamma^p \tag{2}$$

Together with Fowkes' theory, they established the following relation, assuming the geometric mean approach (Equation 3):

$$\gamma_{sl} = \gamma_s + \gamma_l - 2\left(\sqrt{\gamma_s^d \gamma_l^d} - \sqrt{\gamma_s^p \gamma_l^p}\right) \tag{3}$$

In combination with Equation 1, it can be converted into a linear equation:

$$\frac{(1+\cos\theta)\gamma_l}{2\sqrt{\gamma_l^d}} = \sqrt{\gamma_s^p}\sqrt{\frac{\gamma_l^p}{\gamma_l^d}} + \sqrt{\gamma_s^d} \tag{4}$$

By using at least two liquids with known γ_l^p and γ_l^d, the data points can be approximated by a line. In consequence, γ_s^p is determined from the square of the slope and γ_s^d from the square of the ordinate intercept. This evaluation approach is commonly designated to the method of Owens-Wendt-Rabel-Kaelble [12].

In the scope of this work, dynamic advancing contact angle measurements were performed on the cylindrical part of the packaging containers after cutting off the bottom of the respective container. This ideal cylindrical body was immersed in liquids, namely in ultrapure water, in diiodomethane, and, in exceptional cases, in n-hexadecane. For the calculation of the polar and the dispersive part of the surface free energy, contact angle determinations in water were combined with measurements in one liquid of zero polarity. Table 1 depicts the surface tension and free energy components of the test liquids. In this regard, the ability to perform single-sided measurements was crucial and was enabled by differentiated measurements of the one-sidedly coated and the corresponding untreated sample. This also allowed the surface free energy of e.g. siliconized vials to be determined.

Not only the final resulting contact angle but also the chemical composition of the outermost container surface material may have an impact on protein adsorption phenomena. In this regard, polymeric materials meant for pharmaceutical packaging are less affected by aqueous liquids. Although they are gas-permeable to a minor degree, they normally do not release any leachable components [16]. However, the glass surface is anything but totally inert and was shown to be subject to corrosion in aqueous media [17-19]. Concerning silicate glasses, vitreous silica for instance, is most resistant to water corrosion.

Table 1: Surface tensions and surface free energy components (mN/m) of the test liquids according to Stroem *et al.* [15].

Liquid	Surface tension (γ_l)	Polar component (γ_l^p)	Dispersive component (γ_l^d)
Water	72.8	51.0	21.8
Diiodomethane	58.8	0.0	58.8
Hexadecane	27.6	0.0	27.6

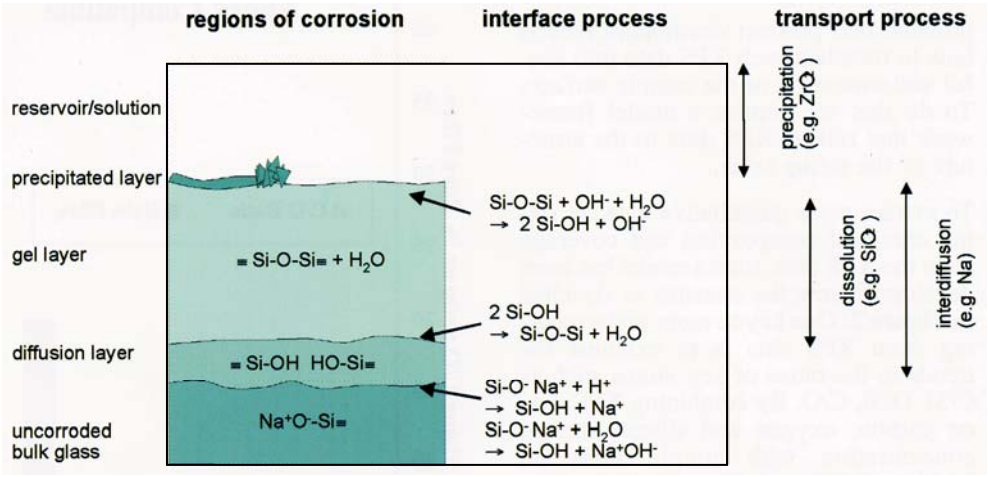

Figure 1: Processes involved in glass corrosion (adopted from Weisser and Bange [24]).

This resistance decreases with the quantity of alkali cations in the glass but is improved again with the addition of alkaline earth oxides [20]. Although the mechanisms are not entirely solved, four major stages are described to play a major role in short-term leaching and glass corrosion [21] (Figure 1 schematically represents the processes involved in glass corrosion):

- The ≡Si–O– network is partially hydrated and a gel layer is formed on the surface. The thickness of this layer was found to increase with exposure time [22].

- Alkali ions (M^+) of the glass are exchanged with monovalent cations of the saline solution (M'^+), according to:

$$(M^+)_{glass} + (M'^+)_{solution} \rightleftharpoons (M^+)_{solution} + (M'^+)_{glass} \quad (5)$$

- The acidic attack on the glass surface is a pure ion exchange process and has been described as *interdiffusion*. Hydronium ions (H_3O^+) are replaced with the alkali cations of the glass surface. The SiO_2-network is not affected by the acid [23]. The reaction rate in very early stages of the reaction has been found to be proportional to $\sqrt{t}$. This implies that the reaction is diffusion-controlled by the exchanging cations [17,20].

$$\equiv Si{-}O^- M^+ + H_3O^+ \rightleftharpoons \equiv Si{-}OH + M^+ + H_2O \quad (6)$$

- In alkaline solutions, a uniform dissolution of the glass matrix is promoted by the OH^- ion. Thereby, the silica network is broken by the nucleophilic OH^-, and the glass network is successively dissolved, showing a linear time dependence (*corrosion*) [24]:

$$\equiv Si{-}O{-}Si\equiv + OH^- \rightleftharpoons \equiv Si{-}O^- + HO{-}Si\equiv \quad (7)$$

A fifth point, which also belongs to the glass corrosion phenomena, is the formation of precipitated layers. This is most distinct when the filling volume is small so that saturation is easily reached.

The critical pH value at which one of the two mechanisms, glass dissolution or alkali depletion, prevails was reported to be around pH 9. Accordingly, a homogeneous dissolution of the glass surface will set in above pH 9, whereas at pH values below depletion of mainly monovalent alkali ions, and, to a minor extent, earth alkaline or other ions will take place under retention of the silica network [23]. With respect to the filling of liquid protein solutions, these effects inevitably occur when the liquid of a certain pH comes in contact with the glass surface. Thus, the adsorption process and glass corrosion processes are taking place at the same time. Finally, it may be conceivable that at certain pH values, parts of the glass surface detach along with the adsorbed proteins. This would interfere with a uniform adsorption process. Glass corrosion affects a variety of different glass properties. The most important ones are a decrease in the total mass, optical changes, modifications of chemical bonding and glass density, as well as topographical changes like increased roughness, and changes in the glass surface composition. The last two seem to have the most direct bearing on the protein adsorption process. In the scope of this work, however, only changes in the glass surface composition at incubation conditions were analyzed. An overview of contemporary and sophisticated methods available for the analysis of glass corrosion is given by Weisser and Bange [24]. A good and reliable method for the sensitive surface analysis is ToF-SIMS, as already mentioned above. It provides information about the chemical composition of the surface-near region with a depth resolution in the nanometer scale [25], whereupon corrosion and contamination phenomena can be sensitively studied.

It was the aim of this study to determine the influence of vial surface properties on the adsorption of an IgG1 antibody. Therefore, containers composed of different materials were studied, while the main focus of the investigations was on borosilicate glass. The surface property of utmost interest was the surface free energy, which was exclusively determined by dynamic contact angle measurements. In this regard, the effect of container pretreatment, storage time, and formulation pH on the surface quality of vials was evaluated on the basis of surface free energy changes. Based on the fact that layers of

adsorbed proteins alter the surface free energy of the substrate as well, tensiometric measurements on IgG1 adsorbates were performed with the objective of correlating surface polarity and the adsorbed protein mass. The ionic composition of the outermost glass surface, which sensitively depends on the pH of the liquid phase, was analyzed by ToF-SIMS depth profiling. Likewise, unspecific surface contamination on the glass was substantiated and further investigated by static SIMS measurements.

2 MATERIALS AND METHODS

2.1 Materials

2.1.1 Protein Formulation

For adsorption experiments, a 2 mg/ml solution of IgG1 (MW ≈ 152 kDa) in 10 mM phosphate buffer and 145 mM NaCl (pH 7.2) was used, which was kindly provided by Merck Serono (Darmstadt, Germany). For ionic strength adjustment, the solution was dialyzed against pure 10 mM phosphate buffer solution by using Vivaflow® 50 tangential flow filtration cartridges (Sartorius-Stedim Biotech, Goettingen, Germany) equipped with a 30,000 MWCO polyethersulfone (PES) membrane. The IgG1 concentration was determined by UV spectroscopy. Variable pH values of the protein formulation had to be adjusted, and, for each pH value, the adequate quantity of NaCl and acid or base was calculated and added to the dialyzed solution in order to retain consistent ionic strength. Ionic strength calculations were performed as described in Chapter 4. Each protein solution including the standard IgG1 formulation was filtered through a hydrophilic 0.2 µm PES membrane filter (Pall GmbH, Dreieich, Germany) before use. Typical protein handling, like dilution and sample preparation, was done in 15 ml and 50 ml polypropylene tubes (GreinerBio-One GmbH, Frickenhausen, Germany).

2.1.2 Glass Vials and Closure Systems

The pharmaceutical containers used for investigations were Fiolax® 2R borosilicate glass vials, kindly provided by SCHOTT AG (Mainz, Germany). Vials were preprocessed (washed and heat sterilized) as described in Chapter 2, unless otherwise stated. Additionally, autoclaving in a Vakulab HP 669-2H R autoclave (Muenchener Medizin Mechanik GmbH, Planegg, Germany) at 121°C for 30 min was applied for individual glass vials after the washing step. A second vial type, siliconized Fiolax® 2R vials (pre-siliconized with

Dow Corning 360), was obtained from SCHOTT AG as well. They were washed in the same way as the glass vials but only dried at 80°C for 1 h. Plastic vials, namely Resin CZ® 2 ml (Daikyo Seiko, Ltd., Japan) made upon COP, were treated analogously. After filling, vials were closed with FluroTec® stoppers and finally sealed with Flip-Off® seals, both from West Pharmaceutical Services GmbH & Co. KG (Eschweiler, Germany). For contact angle measurements, the vials were prepared as described below. Bottoms of the pre-washed and heat sterilized glass vials were carefully cut off with a DREMEL® 300 series rotary tool (DREMEL Europe, Breda, The Netherlands) equipped with a rotating diamond cut-off wheel. Bottoms of pre-washed plastic vials were sawed off with a handsaw. Adherent glass dust or plastic particles of either container type were removed by a flow of pure pressurized nitrogen.

2.1.3 Chemicals / Excipients

Ultrapure water (0.055 µS/cm) for all applications came from a Purelab Plus UV/UF system (ELGA LabWater, Celle, Germany) and was filtrated through a 0.22 µm membrane filter before use. The salts NaCl, NaH_2PO_4, and Na_2HPO_4 were purchased from Merck Chemicals (Darmstadt, Germany). 1 M NaOH and HCl were obtained from Sigma-Aldrich (Munich, Germany). Diiodomethane (99%) and n-hexadecane (≥ 99%) for contact angle measurements were purchased from Sigma-Aldrich as well.

2.2 Methods

2.2.1 Argon Corona Discharge Plasma Treatment of Glass Surfaces

Selected borosilicate glass vials were plasma-treated with argon corona discharge plasma for variable time, subsequent to washing and heat sterilization (Figure 2). The corresponding device was an ambient pressure plasma generator equipped with a Plasmabrush® and was kindly provided by Reinhausen Plasma GmbH (Regensburg, Germany). The discharge was produced by a 12.7 kHz / 6.5 kV power supply. The argon gas flow (argon 5.0 from Air Liquide Deutschland GmbH, Duesseldorf, Germany) was 8 l/min at a pressure of 2.0 bar. According to the manufacturer, the application of Plasmabrush® technology at atmospheric pressure does not exceed surface temperatures above 70°C. The processing time varied from 10 up to 30 sec.

Figure 2: Surface treatment process of 2R borosilicate glass vials with argon plasma.

2.2.2 Contact Angle Measurements

The surface free energy of blank and siliconized glass vials, as well as of COP plastic vials, was determined by dynamic contact angle measurements on a K100MK2 tensiometer (Kruess GmbH, Hamburg, Germany) in combination with the temperature-controlled water bath Julabo F12 (Julabo Labortechnik GmbH, Seelbach, Germany). The vials were fastened in the device with a modified holding clamp. The free energy of the glass vial surfaces was determined from the dynamic advancing angles in water and diiodomethane, whereas for COP polymer vials, water and n-hexadecane were applied. Dynamic contact angles were measured by wetting the axial length from 2 - 6 mm. Data analysis was performed according to the method of Owens-Wendt-Rabel-Kaelble [14,26], using the curve analysis and calculation tools from the Kruess LabDesk 3.1 software. The surface tensions of the test liquids were controlled repeatedly with the Wilhelmy plate method. Furthermore, the software allowed one-sided measurements of the internal surface of siliconized vials via the differential measurement of sample and blank vials. All samples were measured at 25°C and in triplicate, using a new sample vial for each determination. For COP plastic vials, the surface tension was verified using a set of blue testing inks (ISO 8296) from 18 - 32 mN/m (arcotest GmbH, Moensheim, Germany).

2.2.3 UV Spectroscopy

UV spectroscopy for protein concentration measurements was performed on an Agilent 8453 UV/VIS spectrophotometer (Agilent Technologies GmbH, Boeblingen, Germany) at

λ = 280 nm, using quartz cuvettes and an extinction coefficient of 1.40 cm^2/mg for antibodies [27]. The sample temperature during measurement was held at 25°C.

2.2.4 Adsorption Method

The standardized adsorption procedure of IgG1 in containers was discussed in detail in Chapter 2. In the following, only a short description is given. The preprocessed vials were filled with IgG1 solution of 2 mg/ml, closed, and incubated for 24 h in a water bath at 25°C and slow horizontal movement (25 rpm). The vials were emptied using a syringe with an injection needle, and were rinsed in four steps with a buffer solution, correlating to the respective formulation. For desorption of the inherent proteins, the vials were filled with PBS buffer pH 7.2 (10 mM phosphate plus 145 mM NaCl) containing 0.05% SDS, sealed again, and stored at the above conditions over night (14 h). For direct tensiometric measurements of the adsorbed protein layer, glass vials without bottoms were immersed into the protein solution so that adsorption could take place at both wall sides. After 24 h, the incubated vials were successively immersed twice in the respective blank buffer for the removal of loosely adherent molecules, twice in ultrapure water to remove adherent buffer salts, and finally dried in a gentle flow of pure nitrogen.

2.2.5 Size Exclusion High Performance Liquid Chromatography

Desorbed protein quantities were analyzed via Size Exclusion HPLC on an Agilent 1100 device (Agilent Technologies GmbH, Boeblingen, Germany) equipped with a Tosoh TSK gel G3000SWXL and a TSKgel SWXL guardcolumn (Tosoh Bioscience GmbH, Stuttgart, Germany). The mobile phase equaled the desorption buffer described above. The injected sample volume was 400 µl and the run duration 50 min. The protein fluorescence signal at λ_{ex} / λ_{em} = 280 nm / 334 nm was recorded by a Thermo Spectra 3000 fluorescence detector. All chromatograms were integrated manually using the Agilent ChemStation software Rev. B 02.01. In each HPLC batch run, a 10-point IgG1 calibration from 0.1 - 10.0 µg/ml was included.

2.2.6 Time of Flight Secondary Ion Mass Spectrometry

ToF-SIMS glass surface analysis was performed on a ToF-SIMS IV (ION-TOF GmbH, Muenster, Germany). Measurements were carried out using 15 keV Ga^+ ions (area 50 µm x 50 µm) for acquisition. For depth profiling experiments, the surface was sputtered with a 500 eV O_2^+ beam (area 300 x 300 μm^2), which, for glass surface, resulted in an approximated ablation rate of 0.05 nm/s. The timeframe of sputtering was 0 - 300 sec.

3 RESULTS AND DISCUSSION

The impact of a container preprocessing step, such as washing and sterilization, on protein adsorption to pharmaceutical packaging vials has not yet been studied. It could be derived from preliminary tests that the preprocessing of glass vials, a washing step followed by sterilization with moist or dry heat, as commonly performed in the pharmaceutical industry, directly influences the adsorbed IgG1 quantity (data not shown). Adsorption levels were up to 3 - 5 times higher, or even more, than those found in virgin glass vials. Since the identical protein formulation and the same incubation procedure were applied, this phenomenon must be attributed to differences of surface properties. For this purpose, contact angle measurements were found to be insightful, from which the container surface free energies could be deduced.

3.1 Influence of Surface Free Energy on IgG1 Adsorption

Initially, the surface free energy γ_s of borosilicate glass vials after different treatments, i.e. after washing plus sterilization and after different subsequent surface cleaning steps, was determined. All measured contact angle values, as well as the calculated surface free energies with associated polar and dispersive components, are listed in Table 2. Moreover, the latter are diagrammed in Figure 3 and overlaid with the IgG1 binding behavior.

Table 2: Dynamic advancing contact angles, calculated polar (γ_s^p) and dispersive components (γ_s^d) of the surface free energy, surface polarity parameters (γ_s^p / γ_s) and adsorbed amount of IgG1 on glass vials of different pretreatment as well as on siliconized glass and plastic vials.

	Dynamic adv. CA (°) H_2O / CH_2I_2	γ_s^p (mN/m)	γ_s^d (mN/m)	γ_s^p / γ_s	IgG1 adsorbed (mg/m²)
Glass untreated	0.00 / 41.2	37.4	38.9	0.49	0.56 ± 0.10
Glass washed and autoclaved	26.6 / 38.1	30.1	40.5	0.43	0.82 ± 0.22
Glass washed and heat sterilized	46.4 / 13.3	16.2	49.1	0.25	2.50 ± 0.07
Additional heat 300°C 1 h	34.8 / 8.94	21.6	49.9	0.30	2.37 ± 0.05
Additional heat 400°C 1 h	28.2 / 19.8	26.1	46.6	0.36	2.49 ± 0.20
Additional heat 500°C 1 h	15.4 / 33.6	32.6	42.6	0.43	2.01 ± 0.06
Additional heat 600°C 1 h	0.00 / 37.3	36.2	40.8	0.47	1.21 ± 0.30
Additional Ar plasma 30 s	0.00 / 0.00	n/a	n/a	n/a	0.50 ± 0.04
Glass siliconized (one-sided)	78.1 / 31.9	3.9	40.6	0.09	4.41 ± 0.46
Plastic (COP)	80.2 / 0.00[a]	6.4	27.6	0.19	3.70 ± 0.41

[a] n-hexadecane used as measuring liquid

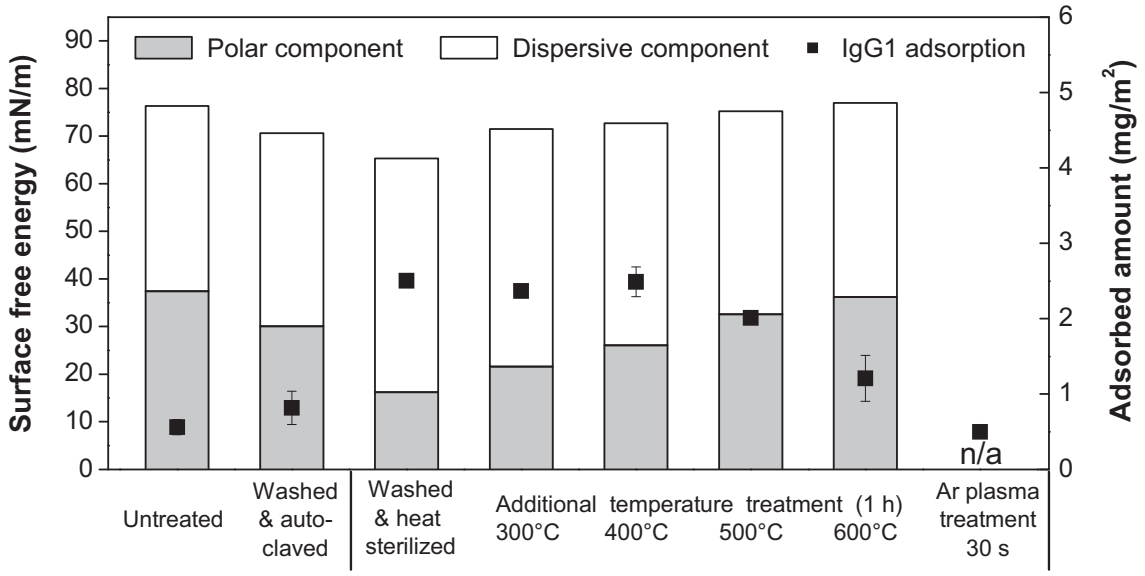

Figure 3: Surface free energy of borosilicate vials after different surface pretreatment procedures; surface free energy is divided into a polar and a dispersion component (bars); overlaid is the resulting quantity of IgG1 adsorbed within 24 h from the standard formulation pH 7.2 (squares) (n = 3).

As expected, all glass vials are primarily hydrophilic and hold contact angles of water in the lower range. Accordingly, the calculated surface free energies were high at approx. 70 mN/m. The markedly high surface tension of the untreated brand-new vials was appreciably reduced by washing plus autoclaving, and, more distinctly by dry heat sterilization. The effect originates from a strong decrease of the polar part. The dispersive fraction of the surface free energy is less susceptible to washing or heating. It is shown in Table 2 that the contact angle of water increased, whereas the contact angle of diiodomethane decreased for the samples in the above order. It can be reasoned that the accessibility of hydrophilic silanol groups was reduced, indicated by an increasing water contact angle. A decrease of the polar fraction of the surface free energy was the consequence. A loss of polar interaction sites was supposed to arise from coverage with a hydrophobic surface contamination due to the washing step. Also lower contact angle values for diiodomethane and, accordingly, a slightly increasing dispersive component were the consequence. To prove the above theory, the washed and heat sterilized vials were further exposed to high temperature in order to clean the surface from contamination and to restore the high surface free energy [23]. As listed in Table 2, water contact angle values decreased, and contact angle values of diiodomethane increased again. Thus, the high temperature treatment gives rise to an increase of γ_s, primarily by means of the polar component (Figure 3). This indicates that presumed organic material on the surface was removed by oxidation, and the bare and highly hydrophilic glass surface was restored.

Plasma cleaning represents an alternative way of glass surface purification. Ar and Ar/air plasma are often applied for treating a variety of materials and causes a high density of electrons, ions, and atoms on the surface. From this, a number of reactive interactions arise [23]. This leads to the removal of surface contamination together with, amongst others, an increase in the number of charged groups. As a matter of fact, the surface free energy was drastically increased, which resulted in total wetting and zero contact angles for water and diiodomethane. For this reason, γ_s together with its polar and dispersive components could not be determined reasonably.

The amount of IgG1 adsorbed from the standard 2 mg/ml / pH 7.2 protein formulation was determined independently. It was highest on glasses of lower surface free energies, i.e. of lower polar components, such as on the washed and sterilized containers. Adsorption was markedly reduced on glasses which were heated up to temperatures of 500°C or higher. The most pronounced reducing effect on the adsorbed amount of IgG1 had the Ar plasma cleaning procedure. This strongly supports the conclusion that varying adsorption quantities can be associated with differences in the energy state of the surface. As mentioned above, changes in the surface free energy were mainly attributable to changes of the polar component γ_s^p, whereas the dispersive component γ_s^d was rather stable. Hence, γ_s^p is of utmost importance. In this context, a new surface parameter can be introduced which reflects the surface polarity and is defined as the quotient of the polar component and the whole surface free energy [28]. It becomes obvious that the adsorbed amount of IgG1 on glass correlates well with the surface polarity. Thus, IgG1 adsorption decreases when the surface polarity increases. To prove the general validity of this result, surfaces different from hydrophilic glass, namely siliconized glass and COP plastic, were additionally tested. The results are shown in Figure 4.

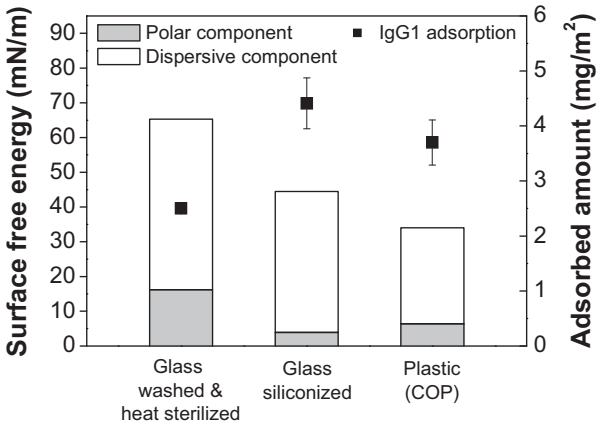

Figure 4: Surface free energy of borosilicate glass vials (reference) compared with surface free energy of siliconized glass vials (one-sided measurement) and COP plastic vials; surface free energy divided into a polar and a dispersive component (bars); overlaid is the resulting quantity of IgG1 adsorbed after 24 h from the standard formulation pH 7.2 (squares) (n = 3).

As expected, siliconized glass exhibits a considerably smaller surface tension than pure glass. The polar fraction reaches values near zero, whereas the dispersive part only diminished to a small extent. This is consistent with the chemical properties of the polydimethylsiloxane (PDMS) oil used for surface hydrophobization [29]. In this regard, water contact angles on PDMS were described to be the same as on paraffin, and it was concluded that the surface of PDMS consists of rather close-packed methyl groups [30]. According to our expectations, a low surface polarity promoted increasing protein adsorption, and the adsorbed amount of IgG1 measured for siliconized glass by far exceeded the values of the uncoated glass surfaces. Tensiometric measurements on the COP plastic container surfaces revealed water contact angles in the same range as those on the siliconized surfaces. Plastic vials were measured in n-hexadecane instead of diiodomethane. This was due to problems with an extremely high buoyancy force of the plastic samples submerged in CH_2I_2. Control measurements with appropriate test inks revealed a surface free energy of the COP vial surface between 30 - 32 mN/m. This value is in accordance with the results determined from the surface free energy calculation (34.0 mN/m) by applying the measured contact angles of water (80.2°) and n-hexadecane (0.0°). Thus, the determination of polar and dispersive components using n-hexadecane as absolutely hydrophobic liquid was seen as reliable. The total surface free energy of the polymer was determined to be less than the value determined for siliconized glass vials. However, the surface polarity of COP is greater, since the polar components represent a greater share of total energy. Also the quantity of IgG1 bound on the polymer surface was lower compared to the amount bound on the siliconized surface. Finally, the above suggested dependence of IgG1 adsorption on the surface polarity was again confirmed. In the course of a detailed investigation of the correlation of surface polarity and protein adsorption, the adsorbed quantities from the standard IgG1 formulation (2 mg/ml, pH 7.2) within 24 h were assumed to cause saturation on all surface types. The degree of surface polarity (γ_s^p / γ_s) was calculated for each glass sample as well as for the hydrophobic materials. In Figure 5, the surface polarity is plotted against the adsorbed amount of protein. It becomes apparent that this correlation can be fit by a straight line, indicating an inverse proportionality with a correlation coefficient of R = 0.94. At the same time, this also means that protein adsorption linearly depends on surface hydrophobicity, with the latter defined as γ_s^d / γ_s.

Although the driving forces and the influencing factors, like pH and ionic strength, are elucidated in more detail in Chapter 4, the situation for adsorption from the standard IgG1 formulation will be outlined briefly. Isoelectric focusing and zeta potential measurements revealed that at pH 7.2 the IgG1 molecules carry a low net positive charge, whereas the glass surface is highly negatively charged. Consequently, protein molecules are electrostatically attracted towards the glass, with the exception of coexisting scattered and negatively charged patches on the IgG1, which in turn are repulsed. As a result, attractive

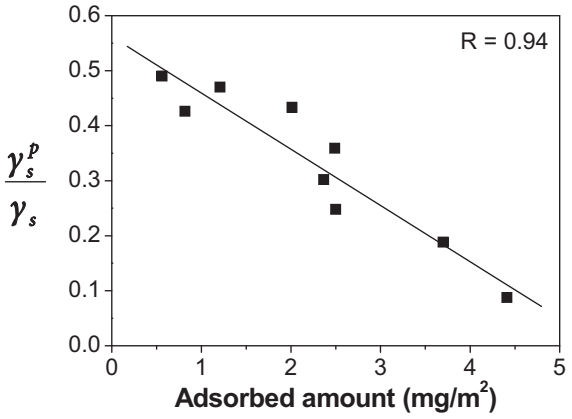

Figure 5: Plot of the surface polarity (γ_s^p / γ_s) against the total adsorbed amount of IgG1, including a linear fit of the data points for various materials tested.

forces should increase with increasing surface polarity, leading to increased adsorption. However, the opposite is true. It will be shown later that electrostatic interactions between protein and surface have a large influence on the adsorption of IgG on glass surface (see Chapter 4). But strong and substantial binding of IgG1 on hydrophobic surfaces, e.g. COP plastic vials, in the absence of pronounced electrostatic protein - surface interactions, emphasizes the high importance of hydrophobic interactions for IgG1 adsorption. Moreover, an increased adsorbed amount on glass with increasing surface hydrophobicity (γ_s^d / γ_s) leads to the conclusion that hydrophobic interactions are the stronger of the two driving forces. This holds true at pH 7.2, where the net charge of IgG is low and electrostatic attraction towards the negatively charged surface is not very pronounced. In all probability, also the shielding of surface charges by hydrophobic contamination layers had contributed to the observed adsorption behavior.

In the context of adsorption driving forces, also the properties of the proteins are crucial. Especially for hydrophilic surfaces, Arai and Norde reported on a widely differing adsorption behavior of proteins [31]. The authors related this to differences in the structural stability of the proteins. Structurally stable “hard proteins” showed adsorption only under electrostatic attraction, whereas “soft proteins”, characterized by a lower structural stability, adsorbed on hydrophilic surface even under electrostatic repulsion. This was ascribed to an extra driving force, the structural rearrangements in the proteins [31]. On hydrophobic surfaces however, proteins were bound under all conditions of charge interactions. Although, in our case, the pH dependency of IgG1 adsorption was not investigated for hydrophobic surfaces, a clearly higher adsorption tendency for IgG1 on hydrophobic surfaces than on hydrophilic ones under electrostatic attraction could be shown. The question whether hydrophobic interactions alone led to this increase in adsorption or

whether alterations of the protein's internal structure contributed to this phenomenon could not be unambiguously clarified so far. Structural investigations on the adsorbed and desorbed protein fractions on/from the glass surface, respectively, will be presented in Chapter 7.

Concerning the correlation of surface polarity and adsorbed protein quantity, similar results were described by Sousa *et al.* [28]. They investigated HSA adsorption on variably treated TiO_2 samples and found less adsorption on surfaces of higher polarity. For surface polarity measurements, they used a similar tensiometric approach. Furthermore, a linear dependency of the adsorbed amount of protein on γ_s^p was described by Michiardi *et al.* in studies on the adsorption of albumin on blank and oxidized nickel - titanium metal surfaces [32]. However, they described just the opposite behavior, namely an increase of adsorption with increasing γ_s^p. We assume that the prevailing adsorption conditions for proteins were completely different from the conditions on insulating glass or polymer surfaces, especially due to the high charge mobility on the conductive metal surfaces. It has to be mentioned that the linear relationship has been shown for only a small range of γ_s^p (8 - 14 mN/m). Furthermore, the findings described above were confined only to albumin. Fibronectin, for example, did not show this dependency. Marsh *et al.* reported of an increased protein adsorption on hydrophobic silica surfaces than on hydrophilic silica surfaces [3]. In this regard, the authors noted differences in the adsorption reversibility. The amount of globular proteins that could be eluted by buffer rinsing, reflecting reversible adsorption, depended on the adsorption time and decreased especially on hydrophobic surfaces due to pronounced molecular reorganizations. In our case, changes in protein adsorption reversibility as a function of surface hydrophilicity and hydrophobicity were not investigated in further detail (for reversibility as a function of pH, see Chapter 5).

With regard to the vial surface characteristics determined above, the high surface free energy of the brand-new glass vials is remarkable. It was described by Schwarzenbach *et al.* that alkali borates condensate on the inner vial surface in the course of the vial formation process [33]. Moreover, this condensation layer was shown to be water-soluble. As a result, it can be assumed that under this layer a pristine glass surface is retained during vial storage. Once the glass gets in contact with an aqueous liquid, the salts dissolve and deposited airborne contaminants are easily removed, giving rise to a high energetic surface. The preceding results indicate that washing and autoclaving increases the contact angle of water and hence decreases the surface polarity. This can be explained by unspecific surface contamination during or after the washing step. The fact that clean glass surfaces are susceptible to air- (or water-) borne hydrophobic organics, leading to a decrease of the surface free energy, was discussed by Mills and Crow [10].

However, it was also shown that a washing and depyrogenation step was capable of causing further surface modifications in terms of morphology and chemical composition.

Heat treatment at 250°C usually leads to the highest density of silanol groups [34], which should result in small water contact angles. However, the opposite was found after the 250°C treatment. Moreover, the contact angle of diiodomethane even decreased, indicating pronounced dispersive interactions. Temperatures of 250°C also involve the complete desorption of water molecules from the surface [34]. Consequently, increasing dynamic advancing water contact angles are the result, as shown for glass slides after an exhaustive drying process [35]. Analogously, Lamb and Furlong described that the exposition to water vapor or air moisture, respectively, leads to decreasing contact angles as a result of a rehydration and rehydroxylation process [36]. This could explain decreasing water contact angles after the autoclaving process under pressurized steam, as opposed to sterilization in dry heat at 250°C. However, the time span between pretreatment and contact angle measurement was several hours and consistent for each pretreatment procedure. Thus, an equilibrium water layer on the glass should have formed on any glass sample, even after heat sterilization. Again, these considerations point to the fact that unspecific surface contamination was the reason for a decreased surface free energy after washing and sterilization. Possible sources of contaminants are the rinse water, which is very unlikely, or the laboratory air, where contaminants are always present [35]. For instance, it was described that hot air drying after the washing step produces high levels of static charge, which increases the risk of recontamination [1]. This could serve as an explanation for increased water contact angles after heat sterilization at 250°C.

By heating up to 600°C and above, the quartz surface is basically rendered hydrophobic since dehydroxylation under formation of siloxane bridges occurs. An increase of water contact angles from 0° to 41° are described [36]. These heat treatment studies were carried out under vacuum, which, however, may substantially differ from the condition in air. In our case, increased water contact angles were not detected after the 600°C treatment. It is assumed that the vial contact to ambient air moisture led to a rehydroxylation of the formed siloxanes [37], as well as to a rehydration of the glass surface, and that both gave rise to an increased surface hydrophilicity. Another possible explanation would be that the heat treatment at elevated temperatures up to 600°C under atmospheric conditions led to a complete oxidation of organic impurities, which resulted in a thorough cleaning of the borosilicate glass surface.

The surface free energy, however, was not as high as that of the glass surface after plasma treatment. The effects of plasma on solid surfaces are manifold. Besides a thorough surface cleaning, a further reason for the complete wetting in connection with the plasma treatment could be an increase in surface roughness. The correlation of contact angles and surface roughness is exemplarily expressed by the equation of Wenzel (Equation 8).

Therein, r equals the roughness ratio parameter and $\hat{\theta}$ the observed contact angle of the roughened surface, having the intrinsic angle θ_0 [38,39].

$$\cos\hat{\theta} = r \cos\theta_0 \tag{8}$$

Thus, for high energetic surfaces, an increased roughness leads to a decreasing water contact angle and, as a consequence, to an increased surface free energy. However, it remains unclear why high-heat-treated or plasma-treated vials did not re-contaminate in the meantime. In the following, it will be dealt with the surface contamination issue in more detail.

In simple terms, any surface will aim to minimize its free energy. According to Equation 9, the change in the Gibbs energy (dG) is proportional to the change in the surface area (dA) and the surface tension or surface energy (γ), respectively.

$$dG = \gamma\, dA \tag{9}$$

Since liquids minimize their Gibbs energy by assuming a globular shape when possible (e.g. at zero gravity), solids as a rule lower their energy by attraction and further deposition of (organic) contamination. Pharmaceutical packaging containers are usually washed before sterilization and filling to reduce particulate as well as unspecific surface contamination [1]. As already assumed for the situation of borosilicate glass vials, inorganic salt deposits are thereby removed, which leads to a SiO_2-rich surface [23]. However, it was also described above that the high energetic glass surface is then particularly susceptible to air or water-borne hydrophobic organics. To substantiate this theory, pretreated glass samples (washed with water and heat sterilized at 250°C) were analyzed in ToF-SIMS in order to gain some indication of unspecific air or water-borne contamination on the topmost glass surface. ToF-SIMS is an extremely surface sensitive method due to its sampling depth of only the first one to two monolayers [40]. Although the method is not absolutely quantitative, changes in the relative signal intensities of different chemical species indicate variations of the species' surface concentrations [40]. It is apparent from Figure 6a that our ToF-SIMS spectra revealed a high mass resolution. $^{27}Al^+$, for example, can be clearly resolved from $^{12}C_2H_3^+$.

The signals from the outermost glass surface were compared with corresponding signals from an essentially salt free IgG1 layer on the glass surface. Thereby, a proteinaceous origin of the adherent contamination should be assessed. Exemplary mass spectra of the washed and heat sterilized glass surface (Figure 6a) and the bulk protein on glass (Figure 6b) are shown in detail around m/z of approx. 27 - 28 and 44 - 45.

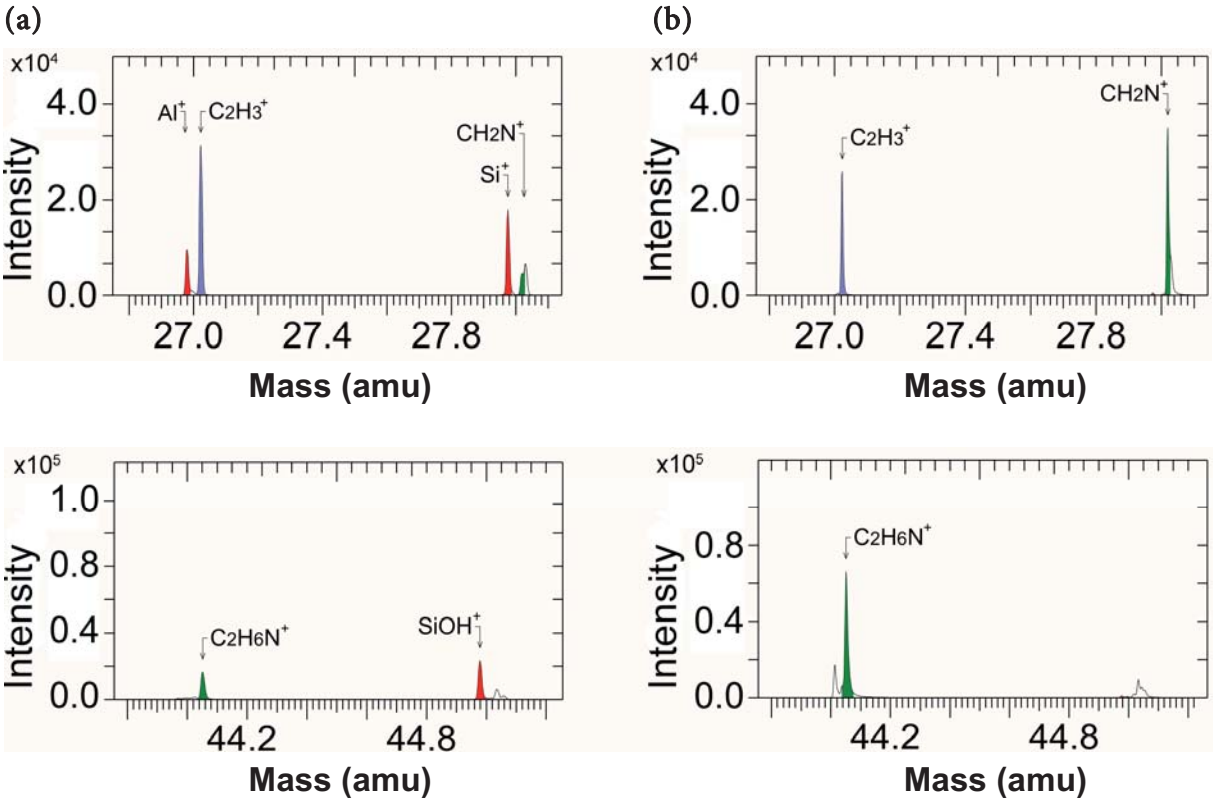

Figure 6: Selected ToF-SIMS spectra sections of (a) the washed and heat sterilized glass surface and (b) the thick IgG1 film without buffer salts put on the glass surface.

According to Figure 6a, characteristic glass components like Al^+, Si^+ and $SiOH^+$ (red peaks) dominate the ToF-SIMS spectra of the glass surface. In addition, fragments whose origin is not from the glass surface, as for instance $C_2H_3^+$, emerge. These fragments represent surface contamination [25] and may originate from volatile air or water-borne hydrocarbons (purple peak). Also, nitrogen-containing species (green peaks) were detectable with significant intensities, which allows the conclusion that deposits other than pure hydrocarbons are present on the glass as well. Traces from equipment cleaning agents, impurities in the ultrapure water, or even proteinaceous components are possible. Altogether, a broad spectrum of most diverse fragments was detected, but none of them is indicative of a definite source. Glass components are missing in ToF-SIMS spectra of the dried IgG1 bulk (Figure 6b). Nitrogen-containing fragments clearly dominate the spectra, as expected. However, $C_2H_3^+$ fragments are detectable in protein samples as well, which, in this case, are predominantly derived from amino acids. A comparison of the protein spectra with the spectra of the pre-washed and heat sterilized glass surface revealed indications of contamination of proteinaceous origin. However, the portion of nitrogen-containing fragments was relatively small, indicating that the majority of contaminants originated from unspecific aliphatic deposits.

3.2 Persistence of Plasma-Mediated Surface Hydrophilicity and Related IgG1 Adsorption Properties after Vial Storage

The influence of storage time on plasma surface-treated borosilicate glass vials and on the subsequent protein adsorption behavior was investigated. All vials were washed and heat sterilized (reference vials). At time point "0", the sample vials were plasma-treated for 10 or 30 sec. The sample vials as well as reference vials were sealed with gray butyl stoppers and stored at ambient conditions in the dark. Subsequently, the adsorbed amount of protein after 24 h incubation from a 2 mg/ml / pH 7.2 IgG1 solution was measured. As shown in Figure 7, IgG1 adsorption on the untreated reference was in the area of 2.3 mg/m^2. In contrast, plasma cleaning at both durations was effective at reducing the adsorbed mass by almost a factor of five. The cleaning effect only sustained for a short time, as the protein adsorption tendency increased quickly within the first two weeks of storage. The adsorbed amount approached the value of the untreated reference after an eight-week storage. Also, the non-plasma-treated reference vials showed a continuous trend to increased protein binding during storage. Thus, although not explicitly measured, storage gives rise to a change of the surface properties. A phenomenon of surface hydrophobicity recovery was recently described for, among others, glass surfaces by Mills and Crow, which they denoted as "dark hydrophilic to hydrophobic process". They ascribed this effect to contamination by airborne hydrophobic organics [10].

As outlined in Chapter 1, multiple factors lead to and govern protein adsorption phenomena. The most important ones are electrostatic attraction, hydrogen bonds, hydrophobic interactions, dispersive interactions, and a driving force on the basis of structural

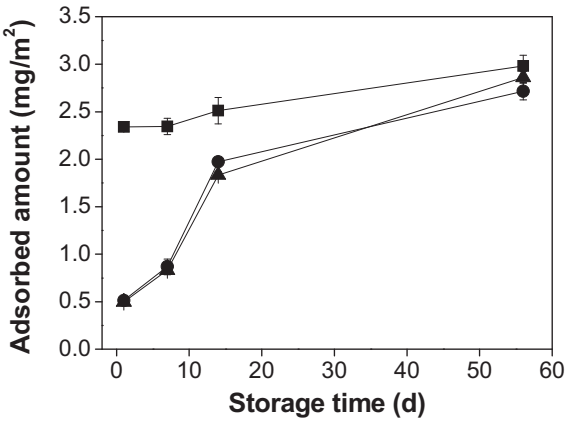

Figure 7: Persistence of the plasma cleaning effect upon storage of borosilicate glass vials; pre-washed and heat sterilized glass containers (■) (= reference) were plasma-treated for 10 sec. (●) or 30 sec. (▲) and stored in the dark at room temperature; adsorbed amount of IgG1 measured after 24 h incubation with 2 mg/ml IgG1 pH 7.2 in PBS (n = 3).

alterations due to decreased protein stability. On the part of the glass surface, ionic interactions are mediated by dissociated hydroxyl groups of the glass, by surface-bound low molecular weight ions from the electrolyte solution or potentially by the glass-incorporated metal ions. As shown above, the adsorbed amount of protein is sensitive to alterations of the surface qualities, which were shown not to be stable over time. This problem could be solved by an alternative surface treatment and may even include the application of appropriate protein-repelling coatings to reduce adsorptive losses to the packaging surface. Relevant proposals are reviewed and evaluated elsewhere [41-44].

3.3 Tensiometric Investigation of Protein-Covered Glass Surface

Tensiometric measurements were carried out on adsorbed protein films deposited from IgG1 solutions of the different pH values 4.0, 7.2, and 8.6, which equal the pH of maximum adsorption at 170 mM ionic strength, the pH of the standard formulation, and the IEP of the IgG1, respectively (see Chapter 4). After immersing them 2 times in correlating blank buffer, the glass samples with adsorbed protein were washed twice in deionized water. The purpose was to remove an excess of unbound protein and buffer salts, respectively. Contact angle measurements of the wet hydrated protein films would have been only reflective of the water present on the analyzed surface, water as a measuring liquid would have completely wet, and the measurements therefore would not have led to success [45]. Thus, adsorbed protein was dried, taking the risk of inducing structural alterations through the removal of the hydration shell (see Chapter 7). In our tensiometric measurements, diiodomethane was used as an unpolar test liquid. In this regard, structural changes of the protein may also arise from the contact with organic liquids during measurements [45]. However, by means of the following measurements, only a basic correlation between surface free energies and the mass of adsorbed IgG1 on the glass surface was to be evaluated. The resulting surface free energies and the corresponding adsorbed IgG1 quantities are shown in Figure 8a, and the measured values are listed in Table 3.

In contrast to the non-incubated reference sample, the protein-covered glass surfaces are accompanied by a virtually complete disappearance of the polar surface energy fraction, whereas the dispersive part remains almost unchanged. This indicates that, among others, the large number of hydrogen-bridge-donating hydroxyl functions of the glass surface has extremely decreased after the surface was covered by proteins. The lack of γ_s^p also indicates the absence of ionic as well as hydrogen bonding entities on the part of the protein in adsorbed and dried state. This is not surprising since air represents a hydrophobic medium itself, and the proteins adapted their structure to this new circumstance. In other

Table 3: Dynamic advancing contact angles, calculated polar (γ_s^p) and dispersive components (γ_s^d) of the surface free energy, surface polarity parameters (γ_s^p / γ_s) of IgG1 films adsorbed from different formulation pH (24 h) on glass vial surface.

	Dynamic adv. CA (°) H_2O / CH_2I_2	γ_s^p (mN/m)	γ_s^d (mN/m)	γ_s^p / γ_s	IgG1 adsorbed (mg/m²)
Incubation at pH 4.0	98.0 / 7.70	0.0	49.5	0.000	4.78 ± 0.08
Incubation at pH 7.2	89.4 / 7.10	0.3	49.6	0.006	2.54 ± 0.10
Incubation at pH 8.6	87.1 / 0.00	0.5	50.8	0.010	1.65 ± 0.11
Reference (blank glass washed and heat sterilized)	46.4 / 13.3	16.2	49.1	0.248	n/a

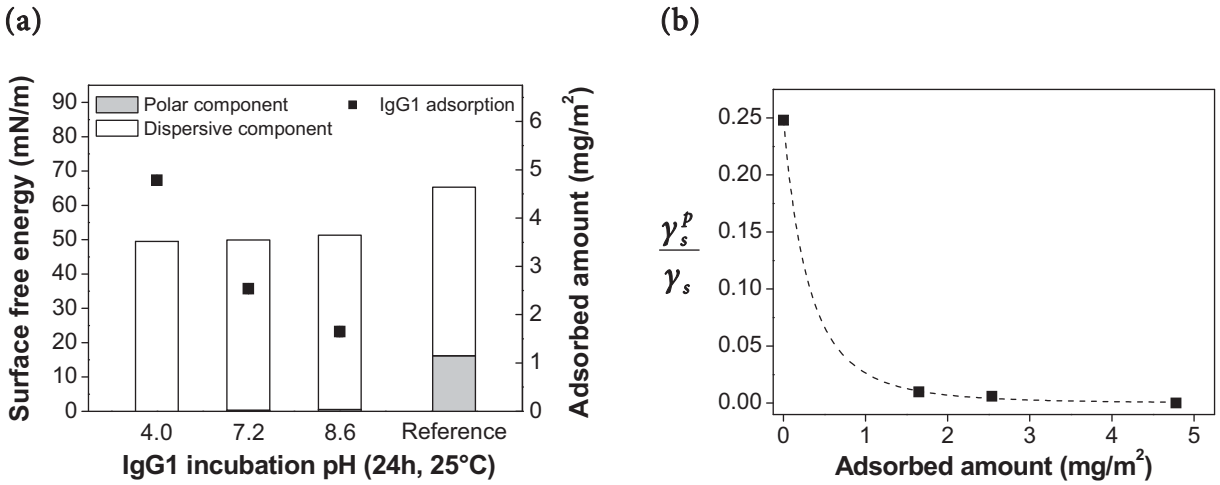

Figure 8: (a) Surface free energy of adherent protein layers (bars) and correlating surface concentrations of IgG1 (■) on borosilicate glass after incubation at the declared pH. (b) Surface polarity (■) as a function of total adsorbed amount of IgG1 including a power function fit.

words, the proteins underwent structural alterations, and predominantly hydrophobic residues were presented towards the atmosphere. However, a residual portion of γ_s^p obviously remains available after adsorption at pH 7.2 and 8.6. This indicates that either the degree of protein unfolding was lower than at pH 4.0, namely with preservation of a residual polar shell of the protein, or the glass surface itself contributed to the measured surface free energy. Although atomic force microscopy of dried IgG1 layers, adsorbed from the respective pH values on glass (see Chapter 7), revealed no homogeneous surface coverage at any pH, it demonstrated that the surface coverage at pH 4.0 was higher than at the other pH conditions. This becomes apparent from the adsorption values of IgG1 at the respective pH as well, which are depicted in Figure 8a.

The relationship between surface polarity and the adsorbed amount of IgG1 on the glass surface is illustrated in Figure 8b. All the surface polarity values for protein-covered samples are in the lower range, but a clear increase can be observed with less protein bound. The assumed resultant curve progression is approximated by a nonlinear curve fit. Thus, according to the power function, only for protein surface concentrations less than approx. 1 mg/m^2 does the surface polarity distinctly increase in order to reach a value of approx. 0.25 for the non-covered blank. In contrast to the findings of Addesso and Lund [45], the extent of IgG1 bound on glass surface may be predicted rather well by means of the measured surface free energy. However, in order to prove the validity of this correlation, some more data points in the lower protein coverage range would have to be determined. Davies *et al.* described the correlation of variable amounts of BSA on different surface types and their water contact angle [40]. They found increasing contact angles on glass with increasing protein coverage as well. Since they investigated dried protein layers, pronounced unfolding of the proteins was also likely. It was proposed that the change in advancing contact angle is not necessarily a linear function of the quantity of adsorbed material [38]. Rather similar advancing contact angle values were obtained for a wide range of different degrees of surface coverage. Johnson and Dettre [38] suggested that with the adsorption of a lower energy phase (protein) on a higher energy phase (glass), the aqueous advancing contact angle reaches the value of the lower energy phase already at approx. 10% surface coverage. This again is in accordance with our findings, as indicated by Figure 8b. For the samples investigated, it could be shown that with decreasing IgG1 surface concentrations, and, consequently, decreasing surface coverage, the surface polarity only changes marginally. Furthermore, an appreciable surface polarity increase does not occur before surface coverage reaches a certain limit.

3.4 Influence of pH on Glass Properties Affecting IgG1 Adsorption

As will be shown in Chapter 4, a characteristic correlation between the protein formulation pH and the adsorbed quantity of IgG1 on the glass vial internal surface exists. Usually, when the influence of pH on protein adsorption is investigated, mainly variable protein characteristics like charge and structure are taken into consideration. Besides, for example, charge, polarity, stability, and aggregation tendency of the proteins, also the surface itself may be affected by heterogeneous solution conditions, contributing to the overall adsorption result. Concerning the glass surface properties, one of the most critical formulation parameters affecting adsorption is probably the pH value. Therefore, the question arose whether and to what extent pH affected the glass surface in terms of charge, composition, and stability of the topmost surface layer during the 24 h incubation step.

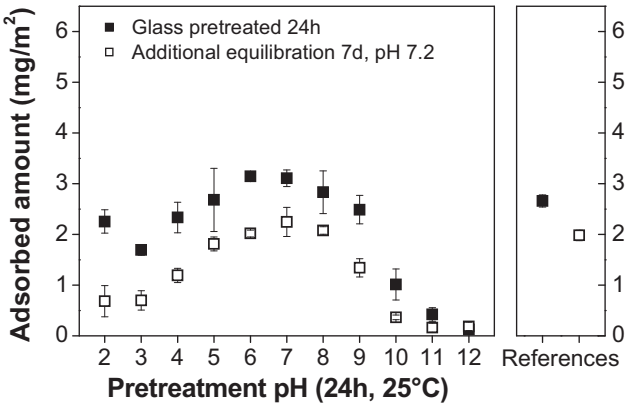

Figure 9: Adsorption profiles of IgG1 (2 mg/ml in PBS pH 7.2, 24 h) depending on the glass pretreatment in PBS buffer of different pH for 24 h (■) and with an additional equilibration step at pH 7.2 for 7 days in PBS buffer subsequent to pH pre-conditioning (□); references: adsorption in not pre-conditioned but washed and heat sterilized vials (■) and washed and heat sterilized vials solely equilibrated at pH 7.2 for 7 days in PBS (□) (n = 3).

In the following, the IgG1 adsorption profile from a 2 mg/ml IgG1 solution pH 7.2 in borosilicate glass vials, pre-conditioned with protein-free formulation buffers in the range from pH 2 - 12 for 24 h, was determined. This preincubation refers to the conditions the glass faces in the course of the standardized adsorption experiment. Before the glass vials were subsequently filled with a protein-containing solution, they were rinsed with ultrapure water. Figure 9 depicts the adsorbed protein quantities as a function of the pretreatment pH. Hardly any effect was observed for vials which were pre-conditioned at pH 7. Adsorption was even slightly higher than for the untreated reference. Towards both higher and lower pH values of preincubation, decreased IgG1 adsorption could be observed. The only data point which does not properly fit in a bell-shaped curve is that of the preincubation at pH 2.0, where the subsequent adsorption value was found to be exceptionally high. A similar bell-shaped curve was obtained when IgG1 adsorption was investigated as a function of the pH value of the protein formulation (Figures 3 and 8, Chapter 4). It seems probable that pH-dependent alterations of the glass properties during incubation may have contributed to these IgG1 adsorption results as well.

It was mentioned above that glass, when in contact with an aqueous solution, usually forms a hydrated gel layer in the surface-near region. Within this well-hydrated layer, the preincubation pH might have been preserved, which might have subsequently influenced the protein behavior in contact with the surface. In order to exclude this possibility, an additional 7 day equilibration step at pH 7.2 was conducted after the pH pretreatment. As already apparent from the reference samples, the equilibration step for 7 days at near-neutral pH is capable of decreasing the adsorbed amount of IgG1 significantly. The same trend was found for the pH-treated glass samples and the bell-shaped curve geometry was

maintained. Hence, it can be concluded that the pronounced adsorption-reducing effect, particularly at extreme pH values, does not arise from a pH memory effect within the hydrated gel layer of the surface-near region. This phenomenon rather originates from other factors concerning the glass properties.

3.4.1 Influence of pH on the Elemental Glass Composition

Borosilicate glass represents a non-inert material whose surface structure and composition may be affected and altered by different solution parameters, as already stated above. For the evaluation of glass corrosion, a possible influencing parameter during the 24 h incubation procedure, i.e. the effect of pH on the chemical composition of the glass surface, was analyzed by ToF-SIMS depth profiling. In Figure 10, glass depth concentration profiles within the top 15 nm of the most important glass components are shown after a corresponding pH pretreatment. Besides the network formers silicon (^{30}Si) and boron (^{11}B), also the additional components like sodium (^{23}Na), potassium (^{39}K), calcium (^{40}Ca), and aluminum (^{27}Al) were analyzed (see the monitored isotopes in parentheses). For better clarity, in each curve only a small fraction of the measured data points is depicted, indicated by the respective symbols. According to the theory, the glass network dissolves in contact with liquids of highly alkaline pH. Thus, a pristine surface is formed, which, in our case, served as pure glass reference. At the beginning of the measurement, it took some seconds, correspondingly a fraction of a nanometer, until equilibrium measurement conditions were reached and surface contamination of any origin was removed. For none of the elements depicted in Figure 10, the surface concentrations obtained after the pH 7.2 incubation deviated markedly from the surface concentrations obtained after the pH 12 incubation. Thus, as expected, a pronounced alteration of the glass surface composition due to the contact with a buffered solution of pH 7.2 was not the case. However, the situation is somewhat different at lower pH values, where metal ions are usually dissolved out of the outermost glass surface in terms of a simple ionic exchange process. In Figure 10a, b, and d it is apparent that Na, K, and Al were depleted to a depth of approx. 2 - 3 nm. By contrast, the leaching effect for Ca (Figure 10c) is more distinct than for other metal ion types. Furthermore, it is remarkable that Ca concentrations do not reach reference values within the first 15 nm. This result is contrary to the findings of Koenderink *et al.* who described a lower extent of divalent cations leaching, as well as smaller depletion depths for Ca than for Na [20]. However, in their studies, they used sodium silicate glasses containing earth alkaline oxides, instead of borosilicate glass. Moreover, their leaching conditions were pH 6.9 (non-constant) and 60°C. In general, between pH 1 and 9, the rate of ion exchange was postulated to only slightly depend on pH [20], whereas in our case, the effect was accelerated more at pH 2 than at pH 7.2. That means the kinetics

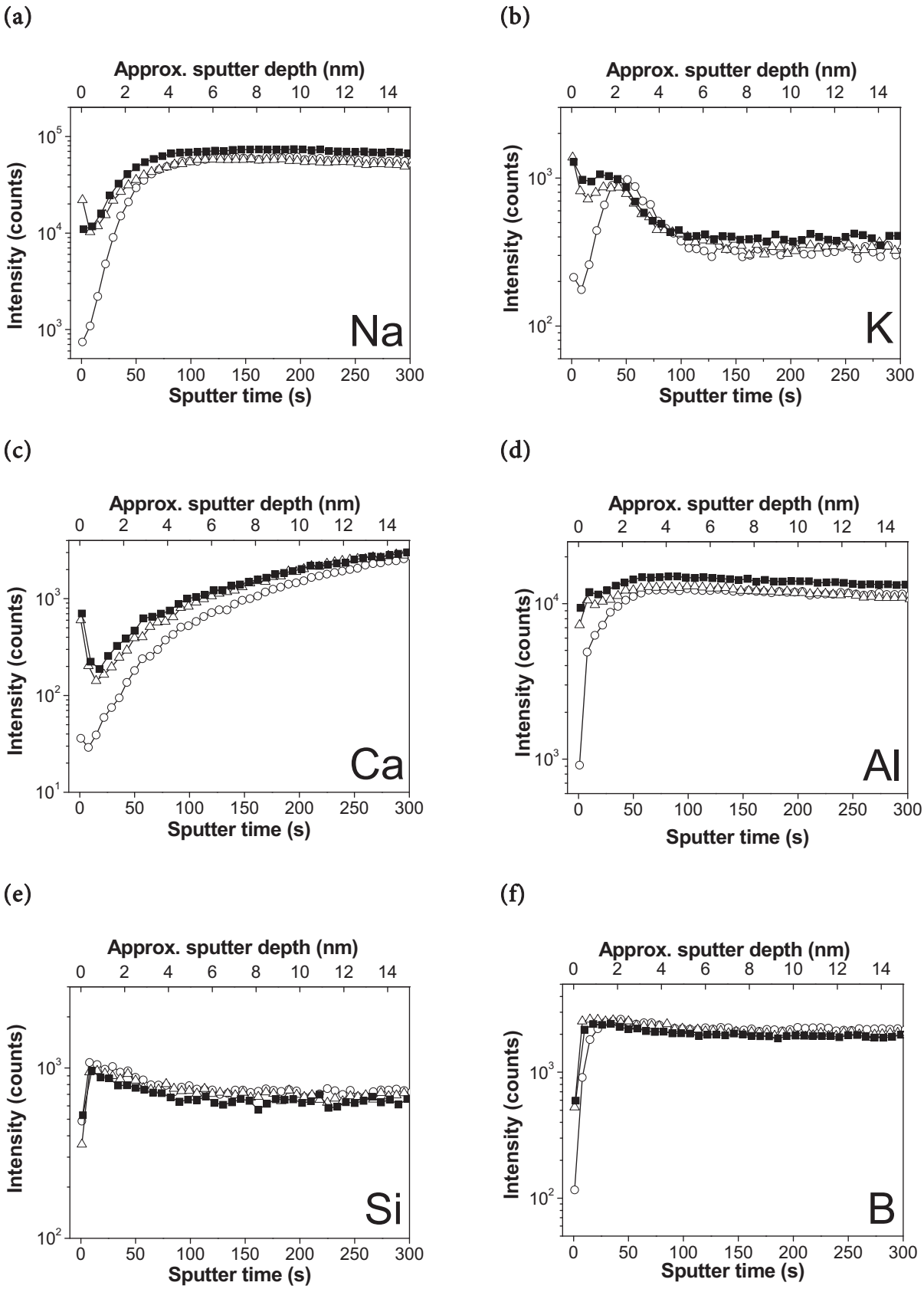

Figure 10: ToF-SIMS depth profiling (approx. 15 nm) on borosilicate glass wall; vials were pre-washed with ultrapure water, heat sterilized and incubated for 24 h with PBS buffer of pH 7.2 (■), 2.0 (○), or 12.0 (△); ToF-SIMS peak areas of selected elements are depicted time and depth-dependent in (a) - (f).

of the interdiffusion process on borosilicate glass clearly changed with pH. By contrast, hardly any or no influence of solution pH is observed on the surface content of the network formers boron and silicon (Figure 10e and f). It is well known that the glass network is not attacked by acids, but rather a gel layer forms whose thickness grows diffusion-controlled [23].

Protein adsorption on glasses of different elemental composition has not been studied yet. Also, in our case, the particular correlation of ionic glass composition and IgG1 adsorption propensity was not investigated in detail. In this regard, it could be clearly shown that the composition of the surface-near region of the glass vials is not stable during the 24 h adsorption experiment, depending on pH. Hence, the possibility of a direct influence of the surface properties on the adsorption characteristics cannot be ruled out. There is probably an interference of protein adsorption and glass matrix dissolution in the alkaline region and one can assume that the establishment of the adsorption equilibrium is thereby counteracted. Decreased adsorption quantities would be the consequence, as observed for the adsorption of IgG1 at highly alkaline conditions (Figure 8, Chapter 4). However, a near-complete decline of adsorption was also observed at pH 7.2, when the glass has only been preincubated at high pH before (Figure 9). Accordingly, the concurrency of adsorption and corrosion cannot be solely accountable for the observed adsorption behavior. Notwithstanding the above, also the depletion of glass components at acidic formulation pH shown above may at least partially affect protein adsorption. This, however, was not examined in detail in the context of this study.

Besides, the resistance of borosilicate glass was also examined at pH 4.0 in order to gain knowledge of the pH dependency of interdiffusion. In Figure 11, ToF-SIMS depth profiling results on borosilicate glass are shown for an incubation term of 30 days with PBS buffer pH 4.0 and are compared with the non-incubated reference. Qualitatively, the findings are in accordance with the results shown before. Within the surface-near region, concentrations of Na, Ca and Al have noticeably decreased after the pH 4.0 treatment. The depletion of these elements is confined to the first nanometer, except for Ca whose surface concentration was reduced within the uppermost 3 - 4 nm. The effect for K is not as distinct as compared to the effect for the other metal ion types. Its initial concentrations are less than those of the reference, but they exceed them within the first nanometer until an equilibrium bulk concentration is reached after 1.5 nm. So far, no clear explanation for this phenomenon exists. Possibly, ionization probabilities for K ions of the different glass samples changed within the first 30 sec. of the measurement and caused fluctuating SIMS intensities. Altogether, the observed effects on the glass composition within 30 days are much less pronounced than after incubation at pH 2 for merely 24 h. This again proves the pronounced dependency of the interdiffusion effect on pH (see above).

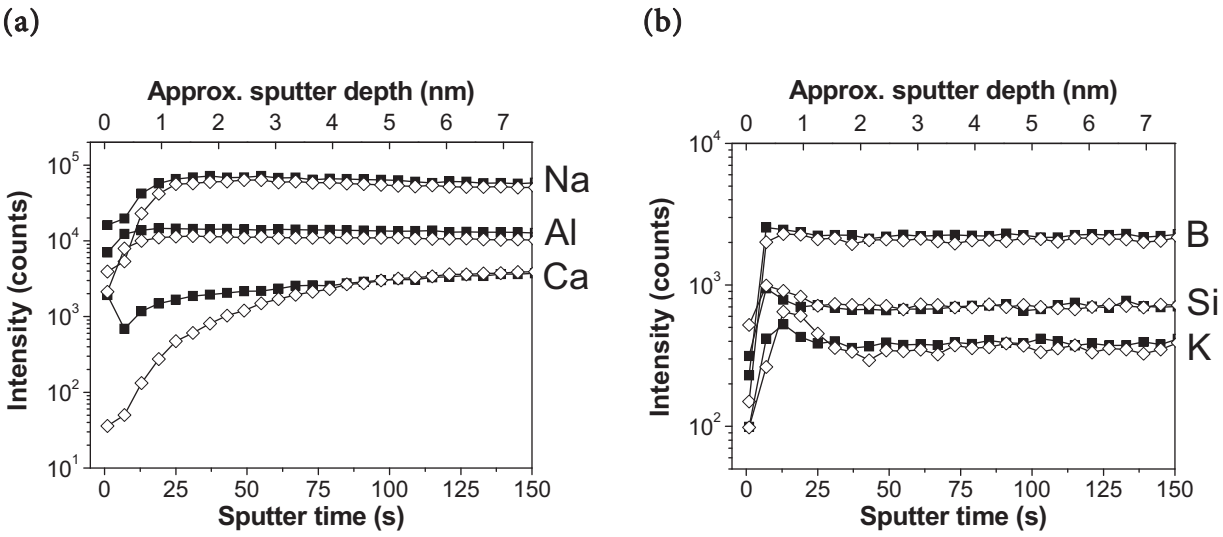

Figure 11: ToF-SIMS depth profiling on borosilicate glass wall after 30 days in pH 4.0 PBS buffer (◇) and on the non-incubated reference (■); beforehand, vials were pre-washed with ultrapure water and then heat sterilized; ToF-SIMS peak areas of selected elements are depicted time and depth-dependent in (a) and (b).

For the network formers Si and B, a total consistency of element concentrations in the surface-near region of the pH-treated sample and the reference sample was detected. This repeatedly indicates that the glass network is not affected at acidic pH.

As a conclusion, it can be stated that corrosion phenomena are likely to play a role in the pH-dependent adsorption of proteins on borosilicate glass. However, the immediate effect has to be investigated in more detail. Acidic buffer solutions were shown to cause corrosion phenomena of the same kind, but the degree of corrosion highly depended on the absolute pH value.

3.4.2 Influence of pH on the Glass Surface Free Energy

The above results reveal that the contact of the borosilicate glass surface with buffered solutions of different pH seriously affects the amount of surface-bound IgG1. This has been discussed within the context of changes in the glass surface composition, which, however, could not be totally proven. But, in the previous sections, the amount of protein adsorbed was clearly shown to be a function of the surface free energy (see 3.1). It stands to reason that the pH value of the buffer solutions may have an effect on the surface free energy as well, which, however, has to be demonstrated. Figure 12a depicts the surface free energy changes of pH pre-conditioned borosilicate glass vials in comparison with the not pretreated reference vials. The surface free energy γ_s appreciably increased for very

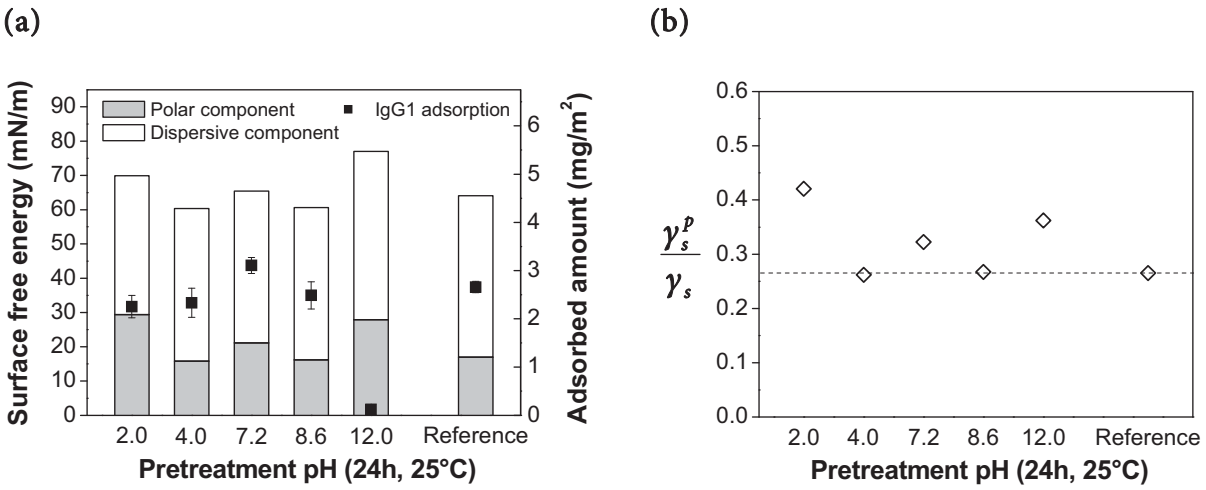

Figure 12: (a) Surface free energy of additionally pH-pretreated borosilicate glass vials at the declared value; reference values are related to the pre-washed and heat sterilized vials; surface free energy divided into a polar and a dispersive component (bars); overlaid is the resulting amount of IgG1 adsorbed from the standard formulation pH 7.2 (n = 3). (b) Surface polarity (γ_s^p / γ_s) as a function of pretreatment pH value; dashed line indicates the polarity value of the reference.

high and very low pH values of glass preincubation, particularly through a pronounced increase of the polar part. Accordingly, the surface polarity increased as well. Previous results already showed that γ_s^p is more subject to change than γ_s^d with regard to different surface states. After the vial preincubation with pH 7.2 buffer, however, both γ_s^p and γ_s did not follow this trend, and higher values than for the reference vials were observed. The amount of IgG1 adsorbed at pH 7.2, the standard formulation pH, is plotted in Figure 12a. As previously depicted in Figure 9, glass preincubation at extreme pH values leads to a decreased protein adsorption from an equal protein solution. This tendency appeared to be very pronounced for pH 12 but less for pH 2. Hardly any change in adsorption was observed for both pH 4.0 and pH 8.6. The already mentioned exceptional increase in surface free energy after the pH 7.2 treatment was not accompanied by a decreased, but by a slightly increased adsorption propensity compared to the reference.

It was shown above that adsorbed quantities correlated best with the surface polarity of the glass. In Figure 12b, the calculated surface polarity parameter is plotted against the pre-conditioning pH. By pretreating vials with an extremely high or low-pH buffer, the surface polarity increased strongly compared to the reference. This goes along with a decrease in IgG1 adsorption (Figure 12a), which is in line with the aforementioned correlation. Both pH 4.0 and pH 8.6 did not cause any change in surface polarity. Moreover, none of the pH values investigated led to a lower polarity than it had been determined for the reference samples. This indicates that at least no (hydrophobic) contamination was additionally deposited on the surface by the buffer. On the contrary, it is presumed that

highly acidic and highly alkaline solutions were effective in increasing surface polarity by the removal of existing contaminants. It was shown above that IgG1 adsorption after pH 2.0 pretreatment was lower than the reference level, but higher than it was expected due to the high surface polarity. Furthermore, the amount of IgG1 adsorbed after the pH 7.2 pretreatment is not in line with the expected value either. An increased surface polarity would have implied a pronounced decrease in adsorption, which, however, was not the case. With the studies conducted so far, a satisfactory explanation for both observations cannot be given. Finally, the adsorption results after pH pre-conditioning may be explained as follows. In alkaline solutions (> pH 9), a uniform dissolution of the glass was favored while an ion exchange was suppressed. Contamination, which had deposited on the outermost surface of the glass samples before, was thereby removed, and a pristine and highly hydrophilic glass surface resulted. In the moderate pH area, the glass composition was neither altered nor was contamination removed from the glass. Highly acidic pH values again promoted metal ion depletion of the glass surface (interdiffusion effect). However, it is questionable whether the adsorption process of proteins is influenced directly by an altered ionic composition of the glass. More likely, adsorption reduction is also due to a surface-cleaning effect by acids [21], by which organic depositions are largely removed. Thus, the results give rise to the conclusion that differences in IgG1 adsorption at uniform pH 7.2 after a pH-dependent pretreatment of the glass containers are most probably due to changes in the surface polarity, even though some measured adsorption results are not fully in line with the above stated polarity adsorption model established in 3.1. Moreover, it cannot be excluded that, during the storage of a pH-adjusted protein solution, cleaning or corrosion effects will interfere with the adsorption process and affect the adsorbed amount.

4 CONCLUSIONS

It could be shown that the adsorption of an IgG1 antibody on hydrophilic borosilicate glass and hydrophobic (siliconized glass and COP plastic) vial surfaces largely depends on the surface properties. The mass of protein adsorbed from a standardized IgG1 solution was found to be inversely proportional to the surface polarity (γ_s^p / γ_s), determined by dynamic advancing contact angle measurements. The elemental composition of the outermost surface layer of borosilicate glass is subject to change upon contact with acidic protein solutions. ToF-SIMS depth profiling confirmed the expected depletion of metal ions in the outermost glass surface upon contact with acidic buffer solutions. In this regard, the extent of ion leaching was found to increase with decreasing pH. A possible direct effect on adsorption was not investigated explicitly. The dissolution of the glass matrix in alkaline solutions could not be proven directly, but was deduced from the results of other investigations. In this regard, a preceding contact of glass with blank buffers of very high and very low pH values was shown to lead to a subsequent decrease in IgG1 adsorption from a uniform pH 7.2 protein solution. It is argued that the surface was cleaned from contamination through the preincubation step, being that the surface polarity significantly increased for both pH-extremes. Hydrocarbon-based organic surface contamination was found on the glass surface by static ToF-SIMS measurements. But a proteinaceous origin to some extent could not be entirely excluded. The source of contamination might be the water used for vial washing, since surface polarity decreased with a precedent water washing step, followed by vial sterilization in moist or dry heat. However, deposition from the laboratory air seems more likely. Besides the cleaning effect of aqueous solutions of extreme pH, also heating up to 600°C and ambient-pressure Ar plasma treating have shown to be well suited for removing surface contaminants and, thus, restoring the highly hydrophilic glass surface. However, both the highly energetic surface state and the associated effect of decreased IgG1 adsorption were evanescent. It could be observed that the amount of surface-adsorbed IgG1 increased with storage time of borosilicate glass vials in air. This equally applied for solely heat sterilized reference vials as well as for glass vials featuring a super-hydrophilic surface after cleaning with plasma. Finally, it can be concluded that a highly hydrophilic container surface is ideal for minimizing adsorptive IgG1 losses. However, the studies also reveal that surface cleaning alone, like heating or plasma treating, cannot ensure an enduring low-binding effect.

5 REFERENCES

[1] Dean, D. A., Evans, E. R., Hall, I. H., Pharmaceutical packaging technology, (Taylor & Francis, London) Ed. 1, 2000.

[2] Haynes, C. A., Norde, W., Globular proteins at solid/liquid interfaces, *Colloids and Surfaces, B: Biointerfaces* **2** (1994) 517-566.

[3] Marsh, R. J., Jones, R. A. L., Sferrazza, M., Adsorption and displacement of a globular protein on hydrophilic and hydrophobic surfaces, *Colloids and Surfaces, B: Biointerfaces* **23** (2002) 31-42.

[4] Elwing, H., Welin, S., Askendal, A., Nilsson, U., Lundstroem, I., A wettability gradient method for studies of macromolecular interactions at the liquid/solid interface, *J. Colloid Interface Sci.* **119** (1987) 203-210.

[5] Mac Ritchie, F., Adsorption of proteins at the solid/liquid interface, *J. Colloid Interface Sci.* **38** (1972) 484-488.

[6] Malmsten, M., Ellipsometry studies of the effects of surface hydrophobicity on protein adsorption, *Colloids and Surfaces, B: Biointerfaces* **3** (1995) 297-308.

[7] Saga, K., Hattori, T., Characterization of trace organic contamination on silicon surfaces in semiconductor manufacturing, *Proc. - Electrochem. Soc.* **3** (2003) 136-149.

[8] Stingeder, G., Grundner, M., Grasserbauer, M., Investigation of surface contamination on silicon wafers with SIMS, *SIA, Surf. Interface Anal.* **11** (1988) 407-413.

[9] Reinhardt, K. A., Kern, W., Handbook of Silicon Wafer Cleaning Technology, (William Andrew Inc., Norwich) Ed. 2, 2008.

[10] Mills, A., Crow, M., A study of factors that change the wettability of titania films, *Int. J. Photoenergy* (2008) 1-6.

[11] Elwing, H., Protein absorption and ellipsometry in biomaterial research, *Biomaterials* **19** (1998) 397-406.

[12] Lechner, H., Die Kontaktwinkelmessung: Ein Verfahren zur Bestimmung der freien Grenzflaechenenergie von Festkoerpern, Kruess GmbH, Wissenschaftliche Laborgeraete, Hamburg (2007).

[13] Fowkes, F. M., Attractive forces at interfaces, *J. Ind. Eng. Chem. (Washington, D. C.)* **56** (1964) 40-52.

[14] Owens, D. K., Wendt, R. C., Estimation of the surface free energy of polymers, *J. Appl. Polym. Sci.* **13** (1969) 1741-1747.

[15] Stroem, G., Fredriksson, M., Stenius, P., Contact angles, work of adhesion, and interfacial tensions at a dissolving hydrocarbon surface, *J. Colloid Interface Sci.* **119** (1987) 352-361.

[16] Qadry, S. S., Roshdy, T. H., Char, H., Del Terzo, S., Tarantino, R., Moschera, J., Evaluation of CZ-resin vials for packaging protein-based parenteral formulations, *Int. J. Pharm.* **252** (2003) 207-212.

[17] Douglas, R. W., El-Shamy, T. M. M., Reactions of glasses with aqueous solutions, *J. Am. Ceram. Soc.* **50** (1967) 1-8.

[18] Jedlicka, A. B., Clare, A. G., Chemical durability of commercial silicate glasses. I. Material characterization, *J. Non-Cryst. Solids* **281** (2001) 6-24.

[19] Bange, K., Anderson, O., Rauch, F., Lehuede, P., Radlein, E., Tadokoro, N., Mazzoldi, P., Rigato, V., Matsumoto, K., Farnworth, M., Multi-method characterization of soda-lime glass corrosion. Part 1. Analysis techniques and corrosion in liquid water, *Glass Sci. Technol. (Frankfurt/Main, Ger.)* **74** (2001) 127-141.

[20] Koenderink, G. H., Brzesowsky, R. H., Balkenende, A. R., Effect of the initial stages of leaching on the surface of alkaline earth sodium silicate glasses, *J. Non-Cryst. Solids* **262** (2000) 80-98.

[21] Frischat, G. H., Reaktionen zwischen waessrigen Loesungen und Glasoberflaechen, *Physikalische Chemie der Glasoberflaeche*, Dunken, H., Wilhelmi, B., Eds. (Friedrich Schiller Universitaet, Jena, 1984) 5-21.

[22] Bange, K., Rauch, F., Surface hydration of glasses and compositional changes, *The Glass Researcher - Bulletin of Glass Science and Engineering* **9** (1999) 4-17.

[23] Dunken, H. H., Baeuer, P., Fink, P., Mueller, E., Tiller, H. J., Winde, H., Physical Chemistry of Glass Surfaces, (VEB Deutscher Verlag fuer Grundstoffindustrie, Leipzig, 1981) Ed. 1, 1981.

[24] Weisser, M., Bange, K., Sophisticated methods available to analyze glass corrosion, *The Glass Researcher - Bulletin of Glass Science and Engineering* **9** (2000) 16-21.

[25] Anderson, O., Scheumann, V., Rothhaar, U., Rupertus, V., Surface and depth profile analysis of insulating samples by TOF-SIMS, *Glass Sci. Technol. (Offenbach, Ger.)* **77** (2004) 159-165.

[26] Rabel, W., Einige Aspekte der Benetzungstheorie und ihre Anwendung auf die Untersuchung und Veraenderung der Oberflaecheneigenschaften von Polymeren, *Farbe und Lack* **77** (1971) 997-1005.

[27] Serra, J., Puig, J., Martin, A., Galisteo, F., Galvez, M., Hidalgo-Alvarez, R., On the adsorption of IgG onto polystyrene particles: electrophoretic mobility and critical coagulation concentration, *Colloid Polym. Sci.* **270** (1992) 574-583.

[28] Sousa, S. R., Ferreira, P. M., Saramago, B., Melo, L. V., Barbosa, M. A., Human serum albumin adsorption on TiO2 from single protein solutions and from plasma, *Langmuir* **20** (2004) 9745-9754.

[29] Mundry, T., Einbrennsilikonisierung bei pharmazeutischen Glaspackmitteln - Analytische Studien eines Produktionsprozesses, Thesis, 1999.

[30] Ogarev, V. A., Rudoi, V. M., Trapeznikov, A. A., Wettability of layers of poly(dimethylsiloxanes) applied on glass by Langmuir's method and obtained by adsorption from solution, *Izv. Akad. Nauk SSSR, Ser. Khim.* (1972) 2488-2493.

[31] Arai, T., Norde, W., The behavior of some model proteins at solid-liquid interfaces. 1. Adsorption from single protein solutions, *Colloids and Surfaces* **51** (1990) 1-15.

[32] Michiardi, A., Aparicio, C., Ratner, B. D., Planell, J. A., Gil, J., The influence of surface energy on competitive protein adsorption on oxidized NiTi surfaces, *Biomaterials* **28** (2006) 586-594.

[33] Schwarzenbach, M. S., Reimann, P., Thommen, V., Hegner, M., Mumenthaler, M., Schwob, J., Guentherodt, H. J., Topological structure and chemical composition of inner surfaces of borosilicate vials, *PDA J. Pharm. Sci. Technol.* **58** (2004) 169-175.

[34] Janczuk, B., Zdziennicka, A., A study on the components of surface free energy of quartz from contact angle measurements, *J. Mater. Sci.* **29** (1994) 3559-3564.

[35] Englaender, T., Wiegel, D., Naji, L., Arnold, K., Dehydration of glass surfaces studied by contact angle measurements, *J. Colloid Interface Sci.* **179** (1996) 635-636.

[36] Lamb, R. N., Furlong, D. N., Controlled wettability of quartz surfaces, *J. Chem. Soc. , Faraday Trans. 1* **78** (1982) 61-73.

[37] Schneider, M., Boehm, H.-P., Versuche zur Hydrolyse der Siloxan-Bindungen an Siliciumdioxid-Oberflaechen, *Kolloid-Zeitschrift und Zeitschrift fuer Polymere* **187** (1962) 128-134.

[38] Johnson, R. E., Jr., Dettre, R. H., Wettability and contact angles, *Surface Colloid Sci.* **2** (1969) 85-153.

[39] Tamai, Y., Aratani, K., Experimental study of the relation between contact angle and surface roughness, *J. Phys. Chem.* **76** (1972) 3267-3271.

[40] Davies, J., Nunnerley, C. S., Paul, A. J., A correlative study of the measurement of protein adsorption to steel, glass, polypropylene, and silicone surfaces using TOF-SIMS and dynamic contact angle analyses, *Colloids Surf. , B* **6** (1996) 181-190.

[41] Holmberg, K., Control of protein adsorption at surfaces, *Encyclopedia of Surface and Colloid Science*, Arthur T. Hubbard, Ed. (Marcel Dekker, Inc., USA, 2002), 1242-1253.

[42] Ostuni, E., Chapman, R. G., Holmlin, R. E., Takayama, S., Whitesides, G. M., A Survey of Structure-Property Relationships of Surfaces that Resist the Adsorption of Protein, *Langmuir* **17** (2001) 5605-5620.

[43] Ademovic, Z., Klee, D., Kingshott, P., Kaufmann, R., Hocker, H., Minimization of protein adsorption on poly(vinylidene fluoride), *Biomol. Eng.* **19** (2002) 177-182.

[44] Bluemmel, J., Perschmann, N., Aydin, D., Drinjakovic, J., Surrey, T., Lopez-Garcia, M., Kessler, H., Spatz, J. P., Protein repellent properties of covalently attached PEG coatings on nanostructured SiO2-based interfaces, *Biomaterials* **28** (2007) 4739-4747.

[45] Addesso, A., Lund, D. B., Influence of solid surface energy on protein adsorption, *J. Food Process. Preserv.* **21** (1997) 319-333.

Chapter 4

Influence of the Protein Formulation on IgG Adsorption to Vials

Abstract

It was the aim of this work to investigate the influence of formulation parameters like pH and ionic strength as well as of common excipients on the adsorption of IgG primarily to borosilicate glass vials. Through the response of IgG to changing conditions, basic knowledge should be gained on the adsorption mechanism and the driving forces of the adsorption process. The charge characteristics of IgG and glass surface were determined by isoelectric focusing and electrokinetic measurements. It could be shown that IgG adsorption highly depends on the formulation pH. Likewise, ionic strength had a large impact on the adsorption process, whereas the final adsorption result changed subject to the prevailing pH. The amount of IgG adsorbed, being a function of pH and ionic strength, was demonstrated to result from an interplay of attractive and repulsive electrostatic interactions between protein molecules and the glass surface as well as among the adsorbed protein molecules. The pH of a minimum ion uptake in the adsorption boundary, which, as a rule, indicates beneficial adsorption conditions in terms of charge - charge interactions, was calculated from electrokinetic measurements. The value coincided well with the adsorption maximum determined from adsorption experiments on glass vials. Further adsorption experiments were conducted in the presence of excipients, stabilizing via preferential exclusion. At pH 4, the presence of Na_2SO_4 gave rise to a stronger increase in adsorption than NaCl at an otherwise equal ionic strength. Compared with this, no difference was observed at e.g. pH 7.2 and 8.6. Various sugars and polyols only had a marginal effect on IgG adsorption, except for trehalose and sorbitol, which slightly but significantly increased adsorption at pH 7.2. Protein adsorption in the presence of nonionic surfactants (polyoxyl 35 castor oil, polysorbate 80, polysorbate 20, and poloxamer 188) mainly decreased with increasing concentrations, whereas the efficiency of adsorption prevention increased with increasing hydrophobicity of the surfactants. The amount of absolute adsorption reduction remained constant for the pH values investigated. In summary, it can be stated that IgG adsorption on borosilicate glass is to a large extent mediated by electrostatic interactions. However, at least in part, the contribution of other driving

forces like hydrophobic interactions or surface-induced structural alterations at the mostly hydrophilic glass surface seems probable.

1 INTRODUCTION

Except for specific interactions of protein molecules with surface groups, the surface contributes to the overall protein adsorption process mainly through an energy gain from dehydration, as well as through an ion transfer and an overlap of its electrical field with that of the proteins [1]. Hydrophobic dehydration often exceeds the strength of electrostatic effects [2]. A pronounced surface hydrophobic effect for pharmaceutical glass containers, arising from the surface hydrophobicity and significantly affecting the adsorption behavior of IgG1, is shown in Chapter 3. Electrostatic interactions, the second major driving force, highly depend on the charge properties of both protein and surface. Charges are to a great extent influenced by factors such as pH and ionic strength (*I*). Hence, the protein formulation is of great importance. Stable protein formulations often include the addition of stabilizing excipients [3,4]. Since structural alterations of the proteins can significantly affect their interfacial behavior, the influence of those stabilizing excipients on protein adsorption is also of particular interest. In adsorption studies of IgG and other proteins, the solvent conditions pH and ionic strength [5-8], as well as sorbent surface properties, such as electrical charge density and hydrophobicity [9,10], have often been used as variables to get information on the driving forces and the adsorption mechanism. With the example of IgG adsorption on hydrophilic and hydrophobic silica, the most important factors that are typically affected by pH and ionic strength have been the adsorption kinetics, the equilibrium adsorbed amount, as well as the degree of adsorption irreversibility [11]. Shifts in pH and ionic strength have also been described to affect the structural state of a protein [10,12,13], which, in addition, may lead to differences in the protein adsorption characteristics. These structural considerations are discussed separately in Chapter 7.

It is a common rule that protein adsorption on hydrophilic surfaces is for the most part governed by charge - charge interactions. As already mentioned above, protein adsorption on a charged surface goes along with an overlap of the electrical double layers of the solvated sorbent surface and the protein. According to our expectations, adsorption, on the one hand, increases through electrostatic attraction in case both the protein and the surface carry a different (net) charge. On the other hand, adsorption becomes more adverse with increasing charge of the same sign [14]. In the latter case, or if either one of the "partners" holds a pronounced charge preponderance, a strong net charge and accord-

ingly a strong electrostatic potential is formed in the interfacial region, which is energetically unfavorable [2]. For judging the electrical state of a protein and a sorbent surface, the zeta potential (ζ) is of utmost importance. It corresponds with the electric potential in the interfacial double layer at the location of the slipping plane versus a point in the bulk liquid away from the particle, and controls the charge - charge interaction between colloids. The formation of the electrical double layer on colloids or other surfaces is largely caused by the dissociation of covalently bound acidic or basic surface groups and/or specific adsorption of low molecular weight ions or other charged species from the surrounding solution due to dispersion forces, ion exchange, Lewis-acid-base reactions, and more [14,15]. This way, a measureable charge even on uncharged surfaces without dissociable groups, such as plastic polymers, may result [16]. First of all, the zeta potential is governed by the chemical nature of the respective material. For proteins, especially the amino acid composition of the molecule surface is determinative, whereas for glass it is the chemical composition of the outermost surface layer. With respect to colloidal systems, possible influencing factors are size and shape of the dispersed phase [17]. Within a common protein formulation, important decisive parameters for ζ are ionic strength, viscosity, temperature, and pH. Regarding the latter, the concentration of protons has the highest influence on the zeta potential, due to their small dimensions and their high charge density [15]. Neutral salts like NaCl contribute to the ionic strength and decrease ζ through double layer compression [16]. Explicitly, the Debye length (κ^{-1}), which is often referred to as the thickness of the double layer, depends on the factor $1 / \sqrt{I}$ (see Equation 4).

In colloids, zeta potentials are accessible from electrokinetic measurements [18,19]. Within the scope of this work, zeta potentials were calculated for borosilicate glass and IgG1 from electrophoretic mobility data. Generally, two basic approximation models relate the measured electrophoretic mobility (μ_e) to the zeta potential. In our case, glass particles exhibit relatively large dimensions compared to κ^{-1}. Accordingly, the Helmholtz-Smoluchowski equation (Equation 1) was used to compute the zeta potential,

$$\zeta = \frac{\mu_e \, \eta}{\varepsilon_0 \, \varepsilon_r} \tag{1}$$

where η equals the viscosity of the liquid, ε_0 and ε_r the permittivity of the free space and the relative permittivity of the medium, respectively [20]. For IgG1, the ratio of protein radius (a) and electrical double layer thickness (κ^{-1}) was largely decreased due to the small protein dimensions.

In the case of a thick double layer, with regard to particle diameter, the zeta potential is determined by applying the Hueckel approximation (Equation 2):

$$\zeta = \frac{3\,\mu_e\,\eta}{2\,\varepsilon_0\,\varepsilon_r} \tag{2}$$

Finally, the electrokinetic charge density (σ_e) can be derived from the zeta potential. The value of σ_e gives a measure of the amount of electric charges per surface area. For symmetric electrolytes, in which the absolute values of the signed units of charge, z_i, are the same for all ions present, the electrokinetic charge density on the surface of particles follows

$$\sigma_e = 4\,\frac{n^0 z\,e}{\kappa}\,sinh\left(\frac{ze\zeta}{2\,kT}\right) \tag{3}$$

where n^0 equals the number of ions per unit volume, z the valency on the ions, e the electron charge, k the Boltzmann constant, and T the absolute temperature [21]. In this regard, the coefficient κ is defined by the term

$$\kappa = \left(\frac{2000\,F^2 I}{\varepsilon_0\,\varepsilon_r\,RT}\right)^{1/2} \tag{4}$$

in units of m^{-1} [21]. F is the Faraday constant and R the gas constant. For diluted solutions of a strong electrolyte, the ionic strength I in $mol \cdot l^{-1}$ is defined by Equation 5 (2.2.1). The objective of measuring σ_e is its use for adsorption-specific mathematical calculations. For example, the amount of low molecular weight ions can be determined, which is integrated in the adsorption boundary and neutralizes unfavorable charge accumulation [18,22]. Further details will be provided in the Results and Discussion section (3.1.2).

Besides their simple contribution to ionic strength, salts can affect the stability of proteins in the formulation. Since most proteins are insufficiently stable in solution at room temperature and neutral pH [23], appropriate stabilizing agents are usually added to the pharmaceutical formulation. The effects of such excipients on proteins were extensively investigated by Arakawa, Timasheff, and coworkers. In general, salts can have either stabilizing or destabilizing effects on proteins [24], in so far as protein solubility and stability are affected by the preferential solvent exclusion properties of the respective salt type [25]. Preferential exclusion arises from an increase of the surface tension of water through the co-solvent, which e.g. also holds true for sugars [26]. Polyols stabilize the compact nature of a folded protein as the surface contact with the solvent becomes

thermodynamically more unfavorable [27]. Another group of stabilizers, namely non-ionic surfactants, are regularly added to protein formulations in order to increase the protein solubility and stability e.g. against shaking or stirring stress [28]. But they have also shown to reduce adsorptive losses to different surfaces [29-31].

It was the aim of these studies to investigate the influence of the most important formulation parameters and excipients on the adsorption behavior of IgG1, mainly on borosilicate glass. Moreover, from the response of the IgG1 to the particular adsorption conditions, basic knowledge on the adsorption mechanism and the driving forces of adsorption should be gained. Special attention was paid to the impact of pH and ionic strength. The influence of the preferential exclusion effect from salts or other stabilizing excipients, such as sugars and polyols, as well as the effect of four different nonionic surfactants on the adsorbed amount of IgG1 was investigated.

2 MATERIALS AND METHODS

2.1 Materials

2.1.1 Protein Formulation

For adsorption experiments a 2 mg/ml solution of IgG1 (MW ≈ 152 kDa) in 10 mM phosphate buffer and 145 mM NaCl (pH 7.2) was used, which was kindly provided by Merck Serono (Darmstadt, Germany). For ionic strength adjustment, the solution was dialyzed against a pure 10 mM phosphate buffer solution (NaH_2PO_4 and Na_2HPO_4 from Merck Chemicals, Darmstadt, Germany), using Vivaflow® 50 tangential flow filtration cartridges (Sartorius-Stedim Biotech, Goettingen, Germany) equipped with a 30,000 MWCO polyethersulfone (PES) membrane. The IgG1 concentration was determined by UV spectroscopy. Variable ionic strengths were adjusted by the addition of NaCl or Na_2SO_4 (Merck Chemicals, Darmstadt, Germany), followed by pH correction using 1M NaOH or HCl (Sigma-Aldrich, Munich, Germany). Also, when a defined solution pH was adjusted, adequate quantities of NaCl were added to the dialyzed protein solution to retain consistent ionic strength. For ionic strength and pH calculations, see 2.2.1. A second protein, IgG from human serum (h-IgG) (Sigma-Aldrich, Munich, Germany) as a salt-free lyophilized powder, was dissolved in the respective buffer solution and quantified by UV spectroscopy. Each protein solution, including the standard IgG1 formulation, was filtered through a hydrophilic 0.2 µm PES membrane filter (Pall GmbH, Dreieich,

Germany) before use. Typical protein handling like dilution and sample preparation was done in 15 ml and 50 ml polypropylene tubes (GreinerBio-One GmbH, Frickenhausen, Germany).

2.1.2 Glass Vials and Closure Systems

The pharmaceutical containers used for investigations were Fiolax® 2R borosilicate glass vials, kindly provided by SCHOTT AG (Mainz, Germany). Vials were preprocessed (washed and heat sterilized) as described in Chapter 2. Resin CZ® 2 ml plastic vials (Daikyo Seiko, Ltd., Japan), made upon a cyclic polyolefin (COP), were washed in the same way as the glass vials but only dried at 80°C for 1 h. After filling, the vials were closed with FluroTec® stoppers and finally sealed with Flip-Off® seals, both from West Pharmaceutical Services GmbH & Co. KG (Eschweiler, Germany).

2.1.3 Glass Powder

Glass powder was prepared from borosilicate glass vials Fiolax® 2R. Vials were shattered and the flinders, apart from the vial neck, were milled in a Pulverisette® 5 laboratory planetary mill (Fritsch GmbH, Idar-Oberstein, Germany) for 8 h, using ZrO_2 grinding beakers and balls. The powder was fractionated in a sieve tower and the particle fraction smaller than 45 microns was collected. Particles were washed 3 times by suspending in water for 5 min and were recovered by centrifugation. The particles were dried at 90°C and heat sterilized at 250°C for 1 h (primary fraction). Electrokinetic measurements required a collective of non-sedimenting glass particles, which was obtained by suspending the primary fraction in water, followed by sedimentation (secondary fraction in the supernatant). A thorough characterization of both fractions is given in Chapter 7.

2.1.4 Chemicals / Excipients

Polysorbate 20, Ph. Eur. (PS 20) and polysorbate 80, Ph. Eur. (PS 80) were purchased from Uniqema (Croda Healthcare Europe, Cowick Hall, UK). Poloxamer 188, Ph. Eur. (P 188) and polyoxyl 35 castor oil, USP/NF (PCO 35) were a gift from BASF (Ludwigshafen, Germany) and were used as received. D-(+)-glucose monohydrate (Ph. Eur.) and sucrose (Ph. Eur.) were purchased from Sigma-Aldrich (Munich, Germany). D-(+)-Trehalose dihydrate was obtained from Ferro Pfanstiehl (Waukegan, IL, USA). Glycerol 85% (Ph. Eur.) was purchased from Sigma-Aldrich, Munich, Germany) and D-sorbitol (Ph. Eur.) as well as D-mannitol (Ph. Eur.) were purchased as powders from Caesar & Loretz GmbH (Hilden, Germany). All excipients were dissolved in blank buffer and

added to the concentrated protein solution. As for glycerol, the amounts of buffer salts as well as NaCl were adapted. Ultrapure water (0.055 µS/cm) for all applications came from a Purelab Plus UV/UF system (ELGA LabWater, Celle, Germany) and was filtrated through a 0.22 µm membrane filter before use.

2.2 Methods

2.2.1 Calculation of Ionic Strength

The interaction of anions and cations in a buffered electrolyte solution leads to a dependence of the equilibrium constants on ionic strength [32]. Therefore, an introduction and a consideration of activity coefficients become necessary. Since the pH varies with the addition of salt, this in turn necessitates an adaption of the amount of acid or base for pH adjustment at different ionic strengths. The overall ionic strength is thereby affected as well. In the scope of this work, ionic strengths along with the volumes of acid or base needed for pH adjustment, but also the amounts of NaCl required for the adjustment of a defined ionic strength, were determined by an iterative calculation process. As a first step, the ionic strength of the system was calculated according to Equation 5 [33], assuming that activity coefficients were 1.

$$I = 0.5 \sum_{i=1}^{n} c_i z_i^2 \tag{5}$$

In this case, c_i is the concentration of ion i in mol·l^{-1} and z_i the valency of the ion, respectively. In the following, pK_{aj}^{*}, the practical dissociation constants of each conjugate dissociation pair j, were calculated with the formula given by Ellis and Morrison [34]:

$$pK_{aj}^{*} = pK_{aj} + (2z + 1)\left[\frac{0.5\sqrt{I}}{1+\sqrt{I}} - 0.1\,I\right] \tag{6}$$

It has to be mentioned that Equation 6 is derived from an approximate form of the Debye-Hueckel equation and therefore valid for dilute solutions. The pK_{aj} values correspond to thermodynamic dissociation constants and were taken from Stoll and Blanchard [35]. As for the phosphate buffer, these were $pK_{a1} = 2.15$, $pK_{a2} = 7.20$ and $pK_{a3} = 12.33$. Furthermore, z equals the charge of the associated conjugate base. Thus, the value of pK_{aj}^{*} varies with the ionic strength and will resemble pK_{aj} for $I = 0$. Calculations were performed with a computer-based spread sheet and iterated until the calculated ionic strength reached a constant value.

2.2.2 Isoelectric Focusing

Isoelectric focusing (IEF) was performed on a Multiphor II™ electrophoresis system combined with an EPS 3501 XL power supply and a MultiTemp III thermostatic circulator (GE Healthcare Europe GmbH, Freiburg, Germany). IEF gels were precast Servalyt® Precotes® Wide Range pH 3 - 10 as well as Range pH 6 - 9 gels (Serva Electrophoresis GmbH, Heidelberg, Germany). Serva Liquid Mix IEF Marker 3 - 10 was used as protein standard. The protein sample concentration was 2 mg/ml in a 10 mM NaCl solution. Final gel staining was accomplished using the Serva Violet 17 staining kit.

2.2.3 Electrophoretic Mobility Measurements by Dynamic Laser Light Scattering

Dynamic laser light scattering was applied to investigate the electrophoretic mobility of both glass particles and IgG1 molecules. Zeta potentials and surface charge densities were derived from this data. Measurements were performed on a Zetasizer Nano ZS (Malvern Instruments GmbH, Herrenberg, Germany), operating with a 4 mW He-Ne laser at 633 nm. Measurements in exclusively "monomodal mode" (50 V const.) were performed in Malvern disposable zeta cells at 25°C in a filtrated aqueous solution of 10 mM NaCl. The IgG1 concentration was 6 mg/ml. For a simplification of both calculations and individual pH adjustment procedures, the addition of buffer salts to the sample medium was avoided. Device control and final data analysis were performed using Malvern Dispersion Technology Software version 5.10 (Malvern Instruments GmbH, Herrenberg, Germany). The pH adjustment of the samples was computer-controlled by a Malvern MPT-2 Autotitrator. A sample volume of 5.0 ml was put in a stirred polypropylene (PP) tube and titrated with 0.1 M NaOH to pH 12 and with 0.1 M HCl to pH 2. For checking purposes, analogous samples were titrated beginning from pH 2.0 to pH 12.0 or conversely.

2.2.4 Determination of the Hydrodynamic Diameter by Dynamic Laser Light Scattering

The hydrodynamic diameter of IgG1 was measured on a Zetasizer Nano ZS (Malvern Instruments GmbH, Herrenberg, Germany). The scattering information was detected in non-invasive back-scatter (NIBS) mode at 173°. The distribution by intensity was calculated from the correlation function with the high resolution multiple narrow mode.

2.2.5 UV Spectroscopy

UV spectroscopy for protein concentration measurements was performed on a temperature-controlled Agilent 8453 UV/VIS spectrophotometer (Agilent Technologies GmbH, Boeblingen, Germany) at 25°C, λ = 280 nm using quartz cuvettes and applying an extinction coefficient of 1.40 cm^2/mg for antibodies [36].

2.2.6 Adsorption Process

The standardized adsorption procedure of IgG1 in containers was discussed in detail in Chapter 2. Briefly, the preprocessed vials were filled with 2 mg/ml IgG1 solution or 1 mg/ml h-IgG solution, respectively, closed, and incubated 24 h in a water bath at 25°C with slow horizontal movement (25 rpm). The vials were emptied using a syringe with an injection needle and rinsed in four steps with buffer solution correlating the respective formulation. For desorption of the inherent proteins, the vials were filled with PBS buffer pH 7.2 (10 mM phosphate plus 145 mM NaCl) containing 0.05% SDS, sealed and stored at the above conditions over night for a further 14 h.

2.2.7 Size Exclusion High Performance Liquid Chromatography

Desorbed protein quantities were analyzed via Size Exclusion HPLC on an Agilent 1100 (Agilent Technologies GmbH, Boeblingen, Germany) equipped with a Tosoh TSKgel G3000SWXL and a TSKgel SWXL guardcolumn (Tosoh Bioscience GmbH, Stuttgart, Germany). The mobile phase equaled the desorption buffer described above. The injected sample volume was 400 µl and the run duration was 50 min. The protein fluorescence signal at λ_{ex} / λ_{em} 280 nm / 334 nm was recorded by a Thermo Spectra 3000 fluorescence detector. All chromatograms were integrated manually by using the Agilent ChemStation software Rev. B 02.01 (Agilent Technologies GmbH, Boeblingen, Germany). In each HPLC batch run, a 10-point IgG1 calibration from of 0.1 - 10.0 µg/ml was included.

3 RESULTS AND DISCUSSION

3.1 Influence of Charge on IgG Adsorption – Formulation Parameters pH and Ionic Strength

As described before, protein adsorption on charged surfaces is governed by electrostatic interactions. Proteins consist of a multiplicity of dissociable groups, and the overall charge of a protein molecule results from an overlay of all dissociation equilibria. For glass, the surface charge primarily arises from the dissociation of surface-exposed ≡Si–OH groups. For proteins, it is mainly the dissociation of amino acid residues that accounts for charges on the surface. Furthermore, the surface potential is altered by the attachment of electrolytes, e.g. salt ions, with or without a specific surface affinity. The effect of surface-attached ions or charged molecules is associated with compensation resp. screening of "free" charges, which similarly affects the protein and the glass surface. Therefore, the influence of the two most important pharmaceutical formulation parameters on the IgG1 adsorption, pH and ionic strength, was investigated.

3.1.1 Charge Characterization of IgG and Glass Surface

Initially, the charge state of glass and the two IgG fractions was characterized according to pH and ionic strength. The area of the isoelectric pH as well as the number of discrete isoforms of both IgG types, the monoclonal IgG1 and the human IgG from pooled serum, were determined with isoelectric focusing. As shown in Figure 1, IgG1 exhibits 6 - 7 characteristic isoforms in the range from pH 7.62 to 8.16. The explicit values for the respective fraction are listed in Table 1. Different isoforms are basically originated from micro-heterogeneities of C-terminal Lysines, from deamidation within several Asn - Gly deamidation sites, as well as from differences in the glycosylation pattern. The situation for human IgG is somewhat different. Here, as expected, no characteristic isoforms, but a broader and consistent distribution is apparent, since the fraction represents a widespread collective of IgG types. The pI range reaches from approx. pH 7.0 to 8.6, and no distinct boundary was observed.

Electrokinetic mobility measurements were accomplished as a function of pH, using IgG1, h-IgG, as well as the borosilicate glass particles. Both colloids, the glass particles and the protein molecules, were treated as spheres with a homogeneously distributed surface charge. The approximate globular shape of the glass particles could be demonstrated by SEM (see Chapter 7), whereas the spherical shape of IgG1 was postulated for all following calculations. Zeta potentials were calculated from electrokinetic mobility data and plotted in Figure 2a.

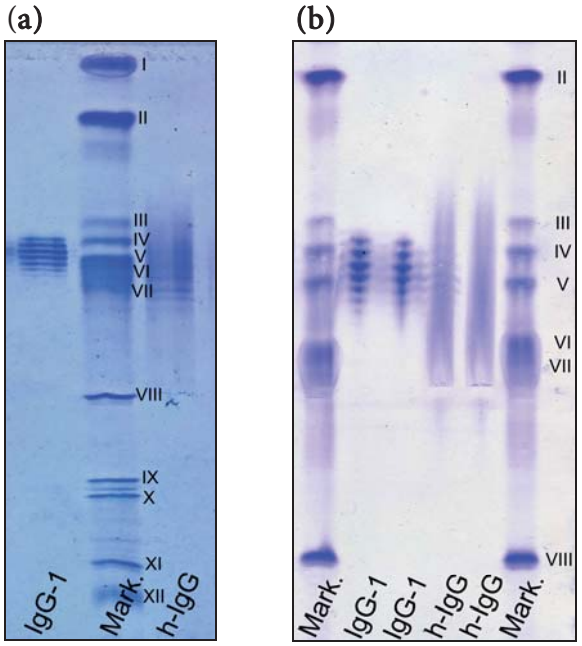

Table 1: Discrete isoforms (pI) of IgG1 and pI range of h-IgG.

	IgG1	h-IgG
maximum	8.16	8.6
	8.07	|
	7.97	|
	7.89	|
	7.80	|
minimum	7.62	7.0

Figure 1: Isoelectric focusing gels for the determination of the IEP of IgG1 and h-IgG in a broad range (a) pH 3 - 10 and a narrow range (b) pH 6 - 9; marker bands can be assigned to the pI values: (I) 10.7; (II) 9.5; (III) 8.3; (IV) 8.0; (V) 7.8; (VI) 7.4; (VII) 6.9; (VIII) 6.0; (IX) 5.3; (X) 5.2; (XI) 4.5; (XII) 4.2.

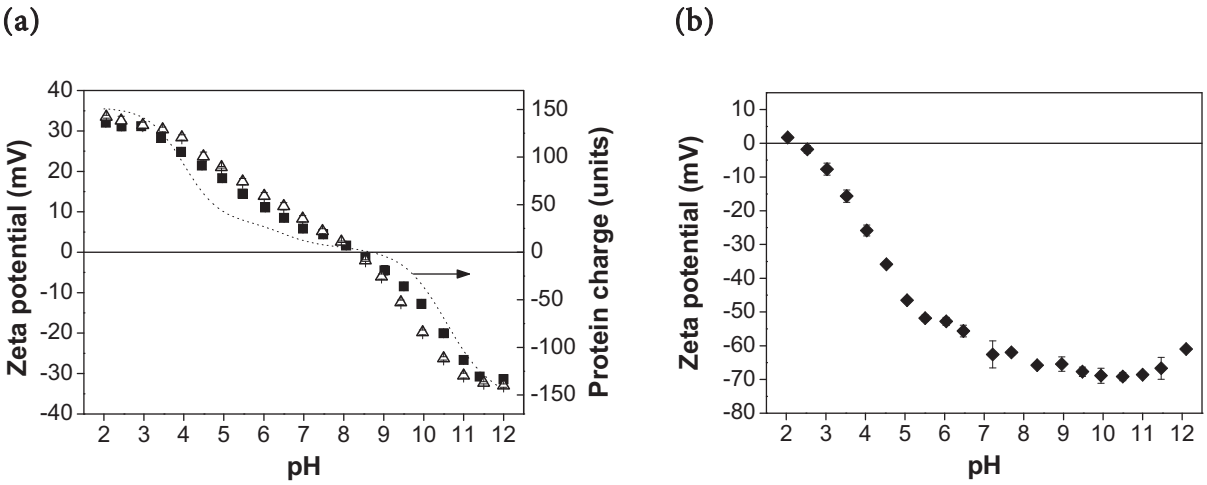

Figure 2: Zeta potential as a function of pH, determined by electrophoretic mobility measurements in 10 mM NaCl solution (n = 3); (a) zeta potential of IgG1 (■) and h-IgG (△) as well as IgG1 theoretical charge distribution determined from the primary sequence (dotted line); the arrow indicates the corresponding axis; (b) zeta potential of washed and heat sterilized (250°C, 1 h) borosilicate glass particles (◆).

For both IgGs, the curves exhibit the shape of a typical protein titration curve. Accordingly, IgG shows a positive net charge at pH values below the IEP and a negative potential above. The mean IEP of IgG1 and human IgG, as the intercept with the x-axis at zero mV, was determined at 8.33 and 8.28, respectively, which corresponds with the results from isoelectric focusing. The isoelectric points of the materials investigated are within the spectrum of pH 5.8 [5] to 9.0 [37], described in literature. Concerning the average charge status of all isoforms, there is hardly any difference between both IgG samples, as indicated by the identical curve shape. The results for IgG1 were verified by comparison with the theoretical charge, which was calculated from the protein sequence using the IEP module of the European Molecular Biology Open Software Suite (EMBOSS) [38] (Figure 2a). It has been described that the net charge estimations based on the amino acid composition, using intrinsic pK values, may deviate to some extent from protein titration experiments [39,40]. One reason would be protein-internal electrostatic interaction, which changes the propensity for ionization [40]. Although the theoretical calculation can only be considered a rough approximation, it coincides well with the curve shape derived from electrophoretic mobility measurements. Minor deviations may have been caused by some of the assumptions stated above. In this regard, it has to be mentioned that due to the titration set-up, ionic strength in the test liquid could not be kept absolutely stable, which may have contributed to curve deviations as well. One example could be the observed flattening of the protein titration curves in the border region. However, this phenomenon is not exceptional and has been described to occur at pH values far from the pI, where molecules are considerably charged [39]. The theoretically calculated IEP is located at 8.69. Since the measured pI does not seriously deviate from the theoretical value, it can be concluded that the zeta potential or the protein net charge in solution is not dramatically changed by preferential adsorption of a certain ion type from the protein solution.

As expected, the glass surface is highly negatively charged in the whole alkaline pH region with zeta potential values down to -70 mV (Figure 2b). This high value does not appreciably vary in the range from pH 12 right up to pH 7. Within this range, surface-exposed ≡Si–OH groups are largely dissociated. With decreasing pH, the surface potential becomes less negative through increased protonation. The glass surface finally reaches its IEP at 2.28. According to literature, the pI of silica is approx. 2 [8,20,41], but may vary in the range from pH < 1 to 5.5, depending on the ions present in the liquid phase [41]. It is not very unlikely that borosilicate glass, which contains a fraction of additional components, like e.g. aluminum oxide and boron oxide, therefore shows a pI different from pure silica. Barz *et al.* have mentioned a pI of borosilicate glass in the range between pH 1.7 - 2.0 [42]. Figure 2b also reveals a certain drift of the zeta potential to less negative values above pH 11, which again was presumably attributed to an increase in the ionic strength

through the titrant solution. Such a phenomenon could not be observed in the acidic threshold region. In the following, the zeta potential is simplified and referred to as "charge" of the respective materials.

Within the scope of this work, the main investigations concerning IgG1 were reduced to three different formulation pH values: pH 4.0, the pH of maximum adsorption at 170 mM ionic strength, pH 7.2, which represents a common protein formulation pH, and pH 8.6, assuming most proteins are in a net uncharged state. Although isoelectric focusing results revealed an IEP between pH 7.6 and 8.2, pH 8.6 was clearly referenced by electrokinetic measurements (pH 8.3) and theoretical calculation (pH 8.7).

3.1.2 Impact of the Formulation pH on IgG Adsorption

3.1.2.1 The Adsorbed Quantity as a Function of pH

The influence of pH on the adsorption of IgG on borosilicate glass vials was investigated in the following. In these studies, adsorption plateau values as a function of pH ($\Gamma_{pl}(pH)$) were determined in the range from pH 2 to 12. According to adsorption isotherms (see Chapter 5), plateau values (Γ_{pl}) for adsorption were assumed for incubation at 2 mg/ml. In the pH experiments, each formulation contained 10 mM phosphate buffer, whereas the ionic strength was adjusted by the addition of an individually calculated amount of NaCl and held constant at 170 mM. In Figure 3a, the Γ_{pl} values are plotted against the formulation pH. For both IgG1 and h-IgG, a bell-shaped dependency is observed, which is common for protein adsorption on solid surfaces [7,43,44]. For monoclonal IgG1, the highest surface concentration is found at approx. pH 4 to 5. Unambiguously, the maximum is not placed at the IEP. From pH 6 on, adsorption steadily decreases towards zero with increasing pH. The most pronounced drop of $\Gamma_{pl}(pH)$ occurs in the upper alkaline pH region. $\Gamma_{pl}(pH)$ also decreases from pH values below 4 towards pH 2, albeit not to the same extent.

The adsorbed amounts of h-IgG compare well with those of IgG1. The pH of maximum adsorption for the h-IgG is located in the same pH region, although slightly shifted towards a higher pH value. However, $\Gamma_{pl}(pH)$ values do not show the same continuous behavior as was observed for IgG1, starting from pH 4.0 towards higher pH values. Remarkably, a second local maximum occurs in the area of the IEP (7.0 - 8.6). A pronounced drop of Γ_{pl} for pH ≈ 9 as well as a decrease of Γ_{pl} towards zero for pH values above pH 9 becomes obvious for both the pooled h-IgG and the monoclonal IgG1. Reasons accounting for the observed differences must be related to intrinsic protein properties. As stated above, the two species differ in their electrostatic properties. It is assumed that the broadening of the bell-shaped adsorption characteristic is due to the wider range of the IEPs of h-IgG, as compared with the discrete isoforms of IgG1, which

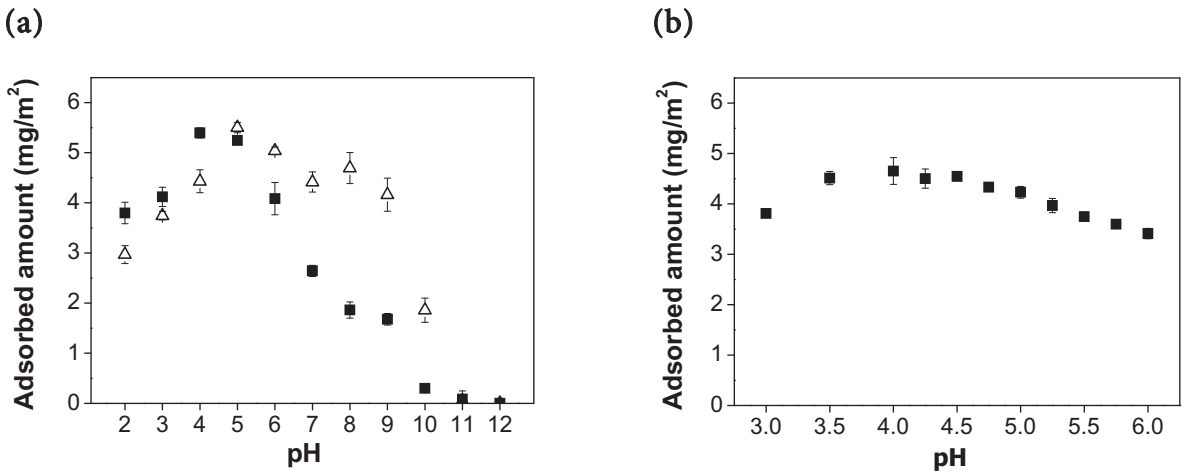

Figure 3: (a) Adsorption profiles of monoclonal IgG1 (■) and pooled human IgG (△) on borosilicate glass depending on pH; incubation for 24 h, 2.0 mg/ml IgG including 10 mM phosphate buffer, 170 mM total ionic strength (n = 3). (b) Detailed investigation in the range of the IgG1 adsorption maximum (n = 3).

were closer together. Figure 3b provides a detailed view of the maximum adsorption area of IgG1. The location of $\Gamma_{pl}(pH)_{max}$ at pH 4.0 is verified. The absolute surface concentration deviated by circa 0.5 to 0.75 mg/m² from the values depicted in Figure 3a because of day-to-day variations or slight inhomogeneities of the vial inner surface.

Protein molecules as well as the borosilicate glass surface in aqueous solution are present in a charged state. Therefore, electrostatic interactions are inevitably involved in the adsorption process. These can be classified into electrostatic interactions between protein and surface, as well as electrostatic interactions between protein molecules on the surface in adsorbed state. As depicted in Figure 2a (3.1.1), the net charge of protein molecules increases with increasing pH values above the IEP, and with it, the repulsive forces between the molecules. Accordingly, for both IgG1 and h-IgG the adsorbed quantity strikingly decreases at pH > IEP. Similar results were described by Zhu *et al.*, who found decreasing protein adsorption with increasing charge difference of the same sign, i.e. increasing repulsion [45]. But it becomes obvious that adsorption does take place to an appreciable extent above the IEP region. It was described that protein adsorption occurs spontaneously even though the surface and the sorbent bear the same charge [7,46,47]. This can be enabled by the incorporation of ions in the inner region of the adsorbed layer to avoid too high of a charge density in the contact region [9]. An extensive investigation of the importance of ionic strength on adsorption is given in 3.1.3. Furthermore, the spatial charge distribution on the surfaces of the protein molecules can have an influence as well. In Figure 4, the surface-exposed areas of acidic and basic character, which represent potential carriers of a charge, are illustrated by means of the IgG1 crystal structure model.

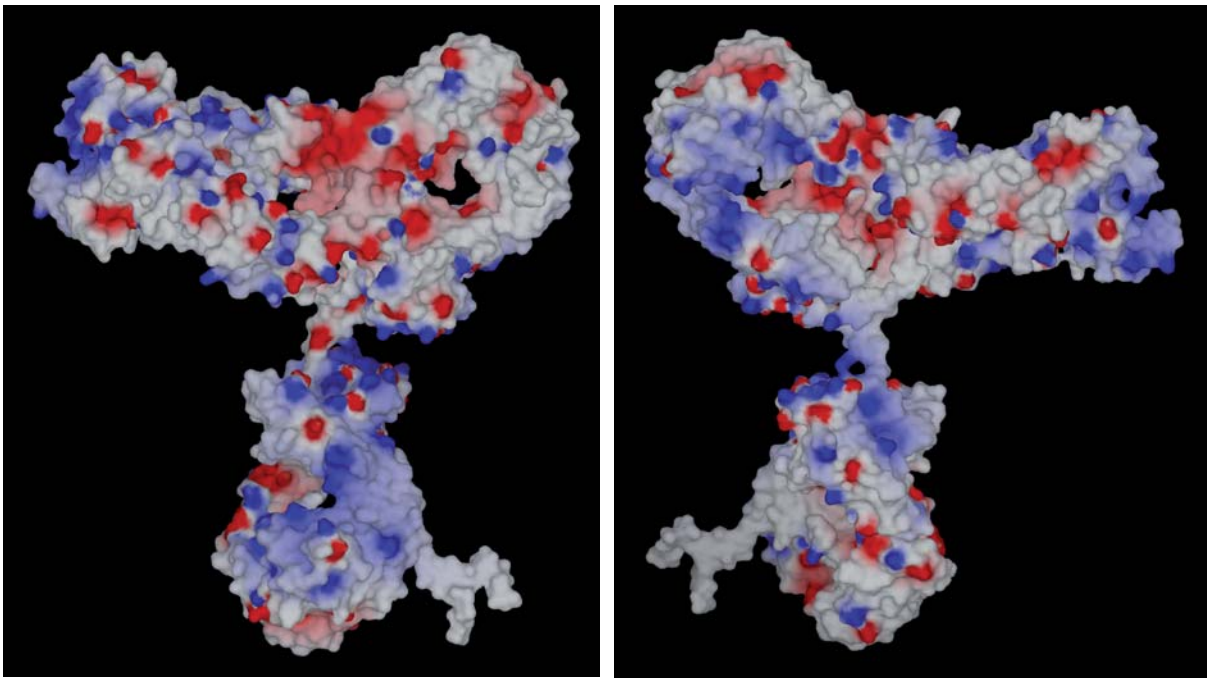

Figure 4: IgG1 crystal structure model indicating the electrostatic surface potential, visualized by VIDA v3.0.0 (OpenEye Scientific Software, Inc., Santa Fe, New Mexico, USA); surface coloring indicates residues/areas of negative (red) and positive (blue) potential; IgG1 front view (left) and back view (right).

It becomes obvious that charges are not uniformly distributed on the surface. Thus, even if the net charge of the molecules is of the same sign as the surface, e.g. for pH above the IEP of the protein, still patches of an opposite charge excess can exist, leading to unhesitant adsorption through electrostatic attraction.

But also a contribution of other adsorption mechanisms than electrostatic interactions was discussed. Structural rearrangements, which outweigh unfavorable contribution of electrostatic repulsion, have been described to allow adsorption at pH values above the IEP [9]. Last but not least, protein adsorption on glass is to a certain extent driven by dehydration reactions (hydrophobic interactions) since the glass surface has turned out to be not completely hydrophilic (see Chapter 3). But at least for high pH values greater or equal than 11, the circumstances become highly unfavorable and adsorption disappears nearly completely.

For IgG1, $\Gamma_{pI}(pH)_{max}$ is located away from the IEP of the antibody and shifted towards lower pH values (pH 4 - 5). It was shown in section 3.1.1 that below pH 8.6, both the glass and IgG1 carry different charge signs, and the differences in zeta potentials initially increase with decreasing pH. The pronounced negative charge of the glass in this pH region is largely preserved. Accordingly, the net electrostatic attraction towards the sorbent surface increases. But with an increasing net charge of IgG, simultaneously, the intermolecu-

lar repulsion forces increase as well. Both aspects have to be taken into account, and the combination is decisive for the resulting adsorbed amount. After passing an optimum in electrostatic conditions, circumstances become more adverse with decreasing pH, since the amount of negative charges on glass decreases and thus the electrostatic attraction towards the glass. Additionally, the electrostatic repulsion among proteins further increases. Below the IEP of borosilicate glass (pH 2.3) when glass becomes net-positively charged, electrostatic attraction towards the surface turns into repulsion, which leads to a further decrease in adsorption.

In several cases, $\Gamma_{pl}(pH)_{max}$ has been found at pH values apart from the protein IEP, e.g. for HSA on colloidal TiO_2 [19] or BSA on negatively charged polyethersulfone membrane [47]. According to the authors, increased electrostatic attraction forces between the oppositely charged protein and sorbent surface below the IEP led to increased adsorption. Consequently, electrostatic interactions between the proteins and the surface outweigh the influence of intermolecular repulsion. Furthermore, according to literature, an increased irreversibility of protein adsorption has occurred in the pH range below the protein IEP because of the local prevalent beneficial electrostatic interactions [48]. Accordingly, the fraction removed by the rinsing step was decreased. In contrast, a multitude of researchers have reported maximal adsorption at the protein IEP, which could be shown for BSA and HSA on hydrophilic silica and other surface types [7,49] and also for several IgGs on hydrophilic and hydrophobic silica surface [11], lattices [43], or polystyrene microspheres [36]. This incident seems to be independent of protein and surface type, or adsorption conditions. An increased protein stability at the IEP and hence a smaller surface area occupied can serve as an explanation for maximum adsorption at the protein pI [11,36,50]. In contrast, if not at their IEP, proteins turn out to be less rigid [50] and their structural stability decreases. Consequently, the space requirement of proteins increases at conditions of reduced structural stability due to a more pronounced unfolding during adsorption (see Chapter 1). Lower $\Gamma_{pl}(pH)$ values than the maximum $\Gamma_{pl}(pH)_{max}$ have been attributed to the progressive structural deformation of the adsorbed protein molecules [46]. For the structurally stable RNase, the influence of pH on Γ_{pl} has been found to be less pronounced than for the more instable HSA [51]. Concerning RNase, it has been assumed that a densely packed monolayer of unperturbed molecules was formed, regardless of the solution pH [51]. On top of that, Bagchi and Birnbaum argued that, for IgG adsorption on negatively charged polymer, solely ionization-induced changes of the protein conformation and changes of the "area per molecule" were decisive for the extent of saturation adsorption [43]. The driving force would then even be completely independent from charge - charge interactions between proteins and the sorbent surface. By contrast, it was also discussed that the amount of adsorbed protein may be dominated by lateral repulsion rather than by attraction between the proteins and the surface. This would cause decreased adsorption at pH values other than at IEP, regardless of increasing

electrostatic attraction towards the sorbent surface [36,49,52]. Considering the situation of both IgG1 and h-IgG on borosilicate glass, electrostatic attraction between surface and protein increases below the IEP, which appears to have a decisive impact on adsorption. As elaborately depicted in Chapter 7, the molecular structure is not or only marginally affected in the pH range from 4 to 9. Likewise, the hydrodynamic diameter of the monomer is not dramatically affected in the pH range investigated (see 3.1.4). In conclusion, the results point to the fact that adsorption of IgG1 on borosilicate glass is to a great extent driven by electrostatic interactions, which is further elucidated in the following.

3.1.2.2 Electrostatic Interactions within the Adsorption Interface

In this section, the adsorption process is considered from the perspective of electrostatic interactions. Upon adsorption, the electrical fields of the solvated protein and solvated glass surface overlap. Hence, charges on both surfaces redistribute, and a charge transfer between protein molecules, the glass surface, and the bulk solution occurs [18]. As a result, a new charge-equilibrium within the protein - glass complex is formed. The pH-dependent electrophoretic characterization of this complex can be helpful for interpreting the location of $\Gamma_{pl}(pH)_{max}$. In this regard, Haynes, Norde, and coworkers emphasized the importance of the electrostatic state after adsorption. They postulated that the pH of maximum adsorption is affected by the charge of the sorbent surface and the protein [2,14]. In particular, maximum affinity for adsorption is observed when the charge of opposite sign of the protein molecule exactly compensates for the charge on the surface. Besides, low molecular weight ions are additionally involved in the adsorption process. They are located on the surface of both the glass and the protein molecules and influence the zeta potential. This ion balance may be reorganized upon the adsorption process [2].

Initially, the isoelectric point of the glass - IgG1 complex was determined. Therefore, glass particles were incubated in a solution of IgG1 at pH values from 4 to 9 in 10 mM PBS buffer. The resulting IgG1 equilibrium concentration after the 24 h adsorption process was 2 mg/ml. Thereafter, particles were carefully centrifuged and washed 4 times with a 10 mM NaCl solution of the corresponding pH. Zeta potentials of the IgG1-surrounded glass particles were determined via electrokinetic mobility measurements by applying the Smoluchowski model (see Equation 1). Although IgG1 adsorption strongly depends on pH, it was assumed that the glass particles were fully covered with IgG between pH 4 to 7. Figure 5 depicts ζ of the IgG1-coated glass particles. ζ of the free IgG1 molecules and the free glass particles are depicted for comparison. As expected, ζ of the IgG1-covered glass particles becomes more negative with increasing pH. The isoelectric point of the complex, however, does not coincide with the IEP of the blank glass (pH 2.3) or with that of the pure IgG1 (pH 8.3), but is located inbetween at pH 5.8. This indicates that the positively

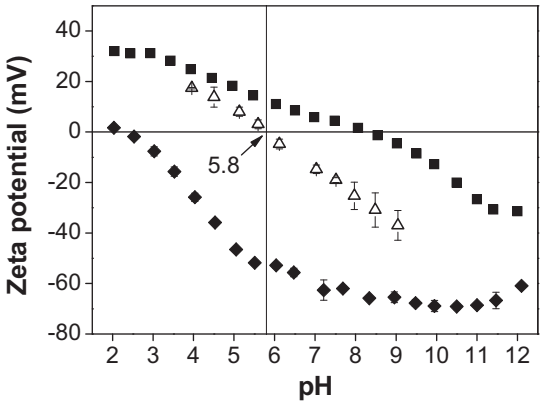

Figure 5: Zeta potential of IgG1-surrounded glass particles at variable pH between 4 and 9 (△); for comparison, zeta potentials of the free IgG1 (■) and free borosilicate glass particles in a protein-free solution (◆) from pH 2 to 12 are shown (n = 3).

charged groups of IgG1 are, at least in part, compensated by the negatively charged groups of the glass surface [22]. It has been found by means of electrokinetic measurements that $\Gamma_{pl}(pH)_{max}$ normally coincides rather with the isoelectric point of the sorbent - protein complex [22,44] than with the isoelectric point of the protein, but not in all cases [5]. As mentioned above, our electrokinetic measurements were performed in solutions of NaCl at 10 mM ionic strength. If a clear relation is to be established, adsorption of IgG1 on glass at low ionic strength has to be used as a basis for comparison. When $\Gamma_{pl}(pH)$ was investigated at low ionic strength of 40 mM (see 3.1.3), $\Gamma_{pl}(pH)_{max}$ was located in the area of pH 5, and thus shifted to a less acidic pH than it was at a moderate ionic strength of 170 mM. Since I in electrokinetic measurements was 10 mM, which is even lower than 40 mM, a further shift towards a more alkaline pH appears very likely. Therefore, also for IgG1 on borosilicate glass surface, $\Gamma_{pl}(pH)_{max}$ seems to coincide roughly with the IEP of the protein - glass complex.

The electric charges of the protein and the sorbent surface will hardly ever match exactly. Some single charges will inevitably accumulate in case the protein and sorbent carry net surface charges of the same sign or in case opposing charges are not fully neutralized. This implicates growing forces of repulsion. Since a very low dielectric permittivity prevails in the protein - surface contact zone, this state is energetically unfavorable. Therefore, low molecular weight ions are transferred from the surrounding liquid to the adsorption layer to prevent accumulation of charges in the contact region [2]. However, this ion transfer also includes a chemical effect which itself has turned out to be energetically unfavorable and which hinders spontaneous protein adsorption [53]. Hence, maximum affinity of proteins to the respective surface type is observed when no further ion incorporation is required [2]. The participation of low molecular weight ions of the solution

can be determined by comparing σ_{ek} before and after protein adsorption. σ_{ek} is obtained from ζ according to the theory of diffuse double layers by Equation 7 [20]:

$$\sigma_{ek} = -\sqrt{8\,\varepsilon_0\,\varepsilon\,c\,R\,T}\;sinh\left(z\,F\,\zeta\,/\,2\,R\,T\right) \tag{7}$$

Therein, ε equals the relative dielectric permittivity of the medium, ε_0 the vacuum permittivity, c the concentration of the symmetric z - z electrolyte (see above), F the Faraday constant, R the gas constant, and T the absolute temperature. In our case, σ_{ek} was calculated from ζ measured in 10 mM NaCl. The extent of incorporated ions was estimated by applying Equation 8 [14,22]. Because of the overall electric charge neutrality, the charge transfer $\Delta_{ads}\sigma_{ek}$ between the adsorbed layer and the surrounding liquid is given by:

$$\Delta_{ads}\sigma_{ek} = \sigma_{ek}(IgG/glass) - \sigma_{ek}(glass) - \sigma_{ek}(IgG)\cdot\Gamma\cdot A \tag{8}$$

σ_{ek} equals the electrokinetic charge density at the slipping layer of the IgG - glass complex, the glass, and the IgG, respectively. The term $\Gamma{\cdot}A$ is the proportion of the cumulated surface of adsorbed protein molecules to the corresponding glass surface. Γ is the mass of protein adsorbed per surface area glass. A equals the surface area per unit mass and is defined by the term:

$$A = \frac{4\,r_h^2\pi\cdot N_A}{M_w} \tag{9}$$

For IgG1, the surface area of one molecule ($4\,r_h^2\pi$) is approx. 335 nm^2, assuming a globular molecule shape and a mean hydrodynamic radius (r_h) of 5.16 nm, determined from PCS measurements (3.1.4). N_A equals Avogadro's number, and M_w equals the molecular weight of IgG1. As an approximation, $\Gamma_{pl}(pH)$-values, measured at I = 40 mM (Figure 8), were used for Γ in the calculations. In the plot of $\Delta_{ads}\sigma_{ek}$ against the formulation pH (Figure 6), the contribution of ions to the adsorption process by means of either an uptake in or a release from the adsorption region of IgG1 on the borosilicate glass surface is depicted. Zero-crossing indicates the energetically favorable state with the least participation of countervailing ions. The data indicates that below pH 6, the negative charge of the glass surface is overcompensated by the positive charges of the IgG1 molecules. Therefore, an incorporation of additional negative charges is required to achieve electric neutrality. Above pH 6, positively charged ions are necessary to compensate for the excess of negative charges on part of the borosilicate glass surface, which had not been sufficiently balanced by adsorbed IgG1 molecules. As stated above, the energetically most

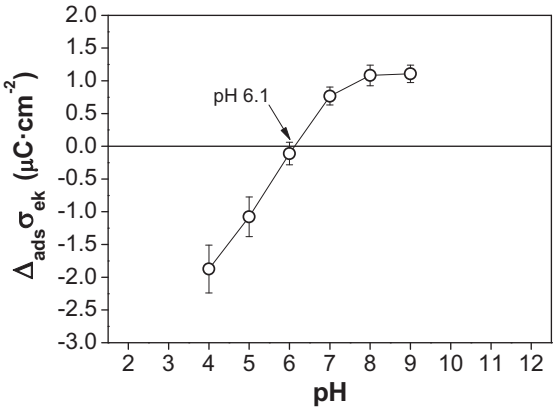

Figure 6: Charge transfer ($\Delta_{ads}\sigma_{ek}$) between the contact region of the adsorbed layer and the surrounding liquid (n = 3); $\Delta_{ads}\sigma_{ek}$ approximated according to Equation 8 (σ_{ek} from electrokinetic mobility measurements in 10 mM NaCl; Γ taken from the pH adsorption profile at I = 40 mM).

favored state is when charges on either surface will more or less precisely match each other. The accurate value (pH 6.1) is in accordance with the IEP of the glass - protein complex (5.8) and the pH of $\Gamma_{pl}(pH)_{max}$ determined at low ionic strength.

The results shown above lead to the conclusion that the location of $\Gamma_{pl}(pH)_{max}$ results from favorable electrostatic conditions with an optimum of both attractive and repulsive forces, indicated by a minimum of low molecular weight ions incorporated in the contact area of adsorption. It has to be mentioned that the results depicted in Figure 6 only represent an approximation of the true circumstances, since ionic strengths in electrokinetic mobility measurements and in vial assay experiments were both in the lower range, but not exactly identical. Therefore, the validity of this theory should be reexamined at uniform conditions. Also, a repeated study at moderate ionic strength conditions, e.g. 170 mM, would be of interest to confirm the location of the corresponding $\Gamma_{pl}(pH)_{max}$ value at pH 4.0. It was stated by Norde and Lyklema that an accurate determination of the ion transfer $\Delta_{ads}\sigma_{ek}$ as a function of pH only provides trends [1]. However, as for IgG1 adsorption on borosilicate glass, where the adsorption process is at least to a large extent governed by pH-dependent electrostatic interactions, this approach has shown to provide further understanding.

3.1.3 Impact of the Formulation Ionic Strength on IgG Adsorption

It was mentioned above that the amount of IgG1 adsorbed on glass is determined by the balance of attractive or repulsive forces between protein and surface as well as between protein molecules within the adsorption layer. Accordingly, the surface coverage is deter-

mined by a combination of both effects [54]. In theory, the importance of each factor may alter in the course of adsorption time. At the beginning, the glass surface is only sparsely populated because protein molecules of the same charge repel each other to some degree. Thus, in the early stages, the main effect arises from the interaction of surface and protein, whereas at higher surface coverage, intermolecular interactions gain in importance through a closer proximity of the proteins. When the surface is completely covered, it significantly loses its influence on further adsorption. Generally, the electrostatic balance of the adsorption process is influenced by small molecular weight ions, which screen charges of the protein and the sorbent surface. Thus, attractive and repulsive forces are equally reduced.

In order to gauge the contribution of electrostatic interactions from IgG1 and the borosilicate glass surface on the adsorbed amount, adsorption experiments with protein solutions containing variable concentrations of NaCl were performed. Again, three characteristic pH values were investigated, namely pH 4.0, pH 7.2, and pH 8.6 representing different charge states of the protein and the glass surface. As shown in Figure 7a, the ionic strength has a different impact on the adsorption behavior of IgG1. At pH 7.2 and 8.6, an increasing NaCl concentration leads to a continuous decrease of the adsorbed amount of IgG1. The electrostatic situation, as elucidated before, can be described as follows. Slight attraction of the marginally positively charged IgG molecules, or rather of positively charged patches, prevails towards the highly negatively charged glass surface. Besides ubiquitous dispersion forces and dehydration phenomena, there is only marginal electrostatic interaction among adsorbed proteins, since the zeta potential equaled (almost) zero. Considering the impact of ionic charge shielding, mainly surface - protein attractive forces are diminished, giving rise to a steady decrease in adsorption. This decrease is more pronounced at the IEP where the system responds more sensitive to changes in charge interaction. In contrast, at pH 4.0, a steady increase of adsorption with increasing ionic strength is observed. As opposed to the situation above, attraction towards the surface is assumed to be increased at this pH since the positive protein net charge increased and the negative charges of glass only decreased to a minor degree. However, with increasing protein net charge, the electrostatic repulsion between the protein molecules continues to gain in importance. Its diminution by ionic charge shielding therefore leads to a denser packaging of IgG on the surface, associated with increasing adsorbed quantities. AFM images of adsorbed protein layers on the glass confirm this tendency (see Chapter 7).

In order to further corroborate the above theory, adsorption experiments were conducted with COP plastic vials. As opposed to glass, the polymer surface has a low surface free energy and is only marginally charged due to the lack of ionizable groups. Although minor specific ion adsorption due to non-electrostatic interaction, e.g. van-der-Waals interac-

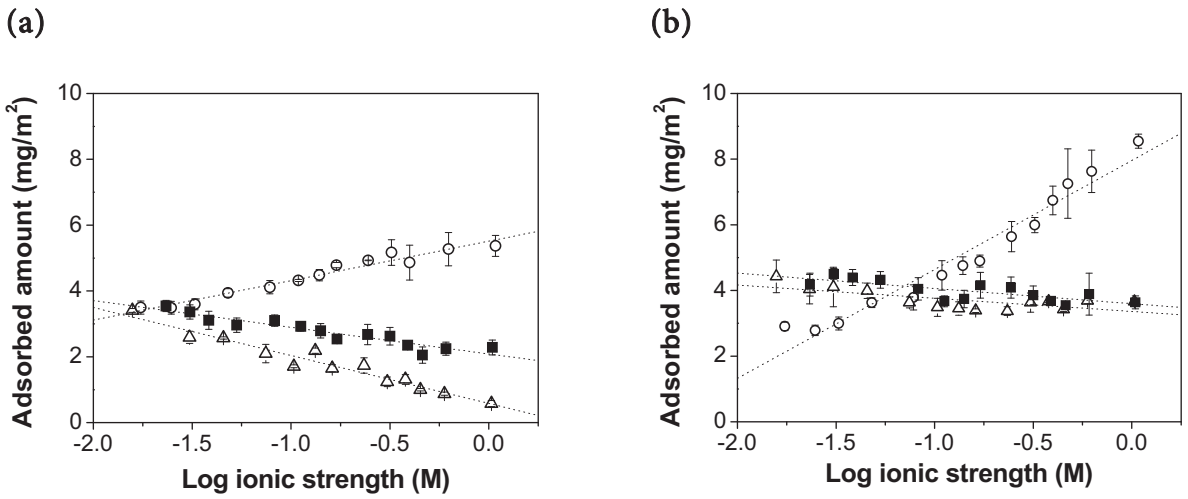

Figure 7: Adsorption of IgG1 on (a) borosilicate glass and (b) COP plastic surface as a function of ionic strength, adjusted with variable amounts of NaCl at three different pH values 7.2 (■), 4.0 (○) and 8.6 (△); protein solution contained 2 mg/ml IgG1 and 10 mM phosphate buffer (n = 3); dotted lines approximate a linear curve progression.

tions, may lead to the formation of an electrical double layer causing a measurable zeta potential [16], electrostatic forces between the surface and the protein were assumed to be missing. Instead, the molecule attachment should be mainly governed by hydrophobic interactions and dispersion forces. But charges still play a major role in protein - protein interactions, thereby affecting the adsorbed amount through intermolecular electrostatic repulsion forces. Thus, by varying the ionic strength in the protein solution, the impact of intermolecular charge - charge interactions on IgG1 adsorption can be evaluated. It can be seen in Figure 7b that adsorption increased on the hydrophobic surface, which was already elucidated in Chapter 3. Furthermore, hardly any impact of the increasing salt concentration is observed at both pH 7.2 and 8.6, and the adsorbed amount remains almost constant. This confirms the insignificance of intermolecular electrostatic interactions in the area of the IEP. At pH 4.0, the high net protein charge causes high electrostatic repulsion, which is an obstacle to favorable protein adsorption. At low ionic strengths, these repulsive forces have the ability to greatly reduce the adsorbed amount, even to values below those observed at the IEP. At the same time, charge shielding leads to a marked increase in adsorption with increasing ionic strength at pH 4.0. Despite the lack of strong electrostatic attraction towards the surface, the increase is even stronger than for the glass surface through the impact of hydrophobic interactions. It has to be mentioned that a logarithmic relationship was found between ionic strength and the adsorbed quantity of IgG1, regardless of the kind of sorbent surface. Finally, intermolecular electrostatic repulsion forces were proven to be an important factor in influencing the amount of adsorbed IgG1. In this regard, adsorption becomes more favorable with

decreasing protein net charge and with increasing ionic strength. For charged surfaces, however, also the concurrent effect of electrostatic protein - surface interactions has to be considered.

For IgG1 adsorption on borosilicate glass, the dependency of Γ_{pl} on pH at an ionic strength of 170 mM has already been outlined (Figure 3). It has also been elaborated that the ionic strength had a heterogeneous influence on the adsorption mechanism, since the two different effects, electrostatic attraction towards the surface and repulsion between protein molecules, vary in importance as a function of the formulation pH. In addition to preliminary adsorption measurements at I = 170 mM, the shape of $\Gamma_{pl}(pH)$ as well as the location of $\Gamma_{pl}(pH)_{max}$ were investigated at I = 40 mM (Figure 8).

For lower ionic strength, $\Gamma_{pl}(pH)_{max}$ is shifted towards the protein IEP (higher pH values) under an approximate retention of the characteristic curve shape. Between pH 2 and 5, where IgG1 has a high net charge, the adsorbed amounts at I = 40 mM range below the respective values determined for I = 170 mM. In this range, intermolecular repulsion forces play a major role, leading to a sparsely covered surface, unless the charges are screened to a certain extent by ions. No change in the adsorbed protein mass is observed at pH 6. This indicates that both the increase in surface attraction and the increase in protein repulsion by lowering the ionic strength from 170 mM to 40 mM are balanced. It could be shown by means of electrokinetic calculations that the ion uptake in the adsorption region between IgG1 and the glass surface is lowest at pH 6.1. This indicates the lowest influence of low molecular weight ions. Hence, it is not surprising that surface concentrations are equivalent at this pH value, despite different ionic strengths. Above pH 6, where the net charge of IgG1 is low, the influence of electrostatic interaction between the protein and the glass surface gains in importance since the glass surface

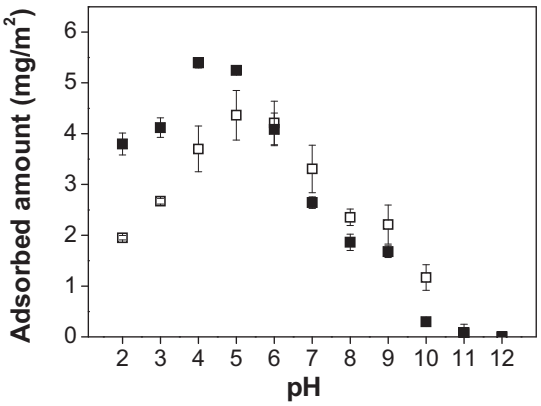

Figure 8: Adsorption profile of IgG1 on borosilicate glass depending on the formulation pH; adsorption was investigated at two different ionic strengths of 170 mM (■) and 40 mM (□); incubation for 24 h, 2.0 mg/ml IgG1 including 10 mM phosphate buffer (n = 3).

becomes increasingly negatively charged. Thus, decreasing the ionic strength leads to slightly increased adsorbed amounts through increasing attractive forces. In the particular case of the protein IEP (pH ≈ 8.6), balanced negative and positive charges on the protein surface cause a low net intermolecular electrostatic attraction [55]. This low attractive force is supposed to prevail towards the charged surface as well. Accordingly, increased adsorption at pH 8.6 for $I = 40$ mM when compared to $I = 170$ mM becomes plausible. This is not necessarily the case for pH values above pH 8.6, where both proteins and glass surface carry net negative charges. A reduction of the electrostatic repulsive forces at higher ionic strengths was expected to increase adsorption, which, however, was not the case. The reasons for the opposite result remain unclear. Similar results have been described by Buijs *et al.*, who studied IgG adsorption on hydrophilic silica [11]. By increasing ionic strength, they also observed a shift of $\Gamma_{pl}(pH)_{max}$ towards a lower pH. Furthermore, adsorption increased at low pH values and decreased towards high pH values of the incubation medium. Also Xu *et al.* found a shift of the adsorption maximum of an IgG1 on hydrophilic silica. $\Gamma_{pl}(pH)_{max}$ was shifted from the IEP at low ionic strength towards a lower pH when ionic strength during incubation was increased [48]. However, not only the ionic strength alone, but also the salt type was described to be capable of shifting $\Gamma_{pl}(pH)_{max}$ due to differences in binding affinities [56]. The influences of the salt type on IgG1 adsorption will be discussed in section 3.2 in more detail. In summary, the above results clearly confirm the synergy of electrostatic intermolecular and electrostatic surface – protein interactions for the adsorption of IgG1 on borosilicate glass. The extent of both is decreased by low molecular weight ions.

3.1.4 IgG1 Monomer Size as a Function of pH and Ionic Strength

It has been mentioned before that pH-induced changes of the protein conformation can alter the space requirement of the molecules in the adsorbed state and can therefore be crucial for the adsorbed amount [43]. Furthermore, it has been described that higher ionic strengths may lead to an increased hydrodynamic diameter (d_h) by a growing hydration shell [13]. In order to judge the importance of this effect, the IgG1 molecule size, determined as hydrodynamic diameter, was investigated as a function of the formulation pH in the range from pH 2 to 12 and as a function of the ionic strength between 23 mM and 1660 mM. The measurements were performed as titrations, starting from pH 7.0 in both directions. d_h of the monomers was taken as the mean value from 3 series of 10 measurements each. The absolute values of d_h depicted in Figure 9 are in very well in line with the findings of Jøssang *et al.* (11.0 - 11.4 nm) [57] or Bagchi and Birnbaum (11.0 - 12.5 nm) [43] for IgG. However, in our case, neither a clear trend of d_h with variable pH nor an expected minimum at the IEP [43] could be observed. For the alkaline and acidic

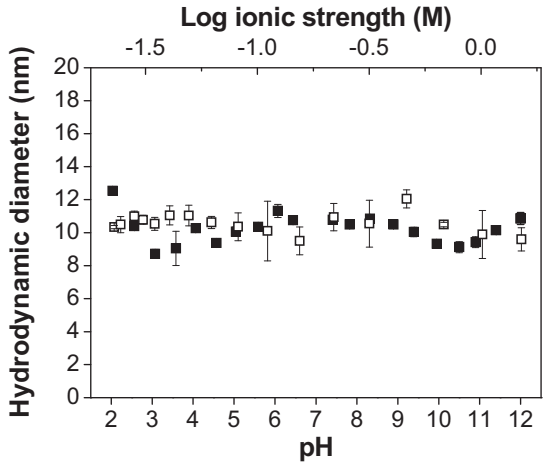

Figure 9: Hydrodynamic diameter of IgG1 monomers as a function of pH at I = 170 mM (■) and as a function of ionic strength at pH 7.2 (□) (n = 3).

range, d_h at first decreases slightly but then increases towards pH 2 and pH 12, respectively. In Chapter 7, it is shown that beginning with pH 10 and above, as well as beginning with pH 4 and below, considerable unfolding as well as increased aggregation with and without increased fragmentation of the IgG1 sets in. According to Figure 9, variable ionic strength did not have a clear impact on the hydrodynamic diameter of the IgG1. Thus, an influence of the monomer dimensions on adsorption, as for example through an increased space requirement on the surface, is excluded for a variable ionic strength or for a variable pH in the range from pH 4 to 10.

3.1.5 Discussion of Other Driving Forces and Influencing Factors

As shown above, a characteristic correlation between the protein formulation pH and the adsorbed amount of IgG on the glass vial internal surface could be observed, with ionic strength having a significant influence on adsorption. Furthermore, the surface itself may be affected by the formulation composition, which can contribute to the overall adsorption result. The question whether pH affects the glass surface in terms of charge, composition, and stability of the topmost layer during the 24 h incubation timeframe was extensively investigated and described in Chapter 3. Besides protein properties like charge and polarity, also the protein's conformational stability and other instabilities like aggregation or fragmentation depend on pH [58-60] and ionic strength [13,61]. It was mentioned that the structural stability of a protein may directly influence the adsorbed mass by affecting its molecular surface area occupied. As shown beforehand, the molecular dimensions of the IgG1 monomer did not change significantly within the pH and ionic strength range investigated (see 3.1.4). According to Arai and Norde, proteins with a strong internal

coherence and a large structural stability are referred to as “hard particles”, and surface interaction is primarily governed by hydrophobic and electrostatic effects [9]. In contrast, “soft particles” hold a relatively low structural stability. This additional internal factor, which is probably related to structural rearrangements in the molecule, leads to an increased conformational entropy and promotes adsorption even under electrostatic repulsion [53]. By this means, considerable IgG1 adsorption at pH values above the IEP (pH 8.6), where the borosilicate glass surface and the IgG1 are both negatively charged, may be explained (Figures 3 and 8). This intrinsic protein property is not necessarily constant but may be subject to change with pH and ionic strength (see Chapter 7). With regard to the protein structure, it is not necessarily the case that the whole protein is equally affected by variable formulation parameters. Especially the $F(ab')_2$ fragment was shown to be highly affected by pH and ionic strength, whereas the adsorption of the Fc part was rather constant [11]. At the same time, differences in the *de*sorption behavior were observed. Consequently, both aspects together will affect the adsorption behavior of the whole IgG molecule.

Structural instability not only concerns the proteins adsorbed on the surface, but also the free form in solution. In this regard, the approach of the favored adsorption of protein aggregates was followed by Nylander [62]. It has been stated that protein monomers exhibit a higher hydrophobicity than aggregates since the association into oligomers is in large part driven by hydrophobic interactions. Accordingly, the adsorption of monomers on a hydrophobic surface would seem more likely, whereas the adsorption of protein aggregates would be favored on a hydrophilic surface. For example, preferential adsorption of larger protein oligomers has been described for β-lactoglobulin [63] and insulin [64], which was associated with an increased adsorption at the same time. In our own studies however, a comparison of desorbed protein fractions revealed significantly less aggregation after adsorption at pH 4 compared to adsorption at moderate pH (see Chapter 7). Moreover, adsorption at pH 3 or below, where the IgG1 aggregate content in the incubation solution was shown to be much higher than at pH 4, rather resulted in decreased surface-bound IgG1 (see Chapter 7). Both aspects support the conclusion that an increased aggregation tendency is not the major driving force for IgG adsorption on borosilicate glass.

Another effect which can influence the pH-dependent adsorption pattern is a variable degree of adsorption reversibility, shown for IgG on silica [11]. Protein adsorption has often been found to be largely irreversible upon dilution [55,65]. But the degree of irreversibility has also been shown to be variable and to increase with adsorption time. Referring to this, the fraction of globular proteins elutable from hydrophilic surface has been demonstrated to decrease with time, already within 30 min to 1 h of adsorption [66,67], reaching a state of minor reversibility thereafter. IgG adsorption irreversibility even has

been stated for different solution parameters, e.g. for fixed pH values between pH 4 and 10 [43]. Thus, for IgG1 on borosilicate glass, a low degree of reversibility was assumed after 24 h of adsorption.

3.2 Influence of Formulation Excipients Including "Hofmeister Considerations"

3.2.1 Influence of the Ionic Strength-Determining Salt Type

As mentioned before, not only the ionic strength itself but also the salt type used may affect the adsorption of proteins. Therefore, adsorption experiments dealing with the influence of ionic strength on adsorption were performed using Na_2SO_4 instead of NaCl for ionic strength adjustment (Figure 10). For better comparability, the linear fits from Figure 7a are overlaid. Adsorption at pH 7.2 and pH 8.6 almost equals the profile that was obtained by using NaCl. This applies for both adsorption at low and high salt content and for the adsorption increment with increasing ionic strength. At pH 4.0, however, increasing ionic strength with Na_2SO_4 leads to a stronger increase in adsorption compared to the adjustment with NaCl. Besides, the linear dependency of the adsorbed IgG1 quantity on the logarithm of ionic strength no longer applies. Above an ionic strength of approx. 0.2 M, the excessive increase stops and equilibrium adsorption clearly decreases.

It has been shown by Van Dulm *et al.* that ions are incorporated in the inner region of the adsorbed protein layer and reduce the charge density therein [46]. This prevents a charge accumulation in a region of low dielectric permittivity. For pH 4.0, it was shown in 3.1.2

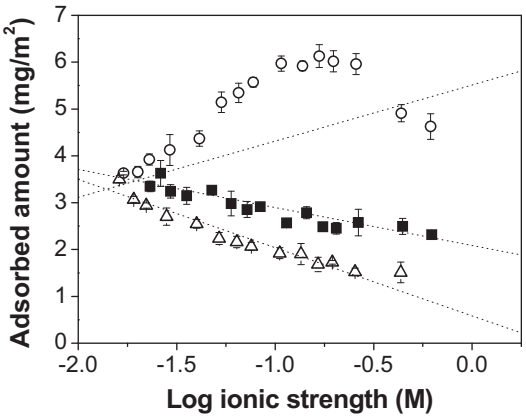

Figure 10: Adsorption of IgG1 on borosilicate glass depending on ionic strength, adjusted with variable amounts Na_2SO_4 at pH 7.2 (■), pH 4.0 (○) and pH 8.6 (△); incubation for 24 h, 2.0 mg/ml IgG1 including 10 mM phosphate buffer (n = 3); dotted lines correspond to the curve progression derived from the use of NaCl (Figure 7a).

that predominantly negative charges are incorporated in the adsorption region. In this case, the incorporation of divalent ions like SO_4^{2-} is preferred because of the higher valency and higher polarizability compared to the monovalent ion types [46]. Especially for lower pH values, such as pH 4.0, where the net charge of the proteins is highly positive and the compensation of interfacial charges is a limiting factor for adsorption, the presence of SO_4^{2-} instead of Cl^- gives rise to this pronounced increase. Furthermore, the high charge screening capacity of SO_4^{2-}, especially with regard to the screening of free charges between the considerably charged proteins at pH 4, would also contribute to increasing IgG1 adsorption due to a higher density of the protein layer. At both pH values beyond 6.1, however, where predominantly cations are incorporated in the boundary layer, no particular effect of Na_2SO_4 can be observed, since in those cases, again Na^+ compensates the excess of negative charges. But the pronounced adsorption decrease at higher Na_2SO_4 concentrations raises questions. Solely charge - charge interactions cannot sufficiently explain this effect and alternative explanation attempts have to be found. One approach is based on the fact that salt can have either a stabilizing or a destabilizing effect on proteins. This depends on whether prevailing repulsive forces within the protein are screened or conformational stabilizing salt bridges are weakened [3]. Another explanation refers to the effect of preferential exclusion of salts. In this regard, it is well known from the Hofmeister series, together with extensive investigations by Arakawa and Timasheff [24], that Na_2SO_4 is a stronger protein precipitant than NaCl, and also shows a stronger preferential hydration and therefore stabilization. Influences of stabilizing salts on protein adsorption are only sparsely described in literature. Adsorption of firefly luciferase on borosilicate glass surface was studied by Suelter and DeLuca [68], who described a decreasing adsorption with increasing concentrations of $(NH_4)_2SO_4$. The studies were carried out at pH 7.5, i.e. above the IEP of luciferase, where molecules are negatively charged (we calculated the IEP ≈ 6.4 from the amino acid sequence "1lci.fasta" using the ProtParam tool on the ExPASy web server [69]). Under these circumstances, the effect on adsorption might be attributed to NH_4^+, which is a better stabilizing ion than Na^+. In our case, however, it could be clearly shown that a SO_4^{2-} concentration below 0.2 M does not lead to dramatic differences in adsorption at pH 7.2 and 8.6, where IgG1 also exists in a rather low net charged state.

Several approaches have to be considered when explaining the effect of specific salts on protein adsorption. Generally speaking, the impact of salting-out systems is an increase of the surface tension of water, whereupon the proteins are preferentially hydrated and these salts are preferentially excluded from the proteins' surface [25]. The associated thermodynamically unfavorable increase in the chemical potential is directly proportional to the surface area of the protein exposed to the solvent. The protein structure is stabilized since a denatured protein has a greater surface than the native one [3]. Accordingly, unfolding of proteins on the sorbent surface upon adsorption is forced back, and the effective area

occupied by a molecule decreases. However, this aspect alone would rather give rise to increasing adsorption. Another approach has been taken by Wendorf *et al.* [70]. They argued that irreversibly adsorbed proteins, which are the only ones that are quantified after a rinsing step, are largely present in a denatured, expanded state. Due to an increased number of interaction sites, proteins in this state are especially strongly bound to the surface. The unfolding process leading to this irreversible binding state was assumed to take place once the molecule is adsorbed. Since the stability of proteins increases in the presence of stabilizing agents (e.g. salting-out salts, sugars, amino acids), the equilibrium is driven to the native form and adsorption becomes less irreversible, and consequently, the determined adsorbed amount decreases. This would be an explanation for the pronounced adsorption decrease at higher Na_2SO_4 concentrations. As a rule, concentrations of a few moles per liter of the stabilizing salt lead to protein precipitation, whereas the formation of oligomers already begins at lower salt concentrations [71]. According to the results outlined in Chapter 7, a slightly increased aggregation tendency arising from the pH shifts towards pH 4 could have been causative for a generally increased surface concentration of the antibody at this pH. However, at increased Na_2SO_4 concentrations, which were assumed to evoke an increased aggregation tendency, surface concentrations rather decrease. It was not evaluated whether aggregation increased in the presence of Na_2SO_4. So the effect of aggregates/agglomerates in this regard is not clear. The most plausible explanation for the adsorption decrease at higher Na_2SO_4 concentrations is again based on electrostatic interactions. Because stabilizing salts increase the surface tension of water, they are preferentially excluded from the surface of the proteins. As a consequence, the compensation of an unfavorable surplus of intermolecular charges is diminished. Consequently, increasing electrostatic repulsion leads to a less compact protein layer, and hence, to decreasing adsorption. With regard to our results, this effect apparently only gains in importance at increased Na_2SO_4 concentrations where preferential exclusion sets in. For lower concentrations, the charge compensation properties of the divalent SO_4^{2-} ion in the area of adsorption initially improve conditions for adsorption and allow higher amounts of adsorbed protein, as described above.

Finally, it can be concluded that in the area of the protein IEP, moderate concentrations of Na_2SO_4 have no effect on the adsorbed amount of IgG1 on glass. The results at pH 4.0 indicate an overlay of the effects of charged ions at lower concentrations and of preferential exclusion at higher concentrations. It has already been denoted by Arakawa and Timasheff that the extent of preferential exclusion depends on the formulation pH [24]. This dependency, in turn, has been described by the same authors to vary with the corresponding salt concentration. This complicates the impact on adsorption. In order to separate the charge effect from preferential exclusion, further investigations were made with the aid of sugars and polyols that are stabilizing but uncharged.

3.2.2 Influence of Sugars and Polyols

It was described in the previous section that salting-out excipients like Na_2SO_4 on the one hand hold protein-stabilizing properties according to the Hofmeister series; on the other hand, however, they are simultaneously involved in charge compensation and charge shielding processes during adsorption. To exclude the charge effect and to analyze solely the stabilization effect, the group of uncharged excipients, namely sugars and polyols, was further investigated. Sugars and polyols belong to the protein-stabilizing agents, which are widely used in protein pharmaceuticals [3]. The stabilizing effect of such co-solutes was shown to depend on their concentration, and according to literature, at least 0.3 M are necessary to significantly stabilize proteins [23]. Chang *et al.* stated that even higher concentrations of 40% and more are needed to achieve a sufficiently stable formulation [72]. As with stabilizing salts, the stabilizing effect of sugars on proteins was described to depend on the pH value [26]. The effect was more pronounced the less stable the protein was at the respective pH. With regard to the stabilization mechanism, "preferential hydration" of proteins also holds true for sugars [25,26]. Accordingly, they stabilize the protein's compact native structure since the asymmetric denatured state with an enlarged surface per molecule is energetically unfavorable [25]. Glycerol and polyols, like sorbitol and mannitol, belong to the group of solvophobic compounds, i.e. they strengthen the hydrophobic effect, and the contact of nonpolar regions of the protein with the solvent becomes thermodynamically more unfavorable than with water [25]. Therefore, the denaturation step with the exposure of internal hydrophobic areas is forced back.

The effect of common sugars and polyols on IgG1 adsorption was initially investigated at pH 7.2 for three concentrations. It is depicted in Figure 11a that the effect of glucose and

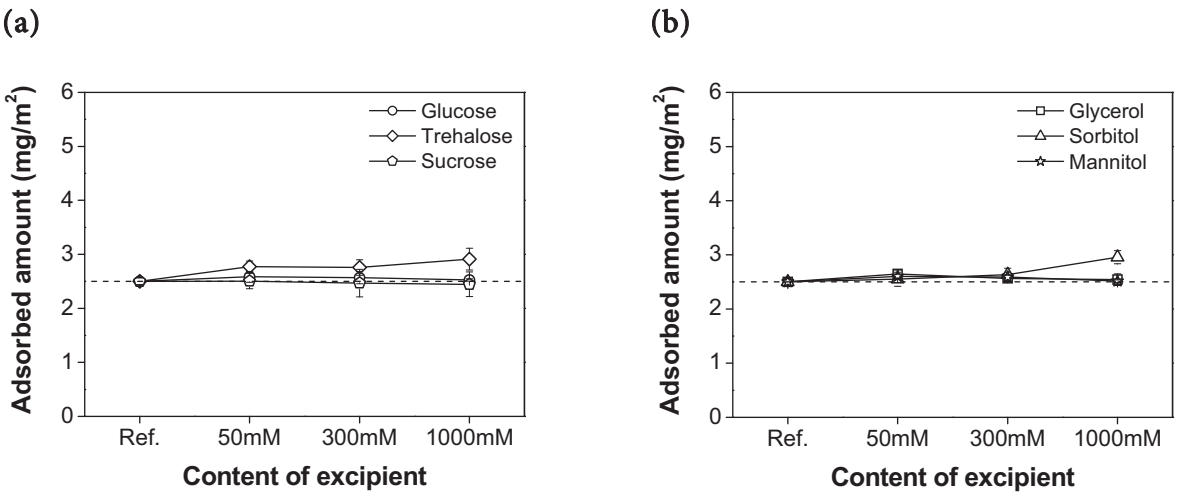

Figure 11: Influence of selected excipients, (a) sugars and (b) polyols, on the adsorption of IgG1 on the borosilicate glass vial surface, determined at pH 7.2, I = 170 mM and 2 mg/ml IgG1 (n = 3); references correspond to the sugar/polyol-free IgG1 solutions.

disaccharide sucrose was negligible. The adsorbed amounts were not significantly different ($\alpha = 0.05$) from the reference. Unlike glucose and sucrose, trehalose caused a distinct and statistically significant increase in IgG1 adsorption at concentrations of 50 and 300 mM. The outcome is not much different for the group of polyols (Figure 11b). The adsorbed amounts are consistent with the reference, except for sorbitol at 1 M which resulted in significantly increased adsorption ($\alpha = 0.05$).

The influence of a broad range of sugars on the adsorption behavior of different proteins (BSA, RNase A and lysozyme) on hydrophilic and siliconized SiO_2/TiO_2 surfaces has been analyzed by Wendorf *et al.* [70], who observed a decrease of adsorption for either surface. This trend does not hold true for our results at pH 7.2. As already mentioned above, Wendorf's approach of interpretation referred to the influence of stabilizing excipients on the denaturation propensity of proteins on the surface and the adsorption reversibility change involved. Matheus investigated the influence of different sugars and polyols, in concentrations up to 300 mM, on antibody stability in highly concentrated IgG1 solutions at a single pH of 6.0 [73]. The studies revealed only a minor improvement of chemical stability. However, the situation might be quite different at another pH. In our case, the influence of sugars and polyols on the adsorbed amount of IgG1 was additionally studied at pH 4.0, where a pronounced effect of stabilizing salts has already been observed. According to Figure 12, the addition of low amounts of both sugars and polyols caused increasing IgG1 adsorption. For higher excipient concentrations of 1 M, however, a drop in adsorption to levels in the range of the reference value for polyols (Figure 12b), or even below for sugars (Figure 12a), was found.

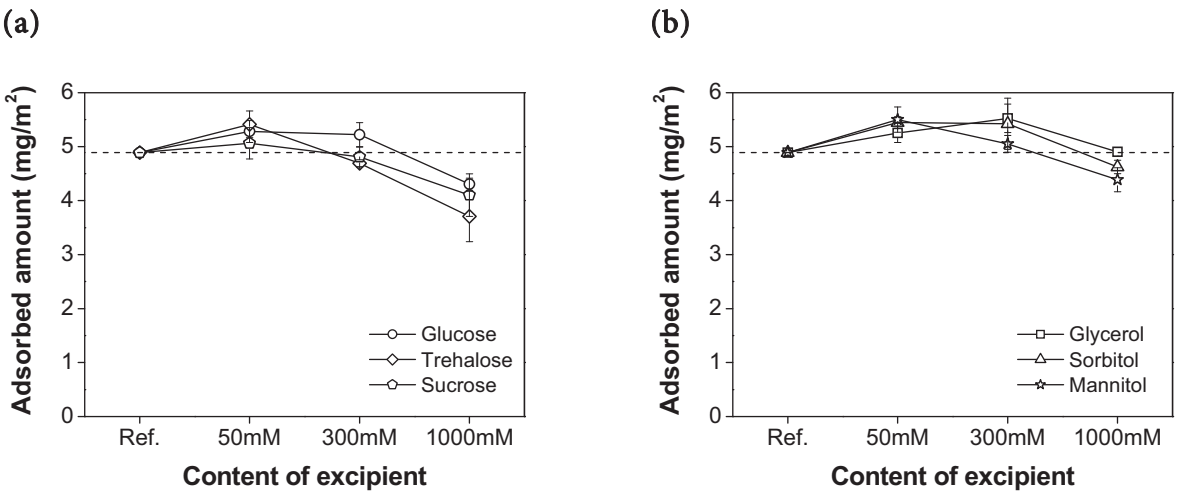

Figure 12: Influence of selected excipients, (a) sugars and (b) polyols, on the adsorption of IgG1 on the borosilicate glass vial surface, determined at pH 4.0, I = 170 mM and 2 mg/ml IgG1 (n = 3); references correspond to the sugar/polyol-free IgG1 solutions.

This decrease in adsorption strongly substantiates the theory of increasing structural stabilization and therefore a decreased adsorption irreversibility at high excipient concentrations. Another attempt to explain the above observation might be based on the adsorption of sugars/polyols to the hydrophilic glass surface. The binding of sugars to negatively charged mica surfaces has been shown by Claesson *et al.*, who concluded a decrease in the long-range electrostatic double layer force, and, as a result, a decrease in the surface charge density [74]. Since a corresponding decrease at pH 7.2, where surface and protein are oppositely charged, is missing, a pH dependence of this excipient surface-binding effect seems probable. Also, an influence of sugars and polyols on intermolecular protein interactions has to be taken into consideration. In this regard, an inherent effect of sugars and polyols is ruled out since they do not bind to the surface of the proteins. They are rather preferentially excluded from the surface, giving rise to a water-rich environment. As a result, especially pH values where the proteins carry a high net charge, repulsive electrostatic protein - protein interactions gain in importance. This might also explain decreasing adsorption at higher excipient concentrations. Finally, it can be concluded that the influence of sugars and polyols on the adsorption of IgG1 on glass is low, especially in the concentration range of pharmaceutical relevance up to 300 mM. Attempts to explain significant effects on the adsorbed amount, especially at high excipient concentrations, could be provided, whereas clear explanations are still missing.

3.2.3 Influence of Surfactants

Surfactants are typically added to protein solutions for stabilization and solubilization purposes [75-77]. By this means, proteins are prevented from e.g. aggregation or unfolding, which often occurs in the context of freeze - thaw stress or mechanical stress with interface effects [28,78]. In this regard, nonionic surfactants are preferred over ionic surfactants since the latter bind stronger to proteins and thus act denaturing [79]. Furthermore, surfactants prevent proteins from unwanted adsorption [29-31,80], were shown to reduce aggregation induced by interaction with solid surfaces [81], and can be used to remove adsorbed proteins [82,83]. The desorption efficiency for removing bound protein molecules is not a consistent property but depends on various factors. Feng *et al.* have found that the elutability decreased in the order HDL > HSA > IgG ≈ Fb for polysorbate 20 (PS 20), which may be explained by differences in interaction strengths between protein and surface [83]. For human γ-globulin bound to surfaces of a broad hydrophilicity range, the desorption efficiency of PS 20 has been found to reach a maximum level on surfaces holding a water contact angle of 40 - 50° [84]. In comparison, the efficiency was relatively small for hydrophilic surfaces. For fibrinogen, the maximum desorption effect was found on surfaces with a water contact angle of about 70°. Nonionic surfactants can prevent proteins from adsorption on solid surfaces through a simple preincubation, as

shown for PS 20 and HSA on polyethylene [83]. In this regard, preincubation of polyethylene with surfactant has been described to lead to the formation of a reversible layer of surfactant molecules on the sorbent, which caused decreased protein adsorption, subject to the surfactant concentration [83]. As mentioned above, surfactants can decrease adsorptive losses to surfaces when added to the protein solution. Complete or significant inhibition of TGF-β1 adsorption has been described for polysorbate 80 at 0.01% [85]. Poloxamer 407 in a concentration of 0.05% could increase the recovery of G-CSF stored in PVC infusion bags to approx. 80%, compared to 60% without the addition of a surfactant. In another case, the adsorption of a hydrophobic cytokine to borosilicate glass within 24 h could be reduced by a factor of 4 through the addition of 0.02% PS 20 to a 0.25 mg/ml solution [86].

In the following, the influence of four nonionic surfactants, approved for parenteral administration, on the IgG1 adsorption to borosilicate glass vials was investigated. The selected surfactants were poloxamer 188 (P 188), polysorbate 20 (PS 20), polysorbate 80 (PS 80), and polyoxyl 35 castor oil (PCO 35). Of the surfactants used, P 188, PS 20, and PS 80 are frequently utilized in protein formulations for solubilization and stabilization of proteins. PCO 35 was included in the studies because of its increased hydrophobicity, indicated by the lower HLB value (see Table 2). An overview of other important properties of the surfactants, like CMC and molecular weight, is also provided in Table 2.

In the adsorption experiments, the molar surfactant concentration was set from 1/10 of the molar IgG1 concentration to an excess of a 1000-fold of the molar IgG1 concentration at two different pH values, namely pH 7.2 or pH 4.0. It is shown in Figure 13a that at pH 7.2, all nonionic surfactants tested were able to reduce the amount of protein bound to the glass surface. For PS 20, PS 80, and PCO 35, the decrease in protein adsorption became pronounced at molar ratios surfactant : IgG1 of 1 : 1. The adsorbed amount decreased by half or even more at this condition. Higher surfactant concentrations did not cause further significant reduction, except for a 1000-fold excess of PS 80 and PCO 35

Table 2: Characteristics of the nonionic surfactants P 188, PS 20, PS 80 and PCO 35.

	P 188	PS 20	PS 80	PCO 35
CMC[a] (mmol/l)	0.48 – 1.14	0.049 – 0.060	0.010 – 0.016	0.040 – 0.080
HLB[b] value	> 24	16.7	15.0	12 – 14
MW[c] (g/mol)	8800	1228	1310	2515
References	[87-90]	[75,91]	[75,91]	[87,88,92]

[a] critical micelle concentration (CMC) in water

[b] hydrophilic/lipophilic balance (HLB)

[c] molecular weight (MW)

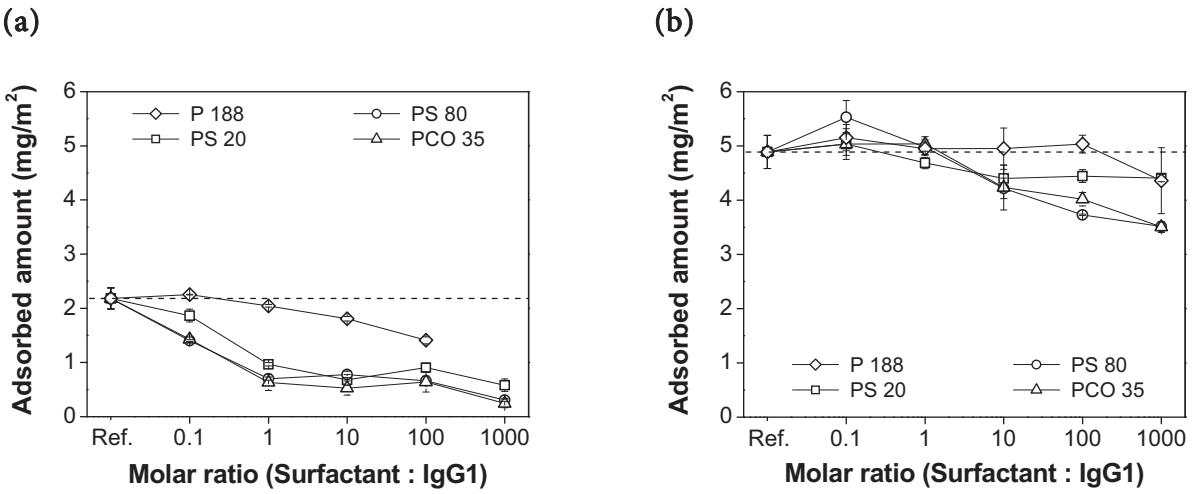

Figure 13: Influence of selected surfactants on the adsorption of IgG1 on the borosilicate glass vial surface, determined at (a) pH 7.2 and (b) pH 4.0; 2 mg/ml (0.013 mM) IgG1 and *I* = 170 mM (n = 3); references correspond to the surfactant-free IgG1 solutions.

over the protein. The maximum decrease in adsorption amounted to approx. 90% (1.9 mg/m^2) of the reference value. In contrast, P 188 did not exhibit a marked effect on adsorption at low surfactant concentrations. Adsorption decreases slightly only at increased concentrations. Unfortunately, no results are available for the molar ratio of 1000 : 1, where the protein quantity could not be determined due to interference effects in the SE-HPLC quantification.

With respect to the reference value of the surfactant-free samples, the adsorption-reducing effect at pH 4.0 was by far less pronounced than it was at pH 7.2 (Figure 13b). The relative reduction reached 30% at the most, whereas the absolute maximum decrease of 1.4 mg/m^2 at a 1000-fold excess of surfactant was in the same range as for pH 7.2. A slight adsorption increase could be observed for very low surfactant concentrations at pH 4. This exceptional phenomenon has been previously described for low surfactant concentrations [93]. It could have derived from a cooperative adsorption mechanism of protein and surfactant or from a change of the protein structure, both times leading to increased surface affinity. Furthermore, it has been discussed that the surface could have been rendered more hydrophobic by low surfactant concentrations, resulting in increased protein binding [94]. The reduction in protein adsorption, however, was most likely due to a combined mechanism. Nonionic surfactants have been described to form a layer on the surface, preventing more protein adsorption the higher the surfactant concentration was during preincubation with surfactant [83]. In most cases, nonionic surfactants do not markedly bind to protein molecules but mainly interact with the surfaces [94]. Even so, a specific interaction with the surface of the proteins is conceivable, where hydrophobic

sites of the protein are covered and hence hydrophobic interactions with surfaces or with other proteins are reduced [30,76]. Another reason for the decrease of protein adsorption is sterical hindrance, which prevents the proteins from coming close to the surface [94].

At pH 7.2, the net charge of the IgG1 is near zero, whereas the charge of the glass surface is highly negative. Thus, only low attractive electrostatic forces are prevalent. A certain degree of hydrophobicity was shown to prevail on the glass surfaces (see Chapter 3). Moreover, hydrophobic patches are usually available also on native proteins. Therefore, a contribution of hydrophobic interactions to the protein adsorption process is assumed. Since nonionic surfactants are able to shield hydrophobic areas on both protein and surface, an important driving force for adsorption at this pH was reduced, leading to a strong prevention of IgG1 adsorption. At pH 4.0, the surfactants were less effective at preventing adsorption. It was shown above that, at this pH, adsorption is mainly driven by electrostatic attraction between IgG1 and glass. None of the nonionic surfactants were able to prevent pronounced electrostatic attraction, e.g. by means of shielding the surface. It has already been mentioned that the absolute decrease in adsorption at pH 4.0 was at the same magnitude as at pH 7.2 (Figure 13b). One may assume that hydrophobic IgG1 - surface interactions played a role for adsorption at pH 4.0 as well. The fact that proteins are able to adsorb on surfaces with hydrophilic and hydrophobic protein patches at the same time reinforces this hypothesis [84]. Consequently, surfactants probably diminished hydrophobic interactions at pH 4.0 as well, which gave rise to the decreased adsorption at pH 4.0.

In Figure 13, another tendency can be observed for both pH values. The higher the hydrophobicity of the surfactants was (i.e. the lower the HLB), the stronger was the adsorption-reducing effect. This is again accounted for by means of the hydrophobic patch approach. Surfactants holding a larger hydrophobic molecule part increasingly shield hydrophobic areas of either protein or sorbent surface, which results in decreased adsorption. In contrast, more hydrophilic surfactants are more readily solvated and less prone to interact with hydrophobic sites. The findings of Duncan *et al.*, that PS 20 was more effective than P 188 in reducing salmon calcitonin adsorption on borosilicate glass, confirm this theory [80].

Generally, in case the binding of surfactants to the surface accounts for the prevention or the reversion of protein adsorption, the CMCs of the surfactants become crucial. At surfactant concentrations above the CMC, the surface is maximally covered. The CMCs of PS 20, PS 80, and PCO 35 are all located in a narrow range (see Table 2). For an IgG1 concentration of 2 mg/ml prevailing at the adsorption experiments, these CMCs correspond to a surfactant : protein ratio between 1 : 1 and 10 : 1. At pH 7.2, IgG1 adsorption does not further decrease above a ratio of 1 : 1, except for drastically high concentrations of the

above surfactants (Figure 13a). By contrast, IgG1 adsorption in the presence of P 188 steadily decreases up to a ratio of 100 : 1. At this point, the CMC of P 188 is not reached, and it may be concluded that adsorption further decreases by increasing the P 188 concentration. When the same surfactant is considered at pH 4.0, the 1000-fold excess of P 188 over the protein is the first concentration where a distinct decrease of adsorption can be observed. This leads to the conclusion that the adsorption-reducing effect of P 188 similarly depends on its CMC. However, no uniform concentration dependency is observed for PS 20, PS 80, and PCO 35 at pH 4.0. It has to be mentioned that the CMCs of the surfactants in the protein solutions were not explicitly measured. The CMC of a surfactant is not a constant value, but varies with, amongst others, ionic strength, pH value, protein concentration, other excipients, and temperature. For example, a high salt content has shown to shift the CMC to lower surfactant concentrations [95,96]. This complicates the interpretation of results obtained at different pH values.

According to literature, a minimum of HSA adsorption on hydrophilic silica surface at the CMC of PS 20 has been found by Zhang and Ferrari [30]. But it has also been described that the CMC of a surfactant does not sufficiently explain concentration-dependent effects on proteins. In this regard, Katakam *et al.* have shown that the stabilizing effect of PS 80 on hGH is not related to the CMC but rather follows certain molar ratios, which indicates a certain binding stoichiometry between the surfactant and the protein [75]. They further stated that a dependency on the CMC would be indicative of a monolayer effect, which implies a complete saturation of interfaces. An effect observed above the CMC may, by contrast, point to a specific binding between surfactant and protein. Our results at pH 7.2 are rather indicative of the monolayer theory, whereas at pH 4.0, the trend is less clear. It would be of particular interest to learn how these surfactants affect protein adsorption on uncharged hydrophobic surfaces.

4 CONCLUSIONS

It was clearly shown that the adsorption of IgG on the surface of borosilicate glass vials is a function of the formulation pH and ionic strength, and depends on the properties of the excipients that are added to the formulation. The outcome of the experiments described above leads to the conclusion that, in general, the adsorption process is to a large extent mediated by electrostatic interactions. During adsorption, attractive or repulsive forces between protein and glass surface as well as repulsive forces between the adsorbed IgG molecules on the surface interact. The magnitude of each factor varies independently by changing pH or ionic strength, respectively. The resulting charge of both sorbent surface

and protein, together with the charge screening strength of the ions present in the solution on both entities, is of fundamental importance. The interplay of the arising forces became apparent, for example, from the shift of the pH of maximum adsorption, when the ionic strength was altered. However, the adsorption of IgG on glass must be, at least in part, mediated by other forces than electrostatic interactions. Especially in the area of the protein IEP, hydrophobic interactions or surface-induced structural changes occur. For pH values below the protein IEP, electrostatic interactions were observed to gain in importance, whereas a residual contribution of other interaction forces is still likely. Electrokinetic measurements on IgG1 and glass particles allowed a deeper insight into the prevailing electrostatic interactions. This includes the uptake of low molecular weight ions into the adsorption boundary layer during the adsorption process, which could be determined in that way. The pH value where ion uptake was minimal, which indicates the most beneficial condition for adsorption from the electrostatic point of view, could be shown to coincide with the pH of maximum adsorption determined from vial adsorption experiments. This again corroborates the broad influence of electrostatic interactions on the adsorption process. The impact of increasing ionic strength on the adsorbed amount is not consistent. Increasing NaCl concentrations can result in either an increase or a decrease of the adsorbed amount of protein, depending on whether protein - surface or intermolecular electrostatic interactions are most pronounced and primarily screened. The SO_4^{2-} ion proved to be more effective than Cl^- in compensating charges due to its higher valency and polarizability. For increased concentrations of Na_2SO_4, which exhibits better protein stabilizing properties than NaCl with respect to the “Hofmeister series”, the preferential exclusion effect reduces its capability to compensate interfacial charges. Uncharged sugars and polyols, which also lead to preferential exclusion, exhibited only marginal effects on adsorption, substantiating the importance of charge interactions. Usually, but not always, the addition of nonionic surfactants led to a decreased IgG adsorption on borosilicate glass. The extent of reduction roughly depended on the hydrophilic/lipophilic balance (HLB) of the surfactants, whereas the absolute reduction was similar for the pH values investigated. This is in line with the contribution of hydrophobic interactions. The CMC turned out to be a critical value for the effect at neutral pH, but this dependency was less profound at acidic pH.

5 REFERENCES

[1] Norde, W., Lyklema, J., Thermodynamics of protein adsorption. Theory with special reference to the adsorption of human plasma albumin and bovine pancreas ribonuclease at polystyrene surfaces, *J. Colloid Interface Sci.* **71** (1979) 350-366.

[2] Norde, W., Adsorption of proteins at solid-liquid interfaces, *Cells and Materials* **5** (1995) 97-112.

[3] Wang, W., Instability, stabilization, and formulation of liquid protein pharmaceuticals, *International Journal of Pharmaceutics* **185** (1999) 129-188.

[4] Hawe, A., Friess, W., Formulation Development for Hydrophobic Therapeutic Proteins, *Pharmaceutical Development and Technology* **12** (2007) 223-237.

[5] Buijs, J., Lichtenbelt, J. W. T., Norde, W., Lyklema, J., Adsorption of monoclonal IgGs and their F(ab')2 fragments onto polymeric surfaces, *Colloids and Surfaces, B: Biointerfaces* **5** (1995) 11-23.

[6] Greene, G., Radhakrishna, H., Tannenbaum, R., Protein binding properties of surface-modified porous polyethylene membranes, *Biomaterials* **26** (2005) 5972-5982.

[7] Norde, W., MacRitchie, F., Nowicka, G., Lyklema, J., Protein adsorption at solid-liquid interfaces: reversibility and conformation aspects, *Journal of Colloid and Interface Science* **112** (1986) 447-456.

[8] Su, T. J., Lu, J. R., Thomas, R. K., Cui, Z. F., Penfold, J., The adsorption of lysozyme at the silica-water interface: a neutron reflection study, *Journal of Colloid and Interface Science* **203** (1998) 419-429.

[9] Arai, T., Norde, W., The behavior of some model proteins at solid-liquid interfaces. 1. Adsorption from single protein solutions, *Colloids and Surfaces* **51** (1990) 1-15.

[10] Buijs, J., Norde, W., Lichtenbelt, J. W. T., Changes in the Secondary Structure of Adsorbed IgG and F(ab')2 Studied by FTIR Spectroscopy, *Langmuir* **12** (1996) 1605-1613.

[11] Buijs, J., van den Berg, P. A. W., Lichtenbelt, J. W. T., Norde, W., Lyklema, J., Adsorption dynamics of IgG and its F(ab')2 and Fc fragments studied by reflectometry, *Journal of Colloid and Interface Science* **178** (1996) 594-605.

[12] Frokjaer, S., Hovgard, L., Pharmaceutical Formulation Development of Peptides and Proteins, (Taylor & Francis Limited, London) Ed. 1, 2000.

[13] Ahrer, K., Buchacher, A., Iberer, G., Jungbauer, A., Thermodynamic stability and formation of aggregates of human immunoglobulin G characterized by differential scanning calorimetry and dynamic light scattering, *J. Biochem. Biophys. Methods* **66** (2006) 73-86.

[14] Haynes, C. A., Norde, W., Globular proteins at solid/liquid interfaces, *Colloids and Surfaces, B: Biointerfaces* **2** (1994) 517-566.

[15] Krajewski, A., Malavolti, R., Piancastelli, A., Albumin adhesion on some biological and non-biological glasses and connection with their z-potentials, *Biomaterials* **17** (1996) 53-60.

[16] Jacobasch, H. J., Simon, F., Weidenhammer, P., Adsorption of ions onto polymer surfaces and its influence on zeta potential and adhesion phenomena, *Colloid Polym. Sci.* **276** (1998) 434-442.

[17] Chae, K. S., Lenhoff, A. M., Computation of the electrophoretic mobility of proteins, *Biophys. J.* **68** (1995) 1120-1127.

[18] Norde, W., Lyklema, J., The adsorption of human plasma albumin and bovine pancreas ribonuclease at negatively charged polystyrene surfaces. III. Electrophoresis, *Journal of Colloid and Interface Science* **66** (1978) 277-284.

[19] Oliva, F. Y., Avalle, L. B., Camara, O. R., De Pauli, C. P., Adsorption of human serum albumin (HSA) onto colloidal TiO2 particles, Part I, *J. Colloid Interface Sci.* **261** (2003) 299-311.

[20] Lyklema, J., Elektrostatische Doppelschichten: Elektrostatik und Elektrodynamik, *Chemie Ingenieur Technik* **71** (1999) 1364-1369.

[21] Hunter, R. J., Colloid Science: Zeta Potential in Colloid Science: Principles and Applications, (Academic Press Limited, London) Ed. 1, 1981.

[22] Elgersma, A. V., Zsom, R. L. J., Norde, W., Lyklema, J., The adsorption of bovine serum albumin on positively and negatively charged polystyrene lattices, *J. Colloid Interface Sci.* **138** (1990) 145-156.

[23] Arakawa, T., Prestrelski, S. J., Kenney, W. C., Carpenter, J. F., Factors affecting short-term and long-term stabilities of proteins, *Adv. Drug Delivery Rev.* **10** (1993) 1-28.

[24] Arakawa, T., Timasheff, S. N., Preferential interactions of proteins with salts in concentrated solutions, *Biochemistry* **21** (1982) 6545-6552.

[25] Timasheff, S. N., Solvent effects on protein stability, *Curr. Opin. Struct. Biol.* **2** (1991) 35-39.

[26] Arakawa, T., Timasheff, S. N., Stabilization of protein structure by sugars, *Biochemistry* **21** (1982) 6536-6544.

[27] Gekko, K., Timasheff, S. N., Mechanism of protein stabilization by glycerol: preferential hydration in glycerol-water mixtures, *Biochemistry* **20** (1981) 4667-4676.

[28] Kiese, S., Papppenberger, A., Friess, W., Mahler, H. C., Shaken, not stirred: mechanical stress testing of an IgG1 antibody, *J. Pharm. Sci.* **97** (2008) 4347-4366.

[29] Johnston, T. P., Adsorption of recombinant human granulocyte colony stimulating factor (rhG-CSF) to polyvinyl chloride, polypropylene, and glass: Effect of solvent additives, *PDA J. Pharm. Sci. Technol.* **50** (1996) 238-245.

[30] Zhang, M., Ferrari, M., Reduction of albumin adsorption onto silicon surfaces by Tween 20, *Biotechnology and Bioengineering* **56** (1997) 618-625.

[31] Williams, R. A., Blanch, H. W., Covalent immobilization of protein monolayers for biosensor applications, *Biosens. Bioelectron.* **9** (1994) 159-167.

[32] de Levie, R., Activity Effects, *Aqueous Acid-Base Equilibria and Titrations*, (Oxford University Press, Oxford, New York, 1999), Chapter 6, 59-66.

[33] Kim, C., Ionic Equilibrium, *Advanced Pharmaceutics - Physicochemical Principles*, (CRC Press LLC, Boca Raton, Florida (USA), 2004), Chapter 2, 45-112.

[34] Ellis, K. J., Morrison, J. F., Buffers of constant ionic strength for studying pH-dependent processes, *Methods in Enzymology* **87** (1982) 405-426.

[35] Stoll, V. S., Blanchard, J. S., Buffers: principles and practice, *Methods in Enzymology* **182** (1990) 24-38.

[36] Serra, J., Puig, J., Martin, A., Galisteo, F., Galvez, M., Hidalgo-Alvarez, R., On the adsorption of IgG onto polystyrene particles: electrophoretic mobility and critical coagulation concentration, *Colloid Polym. Sci.* **270** (1992) 574-583.

[37] Li, G., Stewart, R., Conlan, B., Gilbert, A., Roeth, P., Nair, H., Purification of human immunoglobulin G: a new approach to plasma fractionation, *Vox Sang.* **83** (2002) 332-338.

[38] Rice, P., Longden, I., Bleasby, A., EMBOSS: the european molecular biology open software suite, *Trends Genet.* **16** (2000) 276-277.

[39] Compton, B. J., Electrophoretic mobility modeling of proteins in free zone capillary electrophoresis and its application to monoclonal antibody microheterogeneity analysis, *J. Chromatogr.* **559** (1991) 357-366.

[40] Mosher, R. A., Gebauer, P., Thormann, W., Computer simulation and experimental validation of the electrophoretic behavior of proteins. III. Use of titration data predicted by the protein's amino acid composition, *J. Chromatogr.* **638** (1993) 155-164.

[41] Kosmulski, M., Positive electrokinetic charge of silica in the presence of chlorides, *J. Colloid Interface Sci.* **208** (1998) 543-545.

[42] Barz, D. P. J., Vogel, M. J., Steen, P. H., Determination of the Zeta Potential of Porous Substrates by Droplet Deflection. I. The Influence of Ionic Strength and pH Value of an Aqueous Electrolyte in Contact with a Borosilicate Surface, *Langmuir* **25** (2009) 1842-1850.

[43] Bagchi, P., Birnbaum, S. M., Effect of pH on the adsorption of immunoglobulin G on anionic poly(vinyltoluene) model latex particles, *J. Colloid Interface Sci.* **83** (1981) 460-478.

[44] Shirahama, H., Suzuki, K., Suzawa, T., Bovine hemoglobin adsorption onto polymer latexes, *J. Colloid Interface Sci.* **129** (1989) 483-490.

[45] Zhu, X., Fan, H., Li, D., Xiao, Y., Zhang, X., Protein adsorption and zeta potentials of a biphasic calcium phosphate ceramic under various conditions, *J. Biomed. Mater. Res. Part B* **82B** (2007) 65-73.

[46] Van Dulm, P., Norde, W., Lyklema, J., Ion participation in protein adsorption at solid surfaces, *J. Colloid Interface Sci.* **82** (1981) 77-82.

[47] Salgin, S., Takac, S., Oezdamar, T. H., Adsorption of bovine serum albumin on polyether sulfone ultrafiltration membranes: Determination of interfacial interaction energy and effective diffusion coefficient, *J. Membr. Sci.* **278** (2006) 251-260.

[48] Xu, H., Lu, J. R., Williams, D. E., Effect of surface packing density of interfacially adsorbed monoclonal antibody on the binding of hormonal antigen human chorionic gonadotrophin, *Journal of Physical Chemistry B* **110** (2006) 1907-1914.

[49] Su, T. J., Lu, J. R., Thomas, R. K., Cui, Z. F., Effect of pH on the Adsorption of Bovine Serum Albumin at the Silica/Water Interface Studied by Neutron Reflection, *J. Phys. Chem. B* **103** (1999) 3727-3736.

[50] Norde, W., Adsorption of proteins from solution at the solid-liquid interface, *Advances in Colloid and Interface Science* **25** (1986) 267-340.

[51] Norde, W., Lyklema, J., The adsorption of human plasma albumin and bovine pancreas ribonuclease at negatively charged polystyrene surfaces. I. Adsorption isotherms. Effects of charge, ionic strength, and temperature, *Journal of Colloid and Interface Science* **66** (1978) 257-265.

[52] Su, T. J., Lu, J. R., Thomas, R. K., Cui, Z. F., Penfold, J., The Effect of Solution pH on the Structure of Lysozyme Layers Adsorbed at the Silica-Water Interface Studied by Neutron Reflection, *Langmuir* **14** (1998) 438-445.

[53] Norde, W., Lyklema, J., Why proteins prefer interfaces, *J. Biomater. Sci. Polym. Ed.* **2** (1991) 183-202.

[54] Su, T. J., Lu, J. R., Thomas, R. K., Cui, Z. F., Penfold, J., The adsorption of lysozyme at the silica-water interface: a neutron reflection study, *J. Colloid Interface Sci.* **203** (1998) 419-429.

[55] Haynes, C. A., Norde, W., Structures and stabilities of adsorbed proteins, *Journal of Colloid and Interface Science* **169** (1995) 313-328.

[56] Shirahama, H., Takeda, K., Suzawa, T., Adsorption of bovine serum albumin onto polystyrene latex: effects of coexistent electrolyte anions, *J. Colloid Interface Sci.* **109** (1986) 552-556.

[57] Joessang, T., Feder, J., Rosenqvist, E., Photon correlation spectroscopy of human IgG, *J. Protein Chem.* **7** (1988) 165-171.

[58] Gaza-Bulseco, G., Liu, H., Fragmentation of a Recombinant Monoclonal Antibody at Various pH, *Pharmaceutical Research* **25** (2008) 1881-1890.

[59] Chi, E. Y., Krishnan, S., Randolph, T. W., Carpenter, J. F., Physical Stability of Proteins in Aqueous Solution: Mechanism and Driving Forces in Nonnative Protein Aggregation, *Pharm. Res.* **20** (2003) 1325-1336.

[60] Ahrer, K., Buchacher, A., Iberer, G., Jungbauer, A., Detection of aggregate formation during production of human immunoglobulin G by means of light scattering, *J. Chromatogr. A* **1043** (2004) 41-46.

[61] Brange, J., Physical stability of proteins, *Pharmaceutical Formulation Development of Peptides and Proteins* (2000) 89-112.

[62] Nylander, T., Protein adsorption in relation to solution association and aggregation, *Surfactant Science Series* **110** (2003) 259-294.

[63] Elofsson, U. M., Paulsson, M. A., Arnebrant, T., Adsorption of beta -Lactoglobulin A and B in Relation to Self-Association: Effect of Concentration and pH, *Langmuir* **13** (1997) 1695-1700.

[64] Arnebrant, T., Nylander, T., Adsorption of insulin on metal surfaces in relation to association behavior, *J. Colloid Interface Sci.* **122** (1988) 557-566.

[65] Kim, D. T., Blanch, H. W., Radke, C. J., Direct imaging of lysozyme adsorption onto mica by atomic force microscopy, *Langmuir* **18** (2002) 5841-5850.

[66] Marsh, R. J., Jones, R. A. L., Sferrazza, M., Adsorption and displacement of a globular protein on hydrophilic and hydrophobic surfaces, *Colloids and Surfaces, B: Biointerfaces* **23** (2002) 31-42.

[67] Wahlgren, M., Arnebrant, T., Lundstroem, I., The adsorption of lysozyme to hydrophilic silicon oxide surfaces: comparison between experimental data and models for adsorption kinetics, *J. Colloid Interface Sci.* **175** (1995) 506-514.

[68] Suelter, C. H., DeLuca, M., How to prevent losses of protein by adsorption to glass and plastic, *Anal. Biochem.* **135** (1983) 112-119.

[69] Gasteiger, E., Hoogland, C., Gattiker, A., Duvaud, S., Wilkins, M. R., Appel, R. D., Bairoch, A., Protein identification and analysis tools on the ExPASy server, *Proteomics Protoc. Handb.* (2005) 571-607.

[70] Wendorf, J. R., Radke, C. J., Blanch, H. W., Reduced protein adsorption at solid interfaces by sugar excipients, *Biotechnology and Bioengineering* **87** (2004) 565-573.

[71] Ramsden, J. J., Prenosil, J. E., Effect of Ionic Strength on Protein Adsorption Kinetics, *Journal of Physical Chemistry* **98** (1994) 5376-5381.

[72] Chang, B. S., Beauvais, R. M., Arakawa, T., Narhi, L. O., Dong, A., Aparisio, D. I., Carpenter, J. F., Formation of an active dimer during storage of interleukin-1 receptor antagonist in aqueous solution, *Biophys. J.* **71** (1996) 3399-3406.

[73] Matheus, S., Development of High Concentration cetuximab Formulations using Ultrafiltration and Precipitation Techniques, Thesis, 2006.

[74] Claesson, P. M., Christenson, H. K., Berg, J. M., Neuman, R. D., Interactions between mica surfaces in the presence of carbohydrates, *J. Colloid Interface Sci.* **172** (1995) 415-424.

[75] Katakam, M., Bell, L. N., Banga, A. K., Effect of Surfactants on the Physical Stability of Recombinant Human Growth Hormone, *J. Pharm. Sci.* **84** (1995) 713-716.

[76] Bam, N. B., Cleland, J. L., Yang, J., Manning, M. C., Carpenter, J. F., Kelley, R. F., Randolph, T. W., Tween Protects Recombinant Human Growth Hormone against Agitation-Induced Damage via Hydrophobic Interactions, *Journal of Pharmaceutical Sciences* **87** (1998) 1554-1559.

[77] Nakanishi, K., Sakiyama, T., Imamura, K., On the adsorption of proteins on solid surfaces, a common but very complicated phenomenon, *Journal of Bioscience and Bioengineering* **91** (2001) 233-244.

[78] Mahler, H. C., Mueller, R., Friess, W., Delille, A., Matheus, S., Induction and analysis of aggregates in a liquid IgG1-antibody formulation, *European Journal of Pharmaceutics and Biopharmaceutics* **59** (2005) 407-417.

[79] Frokjaer, S., Otzen, D. E., Protein drug stability: a formulation challenge, *Nat. Rev. Drug Discovery* **4** (2005) 298-306.

[80] Duncan, M. R., Lee, J. M., Warchol, M. P., Influence of surfactants upon protein/peptide adsorption to glass and polypropylene, *International Journal of Pharmaceutics* **120** (1995) 179-188.

[81] Thurow, H., Geisen, K., Stabilisation of dissolved proteins against denaturation at hydrophobic interfaces, *Diabetologia* **27** (1984) 212-218.

[82] Mizutani, T., Decreased activity of proteins adsorbed onto glass surfaces with porous glass as a reference, *Journal of Pharmaceutical Sciences* **69** (1980) 279-282.

[83] Feng, M., Morales, A. B., Poot, A., Beugeling, T., Bantjes, A., Effects of Tween 20 on the desorption of proteins from polymer surfaces, *J. Biomater. Sci. Polym. Ed.* **7** (1995) 415-424.

[84] Elwing, H., Welin, S., Askendal, A., Nilsson, U., Lundstroem, I., A wettability gradient method for studies of macromolecular interactions at the liquid/solid interface, *J. Colloid Interface Sci.* **119** (1987) 203-210.

[85] Gombotz, W. R., Pankey, S. C., Bouchard, L. S., Phan, D. H., Mackenzie, A. P., Stability, characterization, formulation, and delivery system development for transforming growth factor-beta1, *Pharm. Biotechnol.* **9** (1996) 219-245.

[86] Hawe, A., Studies on Stable Formulations for a Hydrophobic Cytokine, Thesis, 2006.

[87] Batrakova, E. V., Han, H. Y., Alakhov, V. Y., Miller, D. W., Kabanov, A. V., Effects of Pluronic block copolymers on drug absorption in Caco-2 cell monolayers, *Pharm. Res.* **15** (1998) 850-855.

[88] Seeballuck, F., Ashford, M. B., O'Driscoll, C. M., The Effects of Pluronic Block Copolymers and Cremophor EL on Intestinal Lipoprotein Processing and the Potential Link with P-Glycoprotein in Caco-2 Cells, *Pharm. Res.* **20** (2003) 1085-1092.

[89] Kabanov, A. V., Batrakova, E. V., Miller, D. W., Pluronic block copolymers as modulators of drug efflux transporter activity in the blood-brain barrier, *Adv. Drug Delivery Rev.* **55** (2003) 151-164.

[90] BASF AG Fine Chemicals Division, Lutrol F68 Technical Information, 2005.

[91] Bendikiene, V., Surinenaite, B., Bachmatova, I., Marcinkeviciene, L., Juodka, B., Tweens and ionic detergents in the hydrolytic activity of Pseudomonas mendocina 3121-1 lipase, *Biologija* **54** (2008) 242-246.

[92] BASF AG Fine Chemicals Division, Cremophor EL Technical Information, 2004.

[93] Wahlgren, M. C., Arnebrant, T., The concentration dependence of adsorption from a mixture of beta -lactoglobulin and sodium dodecyl sulfate onto methylated silica surfaces, *J. Colloid Interface Sci.* **148** (1992) 201-206.

[94] Wahlgren, M., Karlsson, C. A. C., Welin-Klintstroem, S., Interactions between proteins and surfactants at solid interfaces, *Surfactant Sci. Ser.* **110** (2003) 321-343.

[95] Rapoza, R. J., Horbett, T. A., The effects of concentration and adsorption time on the elutability of adsorbed proteins in surfactant solutions of varying structures and concentrations, *J. Colloid Interface Sci.* **136** (1990) 480-493.

[96] Fuguet, E., Rafols, C., Roses, M., Bosch, E., Critical micelle concentration of surfactants in aqueous buffered and unbuffered systems, *Anal. Chim. Acta* **548** (2005) 95-100.

Chapter 5

Modeling of IgG1 Adsorption to Vials – Isotherm Considerations and Affinity Aspects

Abstract

The equilibrium adsorption of IgG1 to hydrophilic borosilicate glass vials as well as to siliconized glass and hydrophobic cyclic polyolefin plastic vials was investigated by means of adsorption isotherms. Variations were made regarding pH value (4.0, 7.2, and 8.6) and ionic strength (40 - 600 mM) of the IgG1 formulation. The adsorption data was analyzed by three adsorption isotherm models, namely the Langmuir, the Freundlich, and the combined Langmuir-Freundlich (Sips) model. The latter, representing a three-parameter isotherm model, was found to be most qualified to empirically describe the experimental data, also with respect to varying surface types and solution compositions. Both the adsorption affinity findings and isotherm plateau values pointed towards a predominantly electrostatically driven adsorption mechanism on glass, but also reflected strong hydrophobic interaction driving forces for the low-energetic surfaces. Differences in surface affinity at varying pH were confirmed by quartz crystal microbalance kinetic measurements on hydrophilic silica model surfaces. Statements on the adsorption cooperativity were derived from the power constant *n* of the Langmuir-Freundlich isotherm model. Cooperativity appeared to be negative at any adsorption condition, thus indicating a consistently decreasing affinity for subsequently attaching molecules. In contrast to the situation on hydrophobic surfaces, where the extent of negative cooperativity was mostly invariable, the extent of negative cooperativity for IgG1 adsorption to borosilicate glass decreased with increasing ionic strength or increasing pH. This was indicative of either reduced intermolecular repulsion forces, including increased charge screening effects, or an increased aggregation tendency, which resulted in enhanced intermolecular attractive forces. Different adsorption isotherm shapes and different plateau values of IgG1 adsorbing on siliconized glass and on hydrophobic cyclic polyolefin plastic might be due to an increased tendency of IgG1 to more pronounced structural alterations in contact with the low-energetic silicon coating.

1 INTRODUCTION

One of the most convenient ways to investigate adsorption phenomena is probably the determination of adsorption isotherms. In isotherms, the adsorbed amount (Γ) is plotted against the concentration (c_{eq}) of the adsorbing species in solution at equilibrium conditions and constant temperature. In general, for protein adsorption on solid surfaces, high affinity isotherms are observed. The isotherms' ascending branch merges the axis of Γ, and plateau values are already reached at low protein concentrations [1]. Thus, the initial curve gradient represents the affinity of the protein to the surface at the respective adsorption condition. Less frequently, protein adsorption manifests in low affinity adsorption isotherms [2,3]. With respect to protein adsorption on solid surfaces, several mathematical equations are commonly used to describe and interpret adsorption isotherm data [4-6]. One of the first and certainly most famous adsorption models has been established by Irving Langmuir (1881 - 1957), and has often been utilized for the interpretation of protein adsorption [7-10]. According to Langmuir, whose model was originally based on the adsorption of gas atoms to solid surfaces, several fundamental postulates are included. If the model is transferred to the situation of proteins, these can be summarized as follows:

1. There is an equilibrium between adsorbed protein molecules ($M\,S$) on the solid surface $S\,(solid)$ and dissolved molecules in the supernatant liquid $M\,(liquid)$ (Equation 1). The rate constants for adsorption (k_a) and desorption (k_d) can be subsumed in an equilibrium constant $K = k_a / k_d$.

$$M\,(liquid) + S\,(solid) \underset{k_d}{\overset{k_a}{\rightleftharpoons}} M\,S \tag{1}$$

2. The proteins are adsorbed on a fixed number of defined sites.
3. All adsorption sites on the solid are energetically equivalent.
4. Adsorption sites are not occupied by more than one molecule.
5. Molecules on separate sites do not exert forces on one another, which in other words, means that lateral interactions within the monolayer are neglected.

The equation by which Langmuir described these adsorption equilibria is:

$$\Gamma = \frac{\Gamma_{max}\, K\, c_{eq}}{1 + K\, c_{eq}} \tag{2}$$

Therein, Γ equals the equilibrium surface concentration of the protein, Γ_{max} is the maximum surface concentration of the protein attainable at monolayer coverage, K is the equilibrium constant (see above), and c_{eq} equals the concentration of free protein in the solution at adsorption equilibrium conditions. However, since adsorption sites are often observed to be non-independent in protein adsorption to solid surface, the Langmuir model would thus be incapable of describing the experimentally obtained isotherms. Another common but strictly empirical model, by which protein adsorption isotherms have also been described [11,12], is the Freundlich isotherm model (Equation 3):

$$\Gamma = k\, c_{eq}^{n} \tag{3}$$

In the above power function, k and c_{eq} are the Freundlich equilibrium constant and the power constant of the Freundlich isotherm, respectively. Although the Freundlich model is limited in that the adsorbed amount increases indefinitely with the adsorbent concentration, it can nevertheless be of theoretical interest to describe adsorption on energetically heterogeneous surfaces. For example, the Freundlich model was reported to fit isotherms where the adsorption energy behaves inversely proportional to the logarithm of the degree of surface coverage [13]. A third model representing a simple generalization of both previously described isotherm models is the combined Langmuir-Freundlich model (Equation 4), which was derived by Sips in 1950 [14]:

$$\Gamma = \frac{\Gamma_{max}\,(K_m\, c_{eq})^n}{1+(K_m\, c_{eq})^n} \tag{4}$$

In analogy to the Langmuir model, Γ equals the adsorbed amount per unit surface, Γ_{max} the maximum attainable surface concentration, and c_{eq} the concentration of free molecules in solution at adsorption equilibrium conditions. In this model, K_m equals the mean binding affinity, which is the mean value of varying bonding energy coefficients K on heterogeneous surfaces, applying a Gaussian-like distribution of these energy coefficients [15,16]. Although not completely equivalent to the Langmuir constant, a higher value of K_m still corresponds to a faster adsorption over desorption [17]. The Langmuir-Freundlich model combines both single models, but can reduce to either at its limits. For $n = 1$, it reduces to the Langmuir isotherm (Equation 2), where K_m equals the binding affinity K. If K_m or c_{eq} reaches 0, the isotherm is reduced to the Freundlich term (Equation 3). The power constant n is of particular interest because it represents the type and the extent of adsorption cooperativity in adsorption of heterogeneous nature [5]. For independent and non-interacting adsorption sites, the n-value is 1, according to the Langmuir model. Positive adsorption cooperativity is indicated by $n > 1$, while negative cooperativity can be

expected when $0 < n < 1$. Therefore, n can be used as an empirical coefficient representing the kind and the degree of cooperativity which prevails during the binding step. Sharma and Agarwal found the combined Langmuir-Freundlich model to be capable of modeling adsorption cooperativity and to be much better suited for approximating heterogeneous adsorption due to its three fitting terms [5].

Within the scope of previous chapters, we have not yet investigated the IgG1 adsorption on either hydrophilic or hydrophobic packaging container surfaces by means of isotherms, but only as one-point determination at one single protein concentration in the upper range. Adsorption isotherms, which illustrate the adsorbed amount Γ over a broad range of concentration c_{eq}, can give further insightful information on the adsorption process. Conclusions can be drawn concerning the predominating extent of electrostatic or hydrophobic interaction as well as structural rearrangements upon adsorption [9,18,19]. As already mentioned above, the initial slope of an isotherm is an indication of the affinity of a protein to the sorbent surface. The appearance of defined plateaus on the isotherm curves furthermore indicates saturation conditions, which can correspond to a state equal to, less than, or even above a complete protein monolayer [19]. The occurrence of steps or inflection points in adsorption isotherms can be indicative of conformational alterations of adsorbed proteins; it can denote a reorientation step or probably the onset of a second protein layer [20].

In our previous work, the influence of the surface quality on IgG1 adsorption, including free energy, was investigated (Chapter 3). Other studies dealt with the impact of the protein formulation composition on the extent of adsorbed IgG1 at saturation conditions (Chapter 4). In this study, the key parameters of both aspects were combined and adsorption isotherms of IgG1 were determined at different pH values on borosilicate glass, on siliconized borosilicate glass, as well as on hydrophobic cyclic polyolefin (COP) plastic. For borosilicate glass, the influence of ionic strength (I) on equilibrium adsorption behavior was also investigated at two characteristic pH values: at pH 4.0 (representing maximum adsorption) and pH 8.6 (the isoelectric pH of IgG1) (see Chapter 4). With the aid of the most qualified isotherm model, the associated adsorption constants were calculated, by which the adsorption behavior under different conditions was subsequently interpreted. In addition to isothermal adsorption investigations, the adsorption kinetics of IgG1 on a hydrophilic silica model surface was studied, which should verify the observed differences in adsorption affinity at extreme pH values and give first insights into adsorption reversibility.

2 MATERIALS AND METHODS

2.1 Materials

2.1.1 Protein Formulation

For protein adsorption experiments, an IgG1 (MW ≈ 152 kDa), dissolved in 10 mM phosphate buffer and 145 mM NaCl (pH 7.2), was used, which was kindly provided by Merck Serono (Darmstadt, Germany). For ionic strength adjustment, the solution was dialyzed against a pure 10 mM phosphate buffer solution (NaH_2PO_4 and Na_2HPO_4 from Merck Chemicals, Darmstadt, Germany) using Vivaflow® 50 tangential flow filtration cartridges (Sartorius-Stedim Biotech, Goettingen, Germany) equipped with a 30,000 MWCO polyethersulfone (PES) membrane. The IgG1 concentration was determined by UV spectroscopy (see 2.2.1). Different volumes of a concentrated solution of NaCl (Merck Chemicals, Darmstadt, Germany) in the above-mentioned phosphate buffer were added to the protein solution. The pH was finally adjusted using 1M NaOH or HCl (Sigma-Aldrich, Munich, Germany). The ionic strength as well as the amount of excipients needed (NaCl, acid, or base) were calculated as described in Chapter 4. All protein solutions were filtered through a hydrophilic 0.2 µm PES membrane filter (Pall GmbH, Dreieich, Germany) before use. Typical protein handling like dilution and sample preparation was done in 15 ml and 50 ml polypropylene tubes (GreinerBio-One GmbH, Frickenhausen, Germany).

2.1.2 Glass Vials and Closure Systems

The pharmaceutical containers used in the investigations were Fiolax® 2R borosilicate glass vials, kindly provided by SCHOTT AG (Mainz, Germany). The vials were preprocessed (washed and heat sterilized) as described in Chapter 2. Resin CZ® 2 ml plastic vials (Daikyo Seiko, Ltd., Japan) made of a cyclic polyolefin (COP) were washed in the same way as the glass vials but dried at only 80°C for 1 h. Siliconized Fiolax® 2R borosilicate glass vials (pre-siliconized with Dow Corning 360), also from SCHOTT AG (Mainz, Germany), were preprocessed in the same manner as the plastic vials. After filling, the vials were closed with FluroTec® stoppers and finally sealed with Flip-Off® seals, both from West Pharmaceutical Services GmbH & Co. KG (Eschweiler, Germany).

2.1.3 Chemicals / Excipients

Ultrapure water (0.055 µS/cm) for all applications came from a Purelab Plus UV/UF system (ELGA LabWater, Celle, Germany) and was filtrated through a 0.22 µm membrane

filter before use. Sodium dodecyl sulfate (SDS) for IgG1 desorption was purchased from Sigma-Aldrich (Munich, Germany).

2.2 Methods

2.2.1 UV Spectroscopy

UV spectroscopy for protein concentration measurements was performed on a temperature-controlled Agilent 8453 UV/VIS spectrophotometer (Agilent Technologies GmbH, Boeblingen, Germany) at 25°C, $\lambda = 280$ nm, using quartz cuvettes and applying an extinction coefficient of 1.40 cm^2/mg for antibodies [21].

2.2.2 Adsorption Process for Isotherm Determination

The standardized adsorption procedure for IgG1 in containers was discussed in detail in Chapter 2. Briefly, the preprocessed vials were filled with IgG1 solution, closed, and incubated for 24 h in a water bath at 25°C with slow horizontal movement (25 rpm). The vials were emptied using a syringe with an injection needle and rinsed in four steps with buffer solution with the same formulation composition. For desorption of the inherent proteins, the vials were filled with PBS buffer pH 7.2 (10 mM phosphate plus 145 mM NaCl) containing 0.05% SDS, sealed, and stored at the above conditions over night for a further 14 h.

2.2.3 Size Exclusion High Performance Liquid Chromatography

Desorbed protein quantities were analyzed via size exclusion HPLC on an Agilent 1100 (Agilent Technologies GmbH, Boeblingen, Germany) equipped with a Tosoh TSKgel G3000SWXL and a TSKgel SWXL guardcolumn (Tosoh Bioscience GmbH, Stuttgart, Germany). The mobile phase equaled the desorption buffer described above. The injected sample volume was 400 µl and the run duration 50 min. The protein fluorescence signal at λ_{ex} / λ_{em} 280 nm / 334 nm was recorded. All chromatograms were integrated manually with the Agilent ChemStation software Rev. B 02.01 (Agilent Technologies GmbH, Boeblingen, Germany). In each HPLC batch run, a 10-point IgG1 calibration from 0.1 to 10.0 µg/ml was included.

2.2.4 (Non-) Linear Curve Fitting

Adsorption isotherms were correlated with theoretical adsorption models by linearization or nonlinear curve fitting by applying Levenberg-Marquardt iterations, using Origin 7 SR4 (OriginLab Corporation, Northampton, MA, USA).

2.2.5 Quartz Crystal Microbalance Measurements

Kinetic adsorption studies were performed on a Q-Sense E4 quartz crystal microbalance with dissipation monitoring (QCM-D) (Q-Sense AB, Gothenburg, Sweden). Thereby, disc-shaped piezoelectric quartz crystals with metal electrodes on both sides were excited to oscillation. In our case, sensors coated with silicon dioxide 50 nm (QSX 303, also from Q-Sense) served as model substrate to simulate the borosilicate glass surface. Buffer and protein solutions were pumped through the cells in a slow and constant flow. In the adsorption experiment, the cells were equilibrated with the corresponding blank buffer first. Subsequently, the protein was allowed to adsorb on the silica surface from IgG1 solutions (0.5 mg/ml) of pH 4.0 and pH 8.6. After a buffer rinsing step, the adsorbed IgG1 was removed with SDS desorption buffer pH 7.2 (described above), followed by another rinsing step with SDS-free blank buffer of the starting pH. The schedule of the 3-hour experiment is depicted in Table 1.

Table 1: Time table of the QCM-D experiment.

Time (h:min)	Medium	Step #
- 0:10 – 0:00	Equilibration with PBS	
0:00 – 0:45	IgG1 (500 µg/ml) in PBS	1
0:45 – 2:05	Rinse with blank PBS	1a
2:05 – 2:35	PBS + 0.05% SDS	2
2:35 – 3:00	Rinse with blank PBS	2a

3 RESULTS AND DISCUSSION

3.1 Fitting of IgG1 Adsorption Isotherms Determined on Borosilicate Glass

IgG1 adsorption isotherms, measured on various vial types at different adsorption conditions, were correlated with each of the three adsorption models elucidated in the introduction. Both the Langmuir and the Freundlich model can be easily converted into a linear equation by simple mathematical transformations. As for the Langmuir isotherm, the semi-reciprocal plot (c/Γ versus c) and the Scatchard plot (Γ/c versus Γ) were applied [22]. With a few exceptions, neither of the transformation plots revealed an acceptable linearization (data not shown). Hence, it was concluded that the Langmuir model does not satisfactorily describe the adsorption system of IgG1 on different container surfaces. With regard to the Langmuirean assumptions described above, this result can indicate a heterogeneous constitution of the adsorption sites on the vial surfaces or of the protein, respectively. Other conclusions could be multiple adsorption sites per molecule or lateral interactions among the adsorbing molecules. The Freundlich isotherm model, which basically equals a power function of solute concentration, can be linearized by plotting in double logarithmic coordinates [11]. Although the Freundlich model was rather appropriate for inhomogeneous adsorption site conditions, a satisfactory coincidence of the isotherms with this model was once more not observed in any instance (data not shown). The Temkin model, also proposed for the situation of reversible heterogeneous adsorption but not further elucidated in the scope of this work, served as an ancillary model. For instance, it has been successfully applied for the description of cytochrome c adsorption on metal affinity chromatographic support [4]. We applied the Temkin model as well in order to fit experimental IgG1 adsorption isotherm data. But it also failed to characterize IgG1 adsorption behavior (data not shown). Most likely, the model's basic assumption of a uniform distribution of binding energies does not apply for the adsorption of protein on both hydrophilic and hydrophobic surfaces.

The Langmuir-Freundlich model, which has been successfully applied to describe protein adsorption processes on solid surfaces [6,17,23] corresponded well with the adsorption data, irrespective of the type of sorbent surface or formulation composition (Figures 1 and 4). As a consequence, the Langmuir-Freundlich model was solely used for the interpretation of our adsorption studies. Adsorption isotherms of IgG1 on borosilicate glass are shown for pH 4.0 (Figure 1a) and pH 8.6 (Figure 1b) at different ionic strengths. As expected from the adsorption results of Chapter 4, pH 4.0 isotherms exhibit higher adsorption plateau levels at the terminal concentration of 2 mg/ml than the pH 8.6 iso-

therms. The affinity of IgG1 to glass, which is indicated by the initial part of the isotherms (the initial gradient of the curve), is apparently higher at pH 4.0. Thus, adsorption values in the range of the plateau are already reached at lower c_{eq} values, whereas at pH 8.6, Γ increases more evenly up to the higher concentration range. The high surface affinity of IgG1 at pH 4.0, especially striking at low c_{eq}, is mainly the result of the high electrostatic attraction between the net-positively charged IgG1 and the net-negatively charged glass

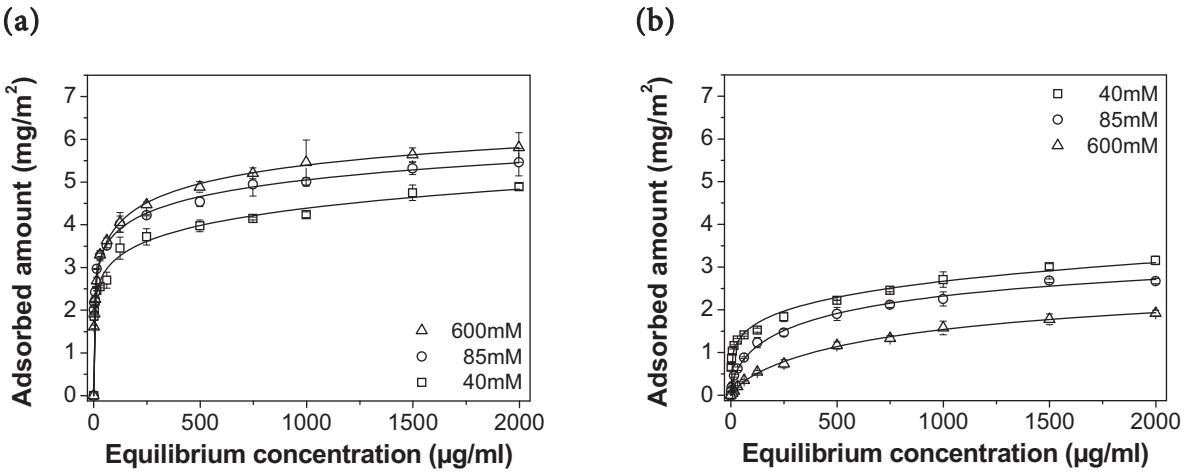

Figure 1: Adsorption isotherms of IgG1 measured on borosilicate glass vials at (a) pH 4.0 and (b) pH 8.6 for I = 40, 85 and 600 mM (n = 3); isotherms fitted by nonlinear curve approximation based on the Langmuir-Freundlich model.

Table 2: Results of the adsorption isotherm nonlinear curve fitting with the Langmuir-Freundlich model for IgG1 on borosilicate glass at pH 4.0 and pH 8.6.

			Langmuir-Freundlich model parameters		
	Ionic strength (mM)	Initial slope [a] (mg·ml/µg·m²)	Γ_{max} [b] (mg/m²)	n [b]	K [b] (ml/g)
pH 4.0	40	0.7482	undefined [c]	0.14	undefined [c]
	85	0.8351	11.54	0.20	0.29
	600	0.6951	8.53	0.31	5.91
pH 8.6	40	0.2670	undefined [c]	0.22	undefined [c]
	85	0.0481	4.08	0.58	1.62
	600	0.0032	3.01	0.78	1.06

[a] determined out of three points per curve (the origin of ordinates and the first two data points of the isotherm)

[b] nonlinear least square fit (Levenberg-Marquardt algorithm)

[c] no value computable

surface, as discussed in Chapter 4. For pH 8.6, where the net charge of IgG1 is in the range of zero, the affinity is appreciably reduced. The low affinity, derived from the low initial curve slope, gives rise to an incomplete surface saturation, which only gradually increases with increasing protein concentration. At both pH values, steps in the isotherm curve shapes are missing and no other defined plateaus emerge. Therefore, it can be stated that the occurrence of multiple layer adsorption as well as structural and/or organizational transitions occurring abruptly at a certain surface coverage, is very unlikely [3]. In the course of curve fitting with the Langmuir-Freundlich model, the three individual model parameters were evaluated by nonlinear regression using the Levenberg-Marquardt algorithm. The initial slope of each isotherm was approximated by a linear fit of the first two data points including the origin of ordinates (Table 2).

It was found in Chapter 4 that the impact of the ionic strength on the adsorbed amount of IgG1 on borosilicate glass changes with the prevailing pH. As expected from these results, at pH 4.0 an increase in the ionic strength from 40 mM, to 85 mM, through to 600 mM led to increasing isotherm plateau levels (Figure 1a). The computed values of Γ_{max} for pH 4.0 (Table 2) however, are not totally in line with the isotherm curve progressions. Given the prevailing attractive electrostatic conditions towards the surface, this increase in adsorption is mainly attributed to the ionic shielding of pronounced intermolecular electrostatic repulsion forces at this pH (see Chapter 4). As a consequence, a denser packaging of molecules on the surface at higher c_{eq} takes place. The initial isotherm slope however, which indicates the overall adsorption affinity towards the surface, is not severely affected by a higher salt content (Table 2 and Figure 2a). This near-complete absence of

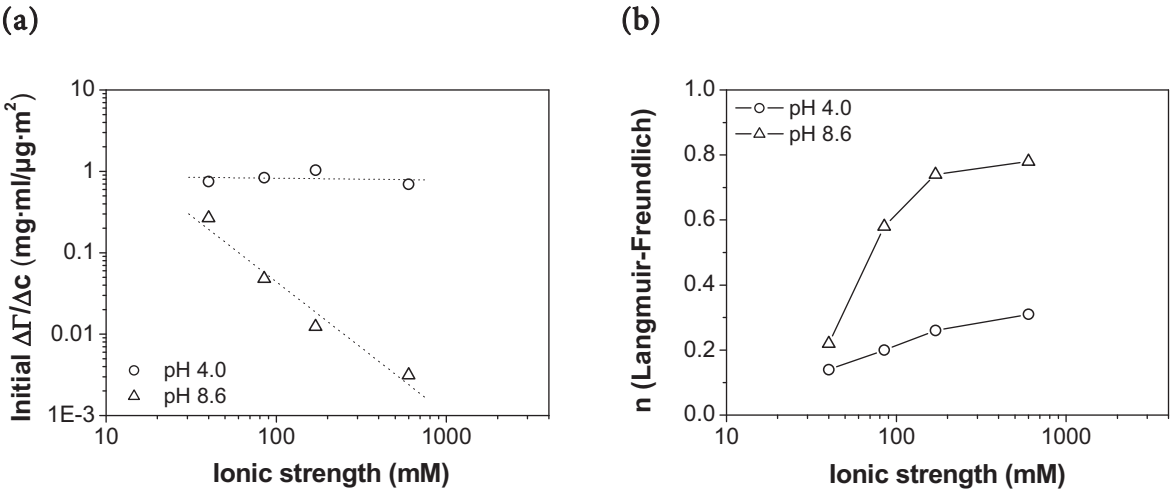

Figure 2: Graphical analysis of the ionic strength dependent (a) isotherm initial slope, indicating adsorption affinity and (b) Langmuir-Freundlich coefficient *n*, indicating type and degree of the adsorption cooperativity for IgG1 adsorption on borosilicate glass at pH 4.0 and pH 8.6.

an ionic strength dependency at low surface coverage confirms the conclusion of Chapter 4, which states that the attenuation of electrostatic attractive forces between IgG1 and the glass surface by ion shielding at pH 4 is irrelevant. By contrast, an increasing ionic strength at pH 8.6 entails the opposite effect (Figure 1b). The initial slope of the isotherms decreases significantly by approx. two orders of magnitude when the ionic strength is increased from 40 mM to 600 mM (Figure 2a). At initial isotherm conditions, intermolecular interactions on the surface play a minor role due to the low surface coverage. Hence, the decrease in adsorption affinity must be due to a reduction of the (small) attractive forces by low molecular ion charge screening, as already assumed in Chapter 4. Evidently, at pH conditions where intermolecular electrostatic repulsion is non-existent or very low (IEP), the decrease in the maximum capacity Γ_{max} with increasing I is similarly attributable to reduced surface attractive forces. Thus, previous findings and interpretations could be well confirmed by the isotherm results.

Unfortunately, not all isotherm specific constants could be determined unequivocally by nonlinear curve fit iterations, especially for low ionic strength conditions. However, from our point of view, this did not interfere with an accurate determination of the Langmuir-Freundlich parameter n. This empirical coefficient was $0 < n < 1$ for all ionic strengths at either pH, indicating negative cooperative adsorption throughout. Thus, once IgG1 molecules have attached to the surface, the affinity of the following molecules decreases because attractive forces decrease or repulsive forces increase. By increasing the ionic strength, n tends to the value of 1, indicating that the extent of negative cooperativity decreased. This is no surprise being that intermolecular repulsive forces were diminished. At the IEP, where these forces are very low by nature, the impact of ionic strength on the degree of negative cooperativity is strong and I values of 170 to 600 mM resulted in an almost non-cooperative adsorption (Table 2 and Figure 2b). But very low ionic strengths entailed a relatively high degree of negative cooperativity at pH 8.6, which was not necessarily expected. A lower IgG1 stability, such as an increased aggregation or denaturation/unfolding propensity upon high or low salt conditions, can be ruled out (see Chapter 7). Hence, this phenomenon most likely stems from long-ranging intermolecular interactions at low salt conditions or from other unknown reasons. At pH 4.0 however, the degree of negative cooperativity remained at a higher level, despite an increasing salt content (Figure 2b). It seems that the shielding efficiency at the prevailing ionic strengths was not sufficient to attenuate the strong repulsion forces; or pronounced intermolecular repulsion forces are not the only cause for the high and persistent degree of negative cooperativity at pH 4.0.

3.2 QCM Kinetic Measurements of IgG1 Adsorption

The aforementioned pH-dependent differences in adsorption affinity of IgG1 on borosilicate glass were verified by quartz crystal microbalance (QCM) kinetic measurements, using a hydrophilic silica model surface. Figure 3 depicts the frequency shift (Δf) for IgG1 adsorbing at the hydrophilic silica-coated sensors at pH 4.0 and at pH 8.6. The pH 4.0 frequency curve shows a rapid decrease in the early stage of adsorption (1), indicating a high adsorption rate and thus a very high affinity. The pH 8.6 solution reveals a significantly less pronounced initial frequency drop. In either case, the initial adsorption phase is followed by a gentle decrease, approaching equilibrium conditions. The pronounced difference in adsorption kinetics underlines the marked difference in adsorption affinity at both pH values. After a short adsorption time of 45 min, rinsing with correlating protein-free sample buffer (1a) reveals only a limited extent of adsorption reversibility in either instance. Although the adsorption process has not reached the final equilibrium state after 45 min, the ratio $\Delta f_{\text{pH 4.0}}$ / $\Delta f_{\text{pH 8.6}}$ after rinsing (≈ 3.5) is well in line with the analogous ratio of adsorbed amounts after 24 h (≈ 3.6) (see section 3.3).

Subsequently, the removability of adsorbed IgG1 by SDS buffer elution was studied. As soon as the surfactant-containing liquid wets the adsorbate (2), the protein is removed. Another equilibrium state is virtually established within 30 min of eluting. The final rinsing step with blank buffer (2a) reveals a disparity of both terminal curves. But considering a certain drift tendency in the course of the adsorption experiment, it can be assumed that IgG1 was exhaustively removed, irrespective of the adsorption pH.

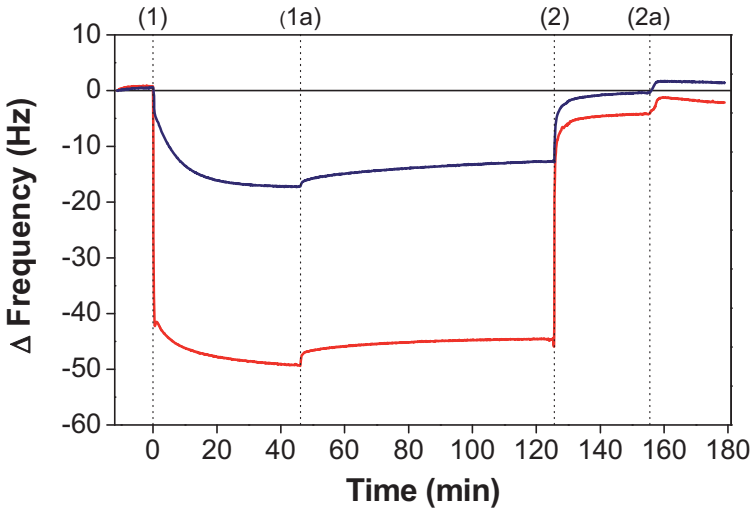

Figure 3: Frequency shift as a function of time for the exposure of IgG1 at pH 4.0 (red) and pH 8.6 (blue) to hydrophilic silica coated QCM sensors.

3.3 Isotherms of IgG1 Adsorption on Different Container Surfaces

In the following, IgG1 adsorption on different surface types (hydrophilic borosilicate glass, hydrophobic siliconized borosilicate glass, and hydrophobic COP plastic) is compared by means of adsorption isotherms at different pH values and constant moderate ionic strength of 170 mM (Figure 4a - c). Again, isotherm data were fitted with the Langmuir-Freundlich model, applying a nonlinear least square fit approximation. The isotherm-specific constants such as the initial slopes and the Langmuir-Freundlich model parameters are summarized in Table 3.

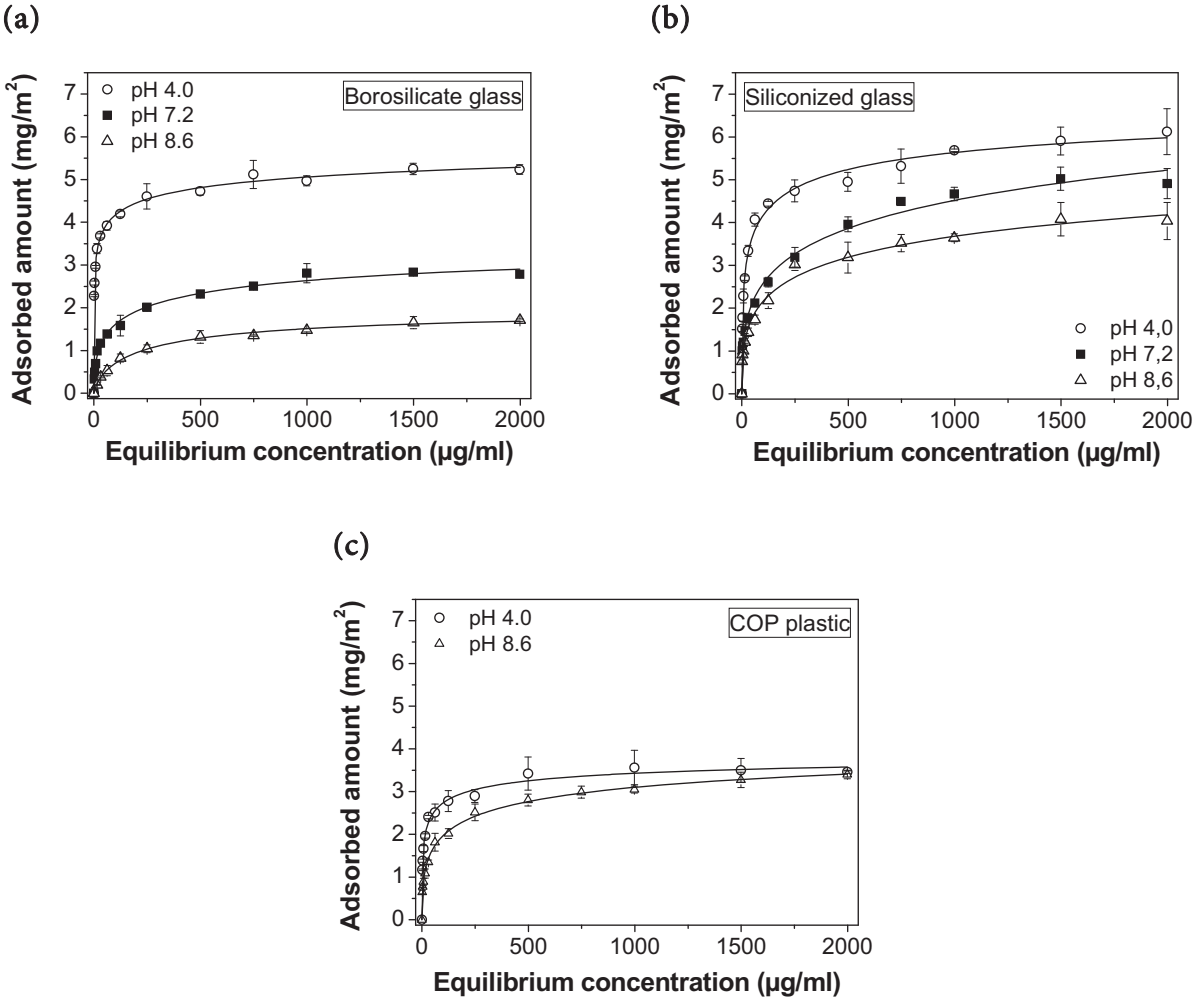

Figure 4: Adsorption isotherms of IgG1 measured on (a) borosilicate glass vials, (b) hydrophobic siliconized glass vials and (c) hydrophobic COP plastic vials at three (two) different pH values, (I = 170 mM) (n = 3); isotherms fitted by nonlinear curve approximation based on the Langmuir-Freundlich model.

Table 3: Results of the adsorption isotherm nonlinear curve fitting with the Langmuir-Freundlich model for IgG1 adsorption on three different container materials (I = 170 mM).

	pH	Initial slope [a] (mg·ml/µg·m²)	Langmuir-Freundlich model parameters Γ_{max} [b] (mg/m²)	n [b]	K [b] (ml/g)
Borosilicate glass	4.0	1.032	6.90	0.26	52.51
	7.2	0.142	4.00	0.46	4.23
	8.6	0.012	2.04	0.74	4.17
Siliconized glass	4.0	0.637	7.48	0.39	18.18
	7.2	0.374	13.23	0.33	0.14
	8.6	0.292	7.92	0.36	0.68
COP plastic	4.0	0.483	4.15	0.39	54.82
	8.6	0.248	4.91	0.41	3.77

[a] determined out of three points per curve (the origin of ordinates and the first two data points of the isotherm)

[b] nonlinear least square fit (Levenberg-Marquardt algorithm)

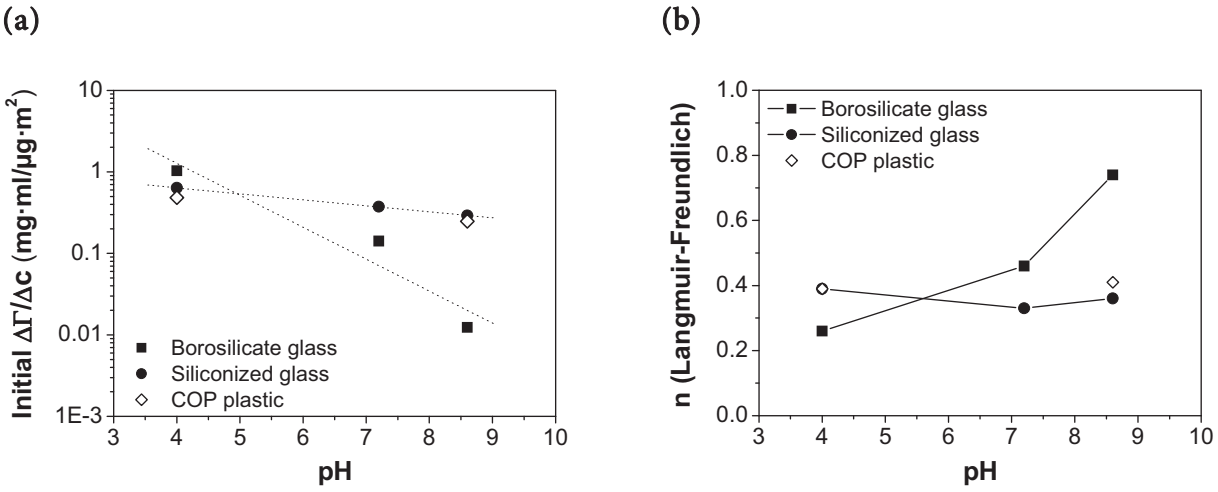

Figure 5: Graphical analysis of the pH-dependent (a) isotherm initial slope, indicating adsorption affinity and (b) Langmuir-Freundlich coefficient n, indicating the type and degree of adsorption cooperativity for IgG1 adsorption on three different container materials.

The isotherms measured on borosilicate glass show an initial slope ranging between two orders of magnitude as a function of solution pH. In contrast, the initial isotherm slopes for the hydrophobic surfaces are consistently on a high level (Figures 4 and 5a). Apparently, the adsorption affinity at pH 4.0 is similarly high for both hydrophilic and hydrophobic surfaces. The decreasing affinity of IgG1 towards the hydrophilic glass surface with increasing pH can be explained by changes in the electrostatic interaction force conditions (see above). In contrast, adsorption on hydrophobic surfaces is rather driven by hydrophobic interactions, which, in turn, are strong and commonly independent of pH. Accordingly, the affinity remains high despite changes in the hydrogen ion concentration (Figure 5a). Beyond that, pH-dependent intermolecular repulsive forces can theoretically impact the adsorbed amount, also on uncharged hydrophobic surfaces. However, as for adsorption affinity, this is unlikely, since intermolecular interactions play a minor role in the initial isotherm region.

In the subsequent isotherm curve progression of glass isotherms and siliconized glass isotherms, a dependence of the isotherm plateau values on solution pH can be observed (Figure 4a and b). For either surface, the adsorbed amount at c_{eq} = 2 mg/ml increases in the order of pH 8.6 < pH 7.2 < pH 4.0, and both at pH 8.6 and 7.2, plateau adsorption on the hydrophobized glass exceeds that of the hydrophilic substrate. In contrast to the hydrophilic glass surface, isotherms measured on the hydrophobized glass seem not to reach defined plateau values at c_{eq} = 2 mg/ml. As mentioned above, for a low free energy surface, protein adsorption increases with increasing hydrophobicity through hydrophobic interactions. Although protein - protein electrostatic interactions are largely missing at low surface coverage, they can gain in importance with increasing surface coverage and affect the adsorbed amount in the terminal isotherm region. The relationships between charge and the adsorption process were extensively elucidated before (Chapter 4). However, more profound insights concerning this matter are expected from IgG1 adsorption isotherms measured on the COP plastic containers. Their hydrophobic surface has an only slightly higher surface free energy compared to that of the siliconized glass (see Chapter 3), but a totally different chemical composition. It was mentioned that the initial isotherm shapes for COP plastic are comparable with those of the siliconized glass, indicating an adsorption affinity independent from pH as well (Figures 4 and 5a). But in the further curve progression, both the pH 8.6 and the 4.0 adsorption level reach the same (mid-level) terminal plateau value. In Chapter 4, uniform adsorbed amounts were observed in adsorption studies at both pH 4.0 and pH 8.6 (c = 2 mg/ml, I = 170 mM) for the COP material. It was concluded that at pH 4.0, where the protein net charge is substantial, an ionic strength of 170 mM led to balanced hydrophobic attraction and intermolecular electrostatic repulsion forces. As a consequence, adsorbed amounts were similar to those at isoelectric pH, where the intermolecular force component was largely missing. However, force equilibrium state considerations fail to entirely explain the increased and espe-

cially the differing isotherm plateau levels of the siliconized glass surface, since intermolecular electrostatic conditions are the same as on the plastic surface. Therefore, other reasons have to be considered. It is known that interactions between hydrophobic protein structures and surfaces of a lower free energy are more likely to cause severe alterations in the protein structure compared to hydrophilic surfaces [24,25]. Hydrophobic interactions, representing strong driving forces for adsorption, are further increased in case the protein loses its globular shape, which thereby increases its surface contact area. Although structural changes of the protein upon surface binding were described to be more probable for low degrees of surface coverage [26], they could have a pronounced effect at advanced adsorption as well. A slightly decreased degree of structural stability of IgG1 at pH 4.0 compared to moderate pH was demonstrated in Chapter 7, which substantiates the above theory. Furthermore, also the degree of adsorption irreversibility has to be considered, which arises from multiple contacts of the protein with the surface [27]. With respect to the surface properties, the silicone oil can be assumed to feature a more pronounced stickiness and thus, a decreased degree of adsorption reversibility, whereas an increased propensity to unfolding seems probable as well.

The adsorption cooperativity type, which was once again analyzed by means of the Langmuir-Freundlich parameter, is negative for all adsorption isotherms irrespective of the surface quality and solution pH (Table 3 and Figure 5b). The main driving forces, both the electrostatic forces on the hydrophilic glass surface and the hydrophobic interactions in the case of the low energetic materials, decrease with an increasing degree of surface coverage resulting in reduced affinity for subsequently adsorbing molecules. While the coefficient n of the hydrophilic glass isotherms increases significantly with a pH change from acidic (pH 4.0) towards the isoelectric point (pH 8.6), it is not affected by pH for the hydrophobic substrates. It was elucidated above that a high protein charge and hence strong intermolecular repulsive forces are responsible for a pronounced negative cooperativity at pH 4.0 on hydrophilic glass, whereas the negative cooperativity effect is reduced at higher pH under less repulsive conditions. Potentially, also structural rearrangements of the molecules bound to the hydrophilic glass surface may play a role, which are increased at higher pH (Chapter 7). However, the reasons for the observed results concerning hydrophobic surfaces are still ambiguous and their clarification would require further investigations.

4 CONCLUSIONS

In this Chapter, IgG1 adsorption on hydrophilic and hydrophobic surfaces was investigated by means of adsorption isotherms at variable surface free energies of the sorbent surfaces and variable solution compositions in terms of pH and ionic strength. The application of three popular theoretical isotherm models on the experimental data revealed that only the combined Langmuir-Freundlich model provides a reasonable mathematical curve description. With a few exceptions, the nonlinear curve fit facilitated the computation of isotherm-associated constants. In the case of the Langmuir-Freundlich model, these are the maximum attainable surface concentration Γ_{max}, the mean binding affinity K_m, and the power constant n, the latter indicating the type and extent of adsorption cooperativity. Furthermore, information on the adsorption affinity could be derived from the isotherm curve progression. For the hydrophilic borosilicate glass surface, the impact of increasing ionic strength on IgG1 adsorption varies depending on the pH conditions during incubation. The results for the initial adsorption affinity, as well as the isotherm plateau values and the adsorption cooperativity, indicated that IgG1 adsorption on glass follows a widely electrostatically dominated adsorption mechanism, which is in accordance with the adsorption theory established in Chapter 4. Quartz crystal microbalance adsorption kinetic measurements on hydrophilic silica, which was taken as a model substrate, corroborated the particularly high adsorption affinity of IgG1 at pH 4.0, especially when comparing it to pH 8.6. By subsequent buffer rinsing, hardly any desorption could be observed in either case. Surface-bound IgG1 was completely removed by SDS, which once again substantiated the excellent applicability of the standard adsorption quantification method developed previously (see Chapter 2). The modeled adsorption cooperativity type on hydrophilic glass was negative at any adsorption condition, indicating a decreasing affinity to the surface for subsequently attaching molecules. A decreasing extent of negative cooperativity with increasing salt concentration was observed for pH 4.0 and pH 8.6, indicating that long-ranging intermolecular electrostatic repulsion forces were causative. In contrast to hydrophilic glass, the high adsorption affinity of IgG1 to the hydrophobic siliconized borosilicate glass was hardly affected by pH. This observation, together with increased isotherm plateau values, is attributed to the presence of pronounced hydrophobic interactions. Although hydrophobic as well, COP plastic material gave rise to lower adsorption in terms of the terminal isotherm progression, which might be due to differences in chemical surface properties that affect adsorption reversibility or structural stability. Both hydrophobic surfaces revealed a high degree of negative adsorption cooperativity, regardless of the apparent pH. This is in marked contrast to the results for the glass surface. Specifically, the effects of the hydrophobic surfaces on structural protein instability upon adsorption should be subject to further investigations.

5 REFERENCES

[1] Norde, W., Haynes, C. A., Reversibility and the mechanism of protein adsorption, *ACS Symposium Series* **602** (1995) 26-40.

[2] Chang, I. N., Lin, J. N., Andrade, J. D., Herron, J. N., Adsorption mechanism of acid pretreated antibodies on dichlorodimethylsilane-treated silica surfaces, *Journal of Colloid and Interface Science* **174** (1995) 10-23.

[3] Norde, W., Adsorption of proteins at solid-liquid interfaces, *Cells and Materials* **5** (1995) 97-112.

[4] Johnson, R. D., Arnold, F. H., The Temkin isotherm describes heterogeneous protein adsorption, *Biochim. Biophys. Acta, Protein Struct. Mol. Enzymol.* **1247** (1995) 293-297.

[5] Sharma, S., Agarwal, G. P., Interactions of Proteins with Immobilized Metal Ions, *J. Colloid Interface Sci.* **243** (2001) 61-72.

[6] Aquino, L. C. L., Miranda, E. A., Duarte, I. S., Rosa, P. T. V., Bueno, S. M. A., Adsorption of human immunoglobulin G onto ethacrylate and histidine-linked methacrylate, *Braz. J. Chem. Eng.* **20** (2003) 251-262.

[7] Tao, Z., Chu, T., On the Applicability of the Langmuir Equation to Estimation of Adsorption Equilibrium Constants on a Powdered Solid from Aqueous Solution, *Journal of Colloid and Interface Science* **231** (2000) 8-12.

[8] Lee, J. E., Saavedra, S. S., Molecular Orientation in Heme Protein Films Adsorbed to Hydrophilic and Hydrophobic Glass Surfaces, *Langmuir* **12** (1996) 4025-4032.

[9] Luey, J. K., McGuire, J., Sproull, R. D., The effect of pH and sodium chloride concentration on adsorption of b-lactoglobulin at hydrophilic and hydrophobic silicon surfaces, *Journal of Colloid and Interface Science* **143** (1991) 489-500.

[10] Luo, Q., Andrade, J. D., Cooperative adsorption of proteins onto hydroxyapatite, *J. Colloid Interface Sci.* **200** (1998) 104-113.

[11] Jennissen, H. P., Evidence for negative cooperativity in the adsorption of phosphorylase b on hydrophobic agaroses, *Biochemistry* **15** (1976) 5683-5692.

[12] Johnston, T. P., Adsorption of recombinant human granulocyte colony stimulating factor (rhG-CSF) to polyvinyl chloride, polypropylene, and glass: Effect of solvent additives, *PDA J. Pharm. Sci. Technol.* **50** (1996) 238-245.

[13] Praus, P., Turicova, M., A physico-chemical study of the cationic surfactants adsorption on montmorillonite, *J. Braz. Chem. Soc.* **18** (2007) 378-383.

[14] Sips, R., The structure of a catalyst surface. II, *J. Chem. Phys.* **18** (1950) 1024-1026.

[15] Umpleby, R. J., II, Baxter, S. C., Chen, Y., Shah, R. N., Shimizu, K. D., Characterization of Molecularly Imprinted Polymers with the Langmuir-Freundlich Isotherm, *Anal. Chem.* **73** (2001) 4584-4591.

[16] Tsai, S. C., Juang, K. W., Jan, Y. L., Sorption of cesium on rocks using heterogeneity-based isotherm models, *J. Radioanal. Nucl. Chem.* **266** (2005) 101-105.

[17] Yoon, J. Y., Kim, J. H., Kim, W. S., The relationship of interaction forces in the protein adsorption onto polymeric microspheres, *Colloids Surf A* **153** (1999) 413-419.

[18] Mac Ritchie, F., Adsorption of proteins at the solid/liquid interface, *J. Colloid Interface Sci.* **38** (1972) 484-488.

[19] Arai, T., Norde, W., The behavior of some model proteins at solid-liquid interfaces. 1. Adsorption from single protein solutions, *Colloids and Surfaces* **51** (1990) 1-15.

[20] Norde, W., Lyklema, J., The adsorption of human plasma albumin and bovine pancreas ribonuclease at negatively charged polystyrene surfaces. I. Adsorption isotherms. Effects of charge, ionic strength, and temperature, *Journal of Colloid and Interface Science* **66** (1978) 257-265.

[21] Serra, J., Puig, J., Martin, A., Galisteo, F., Galvez, M., Hidalgo-Alvarez, R., On the adsorption of IgG onto polystyrene particles: electrophoretic mobility and critical coagulation concentration, *Colloid Polym. Sci.* **270** (1992) 574-583.

[22] Lan, Q., Bassi, A. S., Zhu, J. X., Margaritis, A., A modified Langmuir model for the prediction of the effects of ionic strength on the equilibrium characteristics of protein adsorption onto ion exchange/affinity adsorbents, *Chemical Engineering Journal (Lausanne)* **81** (2001) 179-186.

[23] Lin, P. C., Lin, S. C., Hsu, W. H., Adsorption behaviors of recombinant proteins on hydroxylapatite-based immobilized metal affinity chromatographic adsorbents, *Journal of the Chinese Institute of Chemical Engineers* **39** (2008) 389-398.

[24] Arakawa, T., Boone, T., Davis, J. M., Kenney, W. C., Structure of unfolded and refolded recombinant derived [Ala125]Interleukin 2, *Biochemistry* **25** (1986) 8274-8277.

[25] Lu, J. R., Su, T. J., Thirtle, P. N., Thomas, R., Rennie, A. R., Cubitt, R., The denaturation of lysozyme layers adsorbed at the hydrophobic solid/liquid surface studied by neutron reflection, *J. Colloid Interface Sci.* **206** (1998) 212-223.

[26] Kondo, A., Murakami, F., Higashitani, K., Circular dichroism studies on conformational changes in protein molecules upon adsorption on ultrafine polystyrene particles, *Biotechnol. Bioeng.* **40** (1992) 889-894.

[27] Kamyshny, A., Lagerge, S., Partyka, S., Relkin, P., Magdassi, S., Adsorption of Native and Hydrophobized Human IgG onto Silica: Isotherms, Calorimetry, and Biological Activity, *Langmuir* **17** (2001) 8242-8248.

Chapter 6

Advanced Investigations on Adsorbed IgG1 Molecules with XPS and ToF-SIMS

Abstract

In the scope of this study, the surface sensitive spectroscopic methods, X-ray photoelectron spectroscopy (XPS) and static time-of-flight secondary ion mass spectrometry (ToF-SIMS), were applied to obtain additional chemical information on the borosilicate glass surface used for protein adsorption experiments, as well as on the IgG1 fractions adsorbed at different pH. In comparison to previously established analytical procedures in connection with protein adsorption experiments, a striking feature of both new methods was their capability of providing space-resolved information regarding the glass vial body. Detailed investigations were performed on blank glass vial samples (bottom and wall pieces) after the established washing and heat sterilizing pretreatment as well as on IgG1 layers adsorbed at pH 4.0, 7.2, and 8.6. These pH values correspond to the pH of maximum adsorption, to the standard pH of the IgG1 formulation, and to the isoelectric point of the IgG1. XPS was successfully applied for qualitative as well as for quantitative investigations. Unspecific organic material was detected on the surface of the blank glass samples. Contamination was present in higher quantities on vial walls and less on vial bottoms. ToF-SIMS neither gave indication of the exact nature of the organic material, nor of a particular contaminating source. The amount of adsorbed IgG1 on the glass vial samples correlated with the degree of the above mentioned surface contamination. Both XPS and the established surfactant based desorption quantification procedure revealed that irrespective of the incubation pH, more protein per surface area was bound on the vial wall part. The approximated mean thickness of the dried IgG1 adsorption layers, determined by XPS, reached from 1.1 nm (bottom, pH 8.6) to 4.9 nm (wall, pH 4.0). Additional ToF-SIMS measurements were performed to acquire information on the molecular composition of the topmost area of the IgG1 adsorbates. Principal component analysis turned out to be suitable and most helpful for the simultaneous comparison of an increased number of sample spectra. Protein adsorbates could therefore be classified by means of the incubation pH, as well as by means of the extent of surface coverage. The

heterogeneous fragmentation pattern of IgG1 adsorbates at different solution pH values in ToF-SIMS pointed to differences in the molecular orientation or to a varying degree of denaturation, whereas the prevalence of an influencing matrix effect could not be ruled out.

1 INTRODUCTION

In previous work, sensitive quantification procedures were developed (Chapter 2) and successfully applied to determine the adsorbed amount of IgG1 on borosilicate glass vials as a function of solution parameters, such as pH value, ionic strength or different salt types (Chapter 4). These variables did not only affect properties of the protein molecules, but also sorbent surface qualities, as for instance the surface free energy and the glass surface elemental composition (Chapter 3). As a measure of surface hydrophilicity, the surface free energy has shown to substantially determine the amount of adsorbed IgG1 on the glass surface at otherwise consistent solution conditions. It was proposed that surface contamination effects could have been responsible for an observed decrease in surface free energy. This free energy decrease, in turn, was associated with an increased amount of adsorbed IgG1. A thorough analysis of the chemical state of the outermost glass surface is therefore of particular interest and can be accomplished by means of X-ray photoelectron spectroscopy (XPS) and static time-of-flight secondary ion mass spectrometry (ToF-SIMS). In addition, the utilization of both highly sensitive surface analytical techniques might provide further information on the adsorbed protein molecules such as, for instance, their spatial distribution on the glass surface. Both techniques have been widely applied in the investigation of protein adsorption on solid surface [1-4].

XPS provides qualitative and quantitative information on all elements of the outermost sample surface (except for H and He) in a sampling depth of 20 - 100 Å [5]. This data is commonly observed from XPS survey spectra over a wide range of binding energies. Detailed information on the chemical binding is obtained from high resolution spectra of particular elements. When surface bound protein is investigated, high resolution C1s spectra are mainly composed of three predominating carbon species. The first one, located at the binding energy of 285.0 eV, can be assigned to aliphatic hydrocarbon species (C–H / C–C). The species at 286.5 eV reflects carbon bound to oxygen or nitrogen (C–O / C–N) [6] and can indicate the carbon of the protein backbone (NH–CHR–CO) or the residues. The third peak at a binding energy of 288.2 eV is generally seen as distinctive for protein and can be assigned to the amide carbon (N–C=O) [7]. Since proteins contain a characteristic percentage of amide carbon and nitrogen, they can be well distinguished

from non-proteinaceous organic material on the surface, such as hydrocarbons or carbohydrates. For the quantification of proteins, preferentially on nitrogen free surfaces, the total atomic percentage of nitrogen or the ratio of N and an exclusive surface element can be utilized. For nitrogen containing substrates, the accuracy suffers and quantification usually becomes more challenging. Alternatively, protein may be indicated by an increasing "amide peak" intensity at 288.2 eV or by the reduction of characteristic element signals of the underground by the overlaying protein film [3,7,8]. The sensitivity of protein quantification with XPS is very high. The detection limit of fibrinogen on mica, for example, has been determined by Wagner *et al.* to be approx. 100 - 250 μg/m^2 [7], which matches well with the sensitivity of the SDS protein desorption assay elaborated in Chapter 2. Besides providing sensitive qualitative and quantitative information on the adsorbed protein film and the underlying surface, XPS is also capable of clarifying the three dimensional structure of adsorbed protein films [9,10]. This includes the determination of the (mean) layer thickness of protein adsorbates [5,9,11], from which conclusions on the preferential molecular orientation in the adsorbed state can be drawn. However, a potential alteration of the protein structure, induced by vacuum drying for XPS analysis, has to be critically considered. Despite the versatile fields of applications, XPS lacks detailed macromolecular information on the surface chemistry because of its exclusive specificity for the elemental composition [5]. For that reason, additional ToF-SIMS analysis was necessary.

The interest in ToF-SIMS has continuously increased in life science for the chemical characterization of surfaces. It has also been used in the investigation of adsorbed protein films by the groups of Wagner, Horbett, and Castner [5,7,12], Ferrari and Ratner [11], Lhoest *et al.* [13], and others [14,15]. An important focus regarding protein analysis with ToF-SIMS was the characterization and identification of single proteins and of heterogeneous protein films adsorbed on solid surfaces. In ToF-SIMS, the surface is bombarded with an ion beam (Ga^+, Cs^+, Ar^+, Xe^+, Bi-cluster, or others) with some keV energy. These primary ions penetrate the surface and the primary energy is transferred to target atoms via collisions in a so called collision and energy transfer cascade. By this means, atoms and molecular fragments are emitted from the surface and the positively or negatively charged fragments are analyzed by their mass. Recently, it has been described that the use of Ga^+ primary ions leads to a poor yield of larger protein specific secondary ions, whereas primary ions with a higher mass would improve the ToF-SIMS analysis of protein samples [14]. In a series of studies, two primary ion sources (Ga^+ and Bi-cluster) were compared and could demonstrate that Ga^+ resulted in an increased sensitivity for compositional changes of the glass surface. In contrast, the use of larger Bi-cluster primary ions shifted the fragmentation pattern towards larger fragment sizes and thus enhanced the information content on the organic material (data not shown). One benefit of the ToF-SIMS technique is its very high surface sensitivity down to the femtomolar range, with a

typical sampling depth on surfaces, including (bio-)polymeric materials, of only 10 - 15 Å [16-18]. From this, a lower detection limit than that of XPS follows [3]. Thus, ToF-SIMS may be better suited to determine low amounts of protein on surfaces and to provide information regarding the molecular composition of the outermost sample surface. The group of Wagner and Castner differentiated several proteins by means of their fragmentation pattern [19]. By analyzing single protein film samples and comparing the spectra by using principal component analysis (PCA) they could, therefore, identify unknown protein samples. Ideally, the amino acid composition of the proteins' topmost surface or even the protein molecule orientation in its adsorbed state may be classified. Tidwell *et al.* found a significant influence of adsorption conditions like protein concentration and temperature on the protein fragmentation pattern [17]. Since the shell and the core of a protein molecule differ in their amino acid composition, ToF-SIMS analysis might give some indication on the degree of denaturation after adsorption.

The evaluation of ToF-SIMS spectra is challenging due to the abundance of information contained in each mass spectrum. For protein films of different qualities, unique identifying peaks are missing. PCA enables to distinguish between samples of similar or different properties. Moreover, the selection of crucial signals from the spectra in the course of the PCA sample classification may be helpful to judge the condition of the adsorbed protein film. PCA has become a standard tool in modern data analysis because it is a simple and non-parametric method of extracting relevant information from confusing data sets [20]. By definition, it is a linear transformation of data to a new coordinate system. The greatest variance by any projection of the data is indicated by the first coordinate (the first principal component), the second greatest variance by the second coordinate, and so on [21]. With regard to a ToF-SIMS spectrum comprising n peaks, which can be visualized as a point in an n-dimensional space, PCA can reduce the dimensionality of the space under the retention of a large extent of information of the original data set. Simply spoken, in this mathematical transformation, an m x n matrix X (m spectra comprising n integrated peak areas) is reduced to the cross product of two transposed matrices, a score matrix T and a loading matrix P plus a rest matrix E. The loadings give the relationship between the old variables (in our case the integrated peaks) and the new variables (principal components), which are depicted as axes in the scores plot. The scores, in turn, give the relationship between the samples in the new system [22-24].

In the following ToF-SIMS study, the blank glass vials were investigated in order to obtain detailed information on the surface contamination, which had deposited on the clean samples and which has been found to lower the surface free energy (see Chapter 3). Furthermore, ToF-SIMS together with PCA spectra evaluation was applied to discriminate between IgG1 layers, which adsorbed on borosilicate glass at three different pH values. In this regard, PCA scores and loadings were used to assess differences in the protein surface

coverage, and, possibly, in the preferential orientation and the degree of denaturation of the adsorbed molecules. However, prior to this, the blank glass surface and the IgG1 adsorbates on glass were characterized by means of XPS, providing precise quantitative information on the elemental surface composition. In all studies, special focus was on comparing the surface state and composition of glass vial bottom and wall part, and on the impact of potential differences on the adsorption behavior of IgG1.

2 MATERIALS AND METHODS

2.1 Materials

2.1.1 Protein Formulation

For adsorption experiments, a 2 mg/ml solution of IgG1 (MW ≈ 152 kDa) in 10 mM phosphate buffer and 145 mM NaCl (pH 7.2) was used, which was kindly provided by Merck Serono (Darmstadt, Germany). The initial protein solution was dialyzed against pure water (pH approx. 6 - 7) or against buffer at pH 4.0 or 8.6, using Pierce Slide-A-Lyzer 20K MWCO Dialysis Cassettes (Thermo Fisher Scientific, Rockford, IL, USA). The ionic strength of each solution was adjusted with NaCl, as described in Chapter 4. Simultaneously, the IgG1 concentration was adjusted to 2 mg/ml, controlled by UV spectroscopy. Each protein solution was filtered through a hydrophilic 0.2 µm polyethersulfone membrane filter (Pall GmbH, Dreieich, Germany) before use.

2.1.2 Chemicals / Excipients

Ultrapure water (0.055 µS/cm) came from a Purelab Plus UV/UF system (ELGA Lab Water, Celle, Germany) and was filtrated through a 0.22 µm membrane filter before use. NaCl, NaH_2PO_4 and Na_2HPO_4 were purchased from Merck Chemicals, Darmstadt, Germany. 1 M NaOH and HCl were obtained from Sigma-Aldrich, Munich, Germany.

2.1.3 Glass Preparation

Fiolax® 2R borosilicate glass vials, kindly provided by SCHOTT AG (Mainz, Germany), were preprocessed (washed and heat sterilized) as described in Chapter 2. Vial bottoms were cut off using a DREMEL® 300 series rotary tool (DREMEL Europe, Breda, The Neth-

erlands) equipped with a rotating diamond cut-off wheel. Stripes of approx. 3 - 4 mm in width and 1.5 - 2.0 cm in length were detached from the cylindrical glass wall piece after carefully scratching with glass cutter tools. Adherent glass dust was removed by pure pressurized nitrogen.

2.2 Methods

2.2.1 X-Ray Photoelectron Spectroscopy

XPS analyses were performed on an Axis Nova device (Kratos Analytical, Manchester, U.K.) with a monochromatized Al Kα source ($h\nu$ = 1486.6 eV) at a power of approx. 150 W. Spectra were recorded applying a pass energy of 160 eV for survey spectra and 40 eV for high resolution spectra (n = 6, three measuring points on two independent glass pieces). For all measurements, the analysis spot size was 400 x 800 µm, the takeoff angle 90°, and the vacuum below 10^{-7} mbar. Unwanted charging of the samples was prevented by the system's self-regulating charge neutralizing system, comprising a coaxial low energy electron source. Curve fitting was performed using the CasaXPS software (Version 2.3.14). Atomic concentrations were calculated by determining the integral peak intensities applying a linear background.

2.2.2 Time of Flight Secondary Ion Mass Spectrometry

Static ToF-SIMS was performed using a ToF-SIMS IV instrument (ION-TOF GmbH, Muenster, Germany) equipped with a 30 keV Bi-cluster primary ion source. Charge compensation was applied using a pulsed low-energy electron flood gun. Positive ion SIMS spectra were acquired from m/z = 0 to 200 over an area of 100 x 100 µm^2. Mass calibration was performed on the basis of the peaks of C_xH_y, ^{30}Si, ^{69}Ga, and ^{137}Ba.

2.2.3 Adsorption Process and Sample Preparation

Glass pieces from vial bottom and wall were immersed in 10 ml of a 2 mg/ml IgG1 solution at 25°C for 24 hours in 50 ml round bottom tubes (GreinerBio-One GmbH, Frickenhausen, Germany) for both XPS and ToF-SIMS. After the incubation step, the glass bottoms were immersed twice in 40 ml blank buffer of the corresponding composition for the removal of unbound protein. Afterwards, the bottoms were immersed twice in 40 ml ultrapure water for the removal of salts, which would have crystallized on the surface upon drying and therefore falsified the spectroscopic results. The glass pieces were dried

in a gentle nitrogen flow and were degassed for at least 2 hours at a pressure of 10^{-6} mbar in the pre-vacuum chamber of the respective UHV device. For the sample preparation of pure protein, IgG1 (approx. 2 mg/ml) dissolved in water was repeatedly spread on glass bottoms and dried in a gentle flow of nitrogen.

2.2.4 Principal Component Analysis

ToF-SIMS spectra were analyzed and compared with PCA multivariate analysis by using Solo 4.2 chemometrics software (Eigenvector Research Inc., Wenatchee, WA, USA). A detailed description of PCA in connection with ToF-SIMS data analysis is given by Wagner and Castner [23]. In our studies, a choice of peaks (Table 3) was included in the PCA analysis. Na^+ peaks were excluded from the PCA analysis because of their pronounced intensity. Prior to PCA analysis, peak intensities were normalized within each spectrum (sum of the intensities = 1) and preprocessed (mean centered) by the PCA software. The "leave one out" procedure was chosen as cross validation model.

3 RESULTS AND DISCUSSION

3.1 XPS Investigations of IgG1, Blank Glass Vials and IgG1 Adsorbates

XPS investigations of IgG1 adsorbates on borosilicate glass required a detailed characterization of the pure protein first. An XPS spectrum of the salt free IgG1 is shown in Figure 1a, and the %-elemental composition is summarized in Table 1. The presence of the major elements of proteins N, C, O, and S could be clearly verified, while the quantitative results are in agreement with the theoretical elemental composition of the IgG1. The deviation from the nominal values for the main elements N, C, and O is not more than 9%. A high quality of the measurements is further reflected by consistent N : C ratios (Table 1). The theoretical elemental composition of the IgG1 was derived from its amino acid sequence. In these calculations, an average glycosylation pattern was considered, which, at least slightly, affected the proportion of the main elements. The fact that Si was only hardly detected in these analyses confirmed the presence of a closed protein layer. An evaluation of the IgG1 C 1s high resolution spectrum provides detailed information on the carbon species of different chemical state, as well as their typical proportion within the protein. As stated above, in proteins three main carbon species can be differentiated,

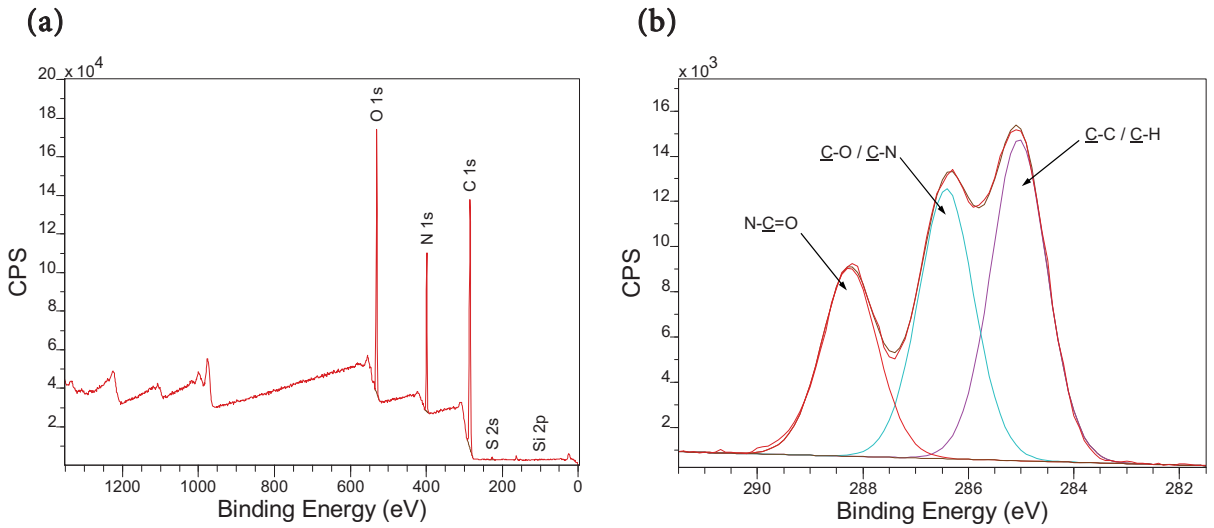

Figure 1: Exemplary (a) XPS survey spectrum and (b) C 1s high resolution spectrum of pure salt-free IgG1 spread on the blank glass surface; carbon species analyzed by peak deconvolution.

namely the aliphatic species (C–C / C–H) at 285.0 eV, the amine or oxygen-bound carbon species (C–N / C–O) at 286.5 eV, and the amide carbon species (N–C=O), shifted to higher binding energies at 288.2 eV. In Figure 1b, C1s peak deconvolution reveals a number of three distinct peaks accounting for the three carbon species. The percentage of each class was determined by peak integration. The results are summarized in Table 2. The characteristic proportion of the carbon species of the pure IgG1 enables to differentiate IgG1 from other organic substances. The most characteristic species for IgG1 as a protein are the amide carbons, which amount to approx. 25% related to total carbon. With regard to the entirety of all elements, the IgG1 consists of approx. 15 - 16% amide carbons.

Subsequently, the inner surface of the blank glass vials was analyzed with XPS. By this means, information on the elemental composition of the outermost glass surface layers was obtained, which the proteins face upon adsorption. Figure 2a shows an XPS survey spectrum of a wall piece sample from a washed and heat sterilized glass vial. Obviously, all major glass bulk elements were qualitatively detected, with Si and O as the main ingredients. The quantitative elemental composition of the sample is summarized in Table 1. The results of the glass surface reflect the theoretical elemental composition of the glass bulk, calculated from the borosilicate glass components [25], but the numbers are not identical. With XPS, a decreased sodium and boron content was measured, for both wall and bottom, than theoretically expected. The results for aluminum and calcium are less unequivocal. Differences between the elemental surface composition of the glass vial and the theoretical bulk composition, on the one hand, may be due to corrosion effects (see Chapter 3), e.g. in contact with liquids or humidity during washing or storage. On the

Table 1: Quantitative elemental composition of different sample surfaces determined by XPS.

Sample	%N	%C	%O	%S	%Si	%Na	%B	%Al	%Ca	N:C	N:Si
Pure IgG1[a]	16.6	62.9	20.1	0.4	0.0					0.26	
Pure IgG1	15.9	65.0	18.4	0.3	0.4					0.24	
pH 4 bottom	9.3	37.1	37.9		14.4	0.2		1.0	0.1	0.25	0.65
pH 4 wall	9.9	39.9	36.6		12.2	0.1		1.2	0.1	0.25	0.81
pH 7.2 bottom	3.0	13.7	57.2		23.1	1.1		1.8	0.1	0.22	0.13
pH 7.2 wall	5.3	21.8	51.4		16.9	1.7		2.8	0.1	0.24	0.31
pH 8.6 bottom	1.1	7.0	63.0		25.4	1.2		2.1	0.1	0.16	0.04
pH 8.6 wall	2.0	14.3	57.8		19.4	2.5		3.9	0.1	0.14	0.10
Glass bulk[b]	0.0	0.0	63.2		26.2	4.7	3.8	1.2	0.8		
Glass bottom	0.5	4.5	65.7		26.5	1.1	0.3	1.3	0.2	0.11	0.02
Glass wall	0.7	8.1	63.1		20.5	1.3	2.7	2.3	1.2	0.09	0.03

[a] calculated from the theoretical amino acid composition including an average glycosylation pattern

[b] calculated from the theoretical glass composition taken from [25]

Table 2: Fractions of different carbon species related to total carbon, received from C1s XPS high resolution spectra through peak deconvolution.

Sample	% N–C=O	% C–O	% CH_2	% N–C=O[a]
Pure IgG1 bulk	24.2	33.8	42.1	15.7
pH 4 bottom	24.0	32.5	43.5	8.9
pH 4 wall	23.6	33.2	43.2	9.4
pH 7.2 bottom	20.3	30.5	49.2	2.8
pH 7.2 wall	21.4	31.4	47.2	4.7
pH 8.6 bottom	12.5	27.2	60.3	0.9
pH 8.6 wall	8.3	28.1	63.6	1.2
Glass bottom	4.1	24.7	71.2	0.2
Glass wall	6.4	26.7	66.9	0.5

[a] amide carbon content referred to the entirety of all elements of the measured samples

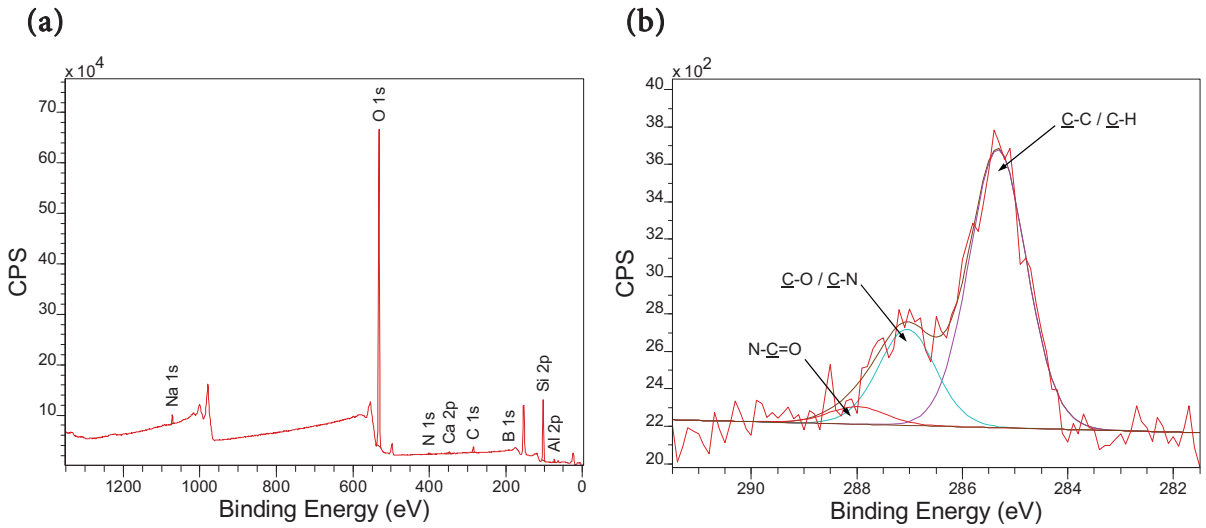

Figure 2: Exemplary (a) XPS survey spectrum and (b) C 1s high resolution spectrum of the blank washed and heat sterilized glass surface.

other hand, such differences may be attributed to a high temperature evaporation of volatile glass components during the hot-forming process (see below). A further comparison of blank vial bottom and wall surfaces revealed differences in their elemental composition. In this regard, a lower content of network modifiers (alkali or alkaline earth elements) and of the network former boron was measured for the vial bottom. This decrease of those additional glass components is associated with an increase in the surface concentration of silicon of the glass vial bottom. Such differences in the chemical surface composition of vial bottom and wall are well known [26]. As shown by Schwarzenbach *et al.* [27], we assume that the high temperatures around 1200°C during the molding process caused alkali diffusion to the surface. These alkali salts subsequently dissolved during the vial washing step. Hence, the above results reveal that a significant difference in surface chemistry of vial bottom and wall exists, which may be accompanied by differences in the adsorption behavior of proteins.

In Chapter 3, the occurrence of glass surface contamination was described, which caused a decrease in the surface free energy for stored vials when compared with the thoroughly cleaned samples. Unspecific contamination of glass usually involves the deposition of carbon and nitrogen from the atmosphere [27]. As expected, XPS measurements on the borosilicate glass samples confirmed an appreciable carbon and a minor nitrogen fraction on the surface. Such compounds were also observed in ToF-SIMS surface analysis (see Chapter 3). Quantification with XPS revealed twice as much contamination on the vial wall than on the bottom. C1s high resolution spectra of blank glass surfaces were recorded (Figure 2b) to specify the kind and origin of the deposited material. The %-contents are again summarized in Table 2. This closer investigation revealed mainly aliphatic (C–C / C–H), as well as nitrogen or oxygen bound carbon species (C–N / C–O). In contrast to

the situation of pure IgG1 (Figure 1b), where the fraction of amide carbon species in the C1s signal amounted to approx. 25%, it was only a share of 4 - 6% of the total carbon on the blank glass sample. Thus, a proteinaceous origin of the contaminating material can be largely excluded, which also corresponds to previous ToF-SIMS results (see Chapter 3).

The effect of surface contamination on the amount of adsorbed IgG1 was already discussed in the context of a decrease in surface free energy (see Chapter 3). There, the average protein adsorption over the whole container surface was analyzed by means of SDS desorption. In contrast, XPS was applied here to quantify glass bound protein in a direct manner. Thus, XPS represents another way to corroborate the indirectly obtained quantification results. Besides, XPS offers the possibility of space resolved measurements along with the ability to compare adsorption at different locations within the vial. With XPS, the protein mass can be inferred from the total nitrogen content. With regard to an ideal glass substrate, nitrogen is significant for the organic adsorbate. However, borosilicate glass vial samples were shown to carry some nitrogen-containing contamination. We rather took the ratio of N1s/Si2p for a more precise quantification of adsorbed protein, since Si was exclusively present in the glass surface and was increasingly attenuated with the mass of bound protein. On the contrary, it has to be noted that the protein mass may be overestimated by large amounts of contaminating material, since the Si signal would thereby be increasingly reduced.

In the following, the amount of IgG1 on glass wall and bottom samples, adsorbed at different pH, is compared. The XPS elemental surface concentrations of the pH 4.0, 7.2, and 8.6 samples are summarized in Table 1. For all samples, the nitrogen content of the pure protein bulk (15.9%) was not reached, since the underlying glass surface contributed to the XPS signal. This circumstance points to the presence of a non-closed (inhomogeneous) protein layer or a layer thickness below the XPS information depth of approx. 100 Å. The visualization of dried IgG1 adsorbates by atomic force microscopy (AFM) confirmed both issues (Chapter 7). Due to concerns of the validity of protein quantification results by means of the N1s to Si2p ratio with respect to the prevalent surface contamination, an alternative approach was applied. For checking purposes, the adsorption of IgG1 was monitored by means of the absolute amide carbon content. The amide carbon species was shown to be only scarcely present (approx. 0.2 - 0.5%) on the blank glass surface, including contamination. Table 2 depicts the amide carbon fraction referred to the entirety of surface elements, which correlates well with the N1s/Si2p ratio. In Figure 3a, the adsorbed IgG1 amount on both glass bottom and wall is graphically depicted for different adsorption pH values on the basis of the N1s/Si2p intensity ratios. With respect to the entire glass vial, the mean adsorbed protein mass was found to be highest for IgG1 at pH 4.0, followed by pH 7.2 and 8.6, reflecting decreasing amounts of protein on the glass with increasing incubation pH. The same trend could be shown by SDS desorption quantifica-

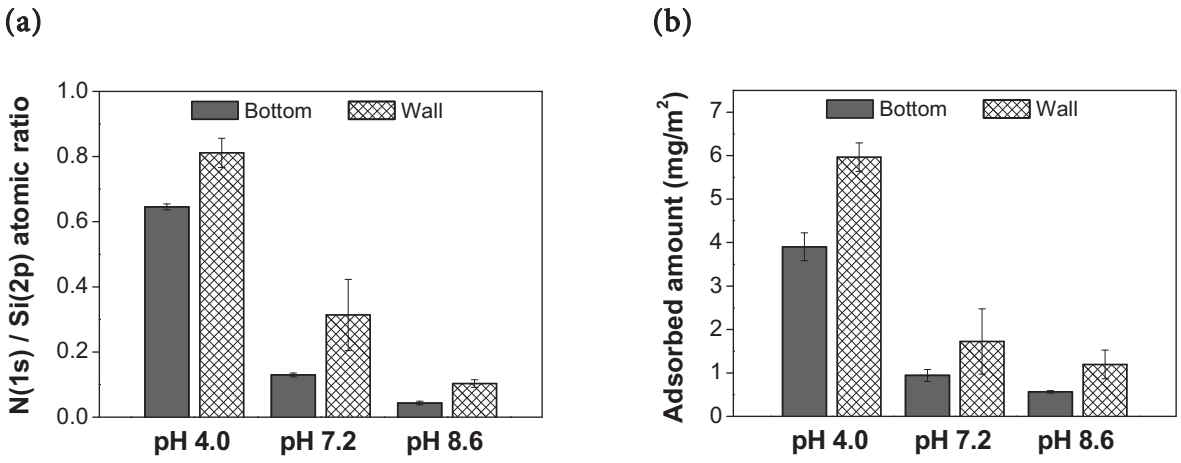

Figure 3: (a) Adsorbed IgG1 on separate borosilicate glass vial parts derived from the XPS N1s/Si2p intensity ratio (n = 6). (b) Adsorbed amount of IgG1 on separate vial bottoms and cylindrical walls part determined by SDS desorption assay (n = 3); in both cases 24 h adsorption at *I* = 170 mM.

tion within this pH range (see Chapter 4). Furthermore, it becomes apparent that a higher amount of IgG1 adsorbed on the cylindrical vial part and less on the vial bottom. This tendency becomes apparent from the N1s (400.1 eV) (Table 1) and amide carbon (288.2 eV) intensities (Table 2). The differences between bottom and wall are not very pronounced at pH 4.0, where the total protein load on the surface is high. However, at pH 7.2 and 8.6, the amount of protein on the wall becomes approx. twice as high as it was on the bottom. In order to confirm the validity of these striking results, the established SDS desorption quantification approach of IgG1 was applied to separate vial bottoms and walls. For this purpose, IgG1 was adsorbed on the vial inside and after the removal of unbound protein, the vial parts were separated. The averaged IgG1 surface concentration over the surface area of vial bottoms or walls is depicted in Figure 3b. The XPS results could be confirmed nicely. Possibly, deviations in the chemical glass surface composition of bottom and wall, such as a variable content of network modifiers of the outermost glass surface or a variable degree of surface contamination, were decisive for differences in IgG1 adsorption. Both instances could be proven by XPS analysis for vial bottom and wall (see Table 1). It is remarkable that the values for IgG1 adsorption on the vial wall show a higher variability than it is the case for the vial bottom, as can be seen from the standard deviations. This circumstance may be caused by the marked chemical and/or sterical inhomogeneity of the cylindrical part, resulting in different zones [28].

According to Wagner *et al.*, the thickness of adsorbed protein layers can be estimated by applying the Beer-Lambert model on XPS data [9]. Accordingly, a linear relationship between the ln(N1s/Si2p) and the thickness of the protein layer exists. Figure 4 depicts the

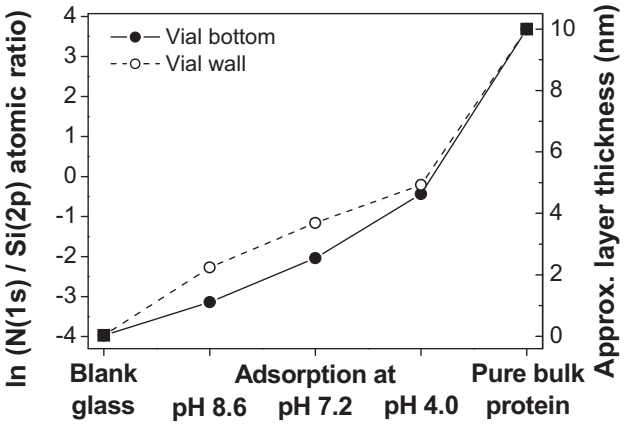

Figure 4: Relative (left ordinate) and approximated absolute IgG1 layer thickness (right ordinate) on vial bottom and wall after adsorption at different pH values.

alleged IgG1 layer thickness adsorbed at different pH, related to the blank glass surface and to the pure protein sample of an estimated finite thickness. Based on the assumption of a homogeneous layer structure, the relative layer thickness is aligned with the results for the protein content determined on the glass surface. At pH 8.6 and 7.2, a higher protein film thickness on the vial wall than on the vial bottom becomes apparent. The absolute IgG1 layer thickness can be approximated by equating the blank glass surface with a thickness of zero and putting the thickness of the pure protein layer on a level with the XPS information depth of around 100 Å [29]. This assignment is justified by the fact that the bulk protein sample still featured a Si signal from the underlying glass surface, which was, however, extremely weak. Furthermore, the above information depth of 100 Å can be assumed as a realistic value for the upper protein layer thickness, considering inelastic mean free paths (IMFPs) of N-derived or Si-derived electrons in organic compounds. Representative IMFP values in layers of bovine plasma albumin (BPA) were calculated by Tanuma *et al.* [30]. Taking all above assumptions into account, the mean layer thickness of dried IgG1 on borosilicate glass ranges between approx. 1.1 nm (bottom, pH 8.6) and approx. 4.9 nm (wall, pH 4.0). Furthermore, the mean layer thickness of IgG1 adsorbed on vial bottom at pH 7.2 is estimated to 2.5 nm. With regard to the latter value, AFM measurements on an equivalent sample revealed only the half of this layer thickness (see Chapter 7). A potential imprecision arises from the data of the pure bulk protein sample, since small variations in the residual Si2p peak intensity seriously affect the approximation. However, irrespective of the absolute precision of the determination, the result of the XPS layer thickness approximation points to structural alterations of adsorbed proteins. There is a discrepancy between the smallest dimension of the IgG1 (6.9 nm), determined from the crystal structure, and the apparent thickness of the dry protein layer. Thus, one may assume that molecules either considerably shrunk or spread on the glass.

It has been pointed out that vacuum conditions and dehydration effects alter the protein structure, for example towards the formation of a reticulation, which is not at all comparable with the situation of natively adsorbed protein [31]. From this point of view, it is difficult or even impossible to draw conclusions on the preferential orientation of dried adsorbed IgG1 on glass. It has been described that the native film structure could be retained in ultrahigh vacuum by applying a preceding freeze drying technique, or by trehalose coating [31,32]. From this, the impact of the drying step on the protein film thickness could be evaluated. For IgG1 on borosilicate glass, the differences in layer thickness between the native and the dried IgG1 adsorbates were investigated with the aid of AFM measurements, as described in Chapter 7.

The protein film thickness calculations were based on a number of assumptions. More precise information on the layer thickness can be received from XPS data determined at different take-off angles, as performed by Ferrari and Ratner [11]. For instance, they measured a layer thickness of approx. 4 nm for albumin adsorbed on hexafluoropropylene. Another way of determining the thickness of protein adsorbates has been described by Fitzpatrick *et al.*, who applied energy-resolved depth profiling and obtained the thickness of concanavalin A on mica to 2.8 nm [2]. Despite the fact that both studies investigated different proteins and surfaces, the findings are in the same range as our results. Moreover, different evaluation models (tower or layer model) for the characterization of protein surface coverage by XPS have been described by Ganz, who investigated the protein deposition of rhIL-11 on different carriers after spray drying [33]. Especially the tower model may allow more precise information on inhomogeneous protein structures. However, in the scope of this work, for the sake of simplicity, investigations on protein layers were limited to quantification assuming a closed and uniform occupation. Thus, it could be shown that XPS is a sensitive tool for analyzing protein - surface effects and is capable to, at least, approximate the adsorbed protein content on different vial locations.

3.2 ToF-SIMS Investigations of IgG1, Blank Glass, and IgG1 Adsorbates

A deeper insight into the molecular composition of the above discussed sample surfaces was expected from static ToF-SIMS analyses. Especially the blank glass surface and the nature of its organic contamination were to be further characterized. Moreover, protein layers adsorbed on glass vial bottom or wall at different pH values, comprising a different extent of surface coverage, should be compared by means of their spectra composition. As mentioned introductorily, not only a differentiation by means of the adsorbed protein quantity, but also conclusions on the orientation or potentially, the degree of denaturation of the adsorbed molecules was expected from ToF-SIMS measurements. In this context, the evaluation involved the consideration of single mass spectra, as well as the application of principal component analysis as an aid to compare a plethora of sample spectra at a time.

Initially, the surface of the washed and heat sterilized blank glass vials was characterized. Figure 5a depicts a positive ion spectrum from the glass vial wall inside. As presumed from the outcome of previous contact angle measurements (Chapter 3), and expected from XPS results, ion fragments of organic origin were detected besides the characteristic glass components. These ion fragments comprised pure hydrocarbons as well as nitrogen and oxygen-containing species. Although ToF-SIMS theoretically allows the identification of a particular contaminating source, our search did not provide a unique contaminating species. A number of peaks characteristically points to the presence of proteinaceous contamination (NH_4^+, $C_3H_8NO^+$ (Thr), $C_5H_{11}N_4^+$ (Arg) and $C_9H_8N^+$ (Trp)) (see Table 3), whose origin remains unclear. XPS results demonstrated that the vial inner surface contamination exhibits low nitrogen content and is therefore, for the most part, not attributable to proteins. In Figure 5a, moreover, a high content of the $C_mH_n^+$ ion type is present. From our point of view, this is an evidence for unspecific hydrocarbon deposition, which settled on the glass samples from the air in the timeframe between preparation and measurement. In his paper, Benninghoven mentioned spectra of air-stored samples which were dominated by high intensity peaks arising from hydrocarbon contamination [16]. Another potential source of vial contamination might have been traces of residual cleaning agents or silicone compounds released from hoses of the vial washing machine. In addition, traces of paraffinic oil based lubricants, used as releasing agents in the production process of polypropylene containers [34], could have deposited on the glass surface and contributed to the overall surface contamination. Such containers were applied for example for sample transport and short term storage.

As an example for a pure protein fragmentation pattern, the ToF-SIMS spectrum of IgG1 adsorbed on the glass surface at pH 4.0 is depicted in Figure 5b. It reveals peaks of almost exclusively organic origin, with a lack of typical glass components, indicating a continu-

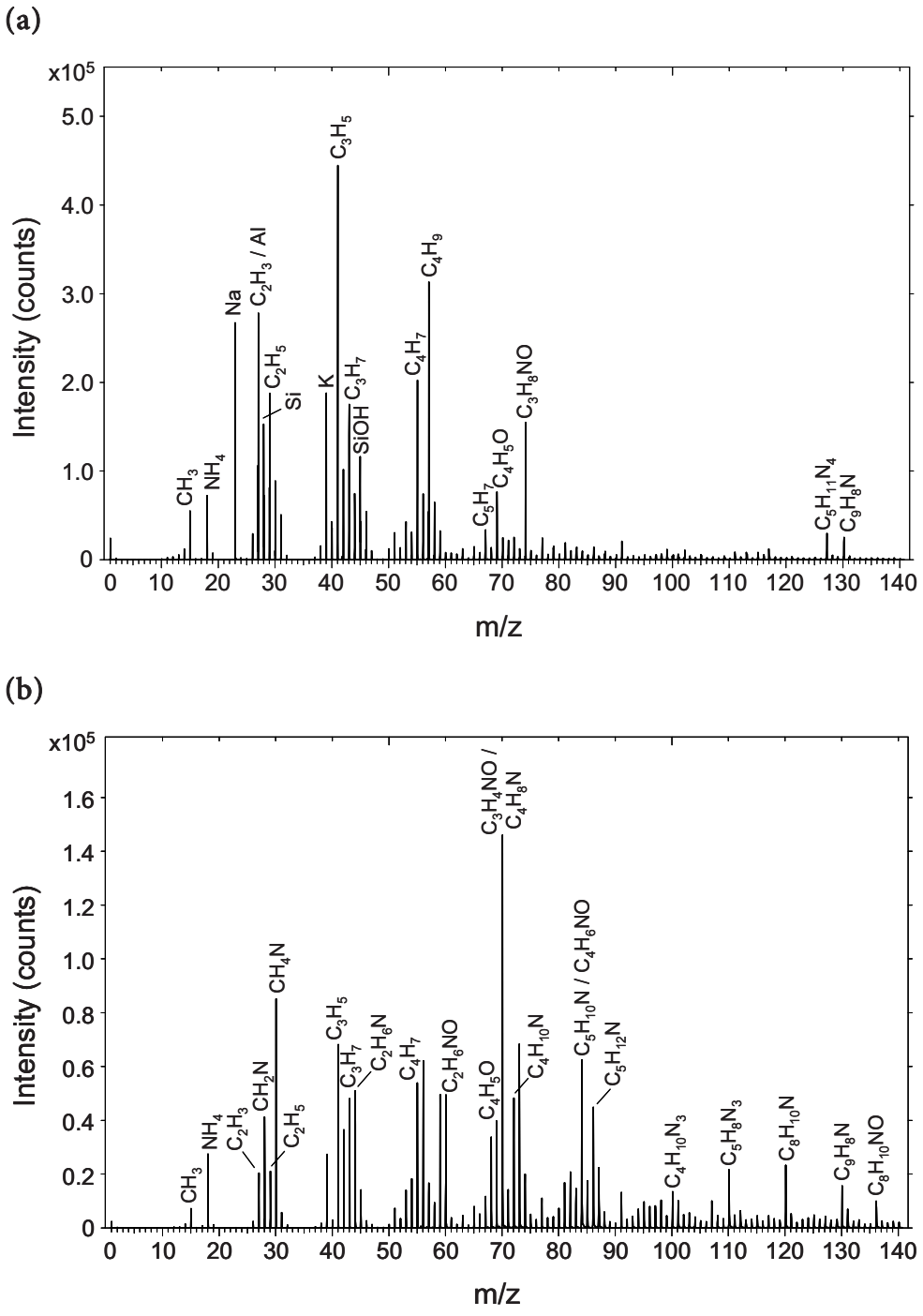

Figure 5: Positive ion ToF-SIMS spectra of (a) blank glass wall surface and (b) IgG1 adsorbed at pH 4.0 on the glass vial wall surface.

ous surface-covering protein layer. The share of unspecific hydrocarbon fragments expectably decreased. Moreover, in contrast to the application of a Ga^+ primary ion source (data not shown), the fragment size distribution is significantly shifted for the benefit of larger size fragments.

Subsequently, the influence of the IgG1 solution pH on the quality and the quantity of the adsorbed protein film on glass vial wall and bottom was investigated with ToF-SIMS on the basis of the fragmentation pattern and the ratio of organic to inorganic secondary ion species. As already stated, the complexity of ToF-SIMS spectra makes it hard to identify the significant differences between the samples. For this reason, principal component analysis was applied. A number of 52 positive ion species were therefore chosen from the spectra, to which the PCA analysis was confined in the following. These ion species were separated into the four groups "glass", "unspecific hydrocarbon", "unspecific proteinaceous", and "amino acids". Regarding the latter, at least one specific peak was ascribed to

Table 3: Positive ion species selected for principal component analysis; peaks were assigned to a collecting group or one characteristic amino acid.

Source	Fragment (m/z)	PCA variable No.
Glass	**7:** Li^+, **11:** B^+, **24:** Mg^+, **27:** Al^+, **28:** Si^+, **39:** K^+, **40:** Ca^+, **45:** $SiOH^+$, **48:** Ti^+, **138:** Ba^+	1-10
Unspecific hydrocarbon	**15:** CH_3^+, **27:** $C_2H_3^+$, **29:** $C_2H_5^+$, **41:** $C_3H_5^+$, **43:** $C_3H_7^+$, **55:** $C_4H_7^+$, **57:** $C_4H_9^+$, **67:** $C_5H_7^+$	11-18
Unspecific proteinaceous	**18:** NH_4^+, **19:** H_3O^+, **28:** CH_2N^+, (**71:** $C_4H_9N^+$)	19-21; (24)
Alanine (Ala)	**44:** $C_2H_6N^+$	26
Arginine (Arg)	**100:** $C_4H_{10}N_3^+$, **101:** $C_4H_{11}N_3^+$, **127:** $C_5H_{11}N_4^+$	41; 43; 49
Asparagine (Asn)	**70:** $C_3H_4NO^+$	22
Aspartic acid (Asp)	**88:** $C_3H_6NO_2^+$	47
Cysteine (Cys)	**76:** $C_2H_6SN^+$	52
Glutamine (Gln)	**84:** $C_4H_6NO^+$	34
Glutamic acid (Glu)	**102:** $C_4H_8NO_2^+$	45
Glycine (Gly)	**30:** CH_4N^+	25
Histidine (His)	**81:** $C_4H_5N_2^+$, **110:** $C_5H_8N_3^+$	39; 32
Isoleucine (Ile)	**86:** $C_5H_{12}N^+$	30
Leucine (Leu)	**86:** $C_5H_{12}N^+$	30
Lysine (Lys)	**84:** $C_5H_{10}N^+$	28
Methionine (Met)	**61:** $C_2H_5S^+$	51
Phenylalanine (Phe)	**120:** $C_8H_{10}N^+$, **131:**$C_9H_7O^+$	36; 44
Proline (Pro)[a]	**68:** $C_4H_6N^+$, **70:** $C_4H_8N^+$	33; 23
Serine (Ser)	**60:** $C_2H_6NO^+$, **71:** $C_3H_3O_2^+$	29; 46
Threonine (Thr)	**69:** $C_4H_5O^+$, **74:** $C_3H_8NO^+$	31; 35
Tryptophane (Trp)	**130:** $C_9H_8N^+$, **159:** $C_{10}H_{11}N_2^+$, **170:** $C_{11}H_8NO^+$	37; 48; 50
Tyrosine (Tyr)	**107:** $C_7H_7O^+$, **136:** $C_8H_{10}NO^+$	42; 40
Valine (Val)	**72:** $C_4H_{10}N^+$, **83:** $C_5H_7O^+$	27; 38

[a] The peak m/z = 70 contains contribution from several amino acids (see text for further elucidation)

each of the 20 amino acids. The peak list of all 52 fragments together with the amino acid attribution is shown in Table 3. A consecutive PCA variable number was assigned to each ion species. The classification of ToF-SIMS peaks to their main characteristic amino acid was performed according to Lhoest *et al.* and Wagner *et al.*, who selected the most intense peak out of the respective poly(amino acid) spectrum for this purpose [7,19]. However, they also emphasized that care must be taken in establishing such an assignment, since influencing effects of different adjacent amino acids on the fragmentation pattern are therefore not considered. Hence, one major peak for an amino acid could be characteristic of another one. Moreover, the fragments of leucine and isoleucine, for example, cannot be unambiguously distinguished because of their isomeric molecular structure. However, despite apparent concerns, such a peak assignment has often been applied and proven to give rise to meaningful results [7,15,32,35].

In the first PCA approach, spectra of the blank glass surface were compared with protein adsorbates at different solution pH (4.0, 7.2, and 8.6) and with the pure IgG1 spread on the glass. The scores plot (Figure 6) illustrates the differences in the sample spectra. First of all, it becomes obvious that more than 95% of the total variance in the system is cap-

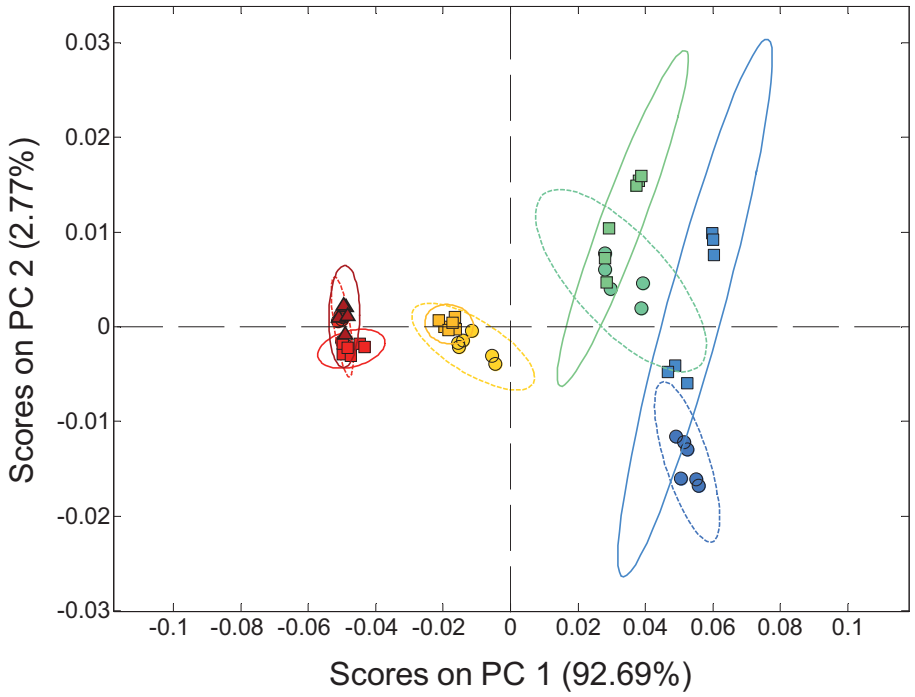

Figure 6: Scores plot from principal component analysis of glass vial bottom (circles) and wall (squares) with adsorbed IgG1 at pH 4.0 (light red), pH 7.2 (yellow), and pH 8.6 (green) applying all fragments of the peak list (Table 3); pure protein bulk samples (dark red triangles) and the blank glass surface (blue) are included in the plot; ellipses indicate the 95% confidence limit for the particular group with regard to PC 1 and PC 2.

tured by the first two principal components (PCs). The differences are for the predominant part described by the first (93%), and to a much lesser part described by the second principal component (3%). At first glance, the extent of the protein coverage is apparently indicated by PC1. According to the results of various adsorption quantification approaches, the spectra are the further apart from each other, the more pronounced the differences in the adsorbed protein mass are. The coincidence of the protein bulk spectra and the spectra of pH 4.0 adsorbed IgG1 again points towards a fully covered surface of the latter sample, as already indicated by the absence of glass components in its native ToF-SIMS spectrum (Figure 5b). Moreover, the spectra of those samples which exhibit a highly protein covered surface, e.g. the pure protein bulk as well as protein adsorbed from pH 4.0 and pH 7.2, are accumulated in a closely confined area with a low variance on both PC1 and PC2. Accordingly, it is not of concern whether IgG1 was adsorbed on the glass bottom or the glass wall. In contrast, the scores of samples with a sparsely protein covered surface (pH 8.6) and the blank glass surface show an increased variance on PC2. In this regard, the overlap of the confidence limits indicates that the spectra of the pH 8.6 incubated vial bottoms are no longer significantly distinguishable from the spectra of the blank glass. This similarity is further substantiated by the poor protein coverage and the small layer thickness of the same samples, obtained by XPS (Figures 3 and 4).

Further information on the crucial ion species is received from the corresponding loading plots of PC1 and PC2 (Figures 7 and 8). Peaks with the highest loadings also exhibit the highest variance, because the principal components capture the directions of the greatest variation in the data. Spectra with negative scores on PC1 (e.g. the dense protein adsorbates) have comparatively more intense peaks at, for example, m/z = 70 (proline). In contrast, spectra with positive scores on PC1 (the blank glass samples) have comparatively more intense peaks of glass components (e.g. Al^+, Si^+, and Ca^+) or even more of hydrocarbon components from the overlying organic glass contamination (e.g. $C_2H_5^+$, $C_3H_5^+$, $C_4H_9^+$, and others). Strikingly, there is a separation of glass surface related inorganic and hydrocarbon fragments (positive loadings) and protein derived nitrogen containing organic fragments (negative loadings) on PC1, which corroborates the decisive role of PC1 with regard to the adsorbed protein quantity. The fact that almost exclusively nitrogen free fragments are associated with the blank glass surface spectra again underlines the marginal importance of proteins with regard to the unspecific surface contamination. On the part of the blank glass surface, no individual prominent peak was recognized, whereas on the part of protein fragments the proline associated fragment m/z = 70 ($C_4H_8N^+$) was striking. The fact that the unspecific proteinaceous fragments, like NH_4^+ or CH_2N^+, hold lower loadings than the larger fragments indicates that the latter play the major role in the differentiation of the blank glass surface and the adsorbed protein.

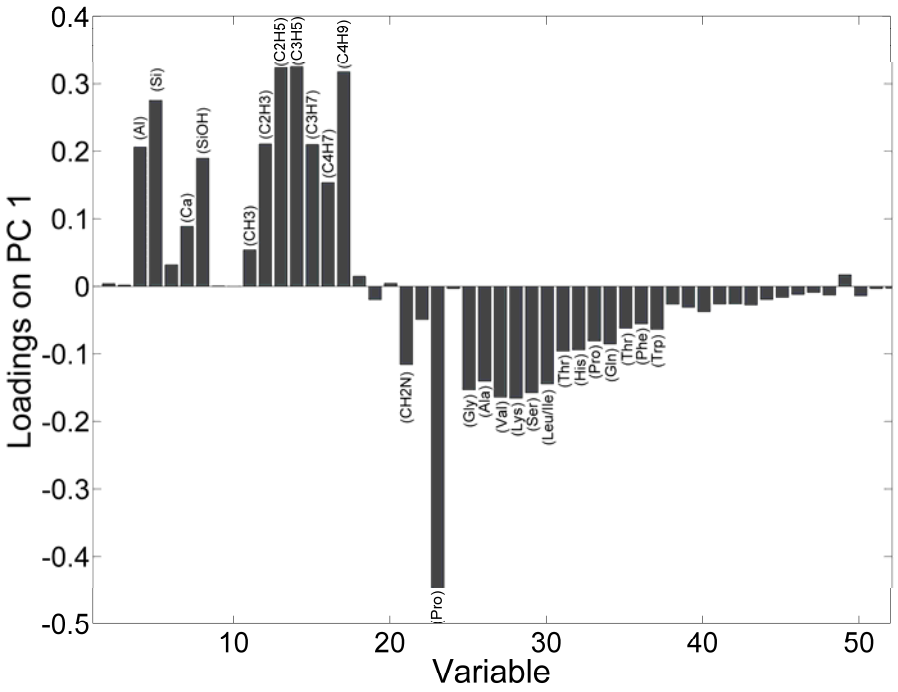

Figure 7: Loadings on PC1; most conspicuous peaks are labeled with the associated ion or the attributed amino acid.

It is apparent from Figure 6 that, as long as the glass surface is densely covered with protein, the spectra are not separated on PC2, but the higher the glass fraction on the surface is, the higher becomes the divergence. Thus, the differences in the underground surface state, namely the glass surface composition and the degree of contamination, are indicated, whereas the protein coverage itself seems to be virtually homogeneous within the scope of this evaluation. The peaks that contribute to this separation on PC2 are Al^+ and K^+ (positive loadings), on the one hand, and $Si^+/SiOH^+$, NH_4^+, fragments of the small residues glycine, and alanine as well as the unspecific organic fragments (negative loadings), on the other hand (Figure 8). The above correlation applies for the spectra of the blank vial bottoms (blue circles), which exclusively hold negative scores on PC2. Vial bottoms have previously shown to exhibit a higher silicon content than the vial wall part (Table 1). Spectra of the cylindrical part of the blank vials, however, are indifferent with regard to their scores on PC2. In contrast, less organic surface contamination was detected on bottoms with XPS, which disagrees with the results of PC2 on the loading plot. At least for the vial wall samples, which show positive and negative scores on PC2, a serious difference in the glass surface composition and/or the degree of contamination is plausible.

It can be concluded that by means of ToF-SIMS measurements together with PCA, differences in the IgG1 surface coverage on the borosilicate glass surface, as well as differences regarding the glass substrate itself could be identified. A further initial objective of using

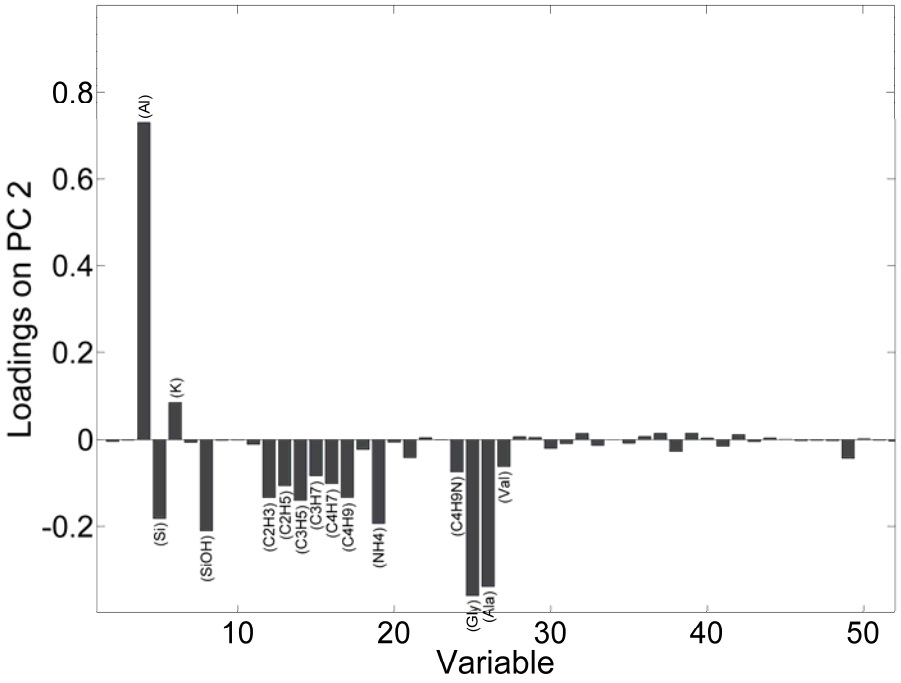

Figure 8: Loadings on PC2; most conspicuous peaks are labeled with the associated ion or the attributed amino acid.

ToF-SIMS was the investigation of the topmost area of adsorbed IgG1 with regard to differences in the amino acid composition and potential information on e.g. the degree of protein denaturation. Therefore, a new PCA approach exclusively considered the amino acid associated peaks (see Table 3). The resulting scores plot (Figure 9) exhibits some marked parallels to the above model. The ratio of PC1 to PC2 is similar to that of the first model, as the first principal component covers the vast majority (> 95%) of the system's variance. The differences between bottom and wall spectra for samples of the same incubation condition are not significant, since the confidence ellipses of both overlap throughout. Neither is a pronounced difference observed between the pure protein bulk and the protein layers adsorbed at pH 4.0, which therefore indicates a similar nature of the topmost molecules of both adsorbates. The distinct separation of the samples on PC1 in the order pH 4.0, pH 7.2, and pH 8.6 is in correlation to the previous model. However, this spectra separation result is based on the processing of protein related ion fragments only and consequently attributable to the amino acid composition of the topmost protein domain. Hence, differences therein may indicate a different orientation of the adsorbed molecules and/or a variable extent of protein unfolding upon adsorption with regard to the incubation pH. In previous work of Lassen and Malmsten, the orientation of adsorbed proteins within a monolayer has been found to change with the degree of surface coverage [36]. The orientation of adsorbed molecules may also change in the course of multi-

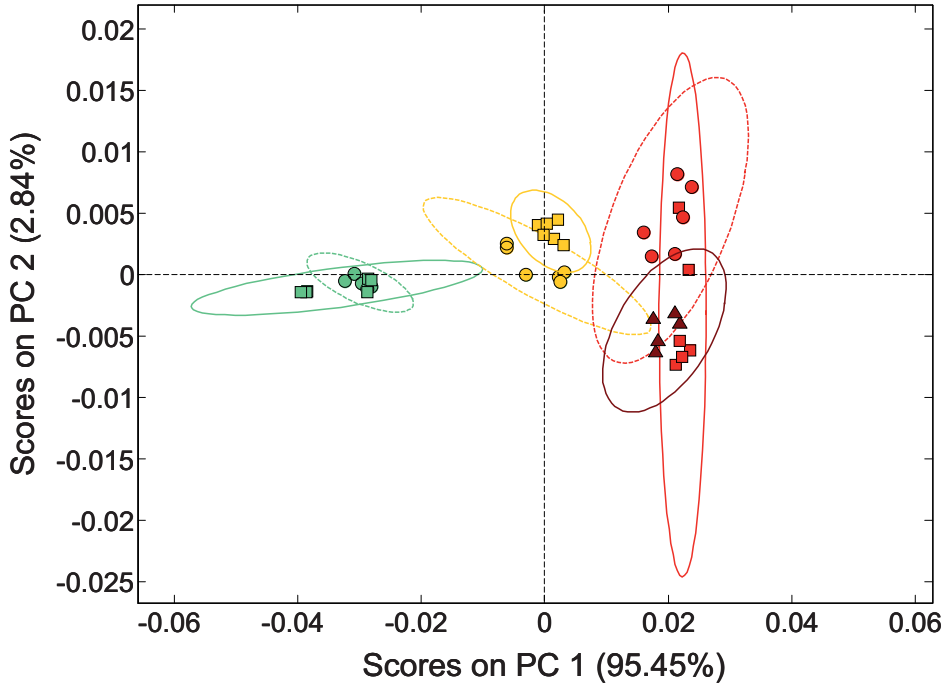

Figure 9: Scores plot from principal component analysis of glass vial bottom (circles) and wall (squares) with adsorbed IgG1 at pH 4.0 (light red), pH 7.2 (yellow) and pH 8.6 (green) on the basis of fragments associated with characteristic amino acid exclusively (Table 3 fragment no. 22-23; 25-52); pure protein bulk samples (dark red triangles) are included; ellipses indicate the 95% confidence limit for the particular group with regard to PC 1 and PC 2.

layer formation of antibodies at higher solution concentrations [37]. Since in our case, different pH values are associated with a varying degree of surface coverage, the evidence of an orientation change by means of the ToF-SIMS results seems probable. However, changes in antibody orientation cannot be clearly distinguished from pronounced protein unfolding. It is further outlined in Chapter 7 that different protein coverage rates and, thus, a varying proportion of antibody in contact to the glass can be associated with a different degree of instability. This means the glass surface itself could have had a significant stabilizing or destabilizing effect on the protein structure, which is reflected by the separation on PC1. Furthermore, IgG1 stability in solutions of different pH has to be considered as well (see Chapter 7). It also has to be taken into account that protein peak intensities in ToF-SIMS can be affected by a matrix effect, induced by the underlying substrate, which has been found to be most pronounced at lowest protein surface concentrations [11].

The loading plots, which outline the contribution of any peak to the separation on each principal component, might further indicate whether protein denaturation was involved. In the native conformation, the hydrophilic amino acids are preferentially located in the exterior of the protein molecule, where they interact with the aqueous environment. Conversely, hydrophobic amino acids are buried in the protein core, where they are mostly

shielded from water contact. Thus, an increased contribution of either hydrophilic or hydrophobic amino acids to the spectra might give some indication of denaturation.

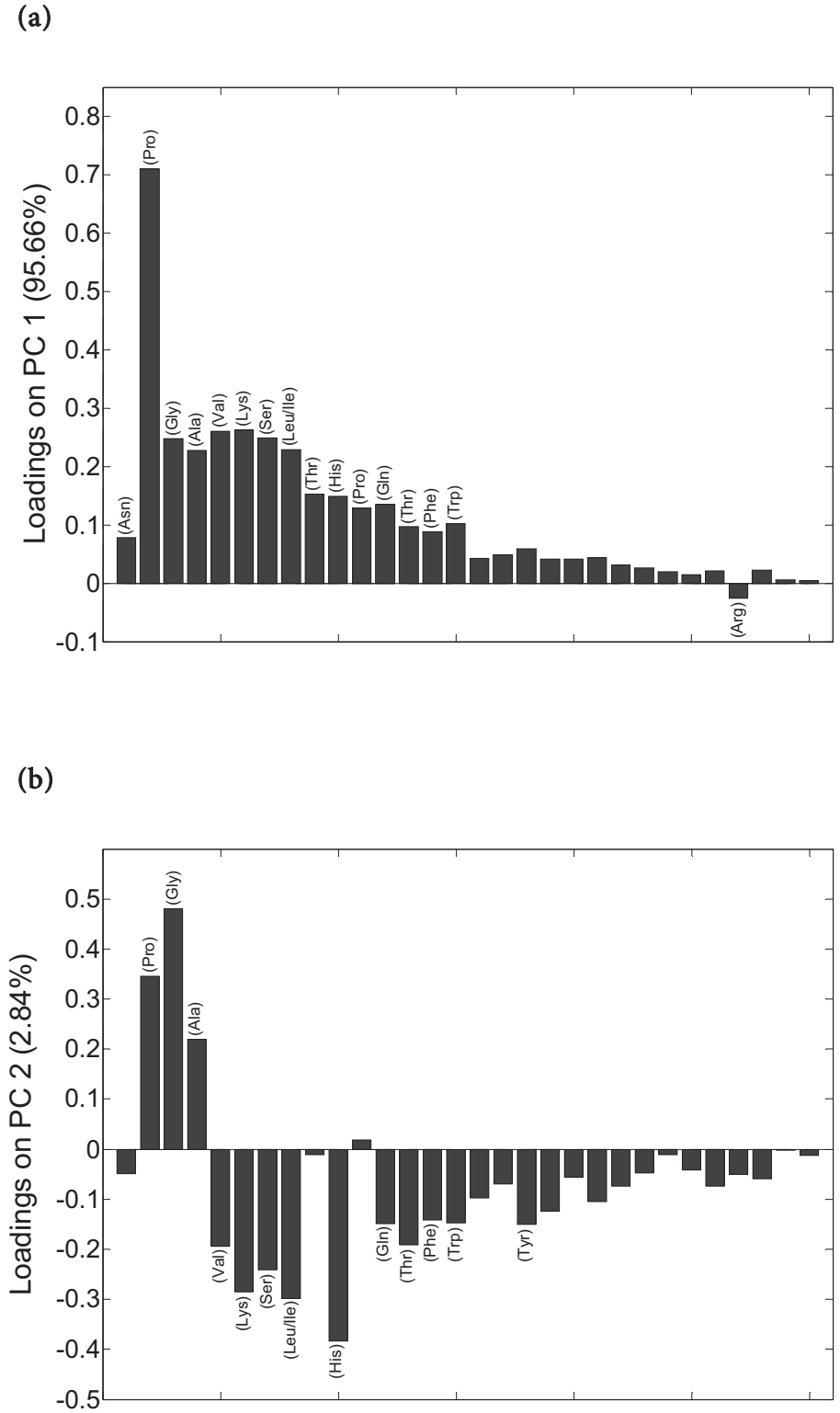

Figure 10: Loadings on (a) PC1 and (b) PC2 of the protein characteristic amino acid PCA plot (Figure 9); most conspicuous peaks are labeled with the attributed amino acid.

The peak m/z = 70 ($C_4H_8N^+$) highly contributes to the separation of the spectra on PC1 (Figure 10a). The associated amino acid proline, which often occurs at turns in the polypeptide chain, is basically nonpolar, but does not occur in the interior of proteins as frequently as, for example, leucine or valine [38]. With regard to the mean solvent accessibility data of the IgG1 amino acid residues (Table 4), proline provides an average mid-level to low solvent accessibility. This implies that it is, by tendency, rather located in the interior of the protein, but is in so far not exclusively indicative of the hydrophobic protein core. The only peak with a negative loading on PC1 is m/z = 127 ($C_5H_{11}N_4^+$), indicative of arginine. As a charged amino acid, it is located in the exterior of the IgG1 and exhibits a high solvent accessibility (Table 4). With the exclusive consideration of these two amino acids and the assumption that the scores reflect the amino acid composition of the

Table 4: Mean solvent accessibility of amino acid residues in the IgG1, obtained from the IgG1 crystal structure by the DSSP program [39]; IgG1 amino acid composition determined by the European Molecular Biology Open Software Suite (EMBOSS) [40].

Amino acid	Mean solvent accessibility (%)[a]	IgG1 composition (mole %)
Cys	41.7	2.4
Lys	36.2	6.5
Arg	**34.3**	**2.7**
Asn	31.2	5.0
Glu	31.1	4.8
Gln	27.8	4.8
Asp	24.1	3.8
Ser	20.3	13.3
His	19.9	2.0
Thr	19.6	7.8
Pro	**19.1**	**6.8**
Tyr	18.6	4.2
Gly	14.1	6.2
Met	13.0	0.6
Ala	11.0	4.4
Leu/Ile	10.6	10.6
Phe	7.9	3.5
Trp	7.7	1.8
Val	7.7	8.7

[a] related to the highest solvent accessibility value occurring in the IgG1

upmost protein layer, molecules without glass contact seem to expose rather their hydrophobic interior. IgG1 adsorbed at higher pH associated with a low surface coverage by contrast exhibits a more hydrophilic protein surface, which accordingly reflects a rather native like IgG1 molecule. However, considering all seven ion species with highest positive loadings on PC1 (highlighted in Table 4), no prevalence of the associated amino acids with regard to their solvent accessibility can be deduced.

Also, other authors reported a high loading of the peak m/z = 70 in their PCA studies of adsorbed protein [32]. They mentioned that other amino acids (Arg, Leu, and Lys) had spectra with similar intensities of this peak and a unique attribution of this peak to leucine would not be reasonable. They further concluded that the peak m/z = 70 could therefore represent e.g. the heterogeneity of the surface concentration of adsorbed protein molecules. Our consideration of the peaks showing high positive or negative loadings on PC2 (Figure 10b) did not reveal any correlation with the solvent accessibility of amino acids or with their frequency in the IgG1 molecule. It is remarkable that exclusively small residues (proline, glycine, and alanine) exhibit high positive loadings on PC2. However, a meaningful conclusion could not be drawn from this result.

With regard to the attempt of investigating the orientation and/or the degree of denaturation of adsorbed IgG1 on the glass surface, two further issues must be discussed. The sample preparation preceding the ToF-SIMS analysis necessarily involves a water rinsing step to avoid buffer salt crystallization in the course of drying. The aqueous medium comprising a low permittivity leads to increased intermolecular and intramolecular electrostatic repulsive or attractive forces, which can readily cause changes within the three dimensional structure of the proteins. Beyond that, the drying step itself was shown to induce structural alterations along with a significant loss of functionality [32]. We observed more dramatic reorganizations in terms of unfolding by AFM film thickness determinations of dry films, which revealed values of only around 1 nm (see Chapter 7). This corresponds to a film thickness of only about 15%, referred to the narrowest dimension of the native hydrated molecule (based on the crystal structure data). Accordingly, the fact that one cannot proceed from the assumption of an intact molecule complicates the interpretation of ToF-SIMS results.

4 CONCLUSIONS

With the aid of the sensitive spectroscopic methods XPS and ToF-SIMS, a number of new insights in the chemical state of the glass substrate and the adsorbed protein layers could be achieved. Via XPS, first the chemical composition of the glass surface was found to differ from the theoretical composition of the bulk, which is ascribed to the manufacturing process or to a pronounced corrosion or leaching process. Moreover, substantial organic contamination was detected on the blank glass vials. A larger amount of contamination was found on the vial wall than on the vial bottom. A low nitrogen signal and an insufficiently high amide carbon fraction indicate a non-proteinaceous origin. ToF-SIMS analyses confirmed the presence of hydrocarbon compounds on the blank glass substrate, but a particular contaminating source could not be identified. With regard to adsorbed protein layers, XPS has shown to be well suited for quantifying adsorbed IgG1 on the glass samples. One advantage over other methods which have previously been established in the scope of this thesis, e.g. eluting with surfactant or acid, was the capability of a direct quantification on the surface avoiding a desorption step. Another advantage of spectroscopic surface examination was the general ability of performing localized measurements. Therefore, increased surface contamination on the vial wall when compared with the vial bottom was seen. Additionally, the adsorbed IgG1 quantities on the vial wall turned out to be increased as well, which was confirmed by separately investigating both sections with the validated SDS desorption quantification. This observation corresponds with the findings described in Chapter 3, where a direct correlation between a decrease in surface free energy and an increase of IgG1 adsorption was described. The increased adsorption tendency on the vial wall was found to be independent of the incubation pH value. This leads to the conclusion that the increased adsorption tendency is not attributable to ionic interactions between glass and protein, therefore less likely due to differences in the glass surface composition, but in all probability due to increased hydrophobic interactions between protein molecules and the organic contamination. Finally, XPS allowed an estimation of the thickness of dried protein layers. The values reached from approx. 1.1 nm (bottom, pH 8.6) to approx. 4.9 nm (wall, pH 4.0). Principal component analysis turned out to be most helpful for the simultaneous comparison of an increased number of ToF-SIMS spectra. With the aid of PCA, the investigated protein samples could be classified by means of the pH value of incubation, as well as the extent of surface coverage. The exclusive consideration of protein derived ion fragments revealed differences in the fragmentation pattern of the protein adsorbates, but the particular reason for this could not be unambiguously clarified. These differences may be attributed to a difference in molecular orientation, to a varying degree of denaturation of the adsorbed molecules, or to an influencing matrix effect, caused by a variable fraction of bare glass underground. In ToF-SIMS, protein adsorbates at pH 4.0 (the pH of maximum adsorption) behaved identical to

the pure protein bulk. This, in turn, proved a closed protein layer for the pH 4.0 samples. Increasing the incubation pH to 7.2 and 8.6 led to an increased glass surface fraction visible in ToF-SIMS. Although fundamental statements were expected from the corresponding loading plots of the PCA models, the determination of a preferential molecular orientation or of the degree of unfolding could not be achieved within the performed measurements, which presents a challenge for future work.

5 REFERENCES

[1] Henry, M., Bertrand, P., Influence of polymer surface hydrophilicity on albumin adsorption, *Surface and Interface Analysis* **36** (2004) 729-732.

[2] Fitzpatrick, H., Luckham, P. F., Eriksen, S., Hammond, K., Use of x-ray photoelectron spectroscopy to study protein adsorption to mica surfaces, *Journal of Colloid and Interface Science* **149** (1992) 1-9.

[3] Kingshott, P., McArthur, S., Thissen, H., Castner, D. G., Griesser, H. J., Ultrasensitive probing of the protein resistance of PEG surfaces by secondary ion mass spectrometry, *Biomaterials* **23** (2002) 4775-4785.

[4] Sweryda-Krawiec, B., Devaraj, H., Jacob, G., Hickman, J. J., A New Interpretation of Serum Albumin Surface Passivation, *Langmuir* **20** (2004) 2054-2056.

[5] Wagner, M. S., Horbett, T. A., Castner, D. G., Characterizing multicomponent adsorbed protein films using electron spectroscopy for chemical analysis, time-of-flight secondary ion mass spectrometry, and radiolabeling: capabilities and limitations, *Biomaterials* **24** (2003) 1897-1908.

[6] NIST X-ray Photoelectron Spectroscopy Database, Version 3.5, (National Institute of Standards and Technology, Gaithersburg, USA), 2003.

[7] Wagner, M. S., McArthur, S. L., Shen, M., Horbett, T. A., Castner, D. G., Limits of detection for time of flight secondary ion mass spectrometry (ToF-SIMS) and X-ray photoelectron spectroscopy (XPS): detection of low amounts of adsorbed protein, *Journal of Biomaterials Science, Polymer Edition* **13** (2002) 407-428.

[8] Wei, J., Ravn, D. B., Gram, L., Kingshott, P., Stainless steel modified with poly(ethylene glycol) can prevent protein adsorption but not bacterial adhesion, *Colloids and Surfaces, B: Biointerfaces* **32** (2003) 275-291.

[9] Wagner, M. S., Horbett, T. A., Castner, D. G., Characterization of the structure of binary and ternary adsorbed protein films using electron spectroscopy for chemical analysis, time-of-flight secondary ion mass spectrometry, and radiolabeling, *Langmuir* **19** (2003) 1708-1715.

[10] Ratner, B. D., Horbett, T. A., Shuttleworth, D., Thomas, H. R., Analysis of the organization of protein films on solid surfaces by ESCA, *Journal of Colloid and Interface Science* **83** (1981) 630-642.

[11] Ferrari, S., Ratner, B. D., ToF-SIMS quantification of albumin adsorbed on plasma-deposited fluoropolymers by partial least-squares regression, *Surface and Interface Analysis* **29** (2000) 837-844.

[12] Wagner, M. S., Castner, D. G., Characterization of adsorbed protein films using time-of-flight-secondary ion mass spectrometry and multivariate analysis, *Applied Surface Science* **203-204** (2003) 698-703.

[13] Lhoest, J. B., Detrait, E., Van Den Bosch De Aguilar, Bertrand, P., Fibronectin adsorption, conformation and orientation on polystyrene substrates studied by radiolabeling, XPS and ToF SIMS, *Journal of Biomedical Materials Research* **41** (1998) 95-103.

[14] Rangarajan, S., Tyler, B. J., Interpretation of static time-of-flight ion mass spectral images of adsorbed protein films on topographically complex surfaces, *Applied Surface Science* **231-232** (2004) 406-410.

[15] Bruening, C., Hellweg, S., Dambach, S., Lipinsky, D., Arlinghaus, H. F., Improving the interpretation of ToF-SIMS measurements on adsorbed proteins using PCA, *Surface and Interface Analysis* **38** (2006) 191-193.

[16] Benninghoven, A., Chemical analysis of inorganic and organic surfaces and thin films using time-of-flight secondary ion mass spectrometry (TOF-SIMS), *Angewandte Chemie* **106** (1994) 1075-1096.

[17] Tidwell, C. D., Castner, D. G., Golledge, S. L., Ratner, B. D., Meyer, K., Hagenhoff, B., Benninghoven, A., Static time-of-flight secondary ion mass spectrometry and x-ray photoelectron spectroscopy characterization of adsorbed albumin and fibronectin films, *Surface and Interface Analysis* **31** (2001) 724-733.

[18] Mathieu, H. J., Time-of-Flight SIMS, *G. I. T. Laboratory Journal* **2007** (2007) 34-35.

[19] Lhoest, J. B., Wagner, M. S., Tidwell, C. D., Castner, D. G., Characterization of adsorbed protein films by time of flight secondary ion mass spectrometry, *Journal of Biomedical Materials Research* **57** (2001) 432-440.

[20] Shlens, J., A Tutorial on Principal Component Analysis, Center for Neural Science, New York University, New York, NY and Systems Neurobiology Laboratory, Salk Insitute for Biological Studies, La Jolla, CA (2009).

[21] Jolliffe, I. T., Principal Component Analysis, (Springer Verlag, Inc., New York, USA) Ed. 2, 2002.

[22] Wise, B. M., Gallagher, N. B., Bro, R., Koch, R. S., Shaver, J. M., Winding, W., Miller, C. E., Principal Component Analysis, *Solo 4.1 / PLS_Toolbox 4.1 Manual*, (Eigenvector Research Inc., 2009), Chapter 5, 99-136.

[23] Wagner, M. S., Castner, D. G., Characterization of adsorbed protein films by time-of-flight secondary ion mass spectrometry with principal component analysis, *Langmuir* **17** (2001) 4649-4660.

[24] Roehl, H., Experimentelle Untersuchung der Wechselwirkung von Fluessigkeiten und Gasen mit Oberflaechen von Magnetspeicherplatten, Thesis, 2007.

[25] SCHOTT AG, SCHOTT technical glasses: Physical and technical properties, 2007.

[26] Pickles, C., Manufacturing Problems, *Pharmaceutical Technology Europe* **11** (2008) 20-23.

[27] Schwarzenbach, M. S., Reimann, P., Thommen, V., Hegner, M., Mumenthaler, M., Schwob, J., Guentherodt, H. J., Topological structure and chemical composition of inner surfaces of borosilicate vials, *PDA J. Pharm. Sci. Technol.* **58** (2004) 169-175.

[28] Schwarzenbach, M. S., Oberflaechencharakterisierung pharmazeutischer Glasbehaeltnisse und Messung verschiedener Wechselwirkungen zwischen Interferon-2a und Glas, Thesis, 2001.

[29] Steffens, G. C. M., Nothdurft, L., Buse, G., Thissen, H., Hocker, H., Klee, D., High density binding of proteins and peptides to poly(DL-lactide) grafted with polyacrylic acid, *Biomaterials* **23** (2002) 3523-3531.

[30] Tanuma, S., Powell, C. J., Penn, D. R., Calculations of electron inelastic mean free paths. V. Data for 14 organic compounds over the 50-2000 eV range, *Surf. Interface Anal.* **21** (1994) 165-176.

[31] Paynter, R. W., Ratner, B. D., Horbett, T. A., Thomas, H. R., XPS studies on the organization of adsorbed protein films on fluoropolymers, *Journal of Colloid and Interface Science* **101** (1984) 233-245.

[32] Xia, N., May, C. J., McArthur, S. L., Castner, D. G., Time-of-flight secondary ion mass spectrometry analysis of conformational changes in adsorbed protein films, *Langmuir* **18** (2002) 4090-4097.

[33] Ganz, M., Herstellung partikulaerer Formulierungen fuer rekombinante Proteine mittels Wirbelschicht, Thesis, 2007.

[34] Thiriez, A., An Environmental Analysis of Injection Molding, Thesis, 2006.

[35] Sanni, O. D., Wagner, M. S., Briggs, D., Castner, D. G., Vickerman, J. C., Classification of adsorbed protein static ToF-SIMS spectra by principal component analysis and neural networks, *Surface and Interface Analysis* **33** (2002) 715-728.

[36] Lassen, B., Malmsten, M., Structure of protein layers during competitive adsorption, *Journal of Colloid and Interface Science* **180** (1996) 339-349.

[37] Xu, H., Zhao, X., Grant, C., Lu, J. R., Williams, D. E., Penfold, J., Orientation of a Monoclonal Antibody Adsorbed at the Solid/Solution Interface: A Combined Study Using Atomic Force Microscopy and Neutron Reflectivity, *Langmuir* **22** (2006) 6313-6320.

[38] Roskoski, R. Jr., Biochemistry, (Elsevier Health Sciences, Philadelphia, USA) Ed. 1, 1995.

[39] Kabsch, W., Sander, C., Dictionary of protein secondary structure: pattern recognition of hydrogen-bonded and geometrical features, *Biopolymers* **22** (1983) 2577-2637.

[40] Rice, P., Longden, I., Bleasby, A., EMBOSS: the european molecular biology open software suite, *Trends Genet.* **16** (2000) 276-277.

Chapter 7

Structural Stability Investigations and Atomic Force Microscopy Imaging of IgG1 Adsorbed on Borosilicate Glass

Abstract

In this Chapter, the stability of dissolved IgG1 was investigated regarding aggregation (SDS-PAGE, SE-HPLC), secondary (ATR-FTIR) and tertiary (fluorescence spectroscopy) structure subject to pH value and ionic strength. The structural properties of IgG1, adsorbed from a solution of 2 mg/ml, were studied on the surface of borosilicate glass particles. In addition, as the adsorption step was shown to be reversible by means of pH shifts of the formulation, also irreversible alterations of desorbed protein could be investigated. The character of the adsorbed antibody was visualized by AFM in dried state as well as submerged in buffer liquid. Finally, the structural integrity of desorbed IgG was assessed by ELISA. The investigations revealed that the IgG1 is structurally stable in the pH range from 4 to 10. Spectroscopic analysis of IgG1 in adsorbed state suggested slight aggregation at the IEP (pH 8.6), but under none of the conditions tested substantial unfolding was observed. Chromatographic and fluorescence spectroscopic investigation of desorbed protein fractions indicated an increasing tendency for aggregation and unfolding in the order pH 4.0 < pH 7.2 < pH 8.6, whereas this trend was less pronounced in FT-IR. In ELISA, an equally reduced structural integrity was found for all three desorbed protein fractions compared to reference. AFM images revealed a completely denatured protein film spread on the glass surface after drying. Imaging of protein films adsorbed from concentrations of 2 mg/ml in submerged state indicated adsorption of IgG1 on the surface in an agglomerated form as patches and a film thickness reflecting multiple protein layers.

1 INTRODUCTION

The interaction of proteins with solid surfaces has, for a long time, been the subject of exhaustive research. A large number of researchers studied changes in secondary or tertiary structure of proteins and determined the biological activity upon surface binding. Very often, specific applications (e.g. immunosorbent assays) are associated with adsorption steps, and the molecular structure together with the protein activity becomes of particular interest. However, the interrelations with respect to protein structure are sophisticated. For example, the overall adsorbed amount of protein is not solely controlled by the attractive and repulsive forces caused by electrostatic and hydrophobic interaction forces, but also depends on the structural stability of the protein in its particular formulation. Thus, the analysis of structural stabilities after adsorption will, at least in part, shed light on the adsorption mechanism of the respective molecule at the given conditions. Irrespective of parameters like the formulation or the intrinsic protein properties, it was described that more profound alterations were induced on hydrophobic surfaces compared to hydrophilic ones [1,2]. Another example of an important factor concerning the remaining protein activity after adsorption is the initial concentration on the surface, as described by Sandwick and Schray [2]. If the initial surface concentration is low, like at the initial part of an adsorption isotherm, the molecules are bound to a greater degree in an inactive or spread form. By contrast, the fraction of proteins in native structure increases when the surface is more crowded. This indicates that sterical reasons are most likely involved in the unfolding of surface bound molecules.

A pool of predominantly spectroscopic analytical methods is applicable to investigate structural alterations with respect to protein adsorption processes. The most common techniques for monitoring changes in the protein secondary structure described in literature so far are, for example, (attenuated total reflection) Fourier transform infrared spectroscopy (ATR) FT-IR [1,3,4], circular dichroism (CD) spectroscopy [5-7], and also nuclear magnetic resonance (NMR) spectroscopy [8]. Moreover, changes in the tertiary structure of proteins are commonly investigated with fluorescence spectroscopy techniques recording either the intrinsic fluorescence of protein chromophores [9] or the fluorescence of extrinsic chromophores like 8-anilino-1-naphthalenesulfonic acid (ANS) [5,10]. Also, a total internal reflection fluorescence (TIRF) setup is widely used in monitoring adsorption induced structural changes and aggregation [11,12]. Further spectroscopic techniques that are capable of investigating protein denaturation in terms of layer thickness are, for example, specular neutron reflection [13,14] or ellipsometry [15,16]. Besides the spectroscopic methods, another common versatile tool is atomic force microscopy (AFM), which has become an established technique for the imaging of “soft” biological samples on solid surfaces [17,18]. The studies focused on (3D) mapping of single

molecules on surfaces [19,20], on imaging the organization and spatial order of adsorbed proteins layers [21,22], and even on following the online adsorption of molecules [23]. Keller provides a good overview of the method regarding the imaging of proteins [24].

However, in many of the aforementioned cases, specific model surfaces with particular requirements are indispensable. That is why these techniques are usually not readily applicable for the investigation of proteins on so-called "real" surfaces such as pharmaceutical containers. Accordingly, only few investigators dealt with containers but with similar substrates instead. Thus, changes of the molecular structure upon adsorption, especially on borosilicate glass, have not yet been exhaustively analyzed. The activity of therapeutic proteins was repeatedly found to decrease upon storage in their primary packaging. The reason for this observation, however, was rather an adsorption induced decrease of the protein concentration in solution (see Chapter 1). Nonetheless, surface induced structural alterations of therapeutic proteins are critical. Besides changes in the secondary or tertiary structure, contact with the surface can also induce clustering or aggregation of proteins. In addition to a loss of function, (partly) denatured proteins in solution can possibly trigger further aggregation, which at worst can cause immunological reactions in the patient. This is a common, but compared to other aspects, a rarely mentioned effect [12]. A short overview of this aspect is given in Chapter 1. Although it could be shown from our previous work, that IgG adsorption on glass container surface is widely irreversible upon dilution (see Chapter 2), a back-diffusion of unfolded or aggregated molecules into the formulation cannot be entirely excluded.

In the context of this work, the protein solution compositions and the surface properties, with respect to material and pretreatment, were to be close to the situation for a recombinant protein drug in a glass vial. Protein concentration, buffer salt and its concentration, as well as total ionic strength were chosen according to established preparations. To increase the effective surface area, glass particles were prepared by grinding glass containers, despite the fact that the surface of the glass particles does not precisely match the chemical surface composition of the inner container surface. Pretreatments like washing and heat sterilizing were considered as well.

The aim of this work was to gain insight into the structural behavior of IgG adsorbed on the borosilicate glass surface. This included the investigation of the secondary and the tertiary structure using ATR-FTIR spectroscopy and fluorescence spectroscopy. Further information should be gained on the surface induced aggregation tendency as well as the residual activity of the adsorbed IgG. The structural properties of IgG were analyzed in two ways, either directly in adsorbed state or after a gentle desorption step with the aid of a pH shift. By these means, the irreversibility of structural rearrangements should be examined. Finally, the adsorbed protein layers were to be visualized on the glass surface by

AFM, both in dried state and submerged in buffer liquid. In all of the structural studies, a main focus was on the impact of the formulation pH value against the background of different protein stabilities.

2 MATERIALS AND METHODS

2.1 Materials

2.1.1 Protein Formulation and Including Excipients

The protein used for the structural studies was a monoclonal IgG1 antibody (IgG1) (MW≈ 152 kDa) in a concentration of 2 mg/ml in 10 mM phosphate buffer and 145 mM NaCl (pH 7.2), which was kindly provided by Merck Serono (Darmstadt, Germany). The second protein investigated was IgG from pooled human plasma (h-IgG) and was purchased as a lyophilized powder from Sigma-Aldrich (Steinheim, Germany). It was further dissolved in the analogous PBS buffer as used for IgG1. The ionic strength of the formulation was calculated to be 170 mM.

Two further 10 mM phosphate buffer solutions of pH 4.0 and 8.6 were prepared. The appropriate amount of NaCl was calculated and added in order to adjust the ionic strength to 170mM. The IgG1 was dialyzed against the buffers, using Vivaspin® 20 centrifugal concentrators (Sartorius-Stedim Biotech, Goettingen, Germany) equipped with a 30.000 MWCO polyethersulfone (PES) membrane. The final solutions were filtered through 0.2 µm PES membrane filters (Pall GmbH, Dreieich, Germany). The protein concentration was determined by UV absorption measurement at 280 nm, and the final protein concentration was adjusted so that the equilibrium concentration after the adsorption experiments was 2 mg/ml. Water for all buffers and applications was ultrapure water (0.055 µS/cm) from a Purelab Plus UV/UF system (ELGA LabWater, Celle, Germany). Bis-ANS (4,4′-Dianilino-1,1′-binaphthyl-5,5′-disulfonic acid dipotassium salt) was purchased from Sigma-Aldrich (Munich, Germany). All chemicals used were of p.a. grade.

2.1.2 Glass Powder

Glass powder was prepared from borosilicate glass vials Fiolax® 2R, kindly provided by SCHOTT AG (Mainz, Germany). Vials were shattered and the flinders, apart from the vial neck, were milled in a Pulverisette® 5 laboratory planetary mill (Fritsch GmbH, Idar-

Oberstein, Germany) for 8 h, using ZrO_2 grinding beakers and balls. The powder was fractionated in a sieve tower and the particle fraction smaller than 45 microns was collected. Particles were washed 3 times by suspending them in water for 5 min and recovered by centrifugation. The particles were dried at 90°C, and the powder was heat sterilized at 250°C for 1 h.

2.1.3 Glass Vials / Glass Vial Bottoms

Fiolax® 2R borosilicate glass vials were washed in a FAW 500 vial washing machine for pharmaceutical purposes (Bausch & Stroebel GmbH+Co. KG, Ilshofen, Germany) with highly purified water and heat sterilized at 250°C for 1 h before use. For AFM measurements, the bottoms of the vials were carefully cut off with a DREMEL® 300 series rotary tool (DREMEL Europe, Breda, The Netherlands) equipped with a rotating diamond cut-off wheel. Contaminating particles were removed by washing with ultrapure water, and the surface was dried under a weak nitrogen flow.

2.2 Methods

2.2.1 Static Laser Light Scattering

The size distribution of different glass particle fractions was analyzed by static laser light scattering in a Horiba LA-950 system (Retsch Technology GmbH, Haan, Germany) according to the Mie scattering theory. The device is equipped with two light sources, a 5 mW 650 nm Laser Diode and a 3 mW 405 nm LED. The optical system consists of inverse Fourier optics and several detectors in forward, side, and reverse direction, ensuring a wide measuring range from upper nm to lower mm range. For measurements, glass powder was suspended in degassed ultrapure water. Data analysis and calculation of values was carried out using the LA-950 software.

2.2.2 Scanning Electron Microscopy (SEM)

For visualization of the glass particles, a JEM 6500F scanning electron microscope from JEOL GmbH (Eching, Germany) was utilized. The particles were deposited on a conductive pad and sputtered with carbon.

2.2.3 Specific Surface Area Analysis

The specific surface area of the glass particle fraction < 45 µm was determined using nitrogen gas sorption in a NOVA 4000e system (Quantachrome GmbH & Co. KG, Odelzhausen, Germany). Before the physisorption of nitrogen, the sample was outgassed at 150°C for 12 h over night. The adsorbed nitrogen volume was determined by differential pressure measurement. The specific surface area was obtained from a multipoint BET by linearization plot in the interval of p/p_0 from 0.05 to 0.20 ($R > 0.9998$; $C >> 0$).

2.2.4 Adsorption Process

250 mg of glass particles were weighed in 2R borosilicate glass vials (n = 3 for each condition). The effective surface area of the powder was calculated by means of the specific surface area. 3.5 ml of protein solution was added to each vial, closed with FluroTec® stoppers and Flip-Off® seals (West Pharmaceutical Services GmbH & Co. KG Eschweiler, Germany). Care was taken that the filling did not wet the stoppers. After incubating the vials at 25°C under slow horizontal movement (25 rpm) for 24 h, the whole volume was transferred to a 5 ml polypropylene (PP) cryogenic tube with screw caps (Brandt GmbH & Co. KG, Wertheim, Germany), using disposable glass pipettes. Particles were centrifuged for 5 min in a Labofuge M at 6000 rpm (Heraeus Sepatech GmbH, Osterode, Germany). The supernatant was removed and 4.0 ml of correlating blank buffer was added. The particles were re-suspended by short-term mixing in a laboratory vortex mixer and centrifuged again. This procedure was repeated 3 times. The particle fraction was either analyzed directly as viscous suspension or the adsorbed protein fraction was desorbed by re-suspending the particles in buffer pH 9.5 for 1 h, removing the glass particles and readjusting the pH to pH 7.2. The protein content of each solution was determined via UV absorption and the concentration adjusted to a uniform value according to each analytical method by dilution. For subsequent ATR-FTIR measurements, the concentration was increased by centrifugation in 30,000 MWCO PES Vivaspin® 500 centrifugal filter units (Sartorius-Stedim Biotech, Goettingen, Germany). An adsorption of IgG1 to the membrane as well as the arising structural alteration caused by binding was neglected because of the short time the protein was in contact with the membrane. An evaluation of protein binding to membrane filter material made of diverse basic raw materials was performed previously (data not shown).

For AFM measurements, glass vial bottom pieces were immersed in 10 ml of a 2 mg/ml protein solution at 25°C for 24 h in 50 ml round bottom tubes (GreinerBio-One GmbH, Frickenhausen, Germany). Care was taken that the inner surface of the bottom pieces was not in contact with the container walls. After the incubation step, the glass bottoms were immersed in 40 ml correlating blank buffer. Altogether, four rinsing steps in a fresh buff-

er, each lasting about 1 min, were accomplished. For investigation of the native protein films, the glass pieces were kept under buffer medium and transferred into the AFM liquid cell. For the analysis of dry protein films, the glass samples were successively dipped very quickly into ultrapure water and dried in a gentle nitrogen flow. Thus, crystallization of salts on the glass surface was avoided.

2.2.5 UV Spectroscopy

UV spectroscopy for protein concentration measurements was performed in a temperature controlled Agilent 8453 UV/VIS spectrophotometer (Agilent Technologies GmbH, Boeblingen, Germany) at $\lambda = 280$ nm / 25°C, using quartz cuvettes and applying an extinction coefficient of 1.40 cm^2/mg for antibodies [25]. For extinction values below 0.1, a calibration curve was used to determine the protein content.

2.2.6 Size Exclusion High Performance Liquid Chromatography (SE-HPLC)

Protein stability was investigated with SE-HPLC on an Agilent 1100 device with UV detection at 280 nm (Agilent Technologies GmbH, Boeblingen, Germany). A Tosoh TSKgel G3000SWXL column combined with a TSKgel SWXL guardcolumn (Tosoh Bioscience GmbH, Stuttgart, Germany) was used with running buffer composed of 10 mM phosphate buffer, 145 mM NaCl pH 7.2 at 0.5 ml/min. All samples were filtrated through a 0.2 µm PES membrane filter (Pall GmbH, Dreieich, Germany). The injection volumes

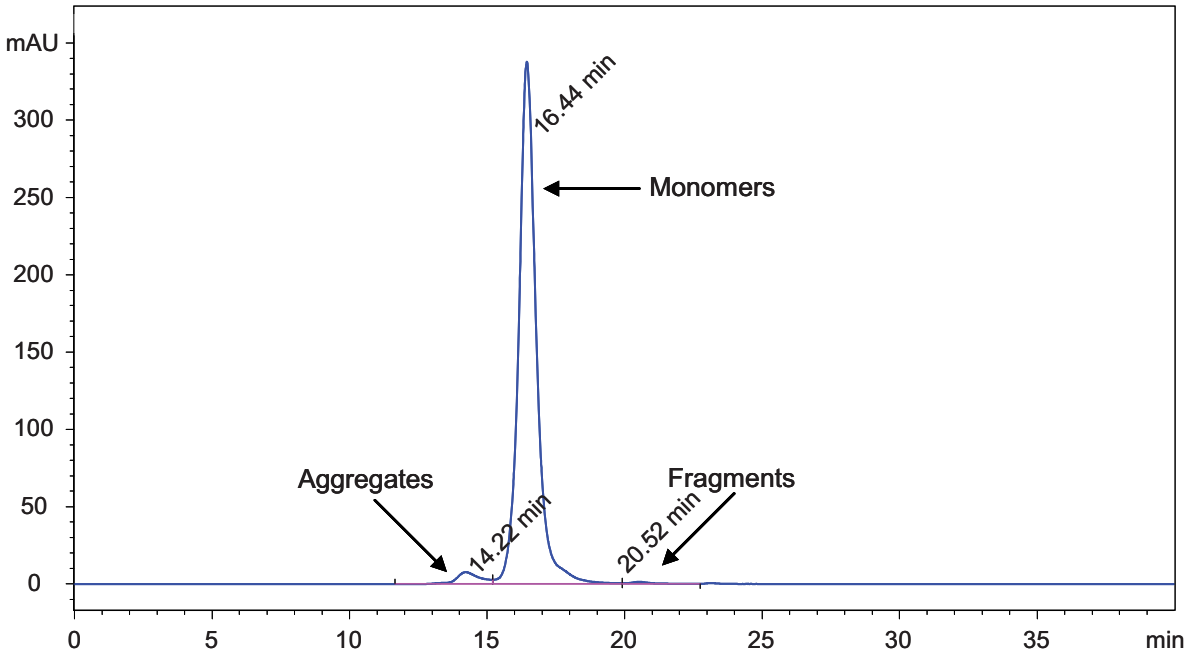

Figure 1: Exemplary SE-HPLC chromatogram of IgG1 with integration procedure.

were 25 µl for 2 mg/ml and 50 µl for 1 mg/ml samples. All chromatograms were integrated manually, using the Agilent ChemStation software Rev. B 02.01. A typical chromatogram is shown in Figure 1.

2.2.7 Fluorescence Spectroscopy

Fluorescence spectra of protein and surface samples were recorded with a Varian Cary Eclipse fluorescence spectrophotometer (Varian Deutschland GmbH, Darmstadt, Germany). For wet solid powder measurements, a front surface sample holder with a powder cell was used. Liquid samples were measured in standard 10 x 10 mm fluorescence quartz cuvettes at 25°C. Intrinsic fluorescence spectra at an excitation wavelength of 280 nm, both excitation and emission bandwidth of 5 nm, were recorded from 270 - 500 nm to cover the region of the Rayleigh scattering as an indicator of potential sample turbidity [26]. For extrinsic fluorescence analysis, bis-ANS was spiked into each sample (final concentration 5 µM). Samples were excited at 385 nm, and emission was recorded from 395 - 700 nm. The protein concentration for all fluorescence measurements was adjusted to 0.05 mg/ml, according to an absorbance of 0.07 at λ_{ex} to neglect the inner filter effect [26]. For each solution, three independent samples were measured and curves were averaged. Emission spectra were corrected for the Raman scattering of the solvent by subtracting the background signal of the corresponding sample buffer. In Figure 2, two exemplary fluorescence measurements of intrinsic IgG1 fluorescence and extrinsic bis-ANS fluorescence are shown.

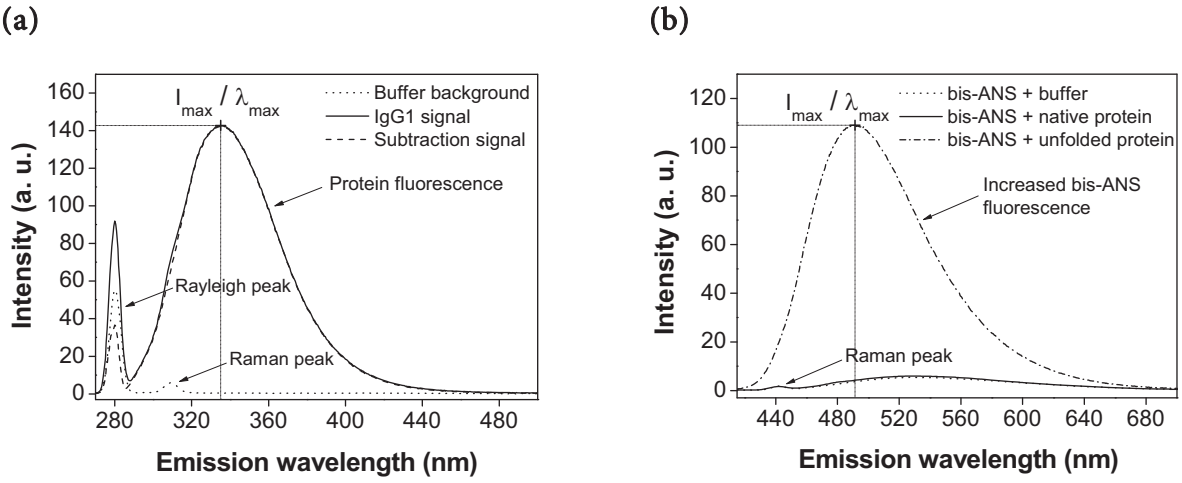

Figure 2: (a) Exemplary buffer background signal and intrinsic protein fluorescence of IgG1 at λ_{ex} = 280 nm. (b) Exemplary bis-ANS buffer background and difference between native and unfolded IgG1 at λ_{ex} = 385 nm.

2.2.8 Fourier Transform Infrared Spectroscopy (FT-IR)

FT-IR measurements were performed on a Tensor 21 spectrometer (Bruker Optics, Ettlingen, Germany), using the Bio-ATR II unit purged with dry nitrogen at 25°C. For each sample, 240 spectra were recorded in the region from 4000 - 850 cm^{-1}. Glass particles were suspended in protein solution of a specific pH value for 24 h, washed 4 times in protein free buffer, suspended in the correlating buffer, and measured after they settled on the ATR crystal. Spectra of blank glass particles were determined in the correlating buffer as well and subtracted to gain protein signal. Liquid protein samples were also measured in the ATR unit and corrected for buffer background. In each case, final spectrum processing included the calculation of the 2nd derivative which included the Savitzky-Golay smoothing algorithm and vector normalization, by using the Bruker OPUS 6.5 software. The protein concentration for adsorption studies, as well as for direct measurements, was 2 mg/ml.

2.2.9 Enzyme-Linked Immunosorbent Assay (ELISA)

For determination of the biological activity of adsorbed h-IgG, a standardized ELISA (IMMUNOtec quantitative human IgG ELISA from ZeptoMetrix Corporation, Buffalo, NY, USA) was conducted. The investigation was comprised of the binding of pH-desorbed h-IgG fractions, which had adsorbed at variable incubation pH on glass particles before, to polyclonal anti-h-IgG antibodies immobilized in the microwells. The captured h-IgG molecules subsequently reacted with a third antibody species against all subclasses of h-IgG, which was moreover coupled with horseradish peroxidase. The activity was quantified by a redox reaction of tetramethylbenzidine and reading the optical density at 450 nm (Figure 3). The working range of the assay was 0 - 125 ng/ml, calibrated with h-IgG. Prior to ELISA, the exact h-IgG concentration of the desorbed protein fractions was determined by UV absorbance, and samples were diluted to a final concentration of both 100 ng/ml and 50 ng/ml by using the assay diluent (PBS buffer containing Triton X-100®).

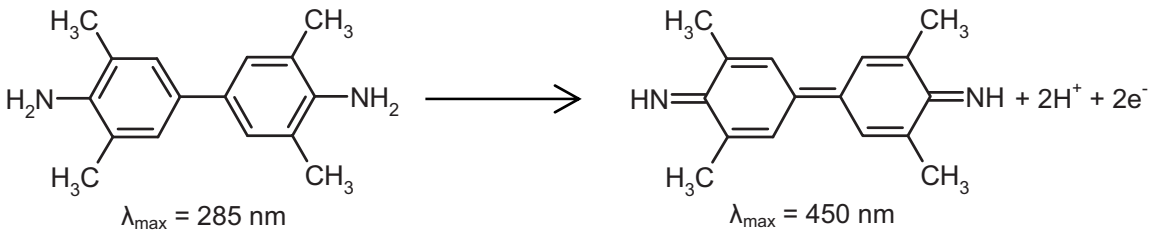

Figure 3: Oxidation of 3,5,3',5'-tetramethylbenzidine as coloring reaction in ELISA (modified from [27]).

Adsorption to test tubes could be a critical step in ELISA sample preparation with regard to the highly diluted protein solutions. Triton X-100® was intended for preserving from adsorptive losses [28]. Each dilution was analyzed in triplicate (n = 2 for the calibration curve). The optical density was read with a FLUOstar Omega microplate reader (BMG LABTECH GmbH, Offenburg, Germany).

2.2.10 Sodium Dodecyl Sulfate Polyacrylamide Gelelectrophoresis (SDS-PAGE)

Non-reducing SDS-PAGE was accomplished by using NuPAGE® Novex 7% Tris-Acetate gels 1.0 mm with NuPAGE® Tris-Acetate SDS running buffer (Invitrogen Ltd., Paisley, United Kingdom), 150 V, 1 h, and intentionally high loading with 5 µg protein. All IgG samples were diluted to a final concentration of 0.25 mg/ml by using NuPAGE® LDS sample buffer (1x) and then heated at 70°C for 10 min. As a marker, 5 µl of HiMark™ pre-stained protein standard (Invitrogen Ltd., Paisley, United Kingdom) were run. Staining was carried out by using Invitrogen's Colloidal Blue Stain.

2.2.11 Atomic Force Microscopy (AFM)

Atomic Force Microscopy was performed on a Digital Instruments Dimension 3100 AFM equipped with a NanoScope V Controller (Veeco Metrology Inc., Santa Barbara, CA, USA). The imaging technique mostly used was the tapping mode. In a few cases, however, the contact mode was used for removing parts of protein from the surface. Dry samples were measured in air at room temperature, using BudgetSensors Tap300Al cantilevers with monolithic silicon probe (Ted Pella Inc., Redding, CA, USA), having a resonant frequency of typically 300 kHz and a tip radius of < 10 nm. Liquid imaging was performed under buffer medium of correlating pH value using a Veeco liquid cell and Veeco DNP-S silicon nitride cantilevers (Veeco Probes, Camarillo, CA, USA) with a spring constant of 0.32 N/m and a tip radius of nominal 10 nm. Scan sizes ranged between 1.0 x 1.0 µm and 10.0 x 10.0 µm.

3 RESULTS AND DISCUSSION

The aim of producing glass particles out of the vial material was to enlarge the effective surface in order to gain an increased amount of adsorbed protein. After desorption, the analysis via chromatographic, spectroscopic, and immunological techniques should be possible. It is indisputable that the newly generated surface of the particles, in spite of pre-washing and heat sterilizing, is not directly comparable to the inner surface of the glass vials, but the greatly enlarged surface should be a very good model for studying IgG adsorption.

3.1 Physical Characterization of Glass Particles

The glass particles received from the milling of borosilicate glass vials were initially characterized physically in terms of shape, size distribution, and specific surface area. Very decisive for further adsorption experiments is the specific surface area of the glass particles, which was determined as $3.53 \pm 0.038\ m^2/g$ by three independent BET sorption measurements. One nitrogen sorption isotherm and the associated BET-plot of one exemplary measurement are shown in Figure 4. The isotherm is a type II isotherm, characteristic of gas adsorption on non-porous solids, whereas first a monolayer, and then, marked by the first inflection point, multiple layers are built up [29]. In the upper range of relative pressure, condensation of liquid nitrogen takes place. Except for a minor hysteresis, the desorption curve depicted in Figure 4a follows the adsorption curve almost exactly. Although the data points in the BET-plot (Figure 4b) are not perfectly fit by a

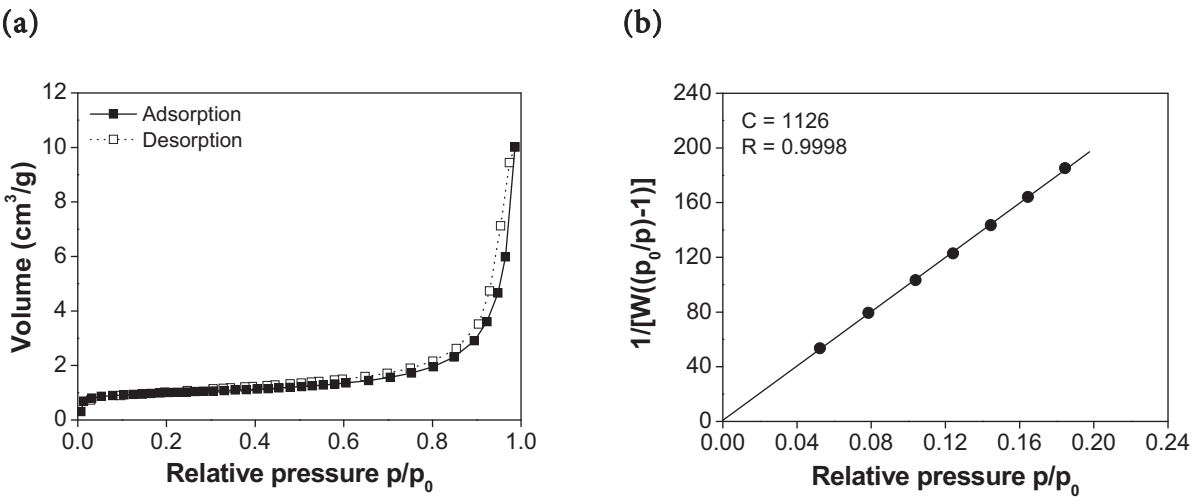

Figure 4: (a) N_2 sorption isotherm of primary glass powder fraction < 45 µm. (b) BET-plot of data points in the linear range of the adsorption curve.

straight line but describe a marginally convex curve, appreciable (micro-) porosity was not expected. The low specific surface area, the positive C-value, and the type of adsorption isotherm argue against it [30]. Most likely, the marginal deviation from BET-theory may be due to the small absolute surface area along with the use of nitrogen as measuring gas. Nevertheless, the value for surface area is realistic, which is shown by calculations based on particle size distribution data (see below).

Only the primary particle fraction (< 45 µm) was measured in BET. Its size distribution was compared with that of a second collective of non-sedimenting glass particles used for electrokinetic measurements (see Chapter 4). The latter fraction was obtained by suspending the primary fraction in water, followed by sedimentation (secondary particle fraction in the supernatant). The size - frequency distributions determined by static light scattering are illustrated in Figure 5. Both graphs offer mono-dispersive distribution characteristics. This was to be expected, as both fractions consist of a homogeneous particle fraction each. The secondary fraction (Figure 5b) shows a slightly narrower distribution as is also indicated by the span value (see Table 1). Being that the size - frequency distribution was measured according to particle volume light scattering measurements, only the volume-based results are presented.

The value of median size d_{50}, i.e. the size for which 50% of the material is finer or coarser, and the geometrical mean value, which is actually only reliable if the distribution is log-normal, are identical as long as logarithm of sizes is normally distributed [31]. The values of median and geometrical mean size are different for the primary fraction, and the deviation from the Gaussian curve becomes apparent in Figure 5a. This may be due to the milling process. The results of the secondary fraction based on sedimentation meet the Gaussian distribution better, which becomes evident when comparing the constants in Table 1.

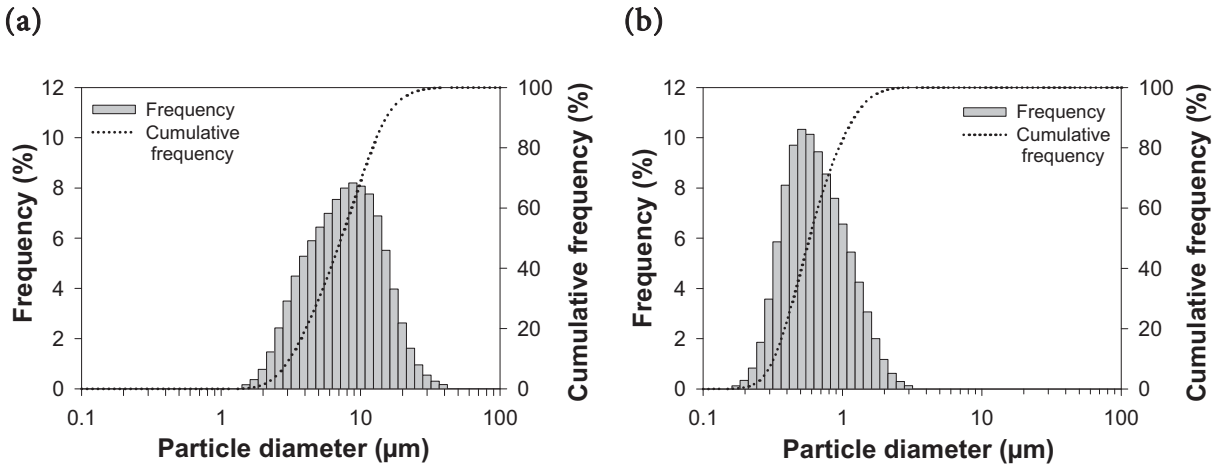

Figure 5: Size - frequency distribution curves of (a) primary particle fraction (< 45 µm) and (b) secondary particle fraction used for electrophoretic mobility measurements, both based on particle volume.

Table 1: Values for primary and secondary particle fractions determined by static light scattering (volume-based).

Particle fraction	Median size d_{50} (µm)	Geom. mean size (µm)	Span $\left(\frac{d_{90}-d_{10}}{d_{50}}\right)$	Specific surface area (m^2/g)[a]
primary	7.27	7.08 (± 1.08)	1.68	0.44
secondary	0.58	0.60 (± 1.06)	1.54	4.82

[a] for calculation a bulk medium density of 2.34 g/cm^3 was used [32]

The specific surface area of the primary particle fraction calculated from light scattering measurements deviates considerably (by a factor of 8) from the gas-sorption data. This is not astonishing, as laser diffraction theory utilizes ideal spherical geometry for calculations. So this is an indication for a certain aberration of the glass particle form from spherical shape. Besides, surface cavities or a certain degree of roughness, which is only considered in gas-sorption experiments, may contribute to the divergence as well. In Table 1, the calculated values for both particle fractions are summarized.

SEM gives a more realistic picture of the particle attributes (Figure 6). In contrast to a short-term milling process, which mainly results in coarser glass grains with an extremely plain fracture surface and straight edges (pictures not shown), the 8 h long-term milling process ends up with more rounded surfaces and a substantial portion of particles with a diameter below 1 µm. In Figure 6a, the tiny particles are seen surrounding the larger ones in the primary particle fraction. The fraction < 1 - 2 µm, generated for electrokinetic measurements, consists of rounded but not-spherical particles (Figure 6b).

(a) (b)

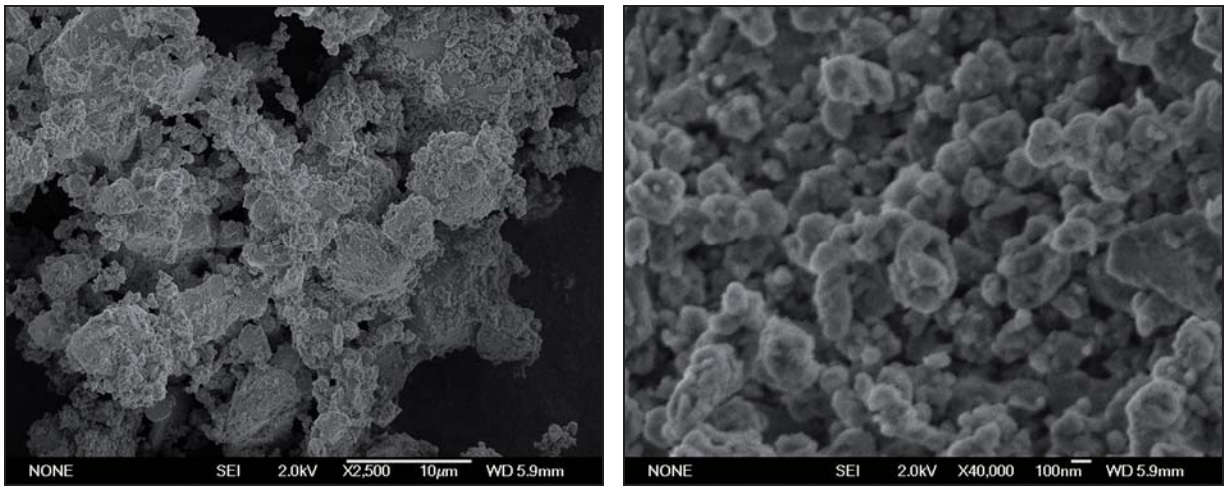

Figure 6: SEM micrographs of (a) primary glass particle fraction (< 45 µm) used for adsorption experiments and (b) second fraction used for electrophoretic mobility measurements.

Thus, compared to the inside of the vial, a large specific surface area for a sufficiently high amount of adsorbed protein was achieved, and as a result, the powdered material was suitable for subsequent protein adsorption experiments. For the following adsorption experiments, exclusively the primary particle fraction (< 45 µm) was used. Calculations of the specific surface area in this regard were exclusively based on the value derived from nitrogen BET measurements.

3.2 Adsorption Studies of IgG1 on Glass Particles – Differences between Vial and Particle Surface

Since a new substrate for adsorption studies with a high surface area was available, the concentration depletion method could be applied, associated with the opportunity of another control for the well-established SDS desorption assay (Chapter 2). Moreover, differences in the protein binding properties on the vial inner surface and the surface of the particles could be evaluated. In the new adsorption assay, the initial weight of particles was about 125 mg (weighed exactly), corresponding to a whole surface area of 0.44 m^2 glass surface. Taking the expected amount of adsorbed protein into account, the initial protein concentration was intentionally set higher so that an equilibrium concentration in the supernatant solution of approx. 2 mg/ml would result after the adsorption step. Figure 7 shows the results for pH-dependent adsorption, obtained from IgG1 adsorbed on the increased glass powder surface and measured by depletion in HPLC against a reference calibration curve. Because of the time dependent variability in the protein structure at the pH extremes, along with an uncertainty in accurate determination of the pro-

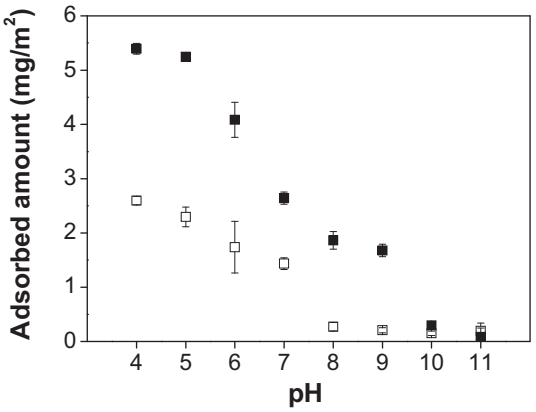

Figure 7: pH-dependent IgG1 adsorption on glass powder determined by solution depletion (□) and pH dependent adsorption of IgG1 in glass vials determined with the SDS desorption assay (■) after 24 h of adsorption in either instance.

tein by SE-HPLC (see section 3.3.1), only pH values from 4 to 11 were evaluated. Lower IgG1 adsorption values on glass powder, as analyzed by the depletion method compared to the vial desorption results, become obvious. Several reasons are possible. As already mentioned, the chemical compositions of the particle and the vial surface are different. For particles originating from vial milling, a surface composition similar to that of the glass bulk can be expected. It is well known that the glass vial surface is greatly influenced by the forming process and therefore differs from the bulk composition [33]. Also, differences in the surface free energy of both the vial and the particle surface are likely. The surface free energy has shown to dramatically affect the adsorbed mass of IgG1 (Chapter 3). To minimize this effect, the vial pretreatment procedure was equally applied to the borosilicate particle fraction prior to the adsorption experiments. It may also be speculated that particles contact each other in the loose sediment, leading to surface regions onto which protein adsorption is hindered. During the 24 h adsorption period, the particles were re-suspended only a few times, since a permanent agitation might have promoted protein denaturation and aggregation [34]. Furthermore, the curved surface geometry of the particles, which is more pronounced the smaller the particles are, has shown to lead to different adsorption conditions [35]. However, in our case, this effect was not considered to be critical for the particle size range investigated. Another reason for decreased adsorbed amounts on the particle surface could be an increased degree of roughness compared to the vial inner surface. For example, it has been shown that the adsorbed amount of albumin on titanium alloys was lower on surfaces with a higher roughness [36]. In this regard, a dependency on the surface free energy is discussed. According to Wenzel's law, the advancing contact angle of a high energetic surface decreases with increasing surface roughness [37]. From the results shown in Chapter 3, this entails a decreased adsorption tendency of IgG1 on the roughened glass surface. Finally, the surface area determined by gas-sorption BET might have been overestimated compared to that accessible by the IgG molecules. However, despite differences in the absolute amount of bound protein, especially in the lower pH range, the trend of pH-dependent adsorption is comparable for both vial and ground glass vial particles, with maximum adsorption at pH 4.0 - 5.0. Thus, the validity of the SDS desorption assay is once again verified.

It was previously mentioned that the structural properties of adsorbed IgG1 were also planned to be investigated after desorption from the surface. Therefore, a thorough evaluation of the adsorption reversibility of IgG1 on glass surface is essential for the subsequent structural studies. According to the common opinion in literature, no or hardly any adsorbed protein can be removed purely by dilution [38,39]. However, it could be shown that the adsorption of protein is reversible when the solution composition is changed in terms of pH or ionic strength [40]. In Figure 8, the result of our own reversibility investigations are depicted.

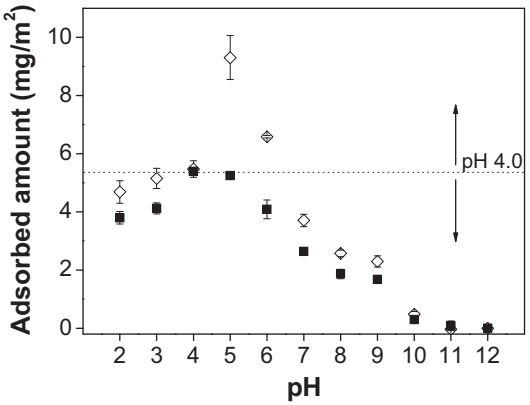

Figure 8: Adsorbed amount of IgG1 in glass vials after 24 h adsorption at pH 4.0, followed by an additional 24 h adsorption step with a solution of the indicated pH value (◇); the dotted line indicates the 24 h pH 4.0 adsorption value; overlaid are the surface concentrations of IgG1 after an exclusive 24 h pH-dependent adsorption in glass vials (■) (see also Chapter 4); in all cases, adsorption quantification was performed by means of the SDS desorption assay.

The adsorption value of pH 4.0 after 48 h coincides with the 24 h value as expected, which confirms the presence of an equilibrium state after 24 h. In the majority of cases however, lower IgG1 surface concentrations than the pH 4.0 reference value can be observed. Thus, it is proven that IgG1 adsorption on glass is widely reversible upon pH shifts. But in most cases, a complete reversibility could not be observed since "default values" were not precisely reached. An increase in adsorption caused by a pH shift from 4 to 5 or 6, respectively, was not expected at all. So far, no plausible explanation could be found for this phenomenon. However, it could be shown that a considerable amount of previously adsorbed protein could be re-dissolved by appropriate pH shifts.

3.3 IgG Stability and Structural Studies

3.3.1 Stability Studies on IgG1

In previous studies, it could be shown that adsorption of IgG1 on the surface of glass containers depends on formulation pH. A timeframe of 24 h was also found to be sufficient for the development of a protein layer in equilibrium state. Further investigations dealt with the question of whether the protein is stable, both during the 24 h adsorption timeframe and in solutions with altered pH, as protein adsorption may be altered or even triggered by instabilities.

3.3.1.1 SDS-PAGE

A first study was carried out by using SDS-PAGE for gaining information on the potential fragmentation and, to a lesser extent, on protein aggregation. Figure 9 shows the SDS-PAGE gels directly after the adjustment of a particular pH value and after 24 h at standard incubation conditions. Directly after pH adjustment (Figure 9a), the same pattern for IgG1 can be seen for all pH values, except for pH 12. Typically, one main band is visible which equals the protein monomer including all isoforms (approx. 152 kDa), directly followed by two minor bands of a marginally less molecular weight. Two further fragments of approx. 110 kDa and 70 kDa can be identified in SDS-PAGE. The short time from pH adjustment to pH 12 and gel filling is enough for an extensive hydrolysis and/or aggregation, but preferential bands are still distinguishable. Figure 9b reflects the situation after 24 h. Here, only the most critical pH values were analyzed. The hydrolysis in the pH 12 sample has advanced to a point to which no more discrete bands are distinguishable. Except for a slight increase in fragmentation for the pH 11 sample, again no significant changes compared to the reference standard are observable.

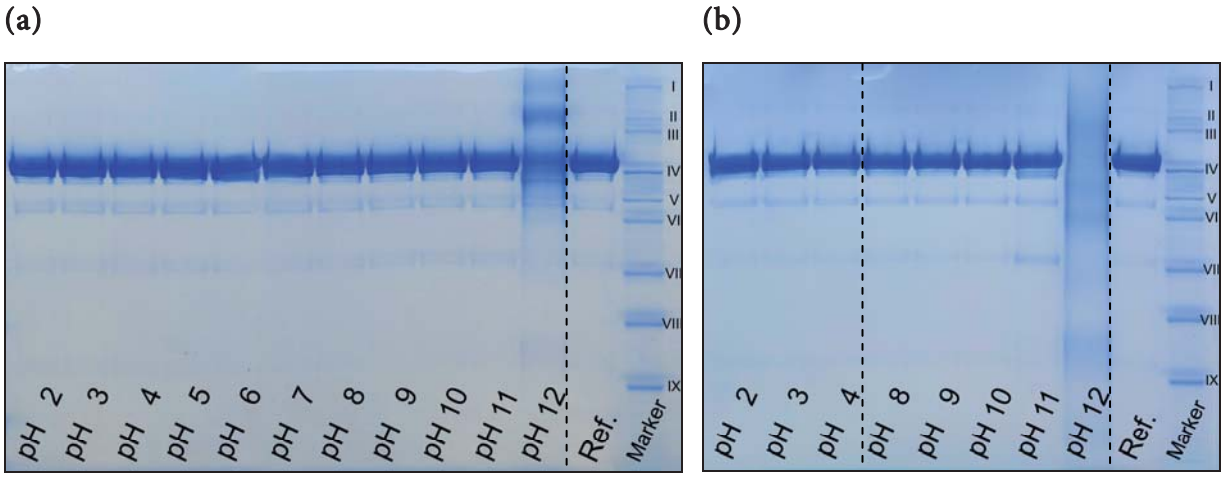

Figure 9: SDS-PAGE of IgG1 (a) directly after adjustment of the pH and (b) selected samples after 24 h storage under adsorption conditions. Molecular weight of the marker proteins: I: 500 kDa; II: 290 kDa; III: 240 kDa; IV: 160 kDa; V: 116 kDa; VI: 97 kDa; VII: 66 kDa; VIII: 55 kDa; IX: 40 kDa.

3.3.1.2 SE-HPLC

It could be shown that the extrema of the pH values are critical in terms of protein stability and they would be worth looking at in more detail. Consequently, time-dependent SE-HPLC analyses of critical samples were conducted for a detailed investigation of protein

behavior during incubation. Five chromatograms for every pH value at consecutive points in time from 0 - 32 h were gained and overlaid. A summary of the results is given in Figure 10. At pH 4.0 (Figure 10a) as well as at pH 10.0 (Figure 10d), the chromatogram of the native IgG1 monomer peak does not alter over time, indicating stability under these conditions. Figures 10b and 10c exhibit the effect of a higher proton concentration in the solution at pH 3.0 and pH 2.0, leading to a decrease of monomer, an increase of aggregated species, and the appearance of a minor fragmentation peak at pH 2.0. The fact that no aggregates are observable in SDS-PAGE suggests the formation of non-covalent aggregates. At pH 11.0 (Figure 10e), a small but steady increase in both aggregates and fragments can be observed, along with a decrease of monomers. Corresponding to the SDS-PAGE results, massive aggregation and degradation occurred at pH 12.0 (Figure 10f). Hence, an overlap of adsorption phenomena and structural alterations has to be considered at extreme pH values. In addition, the stability of IgG1 depending on the ionic strength was studied from 23 mM (solely 10 mM phosphate buffer) to 1 M by the addition of NaCl at pH 7.2. Neither an increased aggregation tendency nor an indication of fragmentation could be observed within the timeframe of 32 h (data not shown).

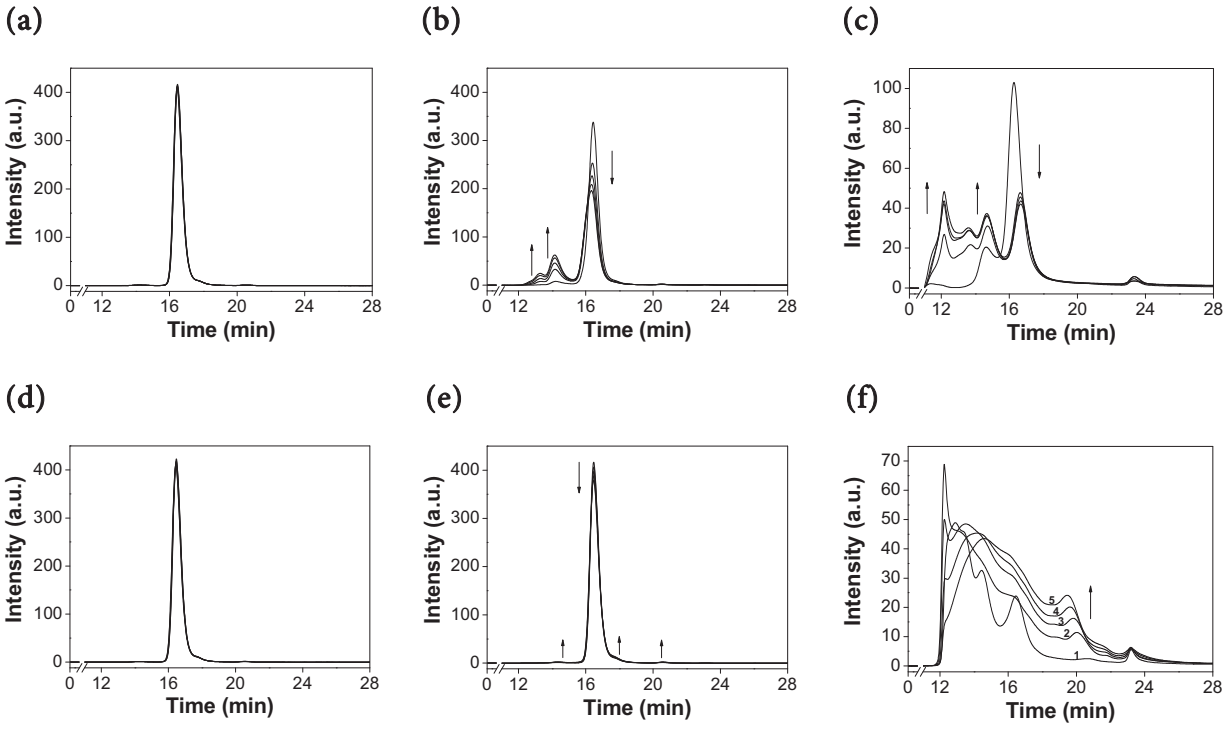

Figure 10: SE-HPLC chromatograms of IgG1 at 25°C: (a) pH 4.0; (b) pH 3.0; (c) pH 2.0; (d) pH 10.0; (e) pH 11.0; (f) pH 12.0. Curves of different time points are overlaid: (1) 0 h; (2) 8 h; (3) 16 h; (4) 24 h; (5) 32 h. Arrows indicate tendencies.

3.3.1.3 Intrinsic and Extrinsic Steady State Fluorescence

Fluorescence spectroscopy is a common and useful technique for monitoring conformal transitions of proteins [41]. Structural alterations of proteins as well as aggregation can be analyzed sensitively by observing intrinsic protein fluorescence or by using extrinsic fluorescent dyes [42,43]. Intrinsic protein fluorescence is mainly based upon light emission of tryptophan, which is a very valuable probe. It has the highest quantum yield within the protein fluorophores, is very sensitive to its microenvironment [41], and can be readily excited at the absorbance maximum of the IgG 280 nm [44]. The band of tyrosine, which marginally fluoresces at this wavelength, is usually not visible in presence of tryptophan [26]. The proteins studied contain a high number of tryptophan residues, 24 determined for IgG1 from its amino acid sequence, but no constant quantity for the human pooled IgG. The fluorescence behavior of a protein, characterized by the emission maximum wavelength λ_{max} and by the fluorescence intensity $F_{\lambda ex/\lambda em}$, depends on the environment polarity of the tryptophan residue and varies from 307 nm to 353 nm [45]. As a rule, the more structural alterations take place, the more the environment polarity of the buried tryptophan residues changes due to an increased accessibility to water. Accordingly, rearrangements can be followed by a (red-) shift of λ_{max}.

The virtually non-fluorescent aromatic dyes ANS or bis-ANS become highly fluorescent in nonpolar environments, i.e. when bound to hydrophobic sites in proteins [42,46]. Besides the increase of quantum yield, the emission maximum is blue-shifted to shorter wavelengths. Bis-ANS, which binds to proteins mainly via hydrophobic interactions, was applied to study surface hydrophobicity, unfolding, and aggregation phenomena [47]. In this regard, it was shown that bis-ANS exhibits a higher affinity to several proteins and an increased sensitivity than ANS [46,48].

The effect of pH on fluorescence properties of IgG1 was studied next. In Figure 11, the intrinsic steady state fluorescence spectra of IgG1 at extreme pH values are summarized. The curves in Figure 11a clearly reveal structural alterations occurring at a low pH indicated by a shift of the intensity maximum wavelength, as well as by a steady increase in intensity. Here, unfolding goes along with a common increase of the quantum yield. This means quenching neighbors change their position relative to the fluorescing amino acid residues. In the pH range in which IgG1 is in native state, λ_{max} is constantly at 334.5 - 335 nm. Towards lower pH values, a larger red-shift, beginning from pH 3 to 2, becomes obvious, indicating changes in protein structure. The shift of λ_{max} to 339 nm at pH 2.0 equals the thermally denatured state after heating to 75°C for 5 min (see Figure 13a).

The more alkaline the pH, the lower the fluorescence intensity is, relative to the native reference, whereas the position of the maximum value remains at approx. 335 nm up to pH 11.0 (Figure 11b). However, drastic alkaline conditions of pH 12 lead to extensive

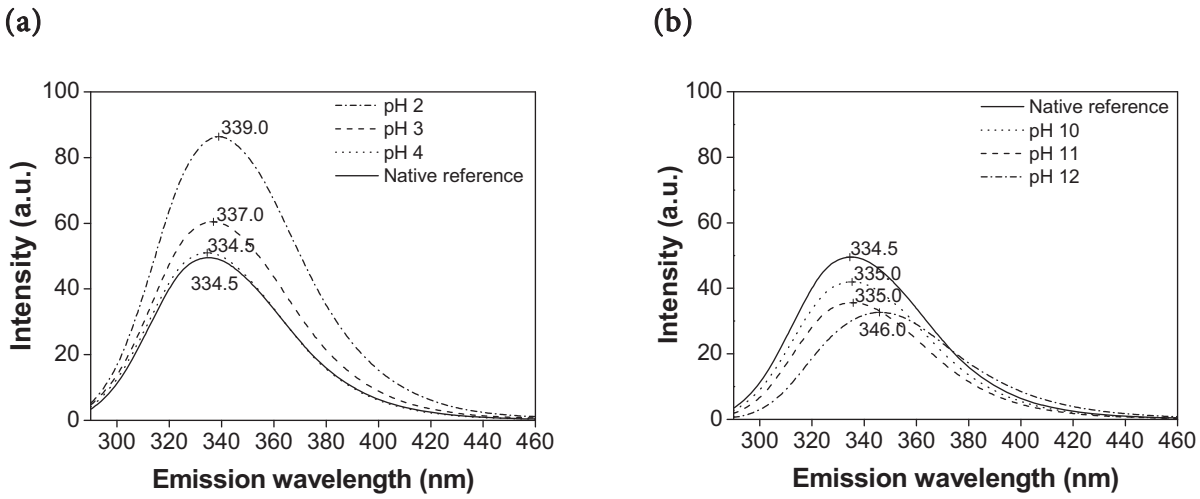

Figure 11: Intrinsic fluorescence spectra of IgG1 at extreme (a) acidic and (b) alkaline pH values compared to the native reference at pH 7.2.

alterations, as shown by SE-HPLC and SDS-PAGE, and are followed by a further decrease in intensity as well as a large red-shift of the wavelength of the emission maximum to 346.0 nm. Consequently, the environment of fluorescent amino acid residues has essentially changed. Longer timeframes at pH 12 finally lead to wavelength shifts up to 352.5 nm and to an increase in fluorescence intensity. According to Ladokhin, this wavelength corresponds to the emission of tryptophan in contact with free water [45]. Thus, complete denaturation up to the point of hydrolysis has occurred.

In Figure 12, the dependency of fluorescence emission maximum wavelength as well as the maximum intensity on pH is shown for the whole range. Thus, fluorescence maximum wavelength of IgG1 was essentially unaffected by pH in the range from pH 4 to 11. With respect to the decrease in fluorescence intensity for increasing pH from 5 to 11 and

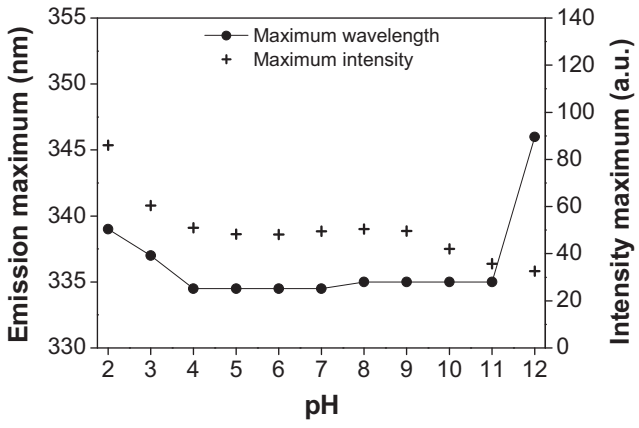

Figure 12: Fluorescence emission maxima and intensity maxima of IgG1 dependent on pH.

the correspondingly decreasing proton concentration, the effect can be related to minor structural alterations of the protein but not to complete unfolding since the emission maximum does not change [49]. The fluorescing behavior is a complex matter, which is dependent on many factors. For example, almost all polar protein residues can account for quenching of tryptophan [45]. In this regard, protonation of neighboring residues to tryptophan can already change their quenching properties, leading to a decrease or increase of the absolute quantum yield.

Fluorescence spectra were also recorded at variable ionic strengths from 23 mM (10 mM phosphate buffer without NaCl) up to 1 M by the addition of NaCl at pH 7.2. Neither the fluorescence intensity nor the wavelength maximum of fluorescence changed, indicating protein stability within the whole range (data not shown).

In further studies, IgG1 was thermally stressed in order to elucidate the response of IgG1 in intrinsic protein and extrinsic bis-ANS fluorescence. Therefore, samples of 0.05 mg/ml IgG1 in pH 7.2 PBS buffer were heat stressed in a water bath at temperatures from 55°C to 75°C for 5 min and analyzed directly or in presence of 5 µM bis-ANS. Heat treatment for 5 min at 75°C was chosen as a standard denaturation treatment for future testing, since a high degree of denaturation was achieved. Flocculation of the protein molecules set in at temperatures around 80°C. As can be observed in Figure 13a, fluorescence intensity increases steadily with an increasing temperature. A shift of the emission maximum wavelength from 334.5 to 339 takes place, indicating a degree of aggregation/denaturation comparable to the situation at pH 2. The increase in intensity can be observed in extrinsic bis-ANS fluorescence as well (Figure 13b). The yield in intensity is higher than for intrinsic fluorescence, which indicates a higher sensitivity.

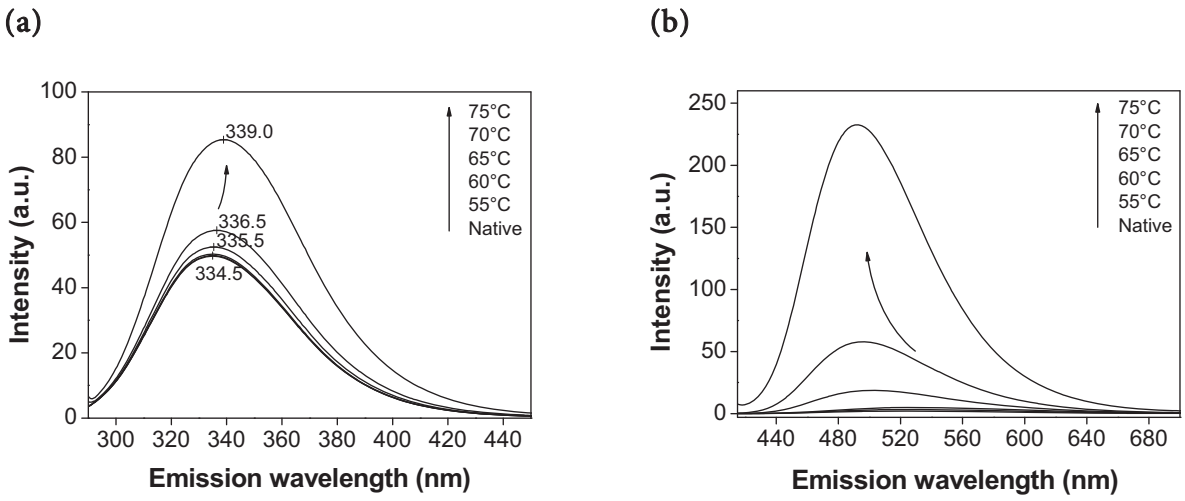

Figure 13: (a) Intrinsic protein and (b) extrinsic bis-ANS fluorescence of heat treated IgG1, 5 min at different temperatures.

Thermal denaturation of IgG1 has previously been investigated using DSC, where irreversible denaturation/aggregation was observed [50,51]. Despite a multi-domain character, a single endothermic transition was observed around 74°C due to the increased rigidity of IgG1 compared to others subtypes [52]. Regarding the mechanistic processes upon heat stress, in general, the aggregation of IgG is forwarded after hydrophobic patches of the molecules are exposed to the surface by denaturation [52].

3.3.1.4 FT-IR

Most of the previous investigations on IgG1 stability and on the response of IgG1 on heat stress were limited to information concerning the tertiary protein structure as well as the interaction of molecules (aggregation). FT-IR spectroscopy is an important tool to analyze the secondary structure of a protein. In this regard, the amide I band between 1700 and 1600 cm^{-1}, which is predominantly due to the C = O stretching vibration of the protein backbone, is of particular importance. FT-IR spectroscopy has shown to be sensitive to the conformation of the protein and is mostly applied in order to receive information on the secondary structure of proteins [4]. In Table 2, the contents of structural elements of native IgG in terms of the amide I band are listed, taken from literature [53].

In the native reference spectrum of IgG1 (Figure 14a/b), important peaks were found at 1638 cm^{-1} and 1688 cm^{-1}. Hence, according to Table 2, these peaks are assigned to β-sheet structures, and positions agree well with those reported for IgG molecules [54]. The minor peak at 1614 cm^{-1} may account for β-sheet structure, but is also described for absorption by side chains of tyrosine and arginine, which is of minor importance for structural interpretations [1]. Other minor bands at 1675 cm^{-1} and 1664 cm^{-1} are related to turns [50]. The content of structural components of the IgG1 was determined from X-ray crystallography data provided by Merck Serono, using the DSSP program described by Kabsch and Sander [55]. The composition was 39% β-sheets, 7% helical structures, 20%

Table 2: Band assignments of the amide I region for FT-IR.

Secondary structure elements	Average (cm^{-1})	Range (cm^{-1})
β-Sheet	~ 1617	1615 – 1620
	~ 1639	1628 – 1645
	~ 1690	1686 – 1697
Non ordered structures	~ 1645	1640 – 1650
α-Helical	~ 1652	1650 – 1658
Turns	~ 1670	1660 – 1667
		1676 – 1680

turns/bends, and 34% loops/irregular elements, whereas a dominance of β-sheets present in native IgG is well known [51]. Although theoretically existent, no FT-IR band indicating α-helical fractions is obvious in the area of 1650 - 1658 cm^{-1}. However, the general information derived from the second derivative spectrum is consistent with the theoretical values from X-ray data and also from other previous FT-IR or CD measurements on IgG1 [50] or other antibodies [53,54].

In the following, the impact of both stressing procedures, i.e. shifting of formulation pH and heating, on the secondary structure of IgG1 was studied, using ATR-FTIR spectroscopy. The results are given in Figures 14 and 15. All spectra recorded at acidic pH values (Figure 14a) exhibit the characteristic band at 1688 cm^{-1}, assigning for β-sheet elements, and a peak or shoulder in the area of 1615 cm^{-1} due to β-sheet or side chain effects [50]. The spectrum at pH 4.0 resembles the profile of the native reference (pH 7.2), whereas with further acidification, the bands of turns at 1675 cm^{-1} are reduced at the expense of a new turn band arising at 1666 cm^{-1}. At pH 2.0, the main band assigning β-sheet at 1638 cm^{-1} is shifted to smaller wave numbers, indicating more pronounced structural alterations. Similar results are obtained at high formulation pH with a small red-shift beginning at pH 10 and increasing up to pH 12 (Figure 14b). At pH 12, a shoulder arises at 1646 cm^{-1}, indicating the formation of unordered elements [56]. At both high and especially low pH, the shift of the main band towards 1625 cm^{-1} is indicative of the formation of intermolecular β-sheet elements [56] and therefore, aggregation. This substantiates the findings of SE-HPLC. However, readjusting the pH of the solutions to 7.2 after 24 h showed full reversibility of any alterations obvious in the spectra, except for the pH extremes 2 and 12 (data not shown). This in turn indicates a reversibility of these structural changes upon pH shifts.

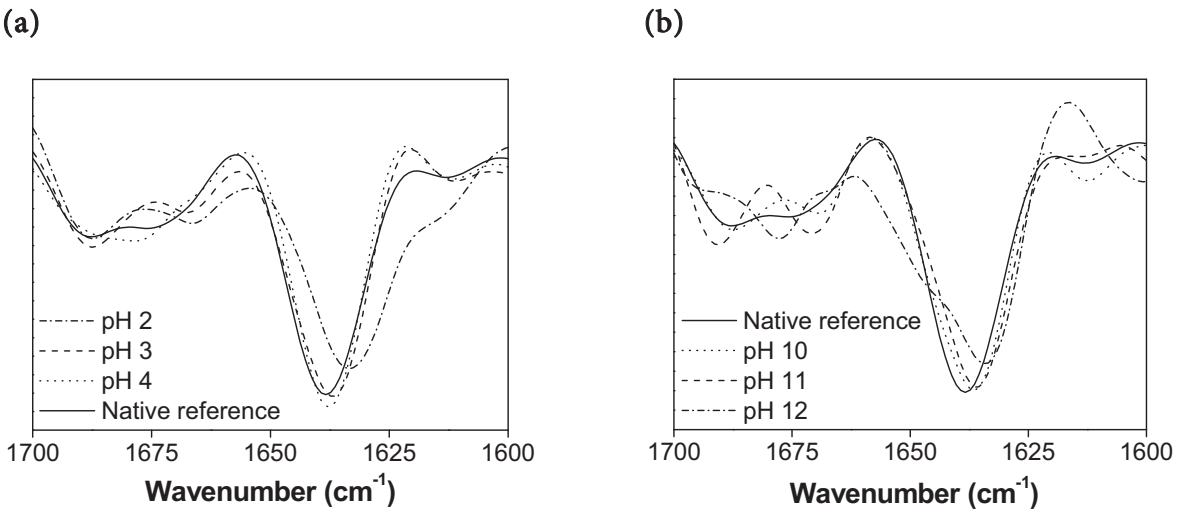

Figure 14: ATR-FTIR second derivative spectra of 2 mg/ml IgG1 bulk protein at (a) acidic and (b) basic pH values.

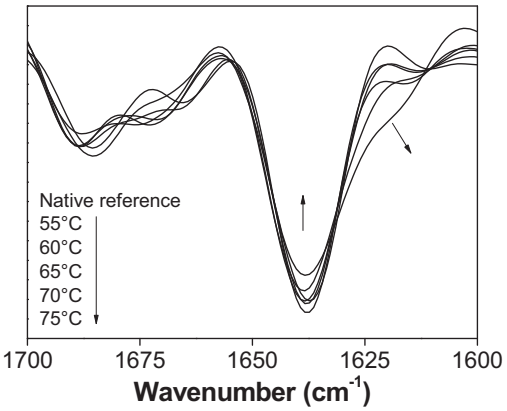

Figure 15: ATR-FTIR second derivative spectra of 2 mg/ml IgG1 bulk protein after heating the pH 7.2 solution for 5 min at the stated temperature.

The temperature treatment of IgG1 (Figure 15) only revealed small changes in the secondary structure. The intensity of the most characteristic band at 1638 cm^{-1} decreased for the benefit of a new band arising at approx. 1625 cm^{-1}, which has already been shown by Matheus *et al.* [50]. As mentioned above, this is indicative of distinct aggregation. Furthermore, all spectra exhibit more or less characteristic bands at 1687 - 1685 cm^{-1} due to β-sheet elements and different bands at 1673 cm^{-1} and 1665 cm^{-1}, both reflecting turn structures, which is, however, less significant regarding structural changes. Since all FT-IR measurements were performed at 25°C, they indicate the state of irreversible structural changes of IgG1 after heat treatment. The thermal and the pH stability of IgG were investigated by Vermeer and Norde in detail using isothermal calorimetry and CD spectroscopy [52]. They described the heat denaturation of IgG at moderate pH as a three-step process, where the final aggregation step accounts for irreversibility. In contrast to their findings, the decrease in β-sheet content was not associated with an increase in α-helical elements in our case (FT-IR band at 1652 cm^{-1}). Their investigations on the IgG secondary structure upon a decrease of pH to 3.5 revealed structural changes as well.

In conclusion, extremely low pH values (pH 2 - 3) lead to an aggregation of IgG1, whereas the secondary structure is much less affected. Under such acidic conditions, an intermediate structure referred to as "molten globule state" was described, showing a high degree of secondary structure, increased hydrophobicity, a native-like maximum wavelength of fluorescence emission, and a tendency toward slow aggregation [43]. Most of those observations could be made for IgG1 as well. At extremely high pH values (pH 11 - 12), an extensive degradation sets in, marked by extreme fragmentation and aggregation. Accordingly, these alterations in structure and especially the increased propensity to aggregation have to be considered when protein adsorption is investigated at extreme pH values. A serious influence on the adsorption of proteins seems probable.

3.3.2 Structural Investigations of IgG1 Directly on the Surface of Glass Particles

In general, investigation of the structural behavior of proteins in the adsorbed state directly on surfaces stands to reason and has often been described in literature. Therefore, protein adsorbed on e.g. flat surface [57] or (nano-) particulates [5,58] was investigated, and studies were performed in dry or semidry state [9]. The ground glass particles exhibit good model material and were used to evaluate protein structure in adsorbed state. The outcome of the previous studies indicated that IgG1 adsorption at pH values above 10 or below 4 is not meaningful, as substantial protein damage occurs. Therefore, the following studies were confined to the three established incubation pH values 4.0, 7.2, and 8.6, which are the pH of maximum adsorption at moderate ionic strengths, the typical formulation pH, and the isoelectric point of the IgG1.

3.3.2.1 Secondary Structure (FT-IR)

The secondary structure of IgG1 molecules after adsorption on glass particle surface from three different formulations (pH 4.0, 7.2 and 8.6) was characterized by ATR-FTIR spectroscopy. Spectra were compared to the correlating (native) protein structure by analyzing the 2nd derivative in the region from 1700 - 1600 cm^{-1}, as shown in Figure 16. All three samples of IgG1, adsorbed at pH 4.0, 7.2, and 8.6, exhibit the characteristic β-sheet band at 1638 cm^{-1} as a predominant secondary structure element, corresponding to the reference protein solutions. This meets the findings of Giacomelli *et al.* [4]. In addition, all reference spectra exhibit a β-sheet band in the area between 1690 - 1687 cm^{-1} and 1616 - 1613 cm^{-1}, respectively, as well as turn structures indicated by bands at 1675 - 1670 cm^{-1}. Besides these usual bands designating β-sheet structures and turns, an additional band at 1658 cm^{-1} indicates the arising of helical structures in IgG1 adsorbed on glass at pH 4.0. At the physiologic pH 7.2, the spectrum of adsorbed protein reveals unordered structures by a band at 1664 cm^{-1} as a striking property. At the IEP, again helical structures emerge but also a band at 1623 cm^{-1} arises, indicating intermolecular β-sheets. Hence, increasing aggregation can be inferred.

The occurrence of an increased aggregate content at pH 8.6 is consistent with the finding for desorbed protein, studied via SE-HPLC (see 3.3.3.2). An often-described conformational state upon adsorption, the molten globule state, is characterized by a tendency of forming aggregates [43]. Hence, this propensity to aggregate, which so far could only be shown for pH 8.6 (IEP) by FT-IR spectroscopy, may be an indication of the formation of a molten globule upon adsorption on the glass surface. By contrast, at low pH (4.0) it is rather the formation of helical structural elements that is most striking. As neither dramatic pH shift nor heat treatment cause any of the structural alterations measured after

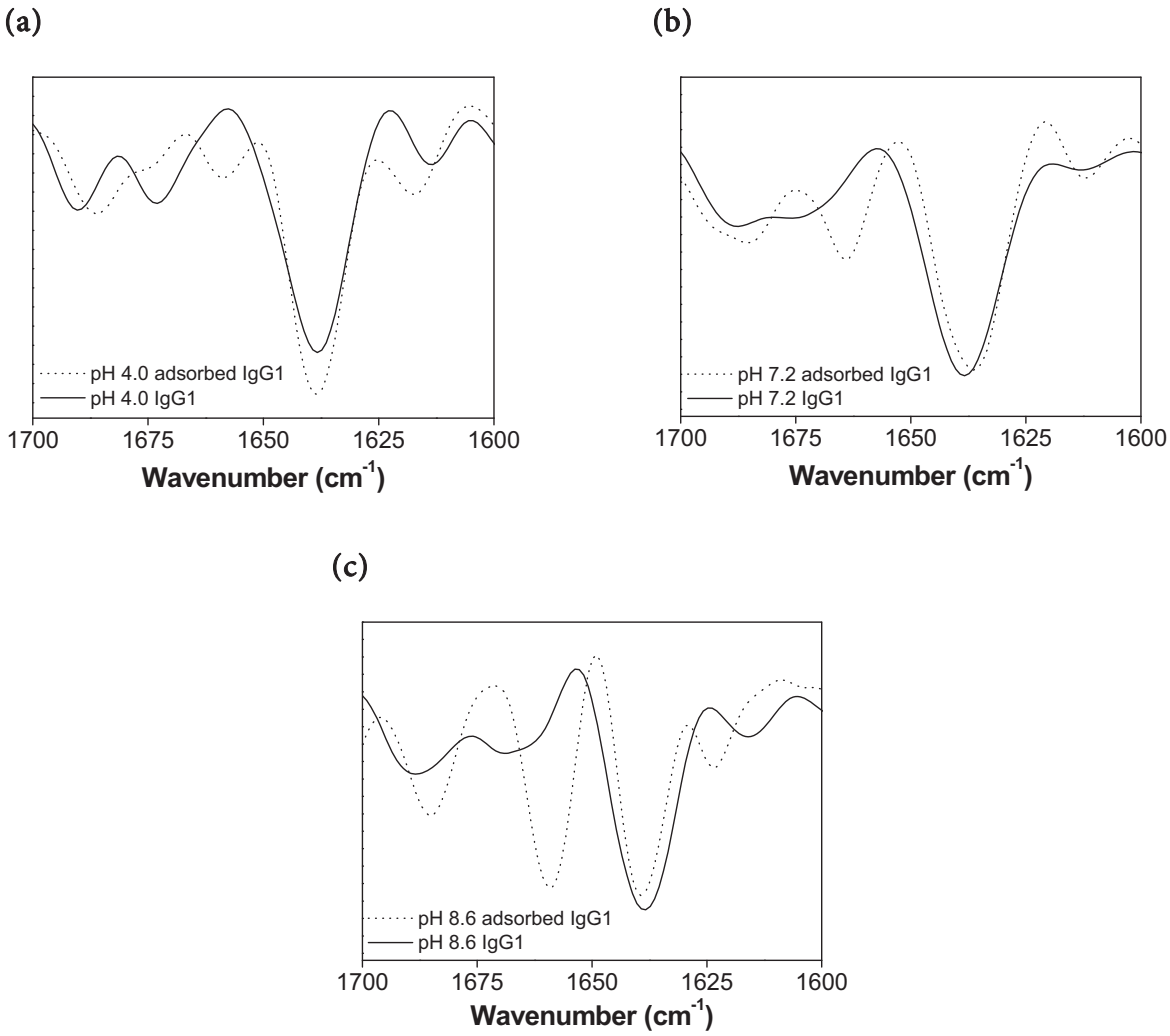

Figure 16: FT-IR second derivative spectra of protein molecules adsorbed on glass particles at (a) pH 4.0, (b) pH 7.2 and (c) pH 8.6, 2 mg/ml IgG1, 24h.

adsorption, the results require further substantiation. By applying ATR-FTIR spectroscopy, Giacomelli *et al.* for example, found a similarity between the secondary structures of free and adsorbed IgG and, if any, only a low content of α-helix [4]. Upon adsorption, the formation of α-helical fractions was also described by Vermeer for IgG on quartz [53]. The extent depended on the surface properties, more pronounced for hydrophobic, but also appreciable for hydrophilic silica [1,53]. The adsorption of IgG1 on hydrophobic Teflon® caused substantial changes in the secondary structure, explicitly a decrease of β-sheets in favor of an increase in α-helix as well as the formation of unordered structures [51]. For IgG but also for other proteins, hydrophobic surfaces usually lead to increased structural alterations compared to hydrophilic surfaces [59]. Concerning the pH of the protein solution, generally more severe effects on the secondary structures are observed when both protein and surface wear the same charge [59,60]. This means that for the

situation of IgG on borosilicate glass, the critical region is from the protein IEP upwards and below the point of zero charge (PZC) of the borosilicate glass surface (pH 2 - 3). However, these areas were not investigated in our case.

Also, difficulties with respect to FT-IR measurements of IgG1 in adsorbed state have to be discussed. The pH of the protein solution greatly influences the adsorbed amount of protein, as shown in Chapter 4. The quality of ATR-FTIR spectra, however, highly depends on the protein quantity adsorbed. Thus, the quality of FT-IR spectra varies with pH, which hampers interpretation and makes comparability very difficult. An additional uncertainty for protein spectra remains, since the amide bands of the proteins are obtained by a subtraction of strong absorption bands of the glass material from the entire spectrum. In this regard, Giacomelli *et al.* were not able to interpret their FT-IR spectra of IgG on hydrophobic silica surface due to the large interfering effect of exchanging water molecules [4]. Furthermore, also the weighting of the degree of structural changes from FT-IR spectra may be delicate, as the 2nd derivative does not necessarily preserve relative intensities of absorption bands [61].

3.3.2.2 Tertiary Structure (Intrinsic and Extrinsic Steady State Fluorescence)

In the following, the tertiary structure of IgG1 is investigated by intrinsic as well as extrinsic fluorescence spectroscopy, using bis-ANS as a sensitive probe. The protein was analyzed in adsorbed state on wet glass particles, using a front surface sample holder. The results of front surface fluorescence did not indicate any structural alterations of IgG1 adsorbed on borosilicate glass at pH 7.2 (Figure 17a). The maximum fluorescence wave-

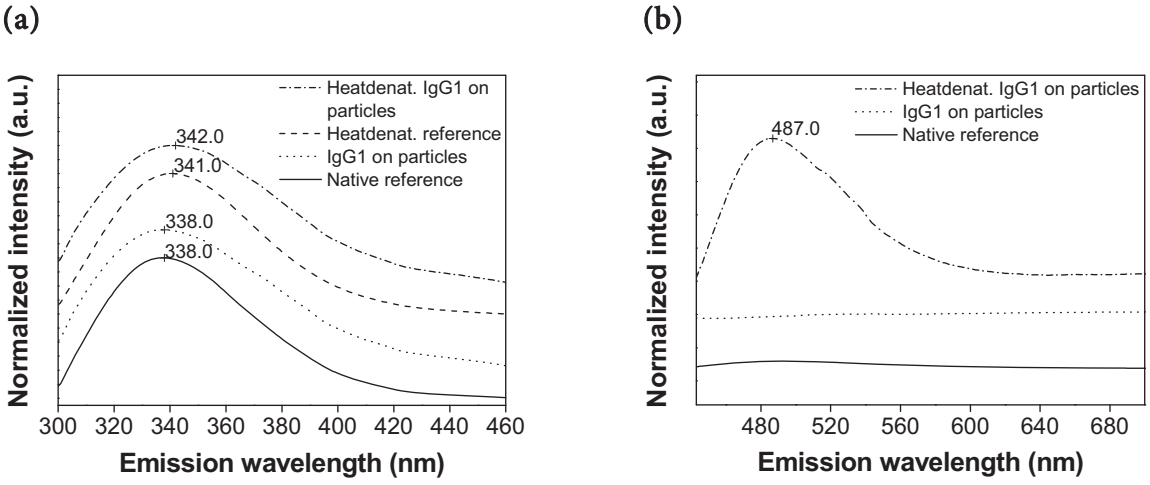

Figure 17: (a) Intrinsic protein fluorescence (b) and extrinsic bis-ANS fluorescence of IgG1 adsorbed on glass particles at pH 7.2, 24 h; particles submerged in (a) sample buffer or (b) sample buffer containing 5 µM bis-ANS.

length of the protein in adsorbed state on the glass was found at 338 nm instead of 335 nm for the free protein in solution (see 3.3.1.3). However, the same maximum could be observed for the native IgG1 investigated in the front face setup as well. So far, no explanation could be found for this evident wavelength shift. In either instance, an additional thermal treatment (75°C for 5 min) caused a red-shift of the maximum by 3 and 4 nm, respectively, indicating that the protein had not been in a severely unfolded or aggregated state before. In Figure 17b, the results of the extrinsic front face fluorescence measurements in the presence of bis-ANS are shown. No indication for structural alterations of adsorbed IgG1 in terms of exposition of hydrophobic protein patches could be observed, since no or only marginal fluorescence was visible for the native reference and the adsorbed protein. As a positive control, further heating of the particles together with the adsorbed protein provided a clear signal. Hence, direct measurements on adsorbed protein have not indicated structural rearrangements for this pH so far.

Front surface measurement of adsorbed protein on particles is a convenient method. In direct comparison, fluorescence spectroscopy of suspended nanoparticles showed the same results as total internal reflection fluorescence spectroscopy (TIRF) on flat silica surfaces, using BSA as model protein [62]. However, in summary, a slight uncertainty exists concerning the results obtained via direct measurements of protein adsorbed on glass. When particles were measured in front face fluorescence setup, an increased light scattering for IgG on suspended particles could be observed, which led to differences in fluorescence intensities [58]. This was also observed in our measurements. Thus, a comparison of only normalized intensities is favorable. In addition, significant background signals caused by scattering or refraction of the incident beam have to be subtracted, and, depending on the signal quality, the error or uncertainty of the information will inevitably increase. For this reason, the desorbed protein fractions from the enlarged surface of the glass particles were investigated in the following in more detail.

3.3.3 Structural Studies on Desorbed IgG1

As mentioned before, various authors examined structural alterations of proteins in adsorbed state by a broad range of appropriate analytical techniques. Alternatively, there is the option of investigating desorbed protein molecules, which were once firmly bound to the surface. For this approach, the irreversibility of protein adsorption to surfaces in terms of dilution is utilized, and the whole formulation including all unbound molecules can be removed by rinsing with corresponding buffer. To exclusively obtain the adsorbed molecules, desorption is not performed with surfactants, as structural alterations could occur, but via a pH shift. Thus, a solution is generated for further analysis, in which formerly adsorbed protein is concentrated. Despite the theoretical potential of refolding or

disintegration of aggregates by this method, more precise and significant statements on the adsorbed protein status should be possible. In return, it allows the estimation of irreversible structural changes persisting after dissociation from the surface. Furthermore, analytical difficulties, such as the analysis of low amounts of protein in adsorbed state on non-ideal surfaces, can be overcome this way and hence, conventional protein analytical methods can be more easily applied. Diverse characterizations of different desorbed protein fractions are presented in the following.

3.3.3.1 SDS-PAGE of Surfactant-Desorbed IgG1

The SDS-desorbed protein from vial pH assay (see Chapter 4) was concentrated and analyzed by SDS-PAGE in a similar way as is described in 3.3.1.1. Again, the result in Figure 18 meets the established pH-dependent adsorption pattern with respect to adsorbed quantity (see Figure 8). But furthermore, in contrast to previous gel electrophoresis, an additional band in the area of approx. 300 kDa became visible, which corresponds to the dimeric form of the IgG1 antibody. The reference sample, which is equivalent to the similarly treated pH 7.2 IgG1 solution, features a very weak dimmer band as well. Aggregation by means of adsorption cannot be excluded, but may also be induced by the desorption step and by the concentration step with increased protein concentrations at the membrane surface. Aggregation in the presence of surfactant points to the formation of covalent aggregates. Hence, interaction with the glass surface or the membrane involves a much stronger impact on IgG1 stability compared to merely pH-adjusted solutions after 24 h (Figure 9b). Below, the structure of adsorbed protein at selected pH values is further investigated after a more gentle desorption step by means of a pH shift.

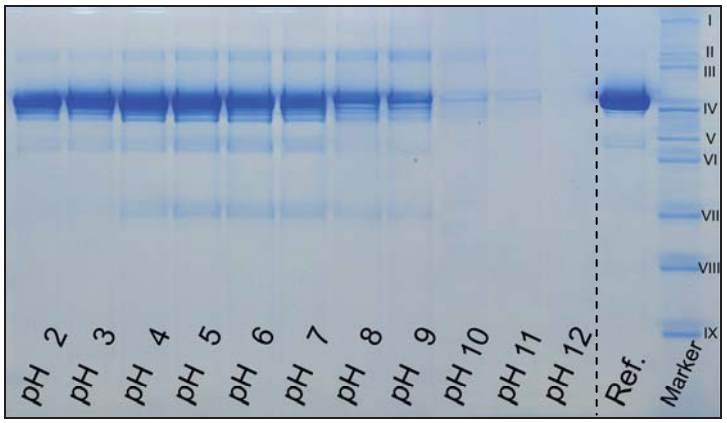

Figure 18: SDS-PAGE of desorbed (SDS buffer) and concentrated (Vivaspin®) IgG1 from pH-dependent vial assay; marker: I: 500 kDa; II: 290 kDa; III: 240 kDa; IV: 160 kDa; V: 116 kDa; VI: 97 kDa; VII: 66 kDa; VIII: 55 kDa; IX: 40 kDa.

3.3.3.2 Aggregation / Fragmentation (SE-HPLC) of pH-Desorbed IgG1

Size exclusion chromatographic studies on desorbed protein from the ground glass vial particles, obtained by shifting pH, reveal an increased disposition to aggregation with glass contact at near-neutral pH and particularly at the IEP. As shown in Figure 19a, at pH 4 the pH shifts themselves led to a decreased starting monomer percentage (A and B). This increased aggregation level could not be observed for the IgG1 desorbed from the glass (C). In contrast, pH adjustment procedures were less damaging at pH 7.2 and 8.6, leading to a lower level of aggregation for initial (A) and reference formulation (B) in Figure 19b and c. But an increased tendency for aggregation was observed for desorbed protein fractions at pH 7.2 and 8.6. FT-IR measurements already indicated that, especially at their IEP, proteins are prone to form aggregates upon contact with the glass surface. It is known that reduced charge repulsion at the IEP, where repelling electrostatic forces are

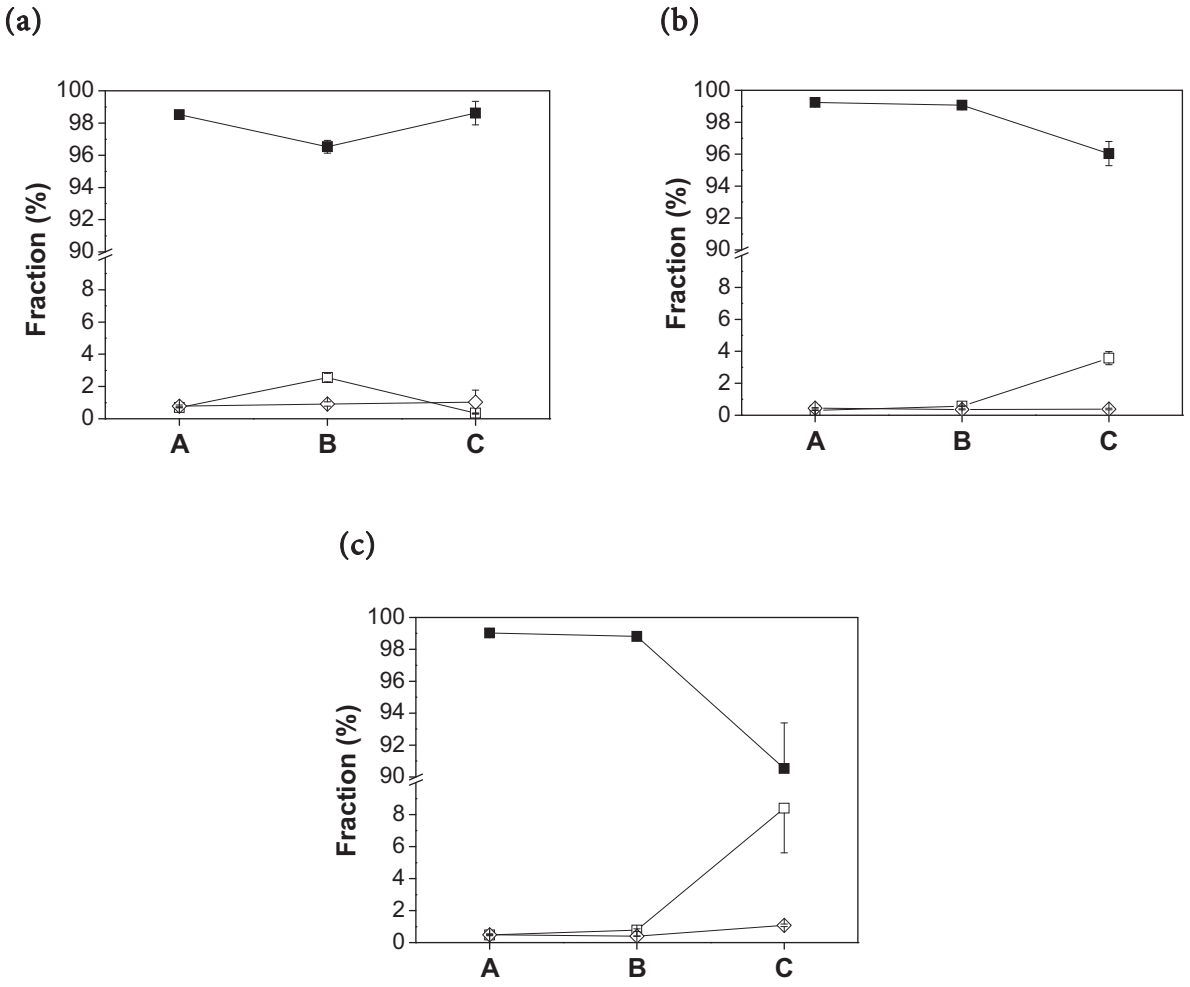

Figure 19: SE-HPLC analysis of IgG1 adsorbed at (a) pH 4.0, (b) pH 7.2 and (c) pH 8.6 with the percentage of (■) monomeric IgG1, (□) aggregated IgG1 and (◇) fragmented IgG1; A: initial incubation formulation at particular pH; B: reference formulation undergone pH shifts; C: IgG1 fractions desorbed from glass particles (B + C measured at pH 7.2).

at their minimum, can result in an agglomeration of protein molecules [63]. Since irreversible aggregation was not observed for IgG1 fractions which have solely undergone the analogous pH shifts (B), the contact of protein molecules with the glass surface must have promoted the formation of stable associates. For all formulations, fragmentation was of minor importance. While the protein structure in agglomerates formed through low electrostatic repulsion is usually native-like and reversible upon pH change, aggregation can also arise from (partially) unfolded intermediates [63]. However, the persistence of the above IgG1 agglomerate fractions, despite the implementation of pH shifts or even of a surfactant treatment, points to more severe structural changes. Below, the structural integrity of the desorbed protein fractions is investigated.

3.3.3.3 Secondary Structure (FT-IR) of pH-Desorbed IgG1

The secondary structure of pH-desorbed IgG1 was characterized by ATR-FTIR spectroscopy. A comparison of the pH-treated reference spectra with the untreated native reference (Figure 20) did not reveal any differences, except for pH 8.6, where a band at 1667 cm^{-1} could be assigned to either turn or unordered structures [4]. The spectrum obtained from protein formerly adsorbed at pH 4.0 (Figure 20a) matches the native standard and the reference. Smaller variations in the peak intensities arising at pH 7.2 (Figure 20b) are presumably due to a reduced protein concentration after desorption, but the fraction exhibits the same structural elements without the indication of structural alterations. The spectrum of IgG1 adsorbed at pH 8.6 (Figure 20c), similarly desorbed at pH 9.5, is of poor quality because the sample concentration is low. Also, a concentration step in advance could not increase the protein content to a sufficient level. Thus, despite the striking differences of IgG1 adsorbed at pH 8.6 when compared to the references, no final conclusions should be drawn.

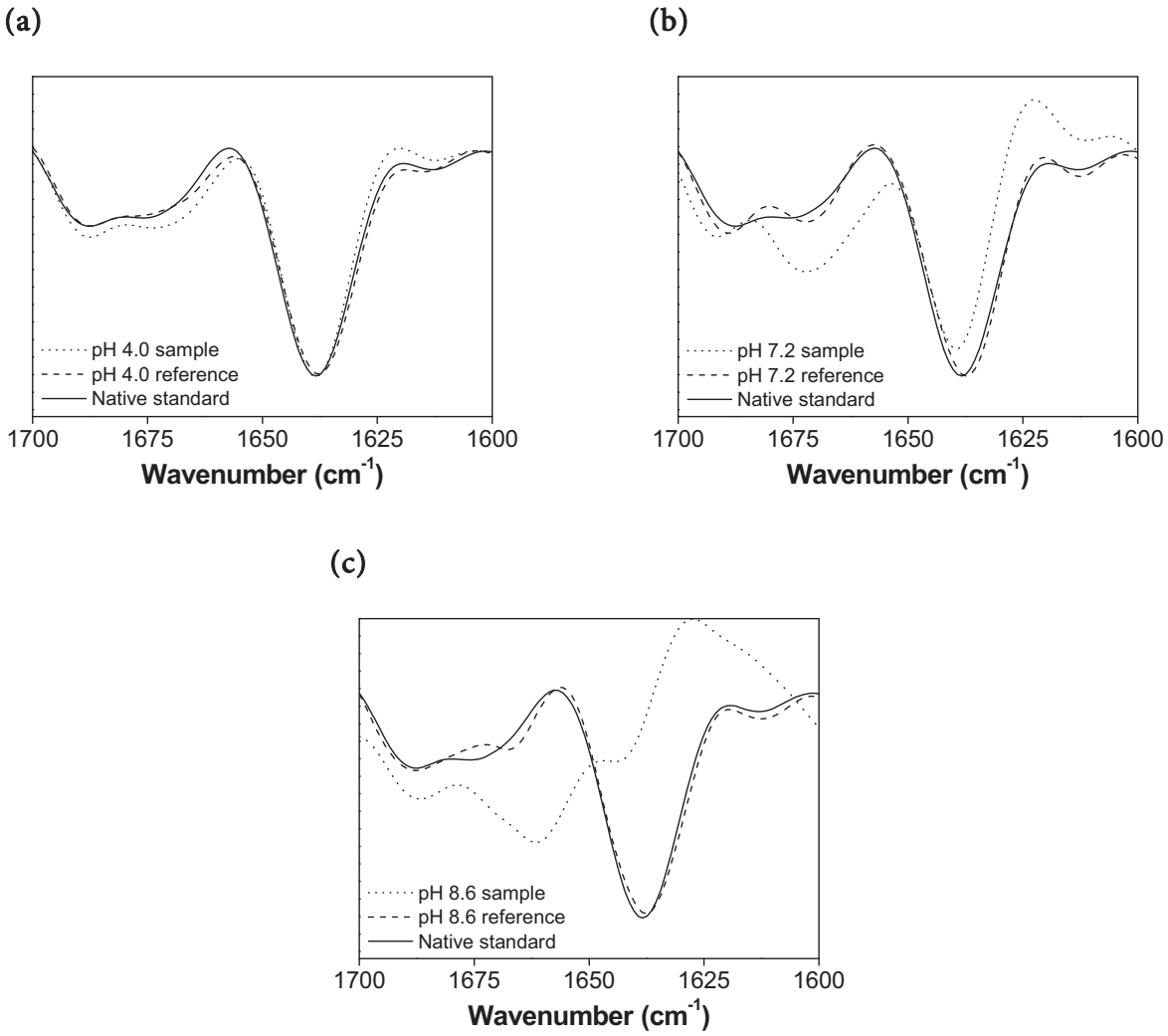

Figure 20: FT-IR second derivative spectra of protein samples adsorbed at (a) pH 4.0, (b) pH 7.2 and (c) pH 8.6; protein sample fractions were obtained by a pH shift to pH 9.5 for 1 h; reference formulation without glass contact underwent identical pH shifts; both samples and references measured after re-adjustment to a uniform pH 7.2.

3.3.3.4 Tertiary Structure (Intrinsic and Extrinsic Steady State Fluorescence) of pH-Desorbed IgG1

The same preparations as analyzed by FT-IR were also subjected to fluorescence spectroscopy. The wavelengths of the emission maxima are identical for all samples. Hence, no dramatic unfolding has occurred through adsorption. In Figure 21, the fluorescence properties of desorbed (a) IgG1 and (b) h-IgG fractions from glass particles are shown. The fluorescence intensity of the IgG1 fraction adsorbed at pH 4.0 is in the same range as the reference. However, a decrease in intensity takes place at the other adsorption pH values, most strikingly for pH 8.6, although the protein concentration was controlled by UV absorption at 280 nm and adapted to a uniform value before. As described above, a

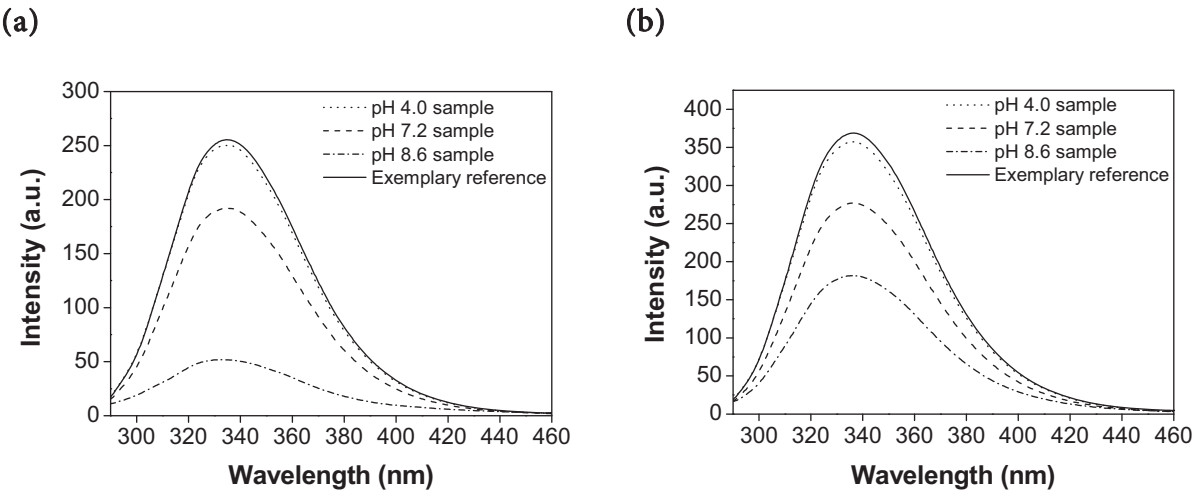

Figure 21: Intrinsic protein fluorescence emission spectra (280 nm) of (a) IgG1 and (b) h-IgG fractions adsorbed at pH 4.0, 7.2 and 8.6; protein sample fractions were obtained by a pH shift to pH 9.5 for 1 h; reference formulation without glass contact underwent identical pH shifts; samples and reference measured after re-adjustment to a uniform pH 7.2 and c = 0.05 mg/ml.

sole decrease in intensity may be evidence for first structural alterations. The same outcome is found for h-IgG. Its quantum yield is higher than that of IgG1, and the fluorescence wavelength emission maximum is slightly red-shifted, which is due to its different amino acid composition and quenching environment. But the intensity decreases in the same manner with increasing incubation pH. This extensive quenching of tryptophan fluorescence along with the decrease in intensity is unlikely to be caused by aggregation only, as the amount of aggregates was less than 10%, which was determined by SEC. The results rather point to substantially unfolded proteins. A similar decrease in fluorescence of an aggregated protein fraction was found by Grillo *et al.* with rhFVIII [42]. They discussed the appearance of this phenomenon in the context of a possible molten globule state.

Additionally, both protein fractions, the desorbed IgG1 as well as the h-IgG, were analyzed in the presence of 5 µM bis-ANS (Figure 22). The dye in buffer alone shows little fluorescence, virtually comparable with the dye added to the native protein. As for the intrinsic fluorescence data, no difference could be observed within the pH-treated reference protein fractions. Hence, for better clarity, only one exemplary curve is presented in Figure 22a and b, respectively. The fluorescence of the protein fraction adsorbed at pH 4.0 is not significantly different from the fluorescence of the reference. However, a significant increase in intensity as well as a blue shift can be observed for pH 7.2 and particularly for pH 8.6. Again, this indicates a change in surface hydrophobicity and unfolding.

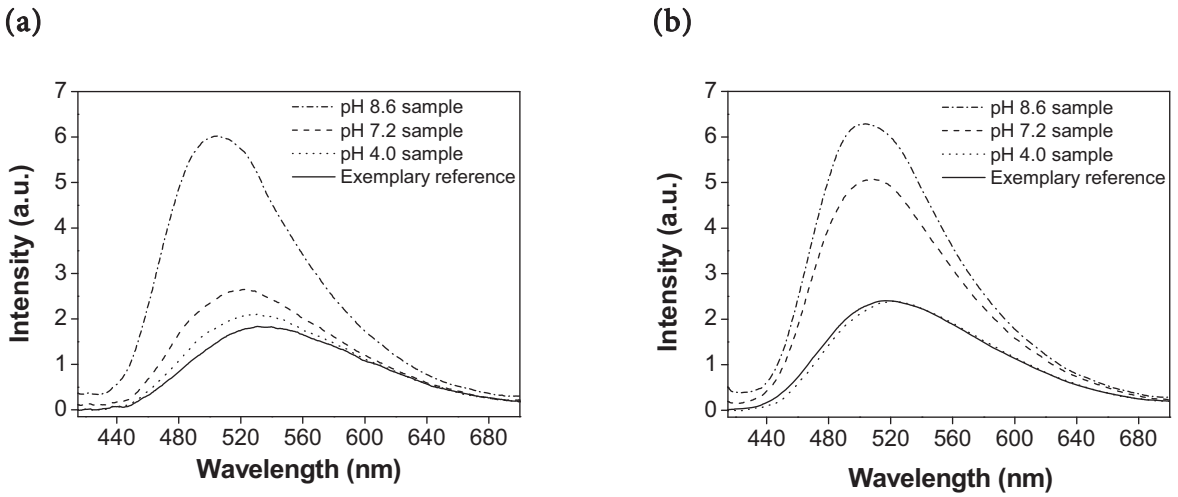

Figure 22: Fluorescence spectra (385 nm) of 5 µM bis-ANS in (a) IgG1 and (b) h-IgG adsorbed at pH 4.0, 7.2 and 8.6; protein sample fractions were obtained by a pH shift to pH 9.5 for 1 h; reference formulation without glass contact underwent identical pH shifts; samples and references measured after re-adjustment to a uniform pH 7.2 and c = 0.05 mg/ml.

In summary, it can be stated that adsorption of IgG on glass causes unfolding and aggregation. The extent to which this takes place depends on the incubation pH. Among the pH values investigated, the structural alterations were most pronounced in the area of the protein IEP and at their lowest at pH 4. This is in marked contrast to stability data of IgG1 in solution, where molecules were shown to unfold/aggregate predominantly at extreme pH values. The extent of structural damage can be related to the degree of surface coverage, as has been described by several authors [6,7,64]. At pH 8.6, where adsorption was low, the distinct glass surface contact caused a pronounced structural damage. Increased adsorption at pH 4 was associated with less structural alterations. Apart from that, one also has to consider a preferential surface binding of unfolded/aggregated protein molecules. In this regard, Christensen *et al.* were able to show that (heat-) aggregated IgG exhibits a higher adsorption tendency on glass than the non-aggregated molecules [65]. This, however, is in contradiction to the very low portion of structurally altered molecules in solution at moderate pH.

3.3.3.5 Biological Activity and Structural Integrity of pH-Desorbed h-IgG

Previous analyses revealed differences between the IgG fractions once adsorbed to the glass surface and the native IgG. The outcome was indicative of an increased aggregation or a (partially) unfolded state, notably through adsorption at the IEP. An enzyme-linked immunosorbent assay (ELISA) can give further information about the conformational integrity of adsorbed proteins [66-69]. But both test parameters and conditions have to be

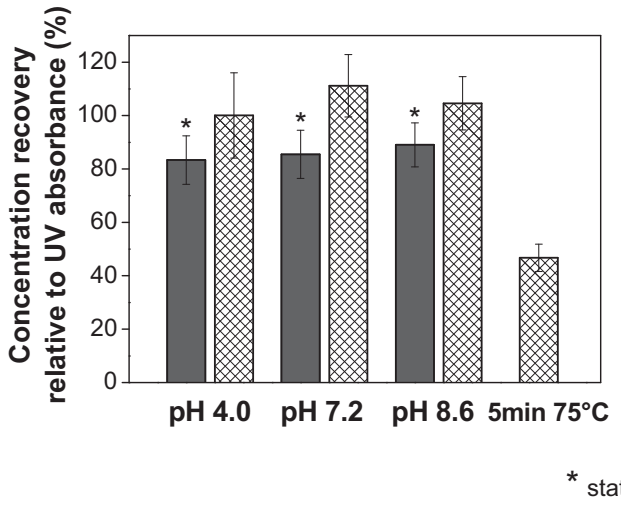

Figure 23: ELISA determined concentration recovery of h-IgG after desorption via pH shift from glass particles; samples (dark gray) adsorbed at the specified pH value; correlating references (white patterned) without glass contact and a denatured reference (heat stressed 5 min, 75°C).

well coordinated for a successful and reproducible outcome of the studies [66]. Our investigations were confined to h-IgG using a standard test kit. This test quantified h-IgG through the binding of anti-h-IgG to a uniform region in human IgGs. Figure 23 shows the %-recoveries from ELISA, related to the UV content of the stock solution, which provides a measure for biological (residual) activity of the desorbed h-IgG fractions after adsorption on borosilicate glass surface. The data is compared to the analogously treated references, except for any glass contact. Each reference fraction exhibits a recovery of around 100%. This proves that both different incubation conditions at each pH and the desorption step with further pH shifts do not negatively influence the h-IgG structure. The IgG fractions once adsorbed on the glass surface show a significantly decreased ELISA recovery ($\alpha = 0.05$) compared to their corresponding reference. This indicates an incomplete structural integrity, equally evident for all incubation pH values investigated. In order to classify the extent of structural damage, a number of reference samples (pH 7.2) were heat stressed at 75°C for 5 min. A concentration recovery of approx. 50% was determined. This result is in line with the findings from previous methods, which reveal that the IgG structure is substantially damaged through the adsorption on glass. But the degree of damage is far from that after heat stress at 75°C. By contrast, previous findings also consistently reveal hardly any structural instability after adsorption at pH 4.0, stronger effects after adsorption at pH 7.2, but less when compared to pH 8.6. This discrepancy may be explained by the presence of Triton X-100® used in the ELISA, which may have forced back aggregation. It is well known that the biological activity is affected by aggregation [70]. Accordingly, reduced aggregation would have led to an

enhanced conformational integrity indicated by ELISA. However, this does not provide a satisfactory explanation for the decreased integrity at pH 4.0. Sandwick and Schray showed that the extent of activity loss due to adsorption is furthermore dependent on protein concentration [2]. At high protein concentrations, the structural alterations were less distinct than at low concentrations. Furthermore, the degree of structural alteration also depends on other factors like temperature, solution characteristics (e.g. pH), time, and the sorbent surface [2,7,71,72].

3.4 Atomic Force Microscopy Investigations on Glass Vial Bottoms

Atomic force microscopy allows a direct visualization of surfaces on the molecular level and has been widely employed for the investigation of glass surfaces [33,73] and IgG deposition on solid surfaces [23,74-76]. Although the elemental compositions of vial bottom and wall surfaces are different [77] and the adsorbed amount of IgG1 on both varies significantly (see Chapter 6), in this study, only the bottoms of glass vials were studied because of their homogeneous surface quality and ease of handling. In comparison, the vial wall has been described to be littered with droplet-shaped structures originating from the vial hot forming process [33]. At first, the blank glass surface was analyzed. A picture of the washed and heat sterilized vial bottom is shown in Figure 24 in an area of 1 x 1 µm and a z-scale of 5 nm. The surface of the vial bottom reveals a very plain and featureless shape and a very low roughness. Hence, the analysis of protein deposits on the glass surface is reasonable.

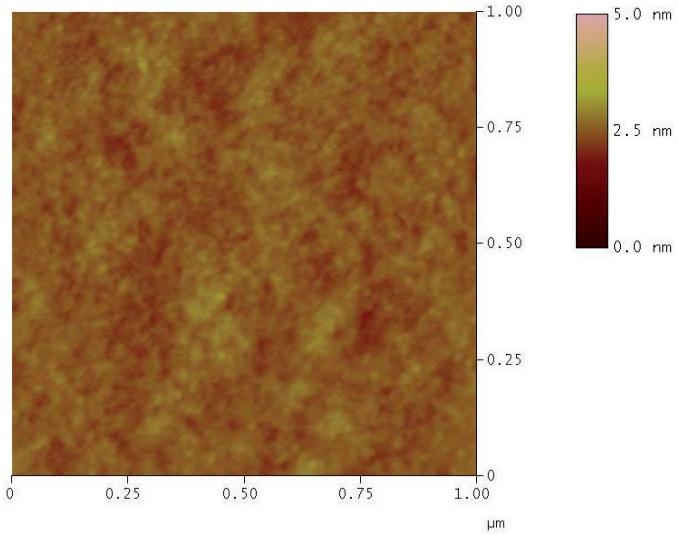

Figure 24: Tapping mode AFM image of the bare dry borosilicate glass vial bottom after washing and heat sterilizing; measurement in air 1 x 1 µm, z-scale = 5.0 nm.

After the adsorption of IgG1 from the standard formulation (2 mg/ml, pH 7.2) on the glass bottom within 24 h, the 3 nm x 3 nm survey scan of the dry glass surface revealed a certain coarseness due to protein deposits (Figure 25a). A detail scan (1 nm x 1 nm) revealed defined round-shaped entities on the surface, which correspond to dried protein structures (Figure 25b). The smallest objects resolved have a diameter in the area of 40 to 60 nm, with an approximate height of 1 nm. Larger formations in the dimension of about 90 - 100 nm appear to arise through the association of smaller objects. The IgG1 dimensions including a common glycosylation pattern are approx. 14.6 x 12.7 x 6.9 nm^3, determined on the basis of the crystal structure. These dimensions correspond to the ones

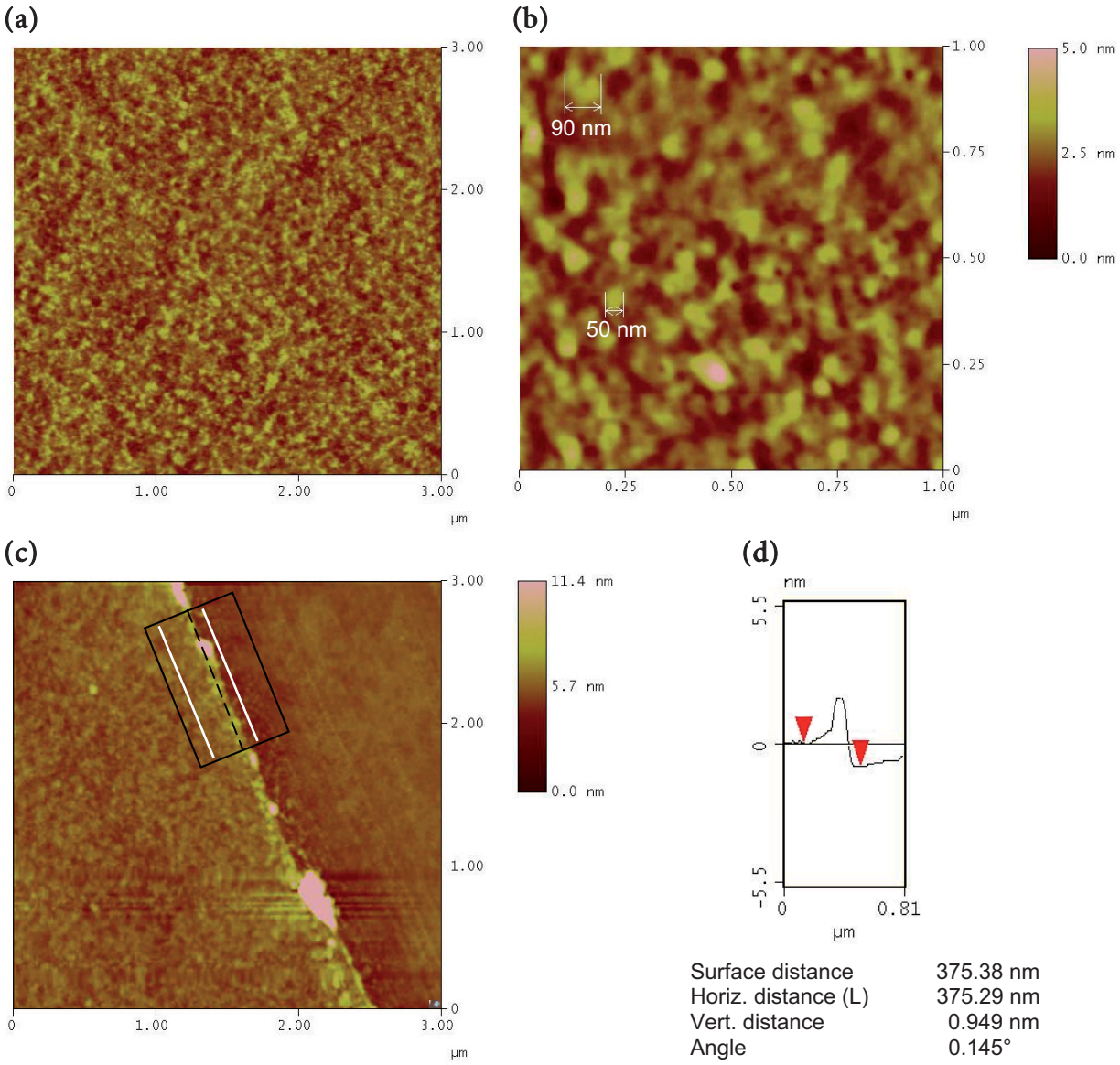

Figure 25: Tapping mode AFM measurements of IgG1 adsorbed (2 mg/ml, 24 h, I = 170 mM) at pH 7.2 (dried) on borosilicate glass vial bottom; measurements in air (a) 3 x 3 µm and (b) 1 x 1 µm, z-scale = 5 nm; (c) protein film partially removed by preparation with an injection needle, z-scale = 11.4 nm; (d) associated cross-section image.

described by other authors for IgG (14.0 x 10.0 x 5.0 nm^3) [74], (14.2 x 8.5 x 3.8 nm^3) [78], (23.5 x 4.5 x 4.5 nm^3) [79], and (14.3 x 13.1 x 5.9 nm^3) [80]. In principle, the existence of a layer thickness smaller than the shortest axis of the molecule seems questionable. Under the chosen condition for adsorption (2 mg/ml), the high IgG concentration led to a high surface coverage, and the base layer suggested in the AFM images cannot essentially be equated with the glass surface. Therefore, another approach of height determination was pursued, in which the protein layer was gently scratched with an injection needle. Care was taken that the glass surface was not damaged. In Figure 25c, it is shown that the tip of the needle waded through the protein layer, resulting in a ridge consisting of protein material. Cross-section analysis confirmed the average protein layer thickness of approx. 1 nm (Figure 25d). Other authors determined the layer thickness of dry IgG films adsorbed on solid surfaces to be 2.0 - 2.5 nm by using AFM [81], and to be 2.9 nm for a wet IgG film, this time by using neutron reflection [78]. Possible reasons for a diminished and shrunk layer thickness may be a compression of the protein layer by the probe tip. It is widely known that forces applied in the AFM technique may modify, distort, or move the analyzed proteins [23], especially well-hydrated proteins in liquid media, as will be described later. However, our measurements were performed in tapping mode, and in repeated scans no alterations were visible and the images remained stable. Another reason for this decreased layer thickness may be the occurrence of pronounced conformational alterations of the molecules due to drying. Protein films shrink depending on the water content at different air humidity values [82], as well as after vacuum treatment [83]. Lu *et al.* found a layer thickness of lysozyme of roughly 1.0 nm on hydrophobic surface and assumed a completely unfolded molecule with loose random structure [14]. The authors hypothesized that a height of 1.0 nm equals the thickness of two average amino acid side chains on top of each other, which would indicate the presence of completely unfolded molecules. Moreover, Tencer *et al.* inferred from a layer thickness of dry BSA, which was smaller than the diameter of the native molecule, that the protein denatured on the surface [17].

As a matter of common knowledge, it should be emphasized that the lateral molecular sizes as seen in AFM images are overstated due to distortions or broadening effects of the AFM tip. Some work has been done on the correction of AFM images via calculations [84], but this is very complex and time consuming. Alternatively, another approach has been described to correct the tip broadening effect regarding a single object. In either case, the tip geometry has to be considered. Assuming a spherical shape of the examined object, the tip broadening effect is described by Equation 1, whereby *W*, the apparent object diameter, can be assessed from the tip radius *R* and the true object radius *r* [73].

$$W = 2\,[(R + r)^2 - (R - r)^2]^{1/2} \qquad (1)$$

As for the broad and flat protein structures, the lateral extension of the objects exceeds the height many times over and the broadening effect should be little. With a height of the protein formation of approx. 1.0 nm (r = 0.5 nm) and a tip diameter of 10.0 nm (R = 5.0 nm), the broadening would be around 5.3 nm, referred to the object diameter.

In the following, it should be investigated whether a molecular resolution was achieved by AFM and whether the round objects could be assigned to single IgG1 molecules. Therefore, the smallest objects resolved were investigated thoroughly. A mean spatial extent was obtained from several independent measurements. The object volume V_o was determined from AFM results according to Equation 2, assuming that the shape of the formations resembles a segment of a sphere [20].

$$V_o = (h/6)\cdot(3r^2 + h^2) \tag{2}$$

In Equation 2, h and r are the height and the radius of the protein object, respectively. The radius r was corrected for the approximated overestimation. For comparison, the molecular volume V_m was theoretically calculated from the molecular weight according to Schneider *et al.* using Equation 3 [20]:

$$V_m = (M_0/N_A)\cdot(V_1 + aV_2) \tag{3}$$

M_0 equals the molecular weight, N_A is Avogadro's number, V_1 and V_2 are the partial specific volumes of the protein and water, respectively. According to Tsai *et al.* [85] and Elwing [86], V_1 was defined to be 0.735 cm^3/g and V_2 was defined to be 1.0 cm^3/g. The extent of protein hydration a was adopted from Schneider *et al.* and set to 0.4 mol H_2O per mol protein [20]. By applying a molecular weight of IgG1 = 152 kDa, V_m equals 286 nm^3 and is therefore in accordance with V_o, which was determined to be 239 nm^3. This confirms the assumption that each of the smaller round objects equals one single protein molecule spread on the glass surface upon drying.

A comparison of dried protein films adsorbed at different solution pH (4.0, 7.2 and 8.6) is shown in Figure 26. The protein film adsorbed at pH 4.0 (a) consists of large irregular-shaped agglomerates which cover wide areas of the surface. A differentiation of single objects becomes difficult as the entities seem to coalesce. The protein film adsorbed at pH 7.2 (b) exhibits a less dense structure, indicating a lower degree of surface coverage. Adsorption at pH = protein IEP (c) reveals a finer structure compared to the other cases, and single entities are distinguishable. With regard to the adsorbed amount of IgG1 at variable solution pH, the coverage rate found from AFM measurements is in line with the results from SDS vial assay quantification (Chapter 4). However, a potential alteration of

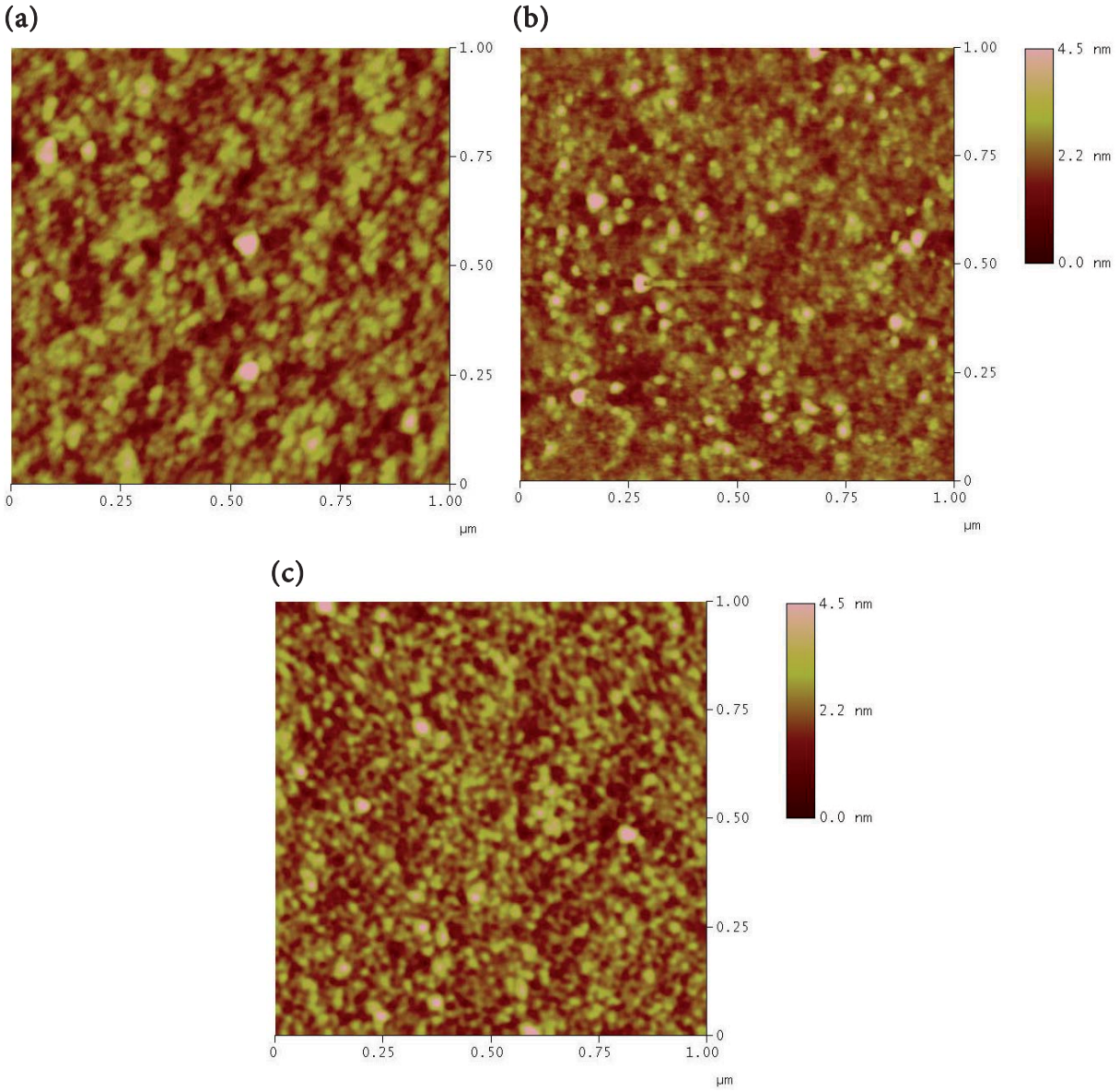

Figure 26: Tapping mode AFM measurements of IgG1 adsorbed (24 h, 2 mg/ml, I = 170 mM) at (a) pH 4.0, (b) pH 7.2 and (c) pH 8.6 on borosilicate glass vial bottom; all samples dried; measurements in air 1 x 1 µm, z-scale = 4.5 nm.

the protein conformation on the surface or a partial desorption by the last rinse with pure water cannot be entirely excluded. According to the results shown above and in Chapter 4, both a pH shift to approx. pH 6 and a drop of the ionic strength are able to decrease the adsorbed amount of IgG1. Also, drying of the adsorbed protein has shown to drastically affect the structure of adsorbed molecules so that the conclusions on protein formation and interaction are less meaningful. In order to avoid such detrimental treatments, the adsorbed protein samples were additionally imaged directly in a more complex setting submerged in buffer medium. That way the molecules are more likely to be in their native conformation as opposed to how they would be in the dried state. However, the proteins might not be sufficiently hard as well as resistant to damage and movement from the

AFM tip [24]. The results of measurements in pH 4.0 are shown in Figure 27 as a survey (a) and in detail (b). In contrast to measurements in air, the images recorded under buffer medium exhibit large bundles of agglomerated (aggregated) IgG1 molecules with a height many times higher than the dried IgG1 adsorbates. A mean object height within the covered surface was determined through cross-section analysis and amounts to 22.0 nm (+/- 6.9 nm). Thus, applying Equation 1, a considerable value for average broadening of each object is expected. Without any correction, the diameters of the vast entities range from roughly 60 nm up to 200 nm and more, corroborating agglomeration of several IgG1 molecules. In analogy to measurements in air, the definite protein layer thickness

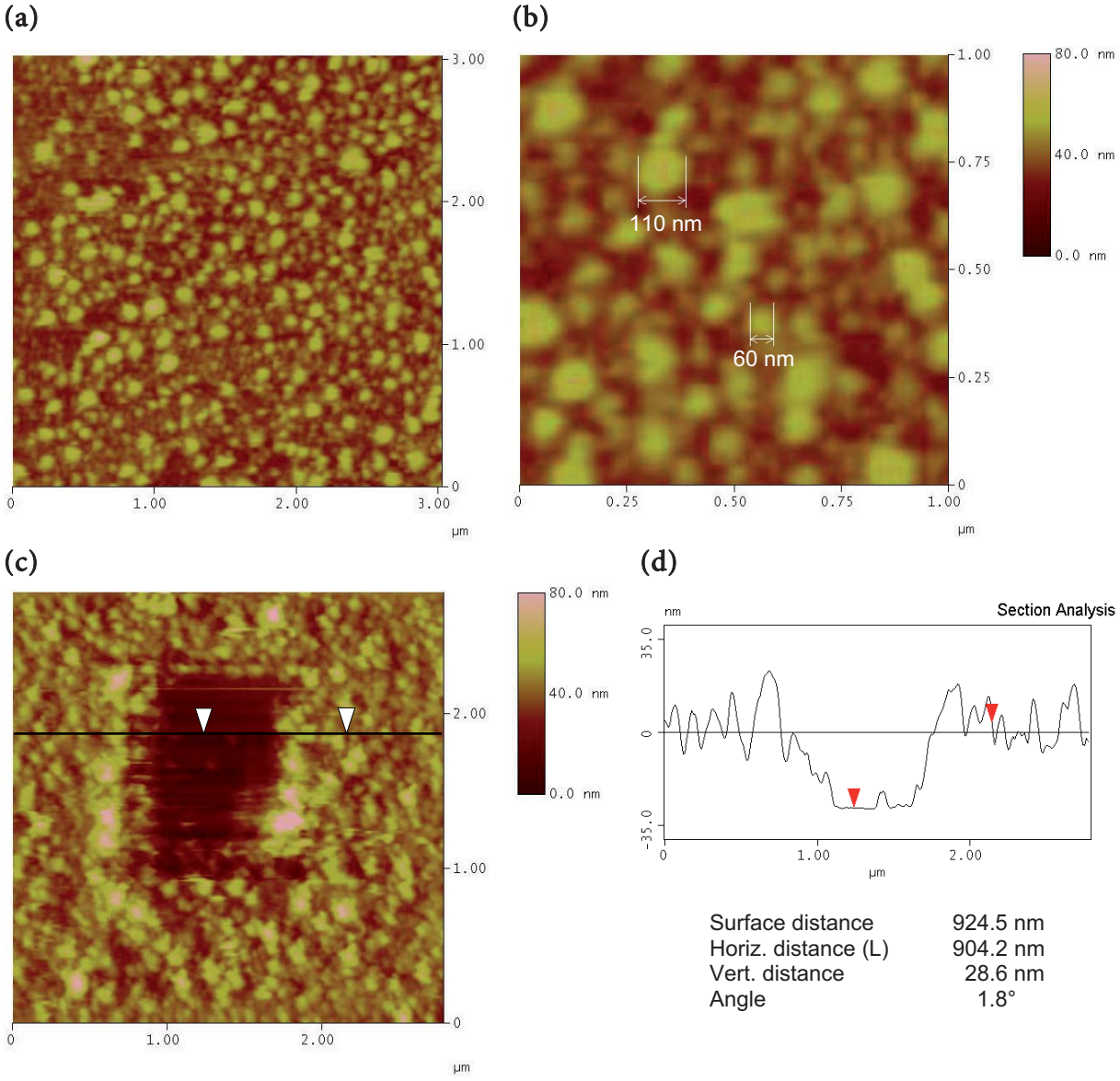

Figure 27: Tapping mode AFM measurements of IgG1 adsorbed (24 h, 2 mg/ml, I = 170 mM) at pH 4.0 on borosilicate glass vial bottom under buffer medium; (a) 3 x 3 µm and (b) 1 x 1 µm; (c) protein layer was removed in the area of 1 x 1 µm by scanning in contact mode; z-scale for all images = 80.0 nm; corresponding section analysis of (c) is shown in (d).

down to the glass is hard to determine because of the crowded surface. The adsorbed proteins did not stick to the glass surface too strongly and were quite easily swept aside within an area of 1 x 1 µm by some scanning procedures in contact mode (Figure 27c), as has also been described by Ton-That *et al.* [87,88]. The average height of the protein structures related to the glass surface is about 30 - 35 nm. This means that more than two perpendicular molecules sit on top of each other and several ones side by side (Figure 27d). If the molecules were lying flat, the number of stacked IgG1 would be increased even further.

In literature, very commonly a monolayer formation model of surface-adsorbed proteins is assumed. According to our results, an IgG1 monolayer formation on glass under the chosen conditions can be clearly disproved. Moreover, both agglomeration and the patchy distribution of proteins complicate the common extrapolation from adsorbed amount to layer thickness and to molecule orientation. Our results are in line with the findings of Zhou *et al.*, who applied AFM/QCM-D on h-IgG adsorbed on solid surface [89]. They suggested a concentration-dependent layer formation of IgG, whereas above a critical value (0.057 mg/ml), multilayer-like structures instead of a monolayer could be observed. Likewise, Su *et al.* limited the monolayer state to low protein concentrations only, e.g. for lysozyme on hydrophilic silica to 0.03 mg/ml [90]. This fact would give rise to further detailed adsorption studies of IgG1 on borosilicate glass at lower protein, and thus, lower surface concentrations.

In contrast to dried protein layers, the space between the hydrated protein molecules may be increased because of the repulsive electric double-layer forces or entropic/thermal fluctuation forces in aqueous electrolyte solutions [91]. Voeroes *et al.* referred to the high amounts of ions and water inside an adsorbed protein layer [92]. Although the share of water in the protein layer decreases with adsorption time, they further argued that the water content (including salt) probably exceeds the mass of protein. This would explain the very voluminous protein structures revealed in hydrated state. Furthermore, the softness of biological samples is problematic when AFM imaging is performed under liquid. Deformation of the sample via compression by the AFM probe was reported [93]. The height determination of biological samples via AFM strongly depends on pH and electrolyte content of the liquid due to electrostatic interactions [94,95]. These interactions can be described by the DLVO (Derjaguin, Landau, Verway, Overbeek) theory. In this regard, Rossell *et al.* found out that a higher ionic strength leads to a decrease in double-layer thickness and forces [95]. Thus, an erroneous imaging of the electrical double layer can be avoided for the benefit of image quality and accurate height measurements. In our case, the ionic strength was chosen to be at a constant value of 170 mM. This should have been sufficient for shielding either attractive or repulsive electrostatic interactions, which generally arise between the AFM tip and the protein surface in solution. But since measured

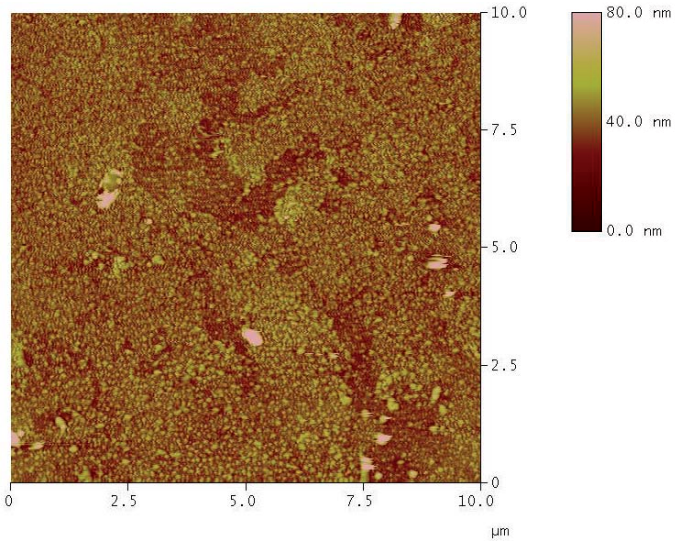

Figure 28: Tapping mode AFM survey image of IgG1 adsorbed (24 h, 2 mg/ml, I = 170 mM) at pH 4.0 on borosilicate glass vial bottom under buffer medium; 10 x 10 µm; z-scale = 80.0 nm.

heights strongly depend on pH [96], the comparison of layer thickness results at different pH values was avoided. Moreover, it turned out to be difficult in our case to receive a stable image at pH values of 7.2 and 8.6, which has also been described by Schneider *et al.* for physiologic pH [20]. The IEP of the Si_3N_4-tip is the area of pH 5 - 6 [97]. The IEP of the protein-covered glass surface was shown to be in the same range (see Chapter 4). Thus, at pH values below as well as above the uniform IEP, both tip and protein loaded surface wear the same charge sign, and the arising rejecting forces favor AFM measurements [95]. It remains unclear whether the bad image quality at neutral to alkaline pH was due to an adverse charge interaction or to other reasons, such as more loosely bound protein [20].

In Figure 28, a 10 x 10 µm survey image of the hydrated pH 4.0 IgG1 sample is shown. Remarkably, no homogeneous adsorption pattern was observed. Although wide areas appear uniformly covered, fields of increased and decreased protein density are distributed over the surface. This allows the assumption that the glass surface chemistry is not homogeneous, thus influencing the protein adsorption pattern or even the aggregation tendency. For example, it could be shown previously by XPS and/or ToF-SIMS measurements (see Chapter 6) that the average adsorbed amounts of IgG1 were different for vial bottom and vial wall, which also must have been due to differences in the glass properties. As proven by the example of vial bottoms (Figure 28), adsorption is not homogeneous in the microscale either.

In summary, it can be stated that AFM imaging is ideally suited for the visualization of protein molecules in surface-adsorbed state. Furthermore, the findings for IgG1 on borosilicate glass are not exceptional. Schneider *et al.*, who imaged single IgG molecules on mica, found heights for IgG adsorbed in dried state similar to ours [20]. The imaging of

adsorbates under buffer has shown to provide more meaningful results, since protein molecules alter extremely upon drying. As mentioned above, difficulties in generating a stable image hampered the AFM analyses under buffer at pH 7.2 and 8.6. For that reason, an increased aggregation tendency observed with other methods at these pH values could not be corroborated with AFM. The pronounced IgG1 agglomeration visualized at pH 4.0 rather leads to the assumption that agglomeration occurs at acidic pH values as well. Most likely, pH-dependent differences in the agglomeration reversibility account for this observation. At the IEP, a decreased IgG1 stability or decreased intermolecular electrostatic repulsion forces may be responsible. Aggregation of IgG on solid surface has already been observed in AFM [23,74], which holds true also for other proteins such as lysozyme [96]. Cullen and Lowe reported a patch-like adsorption pattern of IgG on solid surface as well [23]. From their point of view, nucleation took place, which promoted the adsorption of further molecules. This mechanism is also propagated by Kim *et al.* [96]. Another hypothesis is the formation of aggregates in solution, which subsequently adsorb, forming multiple layers. In our case, the situation became more complex since the high protein concentration during incubation led to a saturated and very crowded surface. Within the scope of this work, the exact mechanism could not be solved conclusively. It might be clarified by monitoring *in situ* adsorption of IgG1 with AFM, using lower IgG1 concentrations. Furthermore, sequential imaging after adsorption at increasing protein concentrations could reveal more differentiated statements upon the adsorption mechanisms. In addition, images in submerged state of IgG1, adsorbed at the so far unsuccessfully tested pH values, would contribute to the mechanistic model as well.

4 CONCLUSIONS

In preliminary studies, the structural stability of IgG1 was investigated in terms of pH, ionic strength, and heat. The IgG1 was stable within the timeframe studied in adsorption experiments over the pH range from 4 to 10 and ionic strengths from 23 mM to 1 M. The adsorption of IgG to borosilicate glass was shown to be at least partially reversible in terms of pH shifts, whereupon the desorbed material could be used for structural investigations. The pH-dependent adsorption characteristic was determined by concentration depletion, using pulverized borosilicate glass. The results from this innovative method were equivalent to those of the vial assay after desorption with SDS buffer. In addition, the secondary, tertiary, and macroscopic structure of IgG1, either in adsorbed state on the well-characterized borosilicate glass powder or after desorption by pH shift, was studied as a function of solution pH. An increased extent of aggregation could be found after adsorption at the isoelectric point of the IgG1 (pH 8.6). The tertiary structure was equally affected by adsorption. Fluorescence spectroscopy results pointed to substantial unfolding, most pronounced at the protein IEP as well. In contrast, the secondary structure of desorbed IgG1 was found to be widely retained. Analysis of the structural integrity of h-IgG after adsorption on borosilicate glass by means of a standardized ELISA revealed a uniformly decreased integrity of only around 80% compared to the native state, which was consistent for all pH values investigated (4.0, 7.2 and 8.6). Besides potential differences in the stability of h-IgG compared to monoclonal IgG1, the decreased integrity, however, may have originated from the ELISA specific sample preparation.

IgG1 adsorbed on borosilicate glass vial bottom could be visualized by AFM in dried state and submerged under buffer. The surface coverage, after adsorption at different pH values (pH 4.0, 7.2 and 8.6), correlated well with the results from quantification assays. AFM measurements revealed an IgG1 layer thickness of approx. 1 nm after drying. Furthermore, AFM imaging resolved small round objects with a diameter of approx. 50 nm. These round entities could be assigned to single IgG1 molecules since their average dimensions corresponded well with the theoretically calculated IgG1 volume. Thus, a spreading of the molecules on the surface along with a loss of their globular molecule shape can be inferred. The imaging of IgG1 adsorbed on the glass surface (pH 4.0) in submerged state revealed agglomeration of molecules and indicated the formation of multiple proteins. The formation of a protein monolayer after incubation at increased equilibrium protein concentrations of 2 mg/ml at pH 4.0 could also be clearly disproved. Further AFM investigations at lower equilibrium concentrations and at different pH values are supposed to give a deeper insight into the adsorption mechanism and the pH-dependence of surface-induced agglomeration.

5 REFERENCES

[1] Buijs, J., Norde, W., Lichtenbelt, J. W. T., Changes in the Secondary Structure of Adsorbed IgG and F(ab')2 Studied by FTIR Spectroscopy, *Langmuir* **12** (1996) 1605-1613.

[2] Sandwick, R. K., Schray, K. J., Conformational states of enzymes bound to surfaces, *J. Colloid Interface Sci.* **121** (1988) 1-12.

[3] Ball, A., Jones, R. A. L., Conformational changes in adsorbed proteins, *Langmuir* **11** (1995) 3542-3548.

[4] Giacomelli, C. E., Bremer, M. G. E. G., Norde, W., ATR-FTIR Study of IgG Adsorbed on Different Silica Surfaces, *Journal of Colloid and Interface Science* **220** (1999) 13-23.

[5] Billsten, P., Freskgard, P. O., Carlsson, U., Jonsson, B. H., Elwing, H., Adsorption to silica nanoparticles of human carbonic anhydrase II and truncated forms induce a molten-globule-like structure, *FEBS Letters* **402** (1997) 67-72.

[6] Kondo, A., Murakami, F., Higashitani, K., Circular dichroism studies on conformational changes in protein molecules upon adsorption on ultrafine polystyrene particles, *Biotechnol. Bioeng.* **40** (1992) 889-894.

[7] Zoungrana, T., Findenegg, G. H., Norde, W., Structure, stability, and activity of adsorbed enzymes, *Journal of Colloid and Interface Science* **190** (1997) 437-448.

[8] Lundqvist, M., Sethson, I., Jonsson, B. H., High-Resolution 2D 1H-15N NMR Characterization of Persistent Structural Alterations of Proteins Induced by Interactions with Silica Nanoparticles, *Langmuir* **21** (2005) 5974-5979.

[9] Sharma, V. K., Kalonia, D. S., Steady-state tryptophan fluorescence spectroscopy study to probe tertiary structure of proteins in solid powders, *Journal of Pharmaceutical Sciences* **92** (2003) 890-899.

[10] Prokopowicz, M., Banecki, B., Lukasiak, J., Przyjazny, A., The measurement of conformational stability of proteins adsorbed on siloxanes, *J. Biomater. Sci. Polym. Ed.* **14** (2003) 103-118.

[11] Czeslik, C., Jackler, G., Royer, C., Driving forces for the adsorption of enzymes at the water/silica interface studied by total internal reflection fluorescence spectroscopy and optical reflectometry, *Spectroscopy (Amsterdam, Netherlands)* **16** (2002) 139-145.

[12] Daly, S. M., Przybycien, T. M., Tilton, R. D., Aggregation of lysozyme and of poly(ethylene glycol)-modified lysozyme after adsorption to silica, *Colloids Surf. B* **57** (2007) 81-88.

[13] Su, T. J., Lu, J. R., Thomas, R. K., Cui, Z. F., Penfold, J., The Conformational Structure of Bovine Serum Albumin Layers Adsorbed at the Silica-Water Interface, *Journal of Physical Chemistry B* **102** (1998) 8100-8108.

[14] Lu, J. R., Su, T. J., Thirtle, P. N., Thomas, R., Rennie, A. R., Cubitt, R., The denaturation of lysozyme layers adsorbed at the hydrophobic solid/liquid surface studied by neutron reflection, *J. Colloid Interface Sci.* **206** (1998) 212-223.

[15] Morrissey, B. W., Smith, L. E., Stromberg, R. R., Fenstermaker, C. A., Ellipsometric investigation of the effect of potential on blood protein conformation and adsorbance, *J. Colloid Interface Sci.* **56** (1976) 557-563.

[16] Sethuraman, A., Han, M., Kane, R. S., Belfort, G., Effect of Surface Wettability on the Adhesion of Proteins, *Langmuir* **20** (2004) 7779-7788.

[17] Tencer, M., Charbonneau, R., Lahoud, N., Berini, P., AFM study of BSA adlayers on Au stripes, *Applied Surface Science* **253** (2007) 9209-9214.

[18] Ohnishi, S., Murata, M., Hato, M., Correlation between surface morphology and surface forces of protein A adsorbed on mica, *Biophys. J.* **74** (1998) 455-465.

[19] Bittencourt, S. E. T., Silva, L. P., Azevedo, R. B., Cunha, R. B., Lima, C. M. R., Ricart, C. A. O., Sousa, M. V., The plant cytolytic protein enterolobin assumes a dimeric structure in solution, *FEBS Letters* **549** (2003) 47-51.

[20] Schneider, S. W., Larmer, J., Henderson, R. M., Oberleithner, H., Molecular weights of individual proteins correlate with molecular volumes measured by atomic force microscopy, *Pfluegers Arch.* **435** (1998) 362-367.

[21] Dufrene, Y. F., Marchal, T. G., Rouxhet, P. G., Probing the organization of adsorbed protein layers: complementarity of atomic force microscopy, X-ray photoelectron spectroscopy and radiolabeling, *Applied Surface Science* **144-145** (1999) 638-643.

[22] Ortega-Vinuesa, J. L., Tengvall, P., Lundstrom, I., Molecular packing of HSA, IgG, and fibrinogen adsorbed on silicon by AFM imaging, *Thin Solid Films* **324** (1998) 257-273.

[23] Cullen, D. C., Lowe, C. R., AFM studies of protein adsorption. 1. Time-resolved protein adsorption to highly oriented pyrolytic graphite, *Journal of Colloid and Interface Science* **166** (1994) 102-108.

[24] Keller, D. J., Scanning Force Microscopy in Biology, *Physical Chemistry of Biological Interfaces*, Baszkin, A., Norde, W., Eds. (Marcel Dekker, Inc., Basel, 2000), Chapter 23, 769-797.

[25] Serra, J., Puig, J., Martin, A., Galisteo, F., Galvez, M., Hidalgo-Alvarez, R., On the adsorption of IgG onto polystyrene particles: electrophoretic mobility and critical coagulation concentration, *Colloid Polym. Sci.* **270** (1992) 574-583.

[26] Pain, R. H., Determining the fluorescence spectrum of a protein, *Current Protocols in Protein Science*, (John Wiley & Sons, Inc., 2004), Chapter 7.7, 1-20.

[27] Josephy, P. D., Eling, T., Mason, R. P., The horseradish peroxidase-catalyzed oxidation of 3,5,3',5'-tetramethylbenzidine. Free radical and charge-transfer complex intermediates, *J. Biol. Chem.* **257** (1982) 3669-3675.

[28] Bakker, A. J., Jellema, B., Prevention of protein adsorption: effect on patient results for microalbuminuria, *Ann. Clin. Biochem.* **36** (1999) 163-167.

[29] Martin, A. N., Physikalische Pharmazie, Leuenberger, Hans, Ed., (Wissenschaftliche Verlagsgesellschaft, Stuttgart) Ed. 4, 2002.

[30] Klank, D., Moeglichkeiten bei der Oberflaechenbestimmung von pulvrigen und poroesen Feststoffen, Quantachrome Workshop: *Oberflaechen und Porenanalytik* (2005).

[31] Vanoni, V. A., Sedimentation Engineering: Manuals and Reports on Engineering Practice No. 54, (ASCE Publications) 2006.

[32] SCHOTT AG, SCHOTT technical glasses: Physical and technical properties, 2007.

[33] Schwarzenbach, M. S., Reimann, P., Thommen, V., Hegner, M., Mumenthaler, M., Schwob, J., Guentherodt, H. J., Topological structure and chemical composition of inner surfaces of borosilicate vials, *PDA J. Pharm. Sci. Technol.* **58** (2004) 169-175.

[34] Kiese, S., Papppenberger, A., Friess, W., Mahler, H. C., Shaken, not stirred: mechanical stress testing of an IgG1 antibody, *J. Pharm. Sci.* **97** (2008) 4347-4366.

[35] Lundqvist, M., Sethson, I., Jonsson, B. H., Protein Adsorption onto Silica Nanoparticles: Conformational Changes Depend on the Particles' Curvature and the Protein Stability, *Langmuir* **20** (2004) 10639-10647.

[36] Deligianni, D. D., Katsala, N., Ladas, S., Sotiropoulou, D., Amedee, J., Missirlis, Y. F., Effect of surface roughness of the titanium alloy Ti-6Al-4V on human bone marrow cell response and on protein adsorption, *Biomaterials* **22** (2001) 1241-1251.

[37] Johnson, R. E., Jr., Dettre, R. H., Wettability and contact angles, *Surface Colloid Sci.* **2** (1969) 85-153.

[38] Docoslis, A., Rusinski, L. A., Giese, R. F., van Oss, C. J., Kinetics and interaction constants of protein adsorption onto mineral microparticles - measurement of the constants at the onset of hysteresis, *Colloids Surf. B* **22** (2001) 267-283.

[39] Wahlgren, M., Arnebrant, T., Lundstroem, I., The adsorption of lysozyme to hydrophilic silicon oxide surfaces: comparison between experimental data and models for adsorption kinetics, *J. Colloid Interface Sci.* **175** (1995) 506-514.

[40] Su, T. J., Lu, J. R., Thomas, R. K., Cui, Z. F., Effect of pH on the Adsorption of Bovine Serum Albumin at the Silica/Water Interface Studied by Neutron Reflection, *J. Phys. Chem. B* **103** (1999) 3727-3736.

[41] Eftink, M. R., The use of fluorescence methods to monitor unfolding transitions in proteins, *Biophys. J.* **66** (1994) 482-501.

[42] Grillo, A. O., Edwards, K. L., Kashi, R. S., Shipley, K. M., Hu, L., Besman, M. J., Middaugh, C. R., Conformational Origin of the Aggregation of Recombinant Human Factor VIII, *Biochemistry* **40** (2001) 586-595.

[43] Buchner, J., Renner, M., Lilie, H., Hinz, H. J., Jaenicke, R., Kiefhaber, T., Rudolph, R., Alternatively folded states of an immunoglobulin, *Biochemistry* **30** (1991) 6922-6929.

[44] Lakowicz, J. R., Weber, G., Quenching of protein fluorescence by oxygen. Detection of structural fluctuations in proteins on the nanosecond time scale, *Biochemistry* **12** (1973) 4171-4179.

[45] Ladokhin, A. S., Fluorescence Spectroscopy in Peptide and Protein Analysis, *Encyclopedia of Analytical Chemistry*, Meyers, R. A., Ed. (John Wiley & Sons Ltd, Chichester, 2000), 5762-5779.

[46] Rosen, C. G., Weber, G., Dimer formation from 1-anilino-8-naphthalenesulfonate catalyzed by bovine serum albumin. Fluorescent molecule with exceptional binding properties, *Biochemistry* **8** (1969) 3915-3920.

[47] Hawe, A., Sutter, M., Jiskoot, W., Extrinsic Fluorescent Dyes as Tools for Protein Characterization, *Pharmaceutical Research* **25** (2008) 1487-1499.

[48] Pastukhov, A. V., Ropson, I. J., Fluorescent dyes as probes to study lipid-binding proteins, *Proteins: Struct. Funct. Genet.* **53** (2003) 607-615.

[49] Holzman, T. F., Dougherty, J. J., Jr., Brems, D. N., MacKenzie, N. E., pH-Induced conformational states of bovine growth hormone, *Biochemistry* **29** (1990) 1255-1261.

[50] Matheus, S., Development of High Concentration cetuximab Formulations using Ultrafiltration and Precipitation Techniques, Thesis, 2006.

[51] Vermeer, A. W. P., Bremer, M. G. E. G., Norde, W., Structural changes of IgG induced by heat treatment and by adsorption onto a hydrophobic Teflon surface studied by circular dichroism spectroscopy, *Biochim. Biophys. Acta, Gen. Subj.* **1425** (1998) 1-12.

[52] Vermeer, A. W. P., Norde, W., The thermal stability of immunoglobulin: unfolding and aggregation of a multi-domain protein, *Biophys. J.* **78** (2000) 394-404.

[53] Vermeer, A. W. P., Conformation of adsorbed proteins, *Encyclopedia of Surface and Colloid Science*, Arthur T.Hubbard, Ed. (Marcel Dekker, Inc., USA, 2002), 1193-1212.

[54] Schuele, S., Friess, W., Bechtold-Peters, K., Garidel, P., Conformational analysis of protein secondary structure during spray-drying of antibody/mannitol formulations, *Eur. J. Pharm. Biopharm.* **65** (2007) 1-9.

[55] Kabsch, W., Sander, C., Dictionary of protein secondary structure: pattern recognition of hydrogen-bonded and geometrical features, *Biopolymers* **22** (1983) 2577-2637.

[56] Dong, A., Kendrick, B., Kreilgard, L., Matsuura, J., Manning, M. C., Carpenter, J. F., Spectroscopic study of secondary structure and thermal denaturation of recombinant human factor XIII in aqueous solution, *Arch. Biochem. Biophys.* **347** (1997) 213-220.

[57] Pompa, P. P., Blasi, L., Longo, L., Cingolani, R., Ciccarella, G., Vasapollo, G., Rinaldi, R., Rizzello, A., Storelli, C., Maffia, M., Optical characterization of glutamate dehydrogenase monolayers chemisorbed on SiO2, *Physical Review E: Statistical, Nonlinear, and Soft Matter Physics* **67** (2003) 041902-1-041902-8.

[58] Maste, M. C. L., Norde, W., Visser, A. J. W. G., Adsorption-induced conformational changes in the serine proteinase savinase: a tryptophan fluorescence and circular dichroism study, *Journal of Colloid and Interface Science* **196** (1997) 224-230.

[59] Noinville, S., Revault, M., Baron, M.-H., Chromatography of biomolecules and biopolymers: an FTIR insight into protein structural changes during the adsorption process, *Encyclopedia of Surface and Colloid Science*, Arthur T.Hubbard, Ed. (Marcel Dekker, Inc., USA, 2002), 1033-1048.

[60] Vermeer, A. W. P., Norde, W., CD spectroscopy of proteins adsorbed at flat hydrophilic quartz and hydrophobic teflon surfaces, *J. Colloid Interface Sci.* **225** (2000) 394-397.

[61] Jiskoot, W., Crommelin, J. A., Methods for Structural Analysis of Protein Pharmaceuticals, Biotechnology: Pharmaceutical Aspects III, (American Association of Pharmaceutical Scientists Press, 2005.

[62] Billsten, P., Carlsson, U., Elwing, H., Studies on the conformation of adsorbed proteins with the use of nanoparticle technology, *Surfactant Sci. Ser.* **110** (2003) 497-515.

[63] Brange, J., Physical stability of proteins, *Pharmaceutical Formulation Development of Peptides and Proteins* (2000) 89-112.

[64] Kamyshny, A., Lagerge, S., Partyka, S., Relkin, P., Magdassi, S., Adsorption of Native and Hydrophobized Human IgG onto Silica: Isotherms, Calorimetry, and Biological Activity, *Langmuir* **17** (2001) 8242-8248.

[65] Christensen, P., Johansson, A., Nielsen, V., Quantitation of protein adsorbance to glass and plastics: investigation of a new tube with low adherence, *J. Immunol. Methods* **23** (1978) 23-28.

[66] Balcells, M., Klee, D., Hocker, H., Quantitative description of protein adsorption processes at polymer surfaces by means of ELISA, *Materialwissenschaft und Werkstofftechnik* **30** (1999) 846-849.

[67] Burns, N. L., Holmberg, K., Surface charge characterization and protein adsorption at biomaterials surfaces, *Prog. Colloid Polym. Sci.* **100** (1996) 271-275.

[68] Jorgensen, P. E., Eskildsen, L., Nexo, E., Adsorption of EGF receptor ligands to test tubes-a factor with implications for studies on the potency of these peptides, *Scandinavian Journal of Clinical and Laboratory Investigation* **59** (1999) 191-197.

[69] Salim, M., O'Sullivan, B., McArthur, S. L., Wright, P. C., Characterization of fibrinogen adsorption onto glass microcapillary surfaces by ELISA, *Lab Chip* **7** (2007) 64-70.

[70] Arakawa, T., Boone, T., Davis, J. M., Kenney, W. C., Structure of unfolded and refolded recombinant derived [Ala125]Interleukin 2, *Biochemistry* **25** (1986) 8274-8277.

[71] Mizutani, T., Decreased activity of proteins adsorbed onto glass surfaces with porous glass as a reference, *J. Pharm. Sci.* **69** (1980) 279-282.

[72] Steiner, G., Tunc, S., Maitz, M., Salzer, R., Conformational Changes during Protein Adsorption. FT-IR Spectroscopic Imaging of Adsorbed Fibrinogen Layers, *Analytical Chemistry* **79** (2007) 1311-1316.

[73] Schwarzenbach, M. S., Reimann, P., Thommen, V., Hegner, M., Mumenthaler, M., Schwob, J., Guntherodt, H. J., Interferon alpha -2a interactions on glass vial surfaces measured by atomic force microscopy, *PDA J. Pharm. Sci. Technol.* **56** (2002) 78-89.

[74] Caruso, F., Rodda, E., Furlong, D. N., Orientational aspects of antibody immobilization and immunological activity on quartz crystal microbalance electrodes, *Journal of Colloid and Interface Science* **178** (1996) 104-115.

[75] Lin, J. N., Drake, B., Lea, A. S., Hansma, P. K., Andrade, J. D., Direct observation of immunoglobulin adsorption dynamics using the atomic force microscope, *Biosens. Technol. [Proc. Int. Symp.]* (1990) 241-249.

[76] Wang, X., Wang, Y., Xu, H., Shan, H., Lu, J. R., Dynamic adsorption of monoclonal antibody layers on hydrophilic silica surface: A combined study by spectroscopic ellipsometry and AFM, *Journal of Colloid and Interface Science* **323** (2008) 18-25.

[77] Pickles, C., Manufacturing Problems, *Pharmaceutical Technology Europe* **11** (2008) 20-23.

[78] Xu, H., Lu, J. R., Williams, D. E., Effect of surface packing density of interfacially adsorbed monoclonal antibody on the binding of hormonal antigen human chorionic gonadotrophin, *Journal of Physical Chemistry B* **110** (2006) 1907-1914.

[79] Malmsten, M., Ellipsometry studies of the effects of surface hydrophobicity on protein adsorption, *Colloids and Surfaces, B: Biointerfaces* **3** (1995) 297-308.

[80] Hook, F., Voros, J., Rodahl, M., Kurrat, R., Boni, P., Ramsden, J. J., Textor, M., Spencer, N. D., Tengvall, P., Gold, J., Kasemo, B., A comparative study of protein adsorption on titanium oxide surfaces using in situ ellipsometry, optical waveguide lightmode spectroscopy, and quartz crystal microbalance/dissipation, *Colloids Surf. B* **24** (2002) 155-170.

[81] Bergkvist, M., Carlsson, J., Karlsson, T., Oscarsson, S., TM-AFM threshold analysis of macromolecular orientation: a study of the orientation of IgG and IgE on mica surfaces, *Journal of Colloid and Interface Science* **206** (1998) 475-481.

[82] Lubarsky, G. V., Davidson, M. R., Bradley, R. H., Hydration-dehydration of adsorbed protein films studied by AFM and QCM-D, *Biosensors & Bioelectronics* **22** (2007) 1275-1281.

[83] Mori, O., Imae, T., AFM investigation of the adsorption process of bovine serum albumin on mica, *Colloids and Surfaces, B: Biointerfaces* **9** (1997) 31-36.

[84] Keller, D. J., Franke, F. S., Envelope reconstruction of probe microscope images, *Surf. Sci.* **294** (1993) 409-419.

[85] Tsai, J., Taylor, R., Chothia, C., Gerstein, M., The Packing Density in Proteins: Standard Radii and Volumes, *J. Mol. Biol.* **290** (1999) 253-266.

[86] Elwing, H., Protein absorption and ellipsometry in biomaterial research, *Biomaterials* **19** (1998) 397-406.

[87] Ton-That, C., Shard, A. G., Bradley, R. H., Thickness of Spin-Cast Polymer Thin Films Determined by Angle-Resolved XPS and AFM Tip-Scratch Methods, *Langmuir* **16** (2000) 2281-2284.

[88] Roberts, C. J., Davies, M. C., Davies, J., Dawkes, A. C., Tendler, S. J. B., Williams, P. M., The use of scanning probe microscopy and surface plasmon resonance for the study of antigen-antibody interactions at immunoassay surfaces, *Polymer Preprints (American Chemical Society, Division of Polymer Chemistry)* **36** (1995) 129-130.

[89] Zhou, C., Friedt, J. M., Angelova, A., Choi, K. H., Laureyn, W., Frederix, F., Francis, L. A., Campitelli, A., Engelborghs, Y., Borghs, G., Human immunoglobulin adsorption investigated by means of quartz crystal microbalance dissipation, atomic force microscopy, surface acoustic wave, and surface plasmon resonance techniques, *Langmuir* **20** (2004) 5870-5878.

[90] Su, T. J., Lu, J. R., Thomas, R. K., Cui, Z. F., Penfold, J., The adsorption of lysozyme at the silica-water interface: a neutron reflection study, *Journal of Colloid and Interface Science* **203** (1998) 419-429.

[91] Israelachvili, J., Wennerstrom, H., Role of hydration and water structure in biological and colloidal interactions, *Nature (London)* **379** (1996) 219-225.

[92] Voeroes, J., The density and refractive index of adsorbing protein layers, *Biophysical Journal* **87** (2004) 553-561.

[93] Radmacher, M., Fritz, M., Hansma, P. K., Imaging soft samples with the atomic force microscope: gelatin in water and propanol, *Biophys. J.* **69** (1995) 264-270.

[94] Muller, D. J., Engel, A., The height of biomolecules measured with the atomic force microscope depends on electrostatic interactions, *Biophys. J.* **73** (1997) 1633-1644.

[95] Rossell, J. P., Allen, S., Davies, M. C., Roberts, C. J., Tendler, S. J. B., Williams, P. M., Electrostatic interactions observed when imaging proteins with the atomic force microscope, *Ultramicroscopy* **96** (2003) 37-46.

[96] Kim, D. T., Blanch, H. W., Radke, C. J., Direct imaging of lysozyme adsorption onto mica by atomic force microscopy, *Langmuir* **18** (2002) 5841-5850.

[97] Senden, T. J., Drummond, C. J., Surface chemistry and tip-sample interactions in atomic force microscopy, *Colloids Surf. A* **94** (1995) 29-51.

Chapter 8

Summary of the Thesis

The adsorption of therapeutic proteins to different surfaces in the course of fill and finish, storage, or administration is critical and has shown to cause severe problems which should not be underestimated. Among them is the loss of content but also, potentially, protein structural changes, accompanied by the risk of therapy failure or immunological reactions. In this context, special attention has to be paid to primary packaging containers, to which the protein has an enduring surface contact.

Against this background, the adsorption of a modern therapeutic protein, i.e. an IgG1 antibody, to vials was investigated within the scope of this thesis. The first priority had borosilicate glass, followed by siliconized borosilicate glass and polyolefin plastic. The use of model surfaces was almost completely avoided. The studies comprise the quantification of surface-bound protein subject to variable formulation compositions and surface qualities as well as a detailed characterization of the adsorbed protein layer including protein structural alterations caused by the adsorption process. In the presented investigations, the main focus was on the equilibrium state of adsorption at conditions mainly within the scope of pharmaceutical relevance, but also beyond, if necessary, for the acquisition of fundamental knowledge on the adsorption mechanism.

The non-ideal surface character of single dose primary packaging containers, together with the limited surface area, required the development of tailored analytical procedures. Desorption of surface-bound protein molecules using SDS, followed by SEC with fluorescence detection, proved excellent suitability and universal applicability for the determination of adsorbed amounts. This was confirmed by various reference techniques in the course of the thesis, such as QCM, XPS, solution depletion, and protein hydrolysis coupled with TOC analysis. The validated SEC method was sufficiently sensitive for the quantification of lowest adsorbed amounts as well as for low container surface-to-volume ratios. LOD and LOQ values were in the range of 0.03 - 0.06 and 0.08 - 0.17 µg/ml IgG, respectively. Moreover, the desorption assay avoids exceptional equipment and the use of model surfaces.

The studies demonstrate that adsorption is strongly affected by the surface quality of the vials. The surface polarity, derived from the ratio of polar and unpolar components of the

surface free energy, turned out to be a key parameter in this regard. Adsorption was shown to decrease linearly with increasing surface polarity. The lowest amount of IgG1 was bound on a highly purified glass surface, whereas organic surface contaminants of either airborne or unspecific origin or hydrophobic vial materials have shown to increase adsorption. The amount of IgG1 adsorbed on borosilicate glass accordingly increased with precedent vial storage time at exposure to air. Therefore, particular attention should be paid to the cleaning procedure as well as to storage conditions and time. An increased extent of organic material on the vial wall part was observed with XPS and ToF-SIMS. Furthermore, it cannot be excluded that experimentally verified differences in the elemental surface composition of both segments or the observed corrosion of the topmost borosilicate glass surface by means of the protein formulation has an effect on the adsorbed quantity as well. Both formulation pH and ionic strength exert a more controllable influence on adsorption by affecting the charge of the protein and the sorbent surface. The adsorption maximum of IgG on glass at an ionic strength of 170 mM was found at pH 4.0 (approx. 5 mg/m^2), thus clearly apart from its IEP at 8.6. It became apparent that the pH of maximum adsorption is a function of the ionic strength and is shifted towards a higher pH with decreasing salt concentration. Ionic strength only has a distinct effect on the adsorbed amount on the hydrophobic plastic surface when IgG1 is considerably charged (e.g. at pH 4.0).

An important outcome of this work is that the main driving forces for IgG adsorption on vials could be elucidated. Electrostatic forces play a major role in the adsorption of IgG on glass. Hydrophobic interactions have shown to be secondary but not entirely insignificant. The adsorbed amount is attributable to the interplay of attractive and repulsive forces, both between protein molecules and between the protein molecules and the surface. Furthermore, this balance is influenced by a charge screening effect of salt ions contained in the protein solution. This could be confirmed by electrokinetic measurements. In the case of a positive charge surplus in the adsorption boundary layer, the doubly charged SO_4^{2-} ion was more effective in preventing charge accumulation than Cl^-. The consequence was a disproportionally increased IgG1 adsorption at an otherwise equal ionic strength. For hydrophobic materials, where hydrophobic protein surface interactions prevail, electrostatic forces affect adsorption by means of intermolecular repulsion. In spite of an intrinsic preferential exclusion and stabilizing effect, uncharged sugar and polyol excipients showed a minor impact on IgG adsorption. In contrast, uncharged surfactants proved to prevent from adsorption by shielding hydrophobic areas on both glass and protein surface. Surfactants of higher hydrophobicity were more effective in reducing the adsorbed amount. Compared to pH 4.0, the adsorption-decreasing effect was more pronounced at pH 7.2 (reductions up to 90%), where hydrophobic interactions contributed significantly to the surface-attractive driving force.

In a theoretical approach, IgG1 adsorption on hydrophilic and hydrophobic vial surfaces was shown to comply with the Langmuir-Freundlich (Sips) isotherm model. The adsorption cooperativity type turned out to be consistently negative. A decreasing extent of negative cooperativity at increasing ionic strengths supports the theory of an electrostatically dominated adsorption mechanism for borosilicate glass. In contrast, the explanation for a pronounced negative cooperativity extent on hydrophobic surfaces throughout requires further investigation.

In the course of structural investigations, AFM imaging revealed interesting insights into the morphology of IgG1 adsorbates, such as adsorption in the form of agglomerates, the absence of a monolayer formation, molecule spreading upon drying, and an inhomogeneous adsorption on the vial surface in the microscale. The thickness of a typical adsorption layer was approx. 1 nm in dried state and amounted up to 30 - 35 nm in its native form submerged. In AFM measurements, individual molecules were resolved on the glass surface. But in most cases, they fused to larger agglomerates. Stability investigations confirmed that the glass surface has a destabilizing effect on the adsorbed IgG1. As expected, the tertiary structure is considerably affected through adsorption, whereas the secondary structure of adsorbed IgG1 is widely retained. The structural alterations observed were increased at the IEP of the antibody and were generally discussed to serve as an additional adsorption driving force.

In summary, the studies contribute to an enhanced and profound understanding of the adsorption of IgG as a therapeutic protein on packaging container surfaces. This thesis presents a set of analytical methodologies which proved to overcome the obstacles of a non-ideal surface in the quantification and the structural investigation of adsorbed protein. The free energy of the surface as well as the pH and the ionic strength of the formulation turned out to be key parameters with regard to the adsorbed amount and the structural stability. The technical experiences gained in the handling of non-ideal surfaces and the knowledge on adsorption mechanisms ought to facilitate a transfer to the question of therapeutic protein adsorption to other packaging components, e.g. syringe plungers or vial stoppers. Finally, the present thesis may encourage and support further research in the field of new packaging materials or innovative container coatings for the minimization of adsorption and the prevention from surface-induced instabilities.

List of Abbreviations

α	significance level
a	protein molecule radius
A	surface area
AFM	atomic force microscopy
ANS	8-anilino-1-naphtalene-sulfonate
API	active pharmaceutical ingredient
ATR	attenuated total reflection
β-hCG	β-subunit of human chorionic gonadotropin
BET	(theory described by) Brunauer, Emmett, and Teller
bis-ANS	4,4′-Dianilino-1,1′-binaphthyl-5,5′-disulfonic acid dipotassium salt
BPA	bovine plasma albumin
c	concentration
CA	contact angle
CD	circular dichroism
c_{eq}	equilibrium concentration
CMC	critical micelle concentration
COC	cyclic olefin copolymer
COP	cyclic olefin polymer
Δ_{ads}	change in thermodynamic function through the adsorption process
$\Delta_{ads}\sigma_{ek}$	charge transfer between the adsorbed layer and the surrounding liquid
Δf	frequency shift
d_h	hydrodynamic diameter
DLVO	(theory described by) Derjaguin, Landau, Verway, and Overbeek
DSSP	define secondary structure of proteins
e	electron charge
ε_0	permittivity of the free space
ε_r	relative permittivity of the medium
ELISA	enzyme-linked immunosorbent assay
EMBOSS	european molecular biology open software suite
EMEA	european medicines agency
ExPASy	expert protein analysis system
η	viscosity of the liquid
F	Faraday constant
Fb	fibrinogen
FDA	food and drug administration
FT-IR	Fourier transform infrared spectroscopy

γ	surface free energy
Γ	mass of protein adsorbed per surface area
γ^d	dispersive component of the surface free energy
γ_l	surface tension of the liquid
Γ_{max}	maximum surface concentration
γ^p	polar component of the surface free energy
Γ_{pl}	adsorption plateau value
γ_s	surface tension of the solid
γ_{sl}	interfacial tension of solid and liquid
γ_s^p / γ_s	surface polarity
G-CSF	granulocyte colony-stimulating factor
h	height
H	enthalpy
HDL	high-density lipoprotein
HEPA	high efficiency particulate air filter
hGH	human growth hormone
h-IgG	human IgG from pooled serum
HLB	hydrophilic / lipophilic balance
HPLC	high performance liquid chromatography
HSA	human serum albumin
I	ionic strength
IC	inorganic carbon
ICH	international conference on harmonisation
IEF	isoelectric focusing
IEP	isoelectric point
IgG	immunoglobulin G
IMFP	inelastic mean free path
κ^{-1}	Debye length
k	Boltzmann constant
K	adsorption equilibrium constant
k_a	rate constant for adsorption
k_d	rate constant for desorption
K_m	mean binding affinity
λ	wavelength of the light
λ_{max}	maximum wavelength
LC	liquid chromatography
LOD	limit of detection
LOQ	limit of quantification
μ_e	electrophoretic mobility

mBCA	micro bicinchoninic acid assay
MW	molecular weight
MWCO	molecular weight cut off
n	cooperativity coefficient
n^0	number of ions per unit volume
N_A	Avogadro's number
NI-assay	non interfering protein assay
NIBS	non-invasive back-scatter
NMR	nuclear magnetic resonance
OWLS	optical waveguide lightmode spectroscopy
P 188	poloxamer 188
PAGE	polyacrylamide gel electrophoresis
PBS	phosphate buffered saline
PC	principal component
PCA	principal component analysis
PCO 35	polyoxyl 35 castor oil
PDMS	poly(dimethysiloxane)
PEG	polyethylene glycol
Ph. Eur.	Pharmacopoea Europaea
pI	isoelectric point
pK_a	thermodynamic dissociation constant
pK_a^*	practical dissociation constant
PMT	photomultiplier tube
PP	polypropylene
PS 20	polysorbate 20
PS 80	polysorbate 80
PTFE	polytetrafluoroethylene
PZC	point of zero charge
QCM	quartz crystal microbalance
QCM-D	quartz crystal microbalance with dissipation monitoring
r	surface roughness parameter
r	true object radius
R	ideal gas constant
R	AFM tip radius
r_h	hydrodynamic radius
rhFVIII	recombinant human factor VIII
RSD	relative standard deviation
σ_e	electrokinetic charge density
S	entropy

SDS	sodium dodecyl sulfate
SE-HPLC	size exclusion high performance liquid chromatography
SEM	scanning electron microscopy
SPR	surface plasmon resonance
T	absolute temperature
TC	total carbon
TGF-β1	transforming growth factor beta 1
TIRF	total internal reflection fluorescence
TOC	total organic carbon
θ	contact angle
$\hat{\theta}$	contact angle of the roughened surface
θ_0	intrinsic angle
USP	United States Pharmacopeia
V_1, V_2	specific volumes
V_m	molecular volume
W	apparent object diameter
XPS	X-ray photoelectron spectroscopy
ζ	zeta potential
z	valency of ions

Curriculum Vitae

Johannes Maximilian Mathes

PERSONAL DATA

Date of birth:	April 24th, 1979
Place of birth:	Oberviechtach, Germany
Nationality:	German
Marital status:	Married, one child

PROFESSIONAL EXPERIENCE

since 08/2009	Licensed pharmacist, Paracelsus Apotheke, Weiden, Germany

EDUCATION

since 08/2005	Ph.D. thesis Department of Pharmacy, Pharmaceutical Technology and Biopharmaceutics, Ludwig-Maximilians-University, Munich Supervisor: Prof. Dr. Wolfgang Frieß In cooperation with Merck Serono GmbH, Darmstadt, Germany and SCHOTT AG, Mainz, Germany
07/2005	License to practice pharmacy
11/2004 - 04/2005	Internship at Neue Apotheke, Neunburg v. W., Germany
05/2004 - 10/2004	Internship at Pharma Stulln GmbH, Stulln, Germany
10/1999 - 04/2004	Study of Pharmacy, University of Regensburg, Germany